VNIVERSITAT DE VALÈNCIA
Doctoral Program in Physiology
Department of Physiology
Faculty of Medicine and Odontology

INHIBITION OF OXIDATIVE STRESS AND NEUROINFLAMMATION AS A NOVEL TREATMENT OF ALS

Doctoral Thesis presented by

Rafael López Blanch

June 2024

Supervised by:

Professor Elena Obrador Pla

Dña Elena Obrador Pla, Titular del Dpto. de Fisiología, Universitat de València

CERTIFICA:

Que la presente memoria, titulada "**INHIBITION OF OXIDATIVE STRESS AND NEUROINFLAMMATION AS A NOVEL TREATMENT OF ALS**", corresponde al trabajo realizado bajo su dirección por D. **Rafael López Blanch**, para su presentación como Tesis Doctoral en el Programa de Doctorado en Fisiología de la Universitat de València.

Y para que conste firma el presente certificado en Valencia, a 10 de junio 2024.

MARIA ELENA| OBRADOR| PLA

Firmado digitalmente por MARIA ELENA| OBRADOR|PLA
Fecha: 2024.06.10 13:37:43 +02'00'

Fdo. Elena Obrador Pla

ACKNOWLEDGEMENTS

Me gustaría comenzar agradeciendo a mi directora de tesis, Elena. Gracias por tu dedicación y por estar siempre disponible cuando te he necesitado. Estoy seguro de que pocos directores se quedan hasta la madrugada para ayudar a sus doctorandos a terminar la tesis. Agradezco la oportunidad de haberte conocido y de que hayas sido una de las personas más influyentes en mi vida. Disfruto mucho de la facilidad con la que puedo hablar contigo sobre cualquier tema. No solo he encontrado en ti a una jefa maravillosa, sino también a una "Mami del lab". Gracias por todo.

Ahora me gustaría agradecer a José. Gracias por tratarme como uno más de vuestra familia. Aún recuerdo nuestra primera reunión sobre lo que iba a hacer durante mi estancia en el laboratorio y lo nervioso que estaba. Nunca imaginé lo a gusto que me sentiría después y cuánto me desarrollaría profesionalmente. Tengo mucho que agradecerte por todas las experiencias que he podido vivir gracias a ti, entre las cuales destaca la oportunidad de realizar esta tesis doctoral que tanto he disfrutado. Al igual que siento que Elena es mi "Mami del lab", tú eres mi "Papi del lab".

Durante estos años en el laboratorio, he conocido a muchas personas que me han ayudado a crecer y a ser quien soy hoy. Quiero agradecer a todos aquellos que he conocido durante este tiempo. Gracias por hacer que los días en el laboratorio sean más llevaderos. He hecho grandes amigos y forjado amistades que, sin importar en qué país se encuentren ahora, siempre encuentran unos minutos para hablar conmigo. Me gustaría hacer una mención especial a mi primera estudiante de TFM, Fátima. Sé que a veces te vuelvo loca con los

experimentos, pero espero que hayas disfrutado tanto como yo de todos los momentos buenos y de la bonita amistad.

I would like to thank the laboratory in Norway that welcomed me so warmly during my stay. The time I spent in Norway marked a turning point in my life, and being able to experience it with such wonderful people is something I wish for every researcher. Thank you for the great moments, and I hope that whenever I go to Norway, I can stop by to say hello.

A mí querida familia:

Primero quiero agradecer a mi prometida Kristine. Gracias por siempre estar conmigo cuando más lo he necesitado. Eres uno de los pilares que sostiene mi vida. La forma en que me entiendes en todo momento te hace única, y conviertes cualquier lugar en "hogar" o "familia" cuando estamos juntos. Solo puedo escribir cosas buenas sobre ti, pero en pocas palabras, quiero decirte que me siento muy orgulloso de la gran profesional y persona que eres. Gracias por ser una bellísima persona y por quererme de la manera que lo haces. Contigo he aprendido el verdadero significado de amar a alguien. Te mereces lo mejor del mundo. Te quiero *muchísisisimo*.

A mi hermano Pedro. No sabes lo feliz que me hace tener un hermano como tú. ¡No podría haber deseado uno mejor! Cada vez que pasamos tiempo junto es el mejor momento del día. Quiero que sepas que estoy muy orgulloso de ti y sé que llegarás muy lejos porque eso es lo que les sucede a las buenas personas como tú. Gracias por animarme tantas veces cuando tengo mis bajoncillos y por cubrirme siempre.

Espero que nuestra relación tan especial se mantenga hasta el último de mis días. Te quiero mucho Tete.

Me gustaría dar las gracias a Belén por portarse tan bien conmigo. Ver que cuidas tan bien a mi hermano me pone muy feliz. ¡También muchas gracias por cuidar de Nico! Eres una gran persona y me alegra mucho que formes parte de la familia. Te quiero.

A mis queridos Yayo Rafa y Yaya Virginia. No sabéis lo afortunado que me siento de haber poder vivido con vosotros. Muchas veces la gente no se da cuenta de los tesoros que tienen al lado, pero yo sí lo hago, y vosotros sois uno de los míos que más aprecio. Os quiero mucho y quiero agradeceros de corazón lo bien que me habéis cuidado todo este tiempo.

Queridos Papá y Mamá. Os quiero dar las gracias por todo. Gracias por la manera en que me habéis querido. Vosotros habéis hecho posible que llegue a donde estoy. Los valores que me habéis enseñado desde pequeño han hecho que nunca me rinda y que trabaje por mis sueños. De vosotros he aprendido lo que es una verdadera familia. No sabéis lo afortunado que me siento de tener unos padres como vosotros. Quiero que sepáis que estoy muy orgulloso de vosotros y espero que vosotros también lo estéis de mí. Siempre habéis sido unos referentes para mí y espero poder contar con vosotros siempre. Os quiero con todo mi corazón.

Quiero agradecer a mi Yaya Elvira y a mi Yayo Pepe. Gracias por cuidarme y apoyarme siempre. Cuando vine a Valencia, siempre estuvisteis ahí cuando lo necesitaba, y es algo que siempre recordaré.

Vosotros siempre confiasteis en mí y espero que lo sigáis haciendo. Os quiero.

También quiero agradecer a mi madrina Bea. Me encanta hablar contigo sobre cualquier cosa. Gracias por nuestras charlas en la playa y por todos los buenos momentos que he vivido contigo desde que era pequeño. Me hace muy feliz que seas mi madrina. Te quiero mucho.

A mi tía Gladys. Muchas gracias por siempre escuchar mis dudas sobre las decisiones que tomar respecto a mi futuro. Me encanta cuando hablamos de ciencia o cuando te comento todas las ideas que se me pasan por la cabeza, y tú pareces incluso más interesada que yo. Te quiero mucho, y quiero que sepas que agradezco todo el esfuerzo que haces por mantener a la familia unida.

A mis queridos amigos:

Quiero mencionar a mis grandes amigos Alex, Alberto, Jordi y Sergi. Los momentos con vosotros no tienen precio. A veces me da pena pensar en cómo pasa el tiempo y cada uno tiene ya su vida, pero después, cuando nos juntamos, parece que el tiempo no ha pasado. Os deseo todo lo mejor, porque personas como vosotras os lo merecéis.

A mi querida amiga Cris. Gracias por estar siempre llena de energía. Eres una de las personas con mejor corazón que conozco y con las que más me río. Sé que la vida tiene cosas muy grandes para ti. Te quiero gamba.

Quisiera agradecer de manera especial a las personas que ya no se encuentran conmigo. Mis queridos yayos Juana y Javier, espero que donde estéis, estéis orgullosos de mí, porque siempre me habéis dicho que podría lograr lo que me propusiera, pero que nunca perdiera la humildad. A mi tío Rafa, aunque nunca llegué a conocerte, siempre he sentido que nos une algo especial. Por último, quisiera agradecer como última persona a mi tío Quique. Aunque lamentablemente ya no estás entre nosotros, quisiera decirte que siempre has sido un referente en mi vida. Aún recuerdo cómo mis padres me contaban lo buen estudiante y trabajador que eras, cosa que me inspiraba a esforzarme cada día más y más para ser como tú. Siempre me sentí muy apoyado por ti, y sinceramente, me hubiera encantado poder celebrar esta etapa de mi vida contigo. Espero que, estés donde estés, puedas leer estas palabras y sentirte orgulloso de mí, tal y como yo siempre lo estuve de ti.

INDEX

FIGURE INDEX

TABLE INDEX

ABBREVIATIONS

Abbreviation	Meaning
Ac	Acetylated
ALS	Amyotrophic Lateral Sclerosis
ALS2	Alsin Rho Guanine Nucleotide Exchange Factor
ALSFRS-R	ALS Functional Rating Scale-Revised
AMPK	AMP-activated Protein Kinase
ANG	Angiogenin
ANOVA	Analysis of Variance
ANT	Adenine Nucleotide Translocator
APS	Ammonium Persulfate
ARE	Antioxidant Responsive Element
AR	Autosomal Recessive
ATXN2	Ataxin 2
ATP	Adenosine Triphosphate
BBB	Blood-Brain Barrier
BCA	Bicinchoninic Acid
BDNF	Brain-Derived Neurotrophic Factor
Bcl-2	B-cell Lymphoma 2
Bax	Bcl-2-associated X Protein
Bak	Bcl-2 Homologous Antagonist Killer
CAT	Catalase
C1q	Complement Component 1q
CCNF	Cyclin F
C/EBP	CCAAT/Enhancer-Binding Protein
CHCHD10	Coiled-Coil-Helix-Coiled-Coil-Helix Domain Containing 10
CHMP2B	Charged Multivesicular Body Protein 2B
CHOP	C/EBP Homologous Protein
cAMP	Cyclic Adenosine Monophosphate
cGMP	Cyclic Guanosine Monophosphate
CNTF	Ciliary Neurotrophic Factor
COX-2	Cyclooxygenase-2
CNS	Central Nervous System
CREB	cAMP Response Element-Binding Protein
CSF	Cerebrospinal Fluid
Cu/ZnSOD	Copper-Zinc Superoxide Dismutase

CyPD	Cyclophilin D
DAPI	4',6-diamidino-2-phenylindole
DCTN1	Dynactin Subunit 1
DHE	Dihydroethidium
DMSO	Dimethyl Sulfoxide
DNA	Deoxyribonucleic Acid
EGTA	Ethylene Glycol Tetraacetic Acid
ELISA	Enzyme-Linked Immunosorbent Assay
EMG	Electromyography
ER	Endoplasmic Reticulum
ETC	Electron Transport Chain
FDA	Food and Drug Administration
FGF	Fibroblast Growth Factor
FALS	Familial Amyotrophic Lateral Sclerosis
FOXO1	Forkhead Box Protein O1
FTD	Frontotemporal Dementia
FUS	Fused in Sarcoma
GADD34	Growth Arrest and DNA Damage-Inducible Protein 34
GAPDH	Glyceraldehyde-3-Phosphate Dehydrogenase
G-CSF	Granulocyte-Colony Stimulating Factor
GDNF	Glial Cell Line-Derived Neurotrophic Factor
GFAP	Glial Fibrillary Acidic Protein
GLN	Glutamine
GM-CSF	Granulocyte-Macrophage Colony-Stimulating Factor
GPX	Glutathione Peroxidase
GRN	Granulin
GSH	Reduced Glutathione
GSSG	Oxidized Glutathione
HBSS	Hank's Balanced Salt Solution
HE	Hematoxylin and Eosin
HEPES	4-(2-hydroxyethyl)-1-piperazineethanesulfonic acid
HGF	Hepatocyte Growth Factor
HLA-DR	Human Leukocyte Antigen – DR isotype

HNRNPA1	Heterogeneous Nuclear Ribonucleoprotein A1
HNRNPA2B1	Heterogeneous Nuclear Ribonucleoprotein A2/B1
HPLC	High-Performance Liquid Chromatography
HRP	Horseradish Peroxidase
Iba1	Ionized Calcium-Binding Adapter Molecule 1
IBU	Ibudilast
ICAM-1	Intercellular Adhesion Molecule 1
IFNγ	Interferon Gamma
IGF-1	Insulin-Like Growth Factor 1
Ikβα	Inhibitor of kappa B alpha
IL-1β	Interleukin-1 Beta
IL-2	Interleukin-2
IL-6	Interleukin-6
IL-10	Interleukin-10
IL-12	Interleukin-12
IL-15	Interleukin-15
IL-17	Interleukin-17
IL-18	Interleukin-18
IL-1α	Interleukin-1 Alpha
IRAK1	Interleukin-1 Receptor-Associated Kinase 1
IRAK3	Interleukin-1 Receptor-Associated Kinase 3
LDH	Lactate Dehydrogenase
LMN	Lower Motor Neurons
L-NAME	L-NG-nitro arginine methyl ester
LPS	Lipopolysaccharide
MAPK	Mitogen-Activated Protein Kinase
MAPT	Microtubule-Associated Protein Tau
MCP-1	Monocyte Chemoattractant Protein-1
MIF	Macrophage Migration Inhibitory Factor
miRNA	MicroRNA
MIP-1α	Macrophage Inflammatory Protein 1 Alpha
MMP	Mitochondrial Membrane Potential
MN	Motor Neuron
mRNA	Messenger RNA
mTORC1	Mechanistic Target of Rapamycin Complex 1

NAD+	Nicotinamide Adenine Dinucleotide
NADH	Nicotinamide Adenine Dinucleotide (Reduced Form)
NADPH	Nicotinamide Adenine Dinucleotide Phosphate (Reduced Form)
NEFH	Neurofilament Heavy
NEK1	NIMA-Related Kinase 1
NF-κB	Nuclear Factor kappa-light-chain-enhancer of activated B cells
NLRP3	NOD-, LRR- and Pyrin Domain-Containing Protein 3
NMDA	N-Methyl-D-Aspartate
NOx	Nitrite/Nitrate
NR	Nicotinamide Riboside
Nrf2	Nuclear Factor Erythroid 2-Related Factor 2
OLE	Oleuropein
OPTN	Optineurin
PARP1	Poly [ADP-Ribose] Polymerase 1
PBS	Phosphate Buffered Saline
PDE	Phosphodiesterase
PFN1	Profilin 1
PGC-1α	Peroxisome Proliferator-Activated Receptor Gamma Coactivator 1-alpha
PKA	Protein Kinase A
PMSF	Phenylmethylsulfonyl Fluoride
PrPC	Cellular Prion Protein
PrPres	Protease-Resistant Prion Protein
PS	Physiological Saline
PT	Pterostilbene
RIPA	Radioimmunoprecipitation Assay
RNS	Reactive Nitrogen Species
ROS	Reactive Oxygen Species
SALS	Sporadic Amyotrophic Lateral Sclerosis
SD	Standard Deviation
SETX	Senataxin
SIRT	Sirtuin
SIRT1	Sirtuin 1

SIRT3	Sirtuin 3
SIRT6	Sirtuin 6
SOD1	Superoxide Dismutase 1
SOD2	Superoxide Dismutase 2
SPF	Specific Pathogen-Free
SPG11	Spastic Paraplegia 11
SPSS	Statistical Package for the Social Sciences
SQSTM1	Sequestosome 1
SSA	Sulfosalicylic Acid
STMN2	Stathmin-2
TBK1	TANK-Binding Kinase 1
TDP-43	TAR DNA-Binding Protein 43
TFEB	Transcription Factor EB
TIA1	T-Cell Intracellular Antigen 1
TLR4	Toll-Like Receptor 4
TNF-α	Tumor Necrosis Factor-alpha
TPMP	Triphenylmethylphosphonium
Tris	Tris(hydroxymethyl)aminomethane
Treg	Regulatory T Cells
TXN	Thioredoxin
UMN	Upper Motor Neurons
VDAC-1	Voltage-Dependent Anion Channel 1
VCP	Valosin-Containing Protein
Xct	Cystine/Glutamate Transporter

ABSTRACT

1. INTRODUCTION

1.1. Amyotrophic Lateral Sclerosis

Amyotrophic lateral sclerosis (ALS) is a neurodegenerative disorder that affects motor neurons (MNs) controlling voluntary muscle movement and breathing. The disease can begin with abnormalities in either upper (UMN) or lower (LMN) motor neurons. UMN disease leads to stiffness and spasticity, while LMN disease causes weakness, muscle atrophy, and fasciculations. A definitive diagnosis of ALS requires the degeneration of both neuron types. ALS progresses rapidly, causing severe disability and ultimately leading to death, typically from respiratory failure within 2-5 years of diagnosis. Only about 30% of patients survive more than five years post-diagnosis, and 10-20% may live beyond ten years. The progression rate and specific symptoms of ALS can vary widely among patients. An example of exceptional longevity with ALS is Stephen Hawking, who lived for several decades after diagnosis. ALS, also known as Charcot's disease, was first diagnosed by Jean-Martin Charcot in 1869. Charcot introduced the term "amyotrophic lateral sclerosis" in 1874, referring to the loss of nerve fibers and subsequent glial scar formation in the spinal cord, which causes muscle atrophy due to lack of nerve stimulation.

1.2. Epidemiology

ALS is considered a rare disease with a global incidence rate of 2-3 cases per 100,000 people, making it the most common form of motor neuron disease. Aging is a significant risk factor, with an average onset age above 60 years and peak incidence in individuals aged 70-79 years. The incidence and prevalence of ALS are slightly higher in men than women, with men typically experiencing earlier onset but longer survival. Factors such as environmental, genetic, and hormonal influences contribute to these gender differences. In Spain, the incidence is about 1.4 new cases per 100,000 inhabitants per year, and the prevalence is slightly higher than global rates. The incidence of ALS varies by ethnicity and geographic location, with lower rates in Hispanic, African, and some Asian populations compared to Caucasians. Eastern Europe reports the highest incidence and prevalence rates, while South Asia has the lowest. The Western Asia region records the highest average survival rates.

1.3. Etiology

The cause of ALS is largely unknown, but genetic, environmental, and lifestyle factors are linked to increased risk. Familial ALS (FALS) occurs when two or more family members have ALS, accounting for 5-10% of cases. Most ALS cases (90-95%) are sporadic (SALS) with no family history. Since the discovery of

SOD1 mutations in 1993, over 40 genes have been linked to ALS, with C9ORF72, SOD1, TARDBP, and FUS responsible for most FALS cases and some SALS cases. The C9orf72 mutation is the most common, associated with 40% of FALS and 7% of SALS cases. The SOD1 gene on chromosome 21q22.11 is linked to 20-25% of FALS cases, involving oxidative stress and protein aggregation. Mutations in TARDBP and FUS genes, which are involved in RNA processing, are linked to 5% and 1% of ALS cases, respectively. Other ALS-associated mutations are less frequent and/or occur in specific geographic locations.

Age and family history are well-established ALS risk factors. Genetic mutations alone do not explain the onset and progression of ALS, suggesting that environmental and metabolic factors also play roles. Exposure to heavy metals, pesticides, electromagnetic fields, solvents, and certain toxins has been linked to ALS risk, primarily through oxidative stress mechanisms. Physical activity, head injuries, and physical trauma are documented ALS risk factors, with higher incidence observed in football players and military veterans. Weight loss is a strong predictor of shortened survival in ALS patients, while increased body mass in earlier life may lower ALS incidence. ALS likely results from interactions between genetic, aging, and environmental factors.

1.4. Symptomatology, diagnosis, and treatments

ALS affects both UMN and LMN, with the sensory system, cognitive functions, eye movements, and anal and bladder sphincters typically remaining intact. ALS is most commonly diagnosed between ages 50-75 for SALS and 40-60 for FALS. Juvenile ALS (JALS) occurs in individuals under 25, often linked to specific genetic variants. Clinical manifestations depend on whether UMN or LMN are initially affected. Spinal involvement of LMN is most common, causing asymmetric strength loss, fasciculations, cramps, hypotonia, muscle weakness, areflexia, atrophy, and paralysis. Bulbar involvement, affecting speech and swallowing, is less common but has a worse prognosis. Primary ALS, affecting only UMN, causes loss of dexterity, stiffness, spasticity, clumsiness, and hyperreflexia. Damage to LMN leads to paralysis, paresis, loss of reflexes, muscle tone, and spontaneous twitches (fibrillations and fasciculations). Pseudo-bulbar syndrome causes uncontrollable emotional expression. Frontotemporal dementia (FTD) is linked to ALS through shared genetic mutations, with 3-20% of ALS patients developing FTD.

Diagnosing ALS can be challenging in its early stages due to its clinical diversity and lack of specific biomarkers. The El Escorial criteria, established in 1990 and revised in 2000, focus on UMN and LMN impairment in four body regions and progressive symptom spreading. Patients are classified into categories of

diagnostic certainty: definite, probable, probable with laboratory support, and possible ALS. The Awaji criteria introduced in 2008 incorporated electrophysiological tests to increase diagnostic sensitivity. Despite improvements, these criteria can be complex and misinterpreted, and they do not predict disease progression. The Gold Coast criteria aim to streamline diagnosis but are not widely used yet. Accurate and rapid diagnosis is crucial for clinical management, entry into trials, and early life planning. Tests supporting diagnosis include electrodiagnostic studies, MRI, cerebrospinal fluid analysis, and genetic studies.

Currently, there is no cure for ALS. Approved medications include Riluzole, Edaravone, Qalsody, and Relyvrio, which can slow disease progression and extend life expectancy. Riluzole, the first drug approved for ALS, reduces glutamate release and inactivates voltage-dependent sodium channels, offering modest survival benefits. Edaravone acts as an antioxidant, neutralizing free radicals and slowing disease progression, particularly in early stages. Relyvrio combines sodium phenylbutyrate and taurursodiol to reduce ER stress and protect mitochondrial function, showing positive effects on function and survival. These medications, though beneficial, are most effective when administered early in the disease course.

In addition to specific pharmacological treatments, managing ALS symptoms and providing supportive therapies are crucial. Symptom relief involves medications for spasticity, sialorrhea, pain, pseudobulbar symptoms, fasciculations, cramps, edema, and constipation. Supportive care includes respiratory support, nutritional assistance, physiotherapy, occupational therapy, speech therapy, and psychological support. This multidisciplinary approach aims to improve patients' quality of life and manage symptoms as the disease progresses.

1.5. Pathophysiology

The pathophysiological mechanisms underlying ALS involve several interconnected processes:

1.5.1. Glutamate-Mediated Excitotoxicity

Glutamate is the main excitatory neurotransmitter in the central nervous system. Elevated glutamate levels can cause TDP-43 translocation to the cytoplasm, leading to ALS. Reduced expression of the EAAT2 transporter in astrocytes, which clears glutamate, is observed in ALS patients and animal models, resulting in excitotoxicity, oxidative stress, and neuronal death.

1.5.2. Axonal Transport Damage

Axonal transport of cell components is crucial for MN function. In ALS, axonal transport is impaired due to mitochondrial

dysfunction, abnormal protein aggregates, and mutations affecting transport proteins. This leads to axonal retraction, denervation, and neuronal death.

1.5.3. Neurotrophic Factor Deficiency

Neurotrophic factors are vital for neuron health. Reduced levels of these factors are seen in ALS patients and models, contributing to MN degeneration. Although supplementation in clinical trials has not been effective, these factors show protective effects in preclinical studies.

1.5.4. Protein Aggregation

ALS is characterized by the accumulation of misfolded proteins in neurons and glia. Mutations in genes like SOD1, C9orf72, FUS, and TDP-43 promote protein aggregation, leading to cytotoxic effects and neuronal death.

1.5.5. Endoplasmic Reticulum Dysfunction

Endoplasmic reticulum (ER) stress plays a critical role in ALS progression. The ER's role in protein folding and calcium signaling is disrupted in ALS, leading to oxidative stress, impaired protein degradation, and neuronal death.

1.5.6. Alterations in Autophagy

Autophagy, the process of clearing protein aggregates, is impaired in ALS due to mutations in genes like SOD1, C9orf72,

TDP-43, and others. This leads to the accumulation of toxic aggregates and neuronal death.

1.5.7. Prion Behavior of Proteins

Proteins involved in ALS, such as SOD1 and TDP-43, can exhibit prion-like behavior, spreading from cell to cell and promoting neurodegeneration.

1.5.8. Neuroinflammation

ALS is characterized by reactive astrocytes, microglia, and infiltration of immune cells in the CNS, leading to chronic inflammation and neuronal death. Early-stage immune response may be protective, but as the disease progresses, it becomes neurotoxic.

1.5.9. Oxidative Stress

Oxidative stress, resulting from an imbalance between reactive oxygen species (ROS) production and detoxification, is a key factor in ALS. MNs are particularly vulnerable due to their high metabolic activity and limited regenerative capacity.

1.5.10. Mitochondrial Dysfunction

Mitochondrial dysfunction is a central aspect of ALS, affecting energy production, calcium homeostasis, and ROS generation. MNs are highly sensitive to mitochondrial damage, leading to neurodegeneration.

1.6. Fundamentals of Our Therapeutic Proposal

Considering the complex mechanisms involved in ALS, a combined therapeutic approach targeting oxidative stress, mitochondrial dysfunction, and inflammation holds promise. Pterostilbene (PT), a stilbenoid found in blueberries, has shown potential in enhancing antioxidant defenses and crossing the blood-brain barrier. Nicotinamide riboside (NR), a precursor to NAD^+, supports energy metabolism and mitochondrial function. In preclinical models, the combination of NR and PT has demonstrated protective effects against oxidative stress, mitochondrial dysfunction, and neurodegeneration, significantly prolonging survival in ALS models.

Adding an anti-inflammatory agent like Ibudilast (IBU) could further enhance the therapeutic efficacy. IBU is a nonselective phosphodiesterase (PDE) inhibitor, particularly effective against PDE4, and has shown promise in reducing neuroinflammation and promoting neurotrophic factors. It modulates immune responses, reduces pro-inflammatory cytokines, and supports mitochondrial function. Clinical trials have demonstrated its potential in neurodegenerative diseases, including ALS.

PDE4 inhibitors, such as rolipram, roflumilast, and apremilast, have shown neuroprotective effects in various models of neurodegenerative diseases by regulating cAMP levels and modulating immune and inflammatory responses. However,

clinical trials have faced challenges due to significant side effects, including gastrointestinal disturbances and psychiatric issues. Despite these challenges, IBU stands out due to its broader anti-inflammatory effects and better safety profile.

In summary, combining PT and NR with IBU could offer a comprehensive approach to managing ALS, addressing multiple pathological mechanisms and potentially improving patient outcomes. This strategy is supported by preclinical evidence and ongoing clinical trials, highlighting the importance of a multifaceted approach in treating this complex disease.

2. HYPOTHESIS AND OBJECTIVES

ALS is a multifaceted neurodegenerative disorder characterized by intricate cellular and signaling network interactions. Our group has demonstrated that PT and NR, as a combined therapy, protect MNs against oxidative stress, slow neurodegeneration, and significantly prolong the survival of $SOD1^{G93A}$ mice. Neuroinflammation (involving reactive astrocytes and microglia, and increased levels of inflammatory mediators) enhances oxidative/nitrosative stress and is involved in ALS progression. Thus, adding an anti-inflammatory agent could help improve the efficacy of PT and NR.

Previous research indicates that PDE inhibitors can reduce glial cell activation, suggesting a potential strategy to mitigate

neuroinflammation. In fact, these inhibitors are being considered as a possible anti-inflammatory strategy for ALS and other neurodegenerative diseases and can be a good option to increase the efficacy of the NR+PT treatment.

Here we propose to test if IBU synergizes with NR and PT treatment for the following reasons:

a) PDE4 is essential for the activation of native immunity and the inflammatory response in the CNS.

b) IBU inhibits the release of pro-inflammatory cytokines, NO and $O_2^{\bullet-}$ production, and has the ability to cross the BBB exerting neuroprotective effects.

c) IBU facilitates the clearance of TDP-43 and SOD1 aggregates in ALS models.

d) As presented in the results (section 4.1), the efficacy of other PDE inhibitors (rolipram, roflumilast, and apremilast) was limited by their side effects in the ALS animal models used in this thesis.

The **general objective** of this doctoral thesis is to investigate whether IBU could enhance the protective effects of the NR and PT in two murine models of ALS (SOD^{1G93A} and FUS^{R521C}), as well as to explore the molecular mechanisms underlying the potential therapeutic efficacy.

Specific Objectives

1. Evaluate the toxicity of PDE4 inhibitors to select the safest therapeutic option.
2. Investigate the effect of NR+PT+IBU on the survival and neuromotor functions in murine models of ALS.
3. Conduct histopathological studies of the spinal cord to obtain direct morphological evidence of the effects of therapy.
4. Evaluate cell death, autophagy/mitophagy, SIRT activities, enzymes, and Nrf2-dependent redox metabolites in MNs isolated from control and treated (NR+PT+IBU) mice to investigate how the treatment affects oxidative/nitrosative stress markers and mitochondrial dysfunction associated with ALS progression.

3. MATERIAL AND METHODS

We utilized two transgenic mouse models, $SOD1^{G93A}$ and FUS^{R521C}, to replicate key features of ALS, with B6SJLF1/J wild-type mice serving as controls. The mice, housed under specific pathogen-free conditions, began experiments at four weeks old. Treatments included PT in feed, NR orally, and IBU in physiological saline, with L-NAME administered intraperitoneally from the 18th week. Neuromotor functionality was assessed using neurological scores and the rotarod test. Pathological

analysis involved perfusing, fixing, embedding, and sectioning spinal cords, with immunostaining for neurons, microglia, and astroglia. Cytokine levels in CSF were quantified using xMAP technology. MNs, astrocytes, and microglia were isolated, cultured, and characterized. Reactive oxygen species (ROS) and NO production were measured, and GSH/GSSG levels were determined. NO and $^{-}$OONO solutions were prepared and characterized. ATP levels, caspase 3 activity, mitochondrial membrane potential, and oxygen consumption were measured, along with mitophagy analysis using specific dyes. Enzyme activities for SOD, CAT, GPX, and NOS were assessed, and expression was analyzed by RT-PCR and western blotting. Statistical analyses were performed using Kaplan-Meier curves, analysis of variance (ANOVA), and t-tests to ensure sufficient significance of the results

4. RESULTS

4.1. PDE Inhibitor Tolerance and Selection

Previous research indicates that PDE inhibitors can reduce glial cell activation, suggesting a potential strategy to mitigate inflammation. Thus, we considered assaying one of them to increase the efficacy of the NR+PT treatment. To select the most suitable option, we evaluated the tolerance of different and currently used PDE4 inhibitors. We tested rolipram, roflumilast,

apremilast, and IBU. Within two weeks of treatment, mice treated with rolipram, roflumilast, or apremilast developed significant side effects, including gastrointestinal disturbances, muscle spasms, and signs of pain. Considering these adverse effects, IBU emerged as the safest and most viable therapeutic option for further studies.

4.2. NR, PT, and IBU Delay ALS-Related Loss of Neuromotor Functions

Neuromotor functions were assessed in $SOD1^{G93A}$ and FUS^{R521C} mice using a neurological scoring system and the rotarod test. The onset of symptomatology appeared around postnatal week 12 in $SOD1^{G93A}$ mice and week 7 in FUS^{R521C} mice. Both IBU alone and the NR+PT treatment delayed the onset of neurological symptoms compared to control groups. However, this delay was most notable in mice treated with the triple combination (NR+PT+IBU), highlighting the synergistic potential of the combined therapy.

4.3. NR, PT, and IBU Extend Survival in Murine ALS Models

Survival studies using our treatments showed that either NR+PT or IBU alone increased survival rates compared to controls. However, the triple therapy (NR+PT+IBU) significantly enhanced survival rates more than either treatment alone. These findings

suggest that NR+PT+IBU could offer substantial benefits in terms of extending life and reducing disease progression in ALS patients.

4.4. NR, PT, and IBU Decrease Microgliosis, Astrogliosis, and MN Degeneration

ALS progression is associated with microgliosis and astrogliosis in the anterior horns of the medulla. Immunohistopathological analysis showed that treatments with NR+PT or the combination of NR+PT+IBU reduced both types of gliosis. However, only the triple combination was significantly more effective in reducing microgliosis. The number of MN cell bodies was better preserved in both mouse models treated with NR+PT or NR+PT+IBU. The histological assessment showed a significant reduction of MNs in control mice, while MNs appeared better preserved in treated mice.

4.5. NR, PT, and IBU Reduce Pro-inflammatory Cytokine Levels

Pro-inflammatory cytokines in CSF samples were measured, showing that NR+PT treatment significantly reduced IFN-γ and IL-6 levels, whereas IBU alone was effective in decreasing TNF-α levels. Comparing the groups treated with NR+PT and those treated with NR+PT+IBU, only a significant difference in TNF-α

levels was observed. These data indicate that, in both ALS models, IBU specifically targets and reduces TNF-α levels.

4.6. Cytokine Induction of Oxidative/Nitrosative Stress

Pro-inflammatory cytokines significantly increased NO and H_2O_2 generation by MNs, astrocytes, microglia, and endothelial cells isolated from ALS mice. This effect was particularly pronounced when all three cytokines were incubated together. The combination of NR, PT, and IBU effectively reduced these stress markers, highlighting its potential to protect MNs from the harmful effects of oxidative and nitrosative stress in ALS.

4.7. NR, PT, and/or IBU Protect MNs Against Oxidative/Nitrosative Stress

Treatment with NR and PT significantly reduced cytokine-induced H_2O_2 and NO production in all cell types, except for H_2O_2 in FUS^{R521C} astrocytes and NO in SOD^{1G93A} astrocytes. IBU alone decreased H_2O_2 production in microglia and endothelial cells. The NR+PT+IBU treatment further reduced H_2O_2 and NO production in microglia and endothelial cells compared with NR+PT treatment, demonstrating significant protection against oxidative/nitrosative stress.

4.8. Metal Presence Enhances RNS/ROS-Induced MN Cytotoxicity

H_2O_2 or NO alone caused minimal cytotoxicity, but their combination resulted in significant MN cytotoxicity due to the formation of potent oxidants like peroxynitrite ($^-$OONO). The Fenton reaction, involving transition metal ions, played a pivotal role in enhancing nitrosative stress. Chelation of metal ions decreased cytotoxicity, while the addition of iron enhanced it. These findings suggest a trace metal-catalyzed process within the mechanism of MN damage.

4.9. The Combined Treatment Attenuates Oxidative/Nitrosative Stress

Microglia and endothelial cells isolated from ALS mice generated higher levels of nitrite (NO_2^-) and $^-$OONO compared to their counterparts from WT mice. The treatment with NR+PT and NR+PT+IBU decreased these levels, with the triple combination being more effective. This demonstrates the ability of the treatment to prevent the generation of highly damaging reactive species, breaking the cycle of oxidative and nitrosative damage in ALS.

4.10. Oxidative and Nitrosative Stress Trigger MN Death

Oxidative/nitrosative stress-induced MN death was mainly apoptotic. The combination of H_2O_2 and NO significantly increased MN cytotoxicity, correlating with molecular alterations related to the activation of apoptosis. Treatments enhanced the clearance of damaged mitochondria, suggesting that protective treatments improve mitophagy and overall cellular health.

4.11. NOS Inhibition Increases Survival in ALS Mice

L-NAME, a NOS inhibitor, reduced nitrosative stress biomarkers and NOx production by MNs, astrocytes, microglia, and endothelial cells. This treatment significantly increased the survival of $SOD1^{G93A}$ and FUS^{R521C} mice, confirming the role of nitrosative stress in ALS progression and supporting the potential of NOS inhibition as a therapeutic strategy.

4.12. NR+PT+IBU Reduces the Cytoplasmic Accumulation of Mutant FUS Protein in MN

The combined treatment decreased the accumulation of mutant FUS protein within MNs but did not alter the intracellular levels of the SOD1 mutant. This suggests that the treatment affects the pathophysiological consequences of the mutation and improves MN function and survival in ALS mice.

5. DISCUSSION

Increasing evidence suggests that neuroinflammation and oxidative stress contribute to neurodegeneration in ALS. As the disease progresses, microglia and astrocytes in the anterior horn of the medulla undergo a phenotypic transition, proliferate, and secrete pro-inflammatory cytokines. Neuroinflammation is associated with the release of cytokines that represent potential apoptosis (i.e., TNF-α, IFN-γ, IL-1β), whereas TNF-α also interferes with the normal electron flow in the mitochondria and increases the generation of ROS. Pro-inflammatory cytokines such as GM-CSF, IL-2, IL-6, IL-15, IL-17, MCP-1, MIP-1α, TNF-α, and VEGF are typically elevated in the CSF of patients and murine models of ALS. Reactive astrocytes in ALS express inflammatory markers, including COX-2, inducible NOS, and neuronal NOS, and inhibitory molecules that block regrowth of a damaged axon. Glial and infiltrated immune cells are major producers of ROS and RNS in pathological conditions of the CNS, and chronic inflammation enhances oxidative stress linked to MN damage.

NAD+ is a vital coenzyme involved in various cellular processes. It functions in redox reactions, serves as a donor of ADP-ribose for ADP-ribosylation reactions, acts as a precursor of cyclic ADP-ribose, and functions as a substrate for SIRTs, which use this cofactor to deacetylate proteins. SIRTs, particularly SIRT1 and SIRT3, regulate mitochondrial biogenesis and function. Sirtuins

also help mitigate oxidative stress by deacetylating and activating antioxidant enzymes. PT can cross the BBB, has intrinsic antioxidant capacity, and has been shown to increase nuclear Nrf2, thus promoting the antioxidant defenses in the CNS. PT mitigates inflammation by decreasing inflammatory mediators, i.e., TNF-α, IL1-β, and IL-6, which may further support its therapeutic potential in ALS treatment.

The efficacy of NR+PT as a potential treatment for ALS is evidenced by several studies performed by our group. NR and PT treatment helps maintain neuromotor functions according to a placebo-controlled double-blind human pilot study in ALS patients (NCT03489200). In this study, NR+PT treatment significantly slowed the progression of ALS as measured by ALSFRS-R score, forced vital capacity, and Medical Research Council grading scale when compared to the placebo group.

My master's thesis results show that NR and PT enhance Nrf2-dependent antioxidant defenses and increase SIRT1 and SIRT3 activity in MNs from $SOD1^{G93A}$ mice. PT promotes SIRT1 overexpression and the nuclear translocation of Nrf2, while NR provides NAD^+ for PARP-1 and SIRT-catalyzed reactions. The NR+PT treatment reduced oxidative stress, potentially decreasing the release of proapoptotic signals from mitochondria through a complex mechanism involving factors, such as Ca^{2+} accumulation, mitochondrial DNA damage, changes

in mitochondrial membrane potential, and alterations in the proapoptotic/antiapoptotic protein balance. The combined treatment slowed the loss of neuromotor functions and significantly prolonged the survival of SOD1^{G93A} mice. PT+NR treatment is now being evaluated in phase II clinical trial (NCT04562831, The NO-ALS Study).

ALS is a multifaceted neurodegenerative disorder, and single-agent therapies have failed to increase survival. Therefore, we consider that a combined strategy is a better therapeutic option, and in our case, the addition of an anti-inflammatory agent has been found to further increase the efficacy of NR and PT. As many anti-inflammatory agents like celecoxib or corticosteroids have failed to demonstrate any survival advantage, we looked at PDE inhibitors for their capacity to cross the BBB and reduce glial cell activation. Rolipram, roflumilast, and apremilast had significant side effects, including diarrhea, muscle spasms, and pain, which necessitated early termination of treatment. In contrast, IBU did not cause significant side effects, making it the safest and most viable therapeutic option. Here we show that treatment with NR+PT+IBU, compared to NR+PT alone, can further delay the progression of neuromotor damage and increase survival in two ALS murine models. Notably, the inclusion of IBU in the combined NR and PT treatment increases survival by 2 more weeks in SOD1^{G93A} mice and by 11 weeks in

FUS^{R521C} mice, compared to the NR+PT treatment alone. These effects were associated with reduced neuroinflammation and decreased levels of various pro-inflammatory cytokines in CSF.

High O_2 consumption is needed to produce ATP to maintain the neuronal membrane potential through Na^+ and K^+ gradients. The mitochondrial respiratory chain, responsible for most oxygen consumption, can leak electrons to reduce molecular O_2 and form $O_2^{\bullet-}$. Although mechanisms exist to eliminate $O_2^{\bullet-}$ from the cell via enzymatic catalysis by SOD enzymes, the kinetically favorable reaction of $O_2^{\bullet-}$ with NO, facilitated by metals like iron, will ultimately lead to $^{-}OONO$ formation before $O_2^{\bullet-}$ can be eliminated. NO is produced by NOS, which are expressed in different isoforms. For example, endothelial cells produce NO through eNOS, neurons through nNOS, and immune cells such as macrophages and microglia through iNOS. Additionally, other cell types, such as astrocytes, can also produce NO using these isoforms. Free radicals are important at physiological concentrations as they can act as cellular signalling molecules, but during oxidative stress, they are produced at high levels and can damage lipids, proteins, and nucleic acids. As MNs are rich in functional lipids, they are especially susceptible to oxidative stress damage. Microglia activated by lipopolysaccharide (LPS) or IgG immune complexes, induced injury in primary cultures of MNs. This injury was prevented by a microglia-iNOS inhibitor, as

well as by CAT or GSH. On the other hand, the cultured embryonic MNs expressing p75(NTR) were not vulnerable to nerve growth factor unless exposed to an exogenous influx of NO. We found that different cytokines (TNF-α, IFN-γ, and IL-1β) increased H_2O_2 and NO generation by MNs, astrocytes, microglia, and endothelial cells isolated from ALS mice. PT alone has been shown to reduce NO production in microglia stimulated by LPS, without directly scavenging NO radicals. Further studies revealed that PT might inhibit LPS-induced NO and TNF-α production in microglia by blocking IkB-α phosphorylation and degradation, presumably preventing NF-κB activation associated with IKβα phosphorylation. The binding of LPS to toll-like receptor 4 (TLR4) of microglia can trigger the activation of downstream signaling pathways such as NF-κB and mitogen-activated protein kinases (MAPKs), subsequently inducing the expression of inflammation-related genes such as COX-2 and various pro-inflammatory cytokines. Taken together, these results suggest that NO plays an important role in the pathophysiological cascade of ALS.

In this doctoral thesis, I demonstrate that the combined treatments, either NR+PT or NR+PT+IBU, cause a significant decrease in NO production in all analyzed cells. IBU significantly reduced TNF-α levels in the CSF and H_2O_2 generation by microglia and endothelial cells. Unexpectedly, exposing MNs to

pathophysiological concentrations of H_2O_2 or NO individually resulted in minimal cytotoxicity. However, the cytotoxicity to MNs was notably increased when H_2O_2 and NO were combined. This can be attributed to the formation of potent oxidants, i.e., $^{\bullet}OH$ and $^{-}OONO$ radicals, through a trace metal-dependent process.

These results suggest that oxidative and nitrosative stress, triggered by pro-inflammatory cytokines, significantly harms MNs, and that different cells in the anterior horn microenvironment play a role in this process, i.e., microglia, astrocytes, endothelial cells, and likely infiltrating immune cells. Importantly, microglia exhibit different phenotypes throughout ALS progression, transitioning from a vigilant state in the early phases to activated M1 and M2 states in advanced stages, characterized by harmful and protective gene expression, respectively. Although our methodology to isolate microglial cells does not differentiate between the different phenotypes, we have evidence that microglia isolated at week 18 of progression release pro-inflammatory cytokines.

The concentrations of H_2O_2 and NO used in the experiments displayed are derived from the amounts generated by different cells present in the anterior horns. Therefore, these concentrations may approach the pathophysiological maximum levels. However, complex tissue architecture, the flow of blood,

lymph, and CSF, along with various regulatory molecules, serve as significant limiting factors that are not present in the in vitro experimental setting. Therefore, it is plausible to expect that, in vivo, MNs are exposed to lower levels of H_2O_2 and NO. Moreover, given that ALS often progresses in sporadic flares, the exposure of MNs to toxic levels of ROS and RNS may not be constant. These observations suggest a scenario more consistent with the gradual deterioration experienced by patients. Additionally, the cellular and neuroanatomical specificity of the ALS-related degeneration is often accompanied by aberrant misfolding, aggregation, and deposition of specific proteins, such as SOD1, TDP-43, or FUS. This is important (and coherent with our findings) because both ROS and RNS can favor abnormal protein aggregation.

Several studies show the importance of metals in the damage induced by oxidative stress. Free iron can react with H_2O_2 via the Fenton reaction, a primary cause of lipid peroxidation and a mechanism that has been implicated in several CNS injuries/disorders, such as, stroke, epilepsy, Friedreich's ataxia, which is also active in ALS. The SOD mutation is involved in oxidative injury through increased generation of hydroxyl radicals, increased peroxidase activity, or increased nitration of tyrosine by $^{-}$OONO. The ALS mutant SODs have reduced affinity for zinc. Furthermore, neurofilament subunits bind zinc with

sufficient affinity to remove zinc from SOD. The increased loss of zinc from SOD will diminish the scavenging of superoxide and increase the catalysis of tyrosine nitration by $^{-}$OONO. Singh et al. were first to suggest that the loss of zinc from SOD may enhance $^{-}$OONO formation and MN death in ALS and also evidenced the importance of the Fenton reactions in the promotion of MN toxicity.

Previous studies have identified iron deposition in the motor cortex as potential pathogenesis of ALS. On the cellular and molecular level, excessive iron deposition may lead to oxidative stress-associated neural apoptosis. Moreover, a recent meta-analysis reported unusual changes in iron status linked to ALS. According to this study, serum ferritin levels were higher and transferrin levels were lower in ALS patients, compared to healthy controls. The ability of transferrin to decrease free iron levels in circulation suggests that this protein may have a protective effect on neurons in ALS progression. The conclusions of the study suggest possible iron metabolism abnormalities in ALS patients, thus supporting the importance of iron in the oxidative stress toxicity on MNs shown in this work. Therefore, controlling metal serum levels, as well as their dietary or accidental intake, could be important for ALS patients.

IBU, an anti-inflammatory drug initially developed to treat asthma, is a cyclic nucleotide PDE inhibitor that acts primarily by

increasing cAMP and cGMP levels, while decreasing pro-inflammatory factors such as TNF-α, MIF, and TLR-4. Pharmacologically, IBU significantly prolongs the time to first relapse and attenuates brain volume reduction in patients with relapsing-remitting and/or secondary progressive multiple sclerosis. Experimentally, IBU's neuroprotective effects are thought to stem from reduced neuroinflammation, apoptosis inhibition, or actions on the ubiquitin-proteasome pathway. The observed reduction of TNF-α levels in the CSF also indicates a potential decrease in the production of mitochondria-derived ROS. Hennet et al. and Goossens et al. first reported that TNF-α promotes ROS formation by mitochondria. Consequently, the reduction in TNF-α levels induced by IBU suggests a probable decrease in mitochondria-derived ROS, positioning IBU as a good candidate to complement the therapeutic benefits obtained by NR and PT. However, although treatment with NR and PT did not show any significant toxicity in the $SOD1^{G93A}$ model or in ALS patients, the use of IBU might encounter challenges due to potential side effects, including gastrointestinal and/or skin disorders. In this study, mouse models were treated with a daily single dose of 12 mg/kg, equivalent to approximately 0.97 mg/kg per day in humans. Therefore, a patient of approximately 70 kg body weight should take a daily oral dose of 67.9 mg, and IBU

shows an excellent safety profile at 60 mg/day based on the FDA-accepted conversion factor.

Our results show that the combination of NR, PT, and IBU enhances the protection of MNs in murine models of ALS. This combined treatment significantly attenuates the oxidative and nitrosative stress caused by pro-inflammatory cytokines, which is highly deleterious to MNs. Thus, the use of NR+PT+IBU or NOS inhibitors currently under investigation in clinical trials emerges as a promising strategy against ALS.

Additionally, this study provides strong evidence that potent oxidants, such as $^{\bullet}OH$ and $^{-}OONO$, which are primarily responsible for lipid, protein, and DNA oxidation, play a crucial role in the cascade of events leading to neuronal damage, involving catalysis by trace metals. This cascade of molecular events likely feed into itself, generating a vicious cycle of accumulated damage.

In conclusion, our results clearly suggest that a judicious combination of several drugs may be more beneficial than the use of individual drugs. The treatment with NR+PT+IBU has significantly improved motor functions and survival in FUS and SOD mice. We believe this treatment could offer substantial benefits to ALS patients. In fact, we are already working to promote the development of a clinical trial involving patients.

6. CONCLUSIONS

Based on the results presented in this doctoral thesis, we can draw the following conclusions:

1. IBU emerged as the most tolerable PDE4 inhibitor, demonstrating a lack of significant side effects in both $SOD1^{G93A}$ and FUS^{R521C} mouse models.
2. The NR+PT+IBU treatment significantly reduces pro-inflammatory cytokine levels (INF-γ, IL-1β, IL-2, IL-6, and GM-CSF) in CSF, with IBU being particularly effective in inhibiting the production of TNF-α. This supports the synergistic anti-inflammatory effect exerted by the combined treatment.
3. Treatment with NR+PT+IBU effectively prevents the production of H_2O_2 and NO in MNs, astrocytes, microglia, and endothelial cells, thereby enhancing the survival of MNs isolated from ALS transgenic mice.
4. The significant increase in survival with L-NAME treatment confirms the critical role of NO-mediated nitrosative stress in ALS progression.
5. Attenuating inflammation reduces oxidative/nitrosative stress, which is a key driver of neurodegeneration in ALS. This not only curbs further inflammation but also improves neuromotor function, effectively breaking the destructive cycle. These findings provide valuable insights into the mechanisms underlying MNs survival in ALS.

6. IBU enhances neuroprotection exerted by NR and PT in the context of ALS. This combined treatment significantly delays the loss of neuromotor functions and increases survival in both $SOD1^{G93A}$ and FUS^{R521C} mouse models.

RESUMEN

1. INTRODUCCIÓN

1.1. Esclerosis lateral amiotrófica

La esclerosis lateral amiotrófica (ELA) es una enfermedad neurodegenerativa severamente incapacitante e irremediablemente mortal. Afecta a las motoneuronas (MNs) responsables del control del movimiento voluntario y la respiración. Inicialmente, pueden verse afectadas MNs superiores (UMN) o inferiores (LMN), pero la confirmación diagnóstica requiere de la afectación de ambas. Tras el diagnóstico la esperanza media de vida no supera los 2-5 años, aunque en un pequeño porcentaje de casos, inferior al 10%, se han descrito supervivencias superiores a los 10 años.

1.2. Datos epidemiológicos

Desde un punto de vista epidemiológico, la ELA es considerada una enfermedad rara (tasa de incidencia global de 2-3 casos por cada 100,000 personas), pero es, tras el Alzheimer y el Parkinson, la tercera enfermedad neurodegenerativa más frecuente. Aunque se dan casos precoces, la edad media de inicio de la enfermedad se sitúa a partir de los 55 años, aumentando la incidencia en la población general hasta alcanzar un pico entre los 70-75 años, disminuyendo la incidencia a edades superiores. Debido al envejecimiento creciente de la población, se estima que en los próximos 20 años los casos de ELA aumentarán en un

69%. El riesgo de sufrir ELA es ligeramente superior en hombres que en mujeres (ratio 1.5:1.2), lo cual es atribuido a factores genéticos, hormonales y ambientales.

1.3. Etiopatogenia

A día de hoy, poco se sabe de la etiopatogenia, pero se reconocen factores de riesgo genéticos, ambientales y asociados a los hábitos de vida. En menos de un 10% de los casos, hay antecedentes familiares de la enfermedad en el momento del diagnóstico, considerándose entonces como ELA familiar. Más de 25 alteraciones genéticas han sido asociadas a casos de ELA familiar, siendo especialmente frecuentes las que afectan a los genes C9orf72, SOD1, TARDBP y FUS que están presentes en casi dos terceras partes de los casos de ELA familiar (40%, 20%, 5% y 5% respectivamente). En ausencia de antecedentes familiares (más del 90% de los casos), la enfermedad es considerada esporádica, sin que se conozcan actualmente causas directamente atribuibles. Entre los factores de riesgo descritos en la literatura destacan la edad, la actividad física, traumatismos craneales, la exposición a tóxicos agrícolas, a metales pesados, a radiaciones, a campos electromagnéticos y a agentes infecciosos, priones, entre otros. Más de un 10% de los casos de ELA esporádica presentan alguna de las mutaciones asociadas a la ELA familiar. Teniendo en cuenta la tardía

presentación de los síntomas y el posible patrón recesivo de la herencia, es factible que algunos casos de ELA familiar sean considerados erróneamente como de ELA esporádica. En cualquier caso, las manifestaciones clínicas de las formas familiares y esporádicas son idénticas, salvo por el hecho de que, en las primeras, la edad de inicio suele ser algo más temprana.

1.4. Sintomatología, diagnóstico y tratamiento

Al principio, los síntomas pueden ser leves e incluso pasar desapercibidos. Además, la sintomatología depende de que inicialmente se vean afectadas las UMN o las LMN. La implicación espinal de las LMN es la más frecuente, causando pérdida de fuerza asimétrica, fasciculaciones y calambres tempranos. La afectación bulbar, aunque menos común, tiene peor pronóstico y provoca dificultades en la deglución y control facial. La ELA primaria afecta a las UMN, resultando en pérdida de destreza, espasticidad y torpeza. La progresión de la enfermedad y los síntomas específicos varían significativamente entre los pacientes, siendo que algunos pueden experimentar un rápido deterioro funcional, mientras que otros tienen una progresión más lenta con períodos de estabilidad. En la mayoría de los casos, el sistema sensorial, las funciones cognitivas, el control ocular y esfínteres permanecen intactos.

Aunque esta fue la definición inicial, la bibliografía de los últimos años evidencia que hasta un 50% de los pacientes con ELA presentan deterioro cognitivo, y hasta un 30% presentan demencia frontotemporal (FTD). Ambas enfermedades neurodegenerativas comparten mutaciones genéticas comunes (C9orf72, TARDBP, FUS, UBQLN2, etc.), y se caracterizan por la presencia de agregados de la proteína TDP-43 en el citoplasma de las neuronas afectadas (lóbulos frontales y temporales del cerebro, en el caso de la FTD).

El diagnóstico de ELA en etapas iniciales puede ser difícil debido a la heterogeneidad de los síntomas y signos clínicos y a la falta de marcadores diagnósticos específicos. Desde los iniciales criterios del Escorial y su versión modificada, varios criterios diagnósticos (Awaji, Gold Coast y otros) han sido propuestos con el objetivo de mejorar la sensibilidad y acortar la demora diagnóstica que limita la eficacia de los escasos tratamientos disponibles.

Actualmente, no existe cura para esta enfermedad mortal. Sin embargo, en algunos países se han aprobado ciertos medicamentos que pueden ralentizar su progresión en algunos pacientes, extendiendo su esperanza de vida y autonomía unos cuantos meses. Estos medicamentos son el Rilutek (riluzole), el Radicava (edaravone), el Qalsody (tofersen) y el Relyvrio (sodium phenylbutyrate/taurursodiol). En cualquier caso, es necesario un

diagnóstico temprano para ver la efectividad de estos tratamientos, lo que refuerza la idea de la necesidad de encontrar otras alternativas más eficaces.

1.5. Fisiopatología de la ELA

Al igual que sucede con la etiología, se desconocen los mecanismos fisiopatológicos que promueven el desarrollo de la enfermedad y por qué solo las MNs se ven afectadas. El conocimiento de las funciones de los genes mutados nos ha proporcionado información sobre algunos de los mecanismos fisiopatológicos implicados en la etiología y progresión de la enfermedad. Entre ellos destacan: la excitotoxicidad mediada por glutamato, alteraciones en la reparación del DNA, el transporte de RNA y el metabolismo proteico, la formación de agregados y/o gránulos de estrés, la eliminación defectuosa de proteínas tóxicas, alteraciones de los microtúbulos y el citoesqueleto, fenotipos reactivos en astrocitos y microglía, neuroinflamación, estrés oxidativo, daño mitocondrial, alteraciones en la autofagia y otros problemas que, de un modo u otro, comprometen el transporte axonal, la liberación de neurotransmisores y causan muerte neuronal. Para introducir los principales objetivos de esta tesis doctoral, revisaremos el papel de algunos de ellos, teniendo en cuenta que no son excluyentes y que influyen unos sobre otros.

La neurotoxicidad del glutamato podría jugar un papel importante en la fisiopatología por varias razones: a) existe una correlación directa entre la severidad de los síntomas y los niveles de glutamato en líquido cefalorraquídeo (CSF) de pacientes; b) otros mecanismos involucrados en la etiopatogenia de la ELA hacen que las MNs sean más sensibles a la excitotoxicidad por glutamato; c) hay una menor expresión de los transportadores EAAT2 en las áreas afectadas del (sistema nervioso central) CNS; y d) el glutamato es un inhibidor competitivo del transporte de GSH a las mitocondrias, y la depleción del GSH mitocondrial y de acumulación Ca^{2+} citosólico son eventos implicados en la activación de la apoptosis. En este sentido, el riluzol es el único tratamiento que ha demostrado prolongar mínimamente la supervivencia de pacientes y animales tratados. Las bases moleculares de sus efectos neuroprotectores son, a día de hoy, todavía discutidas e involucran varios procesos pre y post-sinápticos, como la inhibición de la liberación del glutamato, el bloqueo de receptores, la inactivación de los canales de sodio dependientes de voltaje y la estimulación de una vía de transducción de señal, dependiente de la proteína G. En cualquier caso, sigue sin aclararse si la excitotoxicidad mediada por el glutamato es un agente etiológico primario, o consecuencia de la alteración en la homeostasis neuronal. De hecho, el tratamiento con riluzol solo

muestra cierta eficacia cuando es utilizado en estadios tempranos, y otros otros antagonistas del glutamato (gabapentina, lamotrigina, topiramato) no han mostrado ninguna eficacia clínica. También se han llevado a cabo estudios con fármacos capaces de incrementar la expresión y/o actividad de los EAAT2. En este sentido, la ceftriaxona (un antibiótico β-lactámico capaz de atravesar la barrera hematoencefálica) aumenta la expresión de la proteína EAAT2 en ratones tratados, retrasa la pérdida de MNs (≈2 semanas) y la fuerza muscular (4-6 semanas), y prolonga la supervivencia de ratones $SOD1^{G93A}$ (≈10 días). Desafortunadamente, en los ensayos clínicos no se evidenciaron mejorías con este tratamiento.

Las MNs tienen axones largos que requieren un transporte eficiente de componentes celulares. Las mutaciones en genes como FUS, TDP-43 y C9orf72 conllevan a la acumulación anormal de agregados proteicos, neurofilamentos fosforilados, mitocondrias dañadas y vesículas en los axones de las MN. Todo ello compromete la liberación de neurotransmisores y está involucrado en la muerte de MN. Además, en las muestras obtenidas en pacientes de ELA se ha corroborado el déficit de factores neurotróficos como el BDNF y el GDNF involucrados en la neurogénesis y la plasticidad neuronal. De hecho, los modelos murinos tratados con estos factores parecen mejorar sutilmente su supervivencia y función neuromuscular.

La agregación citoplasmática de proteínas es considerada uno de los rasgos fisiopatológicos característicos de la ELA, con acumulaciones anormales de proteínas como TDP-43 y SOD1 en las MNs y en la glía. La disfunción del retículo endoplásmico (ER) se considera otro mecanismo clave que contribuye la acumulación de proteínas mal plegadas, lo que lleva a la disfunción y muerte neuronal. Por su parte, varias mutaciones vinculadas a la ELA cursan con alteraciones de autofagia que contribuyen a la acumulación de agregados proteicos y aceleran la progresión de los síntomas.

También se ha comprobado que las proteínas codificadas por los genes mutados (SOD1 y TDP-43) pueden comportarse como priones, propagándose de célula a célula de forma semejante a como se produce la neurodegeneración.

La neuroinflamación caracterizada por la presencia de astrogliosis, microglía reactiva y por la infiltración de células inmunes periféricas juega un papel crucial en la fisiopatología de la enfermedad. Las citoquinas proinflamatorias (TNF-α, IL-1β, IL-6, IL-12, e IFN-γ (entre otras) exacerban el daño a las MNs. Cabe destacar que las MNs son altamente dependientes de la función mitocondrial y sensibles al estrés oxidativo debido a su alta actividad metabólica, su elevado consumo de oxígeno y sensibilidad a las alteraciones en la homeostasis del Ca^{2+}. En modelos murinos y muestras de pacientes se ha comprobado la

existencia de alteraciones en la biogénesis y la función mitocondrial y el aumento en los marcadores de estrés oxidativo asociados o no al aumento de citoquinas proinflamatorias que contribuyen a la progresión de la enfermedad.

1.6. Fundamentos de nuestra estrategia terapéutica

Tal y como acabamos de ver, son múltiples los mecanismos involucrados en la fisiopatología de la enfermedad, y de un modo u otro, convergen en el estrés oxidativo, la disfunción mitocondrial y la neuroinflamación. Por ello pensamos que los pacientes podrían beneficiarse de un tratamiento que fuera dirigido en esta línea.

El pterostilbeno (PT) es un análogo estructural del resveratrol con una mayor semivida biológica y liposolubilidad, facilitando la entrada a través de la (barrera hematoencefálica) BBB. El PT induce la expresión de Nrf2 y la actividad sirtuina (SIRT1) y como consecuencia aumenta las defensas antioxidantes en el CNS atenuando los daños asociados al estrés oxidativo y la disfunción mitocondrial del músculo esquelético, problemas habitualmente asociados a la fisiopatología de la ELA. Los efectos antiinflamatorios del PT se asocian a su capacidad de bloquear la activación del NF-κB y disminuir la producción de citoquinas como el TNF-α, la IL-1β y la IL-6.

El NAD^+ es una coenzima esencial para la detoxificación de especies reactivas de oxígeno (ROS) y para el metabolismo energético y la función mitocondrial. A medida que envejecemos, los niveles de NAD^+ disminuyen en ciertos tejidos, afectando las funciones fisiológicas y contribuyendo a enfermedades relacionadas con la edad, como las neurodegenerativas y la degeneración axonal. En la ELA, la alteración de enzimas implicadas en la síntesis de NAD^+ indica que los déficits de NAD^+ están relacionados con la enfermedad. Se ha investigado que la suplementación con precursores de NAD^+ puede aumentar significativamente sus niveles en los tejidos, mejorar la salud cardiovascular, proteger contra la neurodegeneración y aumentar la fuerza muscular. Dado que la depleción de NAD^+ se asocia con la muerte neuronal, incrementar su disponibilidad puede tener efectos neuroprotectores. Además, se ha visto que el NAD^+ y sus metabolitos ayudan a las neuronas a adaptarse al estrés y contrarrestar procesos en enfermedades neurodegenerativas, incluida la ELA. Las sirtuinas (SIRTs) actúan como intermediarios cruciales que vinculan los niveles de NAD^+ con la función mitocondrial y las defensas antioxidantes. En el contexto de la ELA, la disminución de la energía celular puede comprometer la eficacia de las SIRTs. El consumo de NAD^+ sin una reposición adecuada puede reducir la actividad de procesos dependientes

de SIRT, afectando negativamente la biogénesis mitocondrial y la mitofagia. Por ello, garantizar el mantenimiento de los niveles de NAD^+ puede contribuir a retrasar la progresión de la ELA, y utilizar como precursor el ribósido de nicotinamida (NR), fue considerada una buena opción, por su mejor perfil farmacocinético en comparación con otras formas de vitamina B3, como el ácido nicotínico y la nicotinamida.

En mi trabajo de fin de máster, demostré que el tratamiento con NR y PT mejora las defensas antioxidantes dependientes de Nrf2 y aumenta la actividad de SIRT1 y SIRT3 en las MNs de ratones $SOD1^{G93A}$. El PT mostró promover la sobreexpresión de SIRT1 y la translocación nuclear de Nrf2, mientras que el NR aumento los niveles de NAD^+, necesario para las reacciones catalizadas por PARP-1 y SIRT. El tratamiento con NR+PT redujo el estrés oxidativo, disminuyendo la liberación de señales proapoptóticas. Estos resultados sugieren que el NR+PT puede ser un tratamiento viable para la ELA, por su capacidad de atenuar el estrés oxidativo y proteger a las MNs

Teniendo en cuenta que el deterioro neuromotor es acelerado por la respuesta inflamatoria (principalmente mediada por células gliales) y la pérdida de factores neurotróficos, nuestra hipótesis inicial es que es posible aumentar la eficacia del tratamiento con NR+PT añadiendo un fármaco antiinflamatorio. Para seleccionar la mejor opción, realicé una exhaustiva revisión

bibliográfica, en la que verifiqué la escasa eficacia de la mayoría de las terapias antiinflamatorias/inmunosupresoras evaluadas clínicamente para el tratamiento de la ELA. Sin embargo, varios trabajos demostraban el potente efecto antiinflamatorio de los inhibidores de la fosfodiesterasa (PDE), con la ventaja adicional de ser capaces de inhibir la activación glial y atravesar la BBB, lo que los convertía en una atractiva estrategia para el tratamiento de la ELA. Entre ellos, despertaron nuestro interés el rolipram, el roflumilast, el apremilast y el ibudilast (IBU) por ser actualmente utilizado en la clínica. En especial el IBU había demostrado tener potentes efectos neuroprotectores, promover la expresión de factores neurotróficos y prevenir la disfunción mitocondrial. De hecho, actualmente, hay dos ensayos clínicos en curso para evaluar su eficacia en el tratamiento de enfermedades neurodegenerativas como la ELA y la esclerosis múltiple.

2. HIPÓTESIS Y OBJETIVOS

La complejidad e interacción de los mecanismos fisiopatológicos involucrados en la ELA hacen poco probable que un solo agente terapéutico pueda revertir en una mejora clínica de los pacientes. Nuestro grupo ha demostrado que la terapia combinada con NR y PT protege a las MNs frente al estrés oxidativo, ralentiza la neurodegeneración y prolonga significativamente la supervivencia de los ratones $SOD1^{G93A}$. La

inflamación mediada por astrocitos y microglía, y la sobreproducción de citoquinas proinflamatorias potencian el estrés oxidativo/nitrosativo que daña a las MNs. En consecuencia, resulta coherente intentar potenciar la eficacia del tratamiento con NR y PT con la adición de un agente antiinflamatorio.

Los inhibidores de la PDE atraviesan la BBB y han demostrado tener potentes efectos antiinflamatorios y capacidad de reducir la activación de las células gliales. Algunos de ellos están siendo evaluados en ensayos clínicos para el tratamiento de la ELA y otras enfermedades neurodegenerativas, por lo que consideramos que podrían ser una buena opción para aumentar la eficacia del tratamiento con NR+PT.

En esta tesis proponemos utilizar el IBU por las siguientes razones:

a) Su capacidad de inhibir a la PDE4 cuyos efectos implican la activación de la inmunidad innata y la respuesta inflamatoria en el CNS.
b) El IBU es capaz de inhibir la liberación de citoquinas proinflamatorias y la producción de NO y $O_2^{\bullet -}$. Además, tiene efectos neuroprotectores.
c) El IBU facilita la eliminación de agregados de TDP-43 y SOD1 en modelos de ELA.

d) La eficacia de otros inhibidores de PDE (rolipram, roflumilast y apremilast) se vio limitada por sus efectos secundarios en los modelos de ELA utilizados en este trabajo (sección 4.1),

El ***objetivo principal de esta tesis*** es investigar si el IBU es capaz de potenciar la eficacia terapéutica del tratamiento con NR+PT en dos modelos murinos de ELA ($SOD1^{G93A}$ y FUS^{R521C}) y explorar los mecanismos moleculares subyacentes a la posible eficacia terapéutica.

<u>Los objetivos específicos son:</u>

1. Evaluar la toxicidad de los inhibidores de la PDE4 para seleccionar la opción terapéutica más segura.
2. Investigar cómo afecta el tratamiento con NR+PT+IBU contribuye a mantener las funciones neuromotoras y a aumentar la supervivencia de los ratones $SOD1^{G93A}$ y FUS^{R521C}.
3. Realizar estudios histopatológicos de la médula espinal para obtener evidencias morfológicas directas de los efectos de la terapia.
4. Hacer estudios de muerte celular, autogafia/mitofagia, actividad SIRT, enzimas y metabolitos redox dependientes de Nrf2 en MNs aisladas de ratones control y tratados (NR+PT+IBU) para investigar cómo el tratamiento afecta los marcadores de estrés oxidativo/nitrosativo y la disfunción mitocondrial asociada con la progresión de la ELA.

3. MATERIAL Y MÉTODOS

En esta tesis doctoral, se emplearon dos modelos murinos transgénicos ($SOD1^{G93A}$ y FUS^{R521C}) para evaluar los efectos de diversos tratamientos en la ELA. Se administraron NR, PT e IBU a los ratones, utilizando métodos específicos de dosificación para asegurar una ingesta controlada y continua, y se hicieron estudios de supervivencia y funciones neuromotoras. Los ratones también fueron tratados con L-NAME (NG-Nitroarginina Metil Éster) para evaluar los efectos de la inhibición de la síntesis de óxido nítrico.

La actividad y coordinación neuromotora fue evaluada mediante una escala de funcionalidad neurológica y con la prueba de *rotarod*, con el objetivo de monitorizar la progresión de la enfermedad y la efectividad de los tratamientos. Los ratones fueron evaluados semanalmente, registrándose la aparición y progresión de síntomas específicos de la ELA.

Para los estudios patológicos, se analizaron secciones de la médula espinal mediante técnicas histológicas e inmunohistoquímicas para identificar y cuantificar MNs, microglía y astrogliosis. Se aislaron y cultivaron microglía, astrocitos y células endoteliales del CNS para realizar diversos estudios. También se cuantificaron varias citoquinas en el CSF. Además, se realizaron análisis de muerte celular para diferenciar entre apoptosis y necrosis en MNs aisladas de FUS^{R521C}.

Se determinó la generación de ROS y NO mediante técnicas específicas de detección. Se cuantificaron los niveles de glutatión y ATP, así como la actividad de caspasa 3. También se evaluó el potencial de membrana mitocondrial y el consumo de oxígeno en MNs aisladas de FUS^{R521C}.

Para analizar la mitofagia, se utilizó microscopía confocal. Las proteínas específicas se fueron cuantificadas mediante *Western blot.*

El estudio estadístico se llevó a cabo mediante curvas de Kaplan-Meier, análisis de varianza (ANOVA) y la t de student, para garantizar la significación de los resultados del análisis.

4. RESULTADOS

4.1. Tolerancia y selección de los inhibidores de PDE

Para seleccionar el inhibidor de PDE4 más adecuado para nuestros experimentos, evaluamos la toxicidad de los inhibidores de PDE4 que actualmente están en uso clínico (rolipram, roflumilast, apremilast e IBU). Utilizamos el factor de conversión de la "Food and Drug Administration" para ajustar las dosis farmacológicas humanas a equivalentes en ratones.

El tratamiento diario con rolipram, roflumilast y apremilast resultó en importantes efectos secundarios antes de las 2 semanas del inicio del tratamiento. Los ratones tratados con

rolipram presentaron diarrea, el roflumilast indujo espasmos musculares y los tratados con apremilast mostraron signos de dolor. Los experimentos se detuvieron cuando los espasmos musculares o el dolor continuo se hicieron evidentes, o cuando la diarrea provocó una pérdida de peso corporal superior al 20%. Por el contrario, no apreciamos efectos secundarios importantes en los ratones tratados con IBU, siendo por ello la opción terapéutica más viable para este trabajo.

4.2. NR, PT e IBU retrasan la pérdida de funciones neuromotoras relacionadas con la ELA

Las funciones neuromotoras en los ratones $SOD1^{G93A}$ y FUS^{R521C} fueron evaluadas utilizando un sistema de puntuación neurológica estándar y en la prueba de rotarod, que evalúa el equilibrio, la coordinación y la condición física general. La falta de coordinación motora se hizo evidente alrededor de la semana 12 en los ratones $SOD1^{G93A}$ y en la semana 7 en los ratones FUS^{R521C}. Tanto el tratamiento aislado con IBU como el tratamiento con NR+PT retrasaron significativamente la aparición de síntomas neurológicos en ambos modelos murinos de ELA en comparación con el grupo control. Este retraso fue más notable en los ratones que recibieron la triple terapia (NR+PT+IBU) como tratamiento.

4.3. NR, PT e IBU prolongan la supervivencia en modelos murinos de ELA

En comparación con los controles, los ratones $SOD1^{G93A}$ y FUS^{R521C} tratados con NR y PT o con IBU vieron aumentadas sus supervivencias. Sin embargo, la terapia triple (NR+PT+IBU) resultó en un incremento significativo en la supervivencia, superando los resultados obtenidos con los tratamientos individuales de NR+PT o IBU.

4.4. NR, PT e IBU reducen la microgliosis, la astrogliosis y el daño a las MN

La progresión de la ELA se asocia con la microgliosis y astrogliosis en las astas anteriores de la médula espinal. Para poder cuantificar estos cambios, se realizaron análisis inmunohistopatológicos en ambos modelos murinos, utilizando la tinción inmunohistoquímica de Iba1 para la microgliosis y la tinción de proteína ácida fibrilar glial (GFAP) para la astrogliosis. Los tratamientos con NR+PT y NR+PT+IBU, mostraron una reducción significativa en ambos tipos de gliosis relacionada con la neuroinflamación. En el caso específico de la microgliosis, la combinación triple fue significativamente más efectiva que el tratamiento con NR+PT. Además, el número de MNs en las astas anteriores de la médula espinal se preservó mejor cuando ambos modelos murinos fueron tratados con NR+PT o con NR+PT+IBU, siendo muy similar al recuento encontrado en los ratones wild

type (WT). No obstante, debo recalcar que el mantenimiento de la morfología o el número de MNs no garantiza el mantenimiento de la función, requiriéndose para ello de estudios adicionales como los que hemos hecho previamente.

4.5. NR, PT e IBU reducen la producción de citoquinas proinflamatorias

En esta fase del estudio se investigaron los mecanismos involucrados en la activación de la respuesta neuroinflamatoria. Para ello, cuantificamos citoquinas proinflamatorias en muestras de CSF obtenidas de ratones WT, $SOD1^{G93A}$ y FUS^{R521C}. Las muestras procedentes de los ratones $SOD1^{G93A}$ y FUS^{R521C} tratados con suero salino mostraron un aumento importante en los niveles de las citoquinas (TNF-α, IFN-γ, IL-2, IL-6, GM-CSF). El tratamiento con NR+PT redujo significativamente los niveles de IFNγ e IL-6, mientras que el tratamiento con IBU fue notablemente efectivo en la disminución de los niveles de TNFα. Al comparar los grupos tratados con NR+PT, con aquellos tratados con NR+PT+IBU, solo se observó una diferencia significativa en los niveles de TNFα, lo que denota cuál es el mecanismo de acción mediado por el IBU. Estos resultados ponen en evidencia no sólo la eficacia antiinflamatoria del tratamiento, sino también el posible sinergismo.

4.6. Las citoquinas inducen estrés oxidativo/nitrosativo

Dado que el estrés oxidativo y la neuroinflamación son componentes integrales de la fisiopatología de la ELA, investigamos si la exposición citoquinas proinflamatorias, a dosis equivalentes a las obtenidas en CSF, repercutía en un aumento de la producción de NO y H_2O_2 por parte de las células aisladas de los ratones $SOD1^{G93A}$ y FUS^{R521C}. Los resultados demuestran que efectivamente las citoquinas TNFα, IFNγ e IL1β aumentan significativamente la generación de H_2O_2 y NO por parte de MNs, astrocitos, microglía y células endoteliales aisladas de ratones $SOD1^{G93A}$ y FUS^{R521C}, cosa que no sucede en células similares aisladas de ratones WT. El estrés oxidativo/nitrosativo mediado por las citoquinas fue especialmente importante cuando las tres citoquinas se incubaron juntas, reflejando de forma más precisa las condiciones *in vivo*.

4.7. NR, PT y/o IBU protegen a las MN contra el estrés oxidativo/nitrosativo

Se investigó la generación de H_2O_2 y NO en diferentes tipos de células (MN, astrocitos, microglía y células endoteliales) aisladas de ratones control $SOD1^{G93A}$ y FUS^{R521C} que habían sido tratados *in vivo* con NR+PT, IBU o NR+PT+IBU. El tratamiento NR+PT redujo significativamente la producción de H_2O_2 y NO inducida por citoquinas en todos los tipos celulares, excepto para H_2O_2 en astrocitos FUS^{R521C} y NO en astrocitos $SOD1^{G93A}$. El tratamiento

con IBU solo disminuyó la producción de H_2O_2 en células de la microglía y células endoteliales. Tal y como hemos visto en otros resultados de esta tesis, en comparación con el tratamiento con NR+PT, la triple terapia (NR+PT+IBU) redujo más eficazmente la producción de H_2O_2 y NO en la microglía y las células endoteliales.

4.8. La citotoxicidad mediada por RNS y ROS aumenta en presencia de metales

Con el fin de investigar el efecto citotóxico inducido por el estrés oxidativo y nitrosativo, expusimos las MNs aisladas de los ratones, a concentraciones de H_2O_2 y NO equivalentes a las generadas por las células de su entorno (ver apartado anterior). Curiosamente, la exposición aislada al H_2O_2 o al NO, apenas dañó a las MNs (citotoxicidad <10%). Sin embargo, la combinación de ambos resultó en un aumento significativo de la citotoxicidad (aproximadamente un 40% por encima de los niveles de control). El peroxinitrito ($^{-}$OONO) mostró un efecto citotóxico mayor que el H_2O_2 o el NO por separado, sugiriendo que su combinación es responsable del aumento de la citotoxicidad. La presencia de metales, como el hierro ($FeCl_3$), también incrementó la citotoxicidad inducida por H_2O_2 y NO.

La presencia de metales acelera la producción de radicales hidroxilo ($^{\bullet}$OH), con efecto potenciador del estrés nitrosativo. Este proceso, catalizado por iones metálicos como el hierro,

descompone el H_2O_2 para producir $^{\bullet}OH$, una de las especies reactivas de oxígeno más dañinas. La adición de EGTA (quelante de metales) o ebselen (con actividad peroxidasa) reducen el efecto citotóxico sobre las MNs inducida por H_2O_2 y NO, indicando que hay un proceso catalizado por metales que contribuye a la citotoxicidad observada.

4.9. NR, PT e IBU atenúan el estrés oxidativo/nitrosativo

Células endoteliales y microgliales aisladas de ratones $SOD1^{G93A}$ y FUS^{R521C} tienen una mayor producción de nitrito (NO_2^-; que refleja indirectamente la generación de $^{\bullet}OH$ a través de la siguiente reacción: $^{\bullet}OH + {}^{-}NO \rightarrow NO_2^-$) y $^{-}OONO$, en comparación las células obtenidas a partir de los ratones WT.

El tratamiento *in vivo* con NR+PT y con NR+PT+IBU redujo la producción de ambas especies reactivas derivadas del nitrógeno, siendo de nuevo más efectiva la triple terapia NR+PT+IBU.

4.10. El estrés oxidativo/nitrosativo induce apoptosis neuronal

En nuestros resultados demostramos que la exposición al H_2O_2 y NO induce la apoptosis y reduce la viabilidad de MNs aisladas de ratones FUS^{R521C}, siendo el efecto nocivo significativamente más importante en presencia de NO.

Estudios previos demuestran que la disminución de la autofagia/mitofagia induce la muerte neuronal. El tratamiento con NR+PT y, especialmente, la triple terapia (NR+PT+IBU)

induce la mitofagia, favorece la eliminación de mitocondrias dañadas ejerciendo un papel protector sobre las MNs.

4.11. La inhibición de NOS aumenta la supervivencia en ratones con ELA

El L-NAME (Nω-Nitro-L-arginina metil éster) es un inhibidor de la óxido nítrico sintasa (NOS). Tratamos con L-NAME a los ratones $SOD1^{G93A}$ y FUS^{R521C} desde etapas avanzadas e la enfermedad (semana 18) y tal y como cabría esperar, el tratamiento resultó en una significativa reducción de la producción de NOx (NO_2^- más NO_3^-) por parte de las MNs, astrocitos, microglía y células endoteliales obtenidas a partir de los ratones tratados.

Además, el tratamiento con L-NAME aumentó significativamente la supervivencia de los ratones $SOD1^{G93A}$ y FUS^{R521C} en comparación con los ratones de control, lo que evidencia claramente de la importancia del estrés nitrosativo en la progresión de la ELA

4.12. NR+PT+IBU reduce la acumulación citoplasmática de la proteína mutante FUS en MN

Finalmente se investigó si alguno de nuestros tratamientos afectaba a los niveles intracelulares de las proteínas mutantes SOD1 y FUS, y comprobamos que ninguno de ellos afectaba a los niveles intracelulares de la SOD1, descartando con ello que el

efecto terapéutico del tratamiento estuviera vinculado a la expresión genética de la SOD1 mutada.

Sin embargo, en el caso de los ratones FUS^{R521C}, el tratamiento con NR+PT, NR+PT+IBU o con L-NAME disminuyó la acumulación de la proteína mutante FUS en las MNs. Este hallazgo puede interpretarse de diversas maneras: los tratamientos podrían estar influyendo directamente en expresión de la proteína mutada o, también podría ocurrir que, al reducir la producción de citoquinas, ROS o RNS, los tratamientos condujeran indirectamente a una disminución de la transcripción de la proteína mutada. Otra alternativa sería que la eliminación de la proteína mutante FUS se esté viendo favorecida por mecanismos como el sistema ubiquitina-proteasoma. En cualquiera de los casos, la disminución de la acumulación de la proteína mutante FUS dentro en las MNs contribuye al mantenimiento de la función y, consecuentemente, a la supervivencia de los ratones $SOD1^{G93A}$ y FUS^{R521C}.

En conjunto, los resultados de esta tesis doctoral demuestran que los tratamientos con NR, PT e IBU no solo mejoran las funciones neuromotoras y la supervivencia en modelos murinos de ELA, sino que también reducen la neuroinflamación, el estrés oxidativo y nitrosativo, y la acumulación de proteínas mutantes. Estos hallazgos proporcionan una base sólida para futuras investigaciones y potenciales terapias en la lucha contra la ELA.

5. DISCUSIÓN

Cada vez son más las evidencias que demuestran que la neuroinflamación y el estrés oxidativo son factores clave en la neurodegeneración de la ELA. A medida que la enfermedad avanza, la microglía y los astrocitos experimentan una transición fenotípica, proliferan y secretan citoquinas proinflamatorias. Esta neuroinflamación está vinculada con la liberación de citoquinas que inducen apoptosis, como TNF-α, IFN-γ e IL-1β. Además, el TNF-α interfiere con el flujo normal de electrones en las mitocondrias, aumentando la generación de ROS. Las citoquinas proinflamatorias como GM-CSF, IL-2, IL-6, IL-15, IL-17, MCP-1, MIP-1α, TNF-α y VEGF suelen estar elevadas en el CSF de pacientes con ELA y en modelos murinos de ELA. Los astrocitos reactivos sobreexpresan enzimas proinflamatorias como la COX-2, la iNOS y la nNOS. En condiciones patológicas, las células gliales y las células inmunes son las principales productoras de ROS y RNS, por lo que la inflamación crónica aumenta el estrés oxidativo induciendo daños a las MNs.

El NAD^+ es una coenzima vital imprescindible en las reacciones redox, proporciona ADP-ribosa para reacciones de ribosilación, y es sustrato imprescindible para la actividad de las sirtuinas (SIRTs) que catalizan reacciones de desacetilación de proteínas. Las SIRTs, especialmente SIRT1 y SIRT3, regulan la biogénesis y función mitocondrial y ayudan a mitigar el estrés oxidativo

desacetilando y activando enzimas antioxidantes. Por su parte el PT tiene efectos antioxidantes y aumenta la expresión de NRf2, aumentando la expresión de importantes encimas antioxidantes, además de tener importantes efectos antiinflamatorios.

Dos trabajos de nuestro grupo de investigación demuestran que la terapia combinada con NR y PT resulta beneficiosa para el tratamiento de la ELA. En un primer estudio piloto con pacientes de ELA (NCT03489200) demostramos que tratamiento con NR y PT ayuda a mantener las funciones neuromotoras de los pacientes, y en mi trabajo fin de máster demostramos que el tratamiento NR+PT mejora las defensas antioxidantes dependientes de Nrf2 y aumentan la actividad de SIRT1 y SIRT3 en neuronas motoras de ratones $SOD1^{G93A}$. El PT promovió la sobreexpresión de SIRT1 y la translocación nuclear de Nrf2, mientras que el NR proporcionó NAD^+ para las reacciones catalizadas por PARP-1 y SIRT. El tratamiento con NR+PT redujo el estrés oxidativo y la muerte por apoptosis de las neuronas, ralentizó la pérdida de funciones neuromotoras y prolongó significativamente la supervivencia de los ratones $SOD1^{G93A}$. Actualmente, el tratamiento con PT+NR se está evaluando en un ensayo clínico fase II con pacientes de ELA (NCT04562831, The NO-ALS Study: A Trial of Nicotinamide/Pterostilbene Supplement in ALS).

La ELA es un trastorno neurodegenerativo complejo, en el que las terapias aisladas no han logrado aumentar la supervivencia. Por lo tanto, consideramos que una estrategia combinada es una mejor opción terapéutica, y en nuestro caso, la adición de un agente antiinflamatorio puede aumentar aún más la eficacia de NR y PT. Tras revisar en la bibliografía la falta de eficacia de muchos antinflamatorios comunes utilizados habitualmente en la clínica (por ejemplo, el celecoxib, los corticoides, y otros), consideramos interesante utilizar inhibidores de la PDE por su capacidad para cruzar la BBB y reducir la activación de las células gliales. El tratamiento con rolipram, roflumilast y apremilast tuvo importantes efectos secundarios que obligaron a la terminación temprana del tratamiento. En cambio, no observamos toxicidades asociadas al tratamiento con IBU por lo que éste fue considerado la opción terapéutica más segura y viable.

Los resultados de esta tesis demuestran que al combinar el IBU con la NR y el PT, se produce importante retraso en la pérdida de las funciones neuromotoras y aumenta significativamente la supervivencia en ambos modelos murinos de ELA. Más concretamente, en comparación con el tratamiento NR+PT, la triple terapia incrementó la supervivencia en dos semanas en los ratones $SOD1^{G93A}$ y en once semanas en ratones FUS^{R521C}. La eficacia del tratamiento se asocia a la disminución de la

neuroinflamación, evidenciada por el descenso en las citoquinas pro-inflamatorias en CSF y los estudios histológicos.

A bajas concentraciones, los radicales libres actúan como moléculas involucradas en la señalización celular, pero su acumulación induce estrés oxidativo, y causan daños a lípidos, proteínas y ácidos nucleicos, siendo las MNs especialmente sensibles por su elevada semivida biológica.

En cultivos primarios, la microglía activada por lipopolisacáridos (LPS) o por inmunoglobulinas induce efectos citotóxicos en las MNs, toxicidad que resulta revertida mediante tratamiento con un inhibidor de la NOS, con catalasa o glutatión. Por otro lado, las MNs embrionarias que expresan p75(NTR) no son vulnerables al factor de crecimiento nervioso a menos que estén expuestas al NO. Estudios previos demuestran que el PT reduce la producción de NO y TNFα inducida por tratamiento con LPS en las células de la microglía. Este efecto es dependiente del bloqueo de la fosforilación y degradación de IkBα, que evita la activación de NF-κB. Además, la unión de LPS al receptor tipo Toll 4 (TLR4) de la microglía puede desencadenar la activación de de NF-κB y de las MAPKs, induciendo la expresión de genes que codifican citoquinas proinflamatorias y encimas como la COX-2. Todo esto sugiere que el NO juega un papel importante en la cascada fisiopatológica de la ELA.

Los resultados de este trabajo van en la misma dirección ya que demostramos el aumento significativo en los niveles de citoquinas proinflamatorias en el CSF de ratones $SOD1^{G93A}$ y FUS^{R521C}, y que la exposición a estas citoquinas (TNFα, IFNγ e IL1β) aumenta la producción de H_2O_2 y NO por MNs, astrocitos, microglía y células endoteliales aislados de los ratones transgénicos. Además, tanto el tratamiento con NR+PT como la triple terapia (NR+PT+IBU), disminuyen los niveles de las citoquinas proinflamatorias en el CSF y la producción de NO en MNs, astrocitos, microglía y células endoteliales. El IBU disminuye especialmente los niveles de TNFα en el CSF y la generación de H_2O_2 por células endoteliales y microglíales, ejerciendo por ello sinergismo con el PT y la NR.

Sorprendentemente, cuando expusimos a las MNs a niveles fisiopatológicos de H_2O_2 u NO, apenas se evidenciaron efectos tóxicos, siendo el efecto citotóxico superior a la suma de ambos, cuando las MNs se exponen simultáneamente a H_2O_2 y NO. Nuestros resultados evidencian que el potente efecto citotóxico es dependiente de la formación de potentes radicales libres ($^{\bullet}OH$ y $^{-}OONO$) mediado por las reacciones de Fenton catalizadas por las trazas de metales presentes en el medio.

Estos resultados evidencian que el daño a las MNs está mediado el estrés oxidativo/nitrosativo inducido por las citoquinas proinflamatorias y por las células (microglía, astrocitos, células

endoteliales y probablemente células inmunes infiltradas) que rodean el microambiente de las MNs. De hecho, en nuestros experimentos hemos utilizado concentraciones de H_2O_2 y NO semejantes a las que se producen por las células del entorno de las MNs, aunque también es cierto que no hemos podido tener en cuenta el efecto que cursado por la compleja arquitectura tisular, el flujo sanguíneo, linfático y del CSF o por la presencia de moléculas reguladoras, siendo por ello plausible que, in vivo, las MNs estén expuestas a niveles más bajos de H_2O_2 y NO. Además, la ELA progresa en forma de brotes esporádicos, con lo cual la exposición de las MNs a niveles tóxicos de ROS y RNS puede no ser constante. Estas observaciones sugieren un escenario más consistente con el deterioro gradual experimentado por los pacientes.

Es importante recordar que la fisiopatología de la ELA, a menudo, se acompaña del acúmulo citoplasmáticos de proteínas agregadas (SOD1, TDP-43 o FUS). Esto es importante (y coherente con nuestros hallazgos) porque tanto ROS como RNS pueden favorecer la agregación anómala de proteínas.

Varios estudios evidencian la importancia de los metales en el daño inducido por estrés oxidativo. Mediante las reacciones de Fenton, el hierro libre induce la formación de ROS y RNS implicadas en patologías como el ictus, la epilepsia, y otras patologías del CNS. La mutación SOD está involucrada en el daño

oxidativo a través del aumento de la generación de radicales hidroxilo y el aumento de la nitración de la tirosina mediada por $^{-}$OONO. Singh y cols. (1998) fueron los primeros en sugerir que la pérdida de zinc de la SOD1 mutada puede aumentar la formación peroxinitrito asociada a la muerte de las MNs mediada por las reacciones de Fenton. Además, se ha sugerido que el depósito de hierro en las MNs puede estar involucrado en la patogénesis de la ELA, y el exceso de hierro induce la apoptosis neuronal asociada al estrés oxidativo. Finalmente, un reciente metaanálisis informa que, en comparación con los pacientes sanos, los pacientes de ELA presentan niveles séricos de ferritina altos y bajos niveles de transferrina, lo cual puede inducir la acumulación de hierro en los tejidos y daño a las MNs. Las conclusiones del estudio sugieren posibles anormalidades en el metabolismo del hierro en los pacientes de ELA que apoyarían la importancia del hierro en la toxicidad mediada por el estrés oxidativo en las MNs que he evidenciado en esta tesis doctoral. Por lo tanto, sería interesante controlar la sideremia y la ingesta dietética de hierro, con el objetivo de evitar la aceleración del proceso neurodegenerativo.

Tal y como hemos mencionado en la introducción, el IBU es un agente antiinflamatorio utilizado en la farmacopea japonesa para el tratamiento del asma. Es un inhibidor de la migración de macrófagos y de las PDE 3, 4, 10 y 11, siendo especialmente

eficaz en la inhibición de la PDE4. La inhibición de este enzima induce el aumento de los niveles intracelulares de cAMP y cGMP y la consecuente inhibición de la producción de TNF-α, MIF y TLR-4. Ha sido ensayado para el tratamiento de la esclerosis múltiple, donde se ha visto que prolonga significativamente el tiempo hasta la primera recaída y atenúa la reducción del volumen cerebral asociado a la progresión de la enfermedad. Los efectos neuroprotectores del IBU son atribuidos a su acción antiinflamatoria, a sus efectos antiapoptóticos y a sus efectos sobre la vía de ubiquitina-proteasoma. Hennet y Goossens informaron por primera vez que TNF-α promueve la formación de ROS por las mitocondrias. En consecuencia, el IBU puede potenciar los efectos de la NR y el PT mediante un doble mecanismo, la disminución de la producción de ROS y la inhibición de TNF-α.

Es importante mencionar que, aunque el tratamiento con NR y PT no ha mostrado toxicidad significativa en el modelo $SOD1^{G93A}$, ni en pacientes con ELA, algunos estudios señalan que el uso de IBU podría desencadenar trastornos gastrointestinales y/o cutáneos. En este estudio, los modelos murinos han sido tratados con una dosis diaria única de 12 mg/kg, equivalente a aproximadamente 0,97 mg/kg por día en humanos, basándonos en el factor de conversión aceptado por la FDA. Por lo tanto, un paciente de aproximadamente 70 kg de peso corporal debería

tomar una dosis oral diaria de 67,9 mg, y el IBU muestra un excelente perfil de seguridad a 60 mg/día.

Los resultados de esta tesis doctoral demuestran que la combinación de NR, PT e IBU reduce la producción de citoquinas proinflamatorias y a la vez protege a las MNs frente al daño inducido por el estrés oxidativo/nitrosativo asociado a la progresión de la ELA. Así, el uso de NR+PT+IBU o inhibidores de NOS, actualmente en investigación en ensayos clínicos, surge como una estrategia prometedora en el tratamiento de la ELA.

Este estudio también proporciona fuertes evidencias de que los oxidantes potentes, como los radicales $^{\bullet}OH$ y $^{-}OONO$, son responsables de la oxidación de lípidos, proteínas y DNA, jugando un papel crucial en la cascada de eventos que conducen al daño neuronal, involucrando en el efecto citotóxico, la catálisis mediada por los elementos traza, en este caso, el hierro.

En conclusión, nuestros resultados sugieren claramente que una combinación juiciosa de varios fármacos puede ser más beneficiosa que el uso de fármacos individuales. El tratamiento con NR+PT+IBU ha mejorado significativamente las funciones neuromotoras e incrementado de forma muy importante la supervivencia en ratones FUS y SOD. Creemos que este tratamiento podría ofrecer beneficios sustanciales a los pacientes con ELA, y de hecho, ya estamos trabajando para promover el desarrollo de un ensayo clínico con pacientes.

6. CONCLUSIONES

Basándonos en los resultados presentados en esta tesis doctoral, podemos extraer las siguientes conclusiones:

1. El IBU resultó ser el inhibidor de PDE4 mejor tolerado, demostrando no tener efectos secundarios significativos en los ratones $SOD1^{G93A}$ y FUS^{R521C}.
2. El tratamiento con NR+PT+IBU reduce significativamente los niveles de citoquinas proinflamatorias (INF-γ, IL-1β, IL-2, IL-6 y GM-CSF) en el CSF, siendo el IBU particularmente efectivo en la inhibición de la producción de TNF-α. Esto apoya el efecto antiinflamatorio sinérgico del tratamiento combinado.
3. El tratamiento con NR+PT+IBU previene eficazmente la producción de H_2O_2 y NO en MNs, astrocitos, microglía y células endoteliales, mejorando la supervivencia de las MNs aisladas de ratones transgénicos con ELA.
4. El aumento significativo en la supervivencia con el tratamiento de L-NAME confirma el papel crítico del estrés nitrosativo mediado por NO en la progresión de la ELA.
5. La atenuación de la inflamación reduce el estrés oxidativo/nitrosativo implicado en el daño a las MNs, lo cual a su vez frena la respuesta inflamatoria rompiendo un mecanismo de retroalimentación positiva que contribuye la progresión de la ELA.

6. El IBU mejora la neuroprotección ejercida por NR y PT en el contexto de la ELA. Este tratamiento combinado retrasa significativamente la pérdida de funciones neuromotoras y aumenta la supervivencia en los modelos $SOD1^{G93A}$ y FUS^{R521C}.

C

1. INTRODUCTION

1.1. Amyotrophic lateral sclerosis

Amyotrophic lateral sclerosis (ALS) is a neurodegenerative disorder that affects motor neurons (MNs) that control voluntary muscle movement and breathing. ALS may begin with abnormalities of upper (UMN) or lower (LMN) MNs. UMN disease causes stiffness, which is called "spasticity". LMN disease causes weakness, loss of muscle ("atrophy") and muscle twitching ("fasciculations"). However, the degeneration of both neuron types is essential for a definitive diagnosis of ALS [1,2]. ALS is a rapidly disabling and irremediably fatal neurodegenerative disease, that clinically manifests as progressive muscle weakness and atrophy, leading to death, typically from respiratory failure [1,2]. Life expectancy usually does not exceed 2-5 years after diagnosis. Only a small percentage of patients, about 30%, survive more than five years post-diagnosis, although 10-20% may live beyond ten years [3,4].

It is important to note that the rate of disease progression and the specific symptoms experienced can vary widely among ALS patients. Some individuals may experience a rapid decline in function, while others may have a slower progression with periods of stability [5]. Stephen Hawking, who was diagnosed at 21 and lived until 76, is an example of exceptionally long survival in the history of ALS [6].

ALS is also known as Charcot's disease, in recognition of the French neurologist Jean-Martin Charcot, who pioneered its diagnosis in 1869 [7]. In 1874, Charcot introduced the term "amyotrophic lateral sclerosis", making reference to the loss of nerve fibers leading to a "sclerosis" (a term derived from the Greek 'σκλήρωσις', meaning “hardening”) or glial scar formation in the lateral area of the spinal cord, which is mainly occupied by the axons of pyramidal neurons. Additionally, ‘amyotrophic’ comes from Greek, where 'a' means negation, 'mio' refers to ”muscle”, and “trophic” means “nutrition”, illustrating how the lack of nerve stimulation leads to decreased muscle activity and, eventually, to atrophy [8].

In his work, *A Manual of Diseases of the Nervous System*, William Richard Gowers (1845-1915) drew from contemporary literature to propose that progressive motor system disorders, impacting both UMN and LMN pathways to varying degrees, represented syndromic variations of a single disorder. He referred to "primary spastic paraplegia" to identify what is now known as primary lateral sclerosis [9]. Jean-Martin Charcot supported this syndromic view, noting that the clinical features of each syndrome generally correlated with the distribution of pathological traits in the brain. Hermann Oppenheim (1858-1919) also referred to different motor degenerations as related disorders in his textbook [10]. William Russell Brain, in his

popular and influential work *Diseases of the Nervous System*, synthesized these ideas, clarifying that, in his view, the three syndromes of UMN degeneration, LMN degeneration, and mixed UMN and LMN degeneration should be considered manifestations of the same underlying disorder [11,12]. In 1933, Lord Russell proposed the term "MN disease" as a unifying concept for various neurological disorders characterized by the degeneration of MN [13].

1.2. Epidemiology

ALS is considered a rare disease due to its low global incidence rate of 2-3 cases per 100,000 people; however, it is the most common form of MN disease. Aging is a well-established risk factor for ALS, with an average age of onset above 60 years and a peak incidence in people aged 70–79 years [14]. Furthermore, due to the increasing aging process of the world's population, it is estimated that ALS cases will increase by 69% in the next twenty years [15].

Epidemiologic studies indicate a slightly higher incidence and prevalence of ALS in men (1.91 and 5.96 per 100,000, respectively) compared to women (1.36 and 3.90 per 100,000, respectively) [16–18]. Men tend to have an earlier onset but longer survival. Factors such as environmental, genetic and

hormonal factors may play a role in the gender disparities, but the precise mechanisms are still under investigation [19].

In Spain, there are just a few sociodemographic studies on ALS [20]. The incidence is similar to other developed countries, about 1.4 new cases per 100,000 inhabitants per year, while the prevalence (5.4 cases per 100,000 inhabitants) is slightly higher than the global rates [21,22]. Based on these statistics, it is estimated that around 4,400 people are living with ALS in Spain, and 900 new cases are diagnosed each year, equating to roughly 3 new cases per day [21].

Some studies evidence that the incidence of ALS varies by ethnicity and geographic location. Hispanic, African, and some Asian communities exhibit significantly lower incidence rates compared to Caucasian populations [23]. Eastern Europe reports the highest incidence and prevalence rates (2.76 and 9.62 per 100,000, respectively), while South Asia has the lowest (0.42 incidence and 1.57 prevalence per 100,000). Interestingly, the Western Asia region records the highest average survival rates (9.23 years) [22,24].

1.3. Etiology

1.3.1. Familiar and Sporadic ALS

The cause of ALS is largely unknown, but several factors, including genetics, environmental exposures, and lifestyle

habits, have been linked to an increased risk of ALS [25]. ALS is considered familial (FALS) when at least two or more family members have ALS at the time of diagnosis (approximately 5-10% of cases). Consequently, having a family history of ALS is recognized as one of the most significant risk factors for the disease [26]. Despite this, the vast majority of ALS patients (between 90-95%) do not have a familial history of ALS and are classified as having sporadic ALS (SALS) [27].

Since the discovery of superoxide dismutase 1 (SOD1) mutations as a cause of FALS in 1993, our understanding of the genetic architecture of ALS has increased substantially. Currently, it is estimated that 68% of people with FALS have an identified genetic mutation, while in the remaining cases, the affected gene is unknown (Figure 1). More than 40 genes have been linked to the onset or increased risk of ALS. Among these, four genes [C9orf72 (chromosome 9 open reading frame 72), SOD1, TARDBP (TAR DNA-binding protein, which codes for TDP-43), and FUS (fused in sarcoma)] are responsible for about 60% of FALS cases and 10% of SALS cases in populations of European descent (Figure 1) [25,28–30].

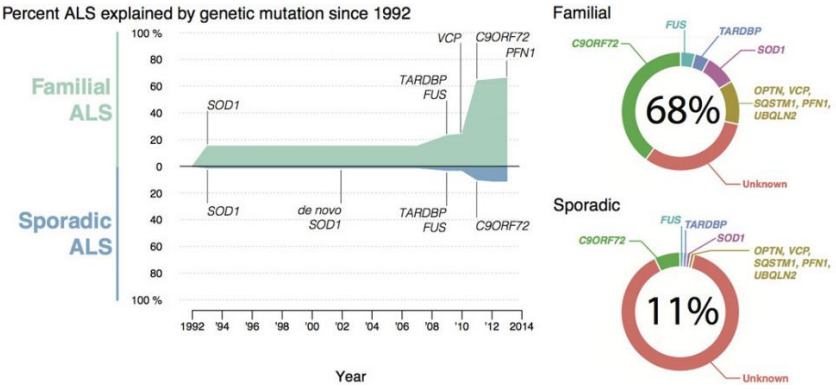

Figure 1. Genetic mutations associated with FALS and SALS [28]. *Abbreviations: SOD1 (Superoxide Dismutase 1), TARDBP (TAR DNA-binding Protein), FUS (Fused in Sarcoma), C9orf72 (Chromosome 9 open reading frame 72), VCP (Valosin Containing Protein), PFN1 (Profilin 1), OPTN (Optineurin), SQSTM1 (Sequestosome 1), UBQLN2 (Ubiquilin 2).*

The intronic hexanucleotide expansion (GGGGCC) of the gene C9orf72 is the most common genetic mutation associated with approximately 40% of FALS and 7% of SALS cases [31]. The number of repeats in healthy individuals is usually fewer than twenty, whereas in ALS patients it can exceed hundreds or even thousands [32,33]. The protein encoded by this gene is involved in the nucleocytoplasmic transport of messenger RNA (mRNA), as well as the control of lysosomal function and autophagy [34].

The SOD family, designated by enzyme code EC1.15.1.1, includes a group of metalloenzymes that play a crucial antioxidant role by catalyzing the conversion of superoxide radicals ($O_2^{\bullet -}$) into oxygen (O_2) and hydrogen peroxide (H_2O_2). This process is fundamental to protecting cells from damage induced by

oxidative stress. In eukaryotic organisms, SOD activity is categorized into three main types of enzymes based on their metal cofactors and cellular localization. These include the copper-zinc SOD (Cu/ZnSOD or SOD1), which is found in the cytoplasm or secreted into the extracellular fluid; manganese-containing SOD (MnSOD or SOD2), located within the mitochondrial matrix; and extracellular SOD (EC-SOD or SOD3) [35–37].

Approximately 20-25% of FALS patients have mutations in the long arm of chromosome 21 (21q22.11), where the gene encoding SOD1 is located [38]. Initially, ALS mutant SOD1 was attributed to increased sensitivity to oxidative stress. However, silent SOD1 mutations in experimental models do not cause ALS [39], and null mutations are not present in ALS patients [40]. Furthermore, mutant SOD1 is unstable and tends to form cytoplasmic aggregates, which include other proteins such as TDP-43. Mutant SOD1 regulates basal autophagy by stabilizing three different mRNAs: atg7, raptor, and dynactin 1 [34,40–42]. Alterations in their folding, solubility, and/or degradation result in neuronal damage [43], consistent with the finding of inclusion bodies immunoreactive against mutant SOD1 in MNs of FALS patients [44–46]. Recent *in vivo* observations have demonstrate that inside the spinal cord, SOD1 aggregates are transported to neighboring MNs, a process assisted by oligodendrocytes

[47,48]. All this suggests that accumulation of mutated proteins is a main cause of toxicity in MNs [39,49,50] and could be part of the underlying mechanism involved in the propagation of the disease (a mechanism still to be elucidated).

Mutations in the genes encoding TDP-43 or FUS (transcription repressor fused oncogene) are associated with 5% and 1% of FALS and SALS cases, respectively [51,52]. As detailed in Figure 2, TDP-43 and FUS are involved in DNA-RNA binding and transcription, RNA splicing, miRNA synthesis, and mRNA transport to the cytoplasm [53].

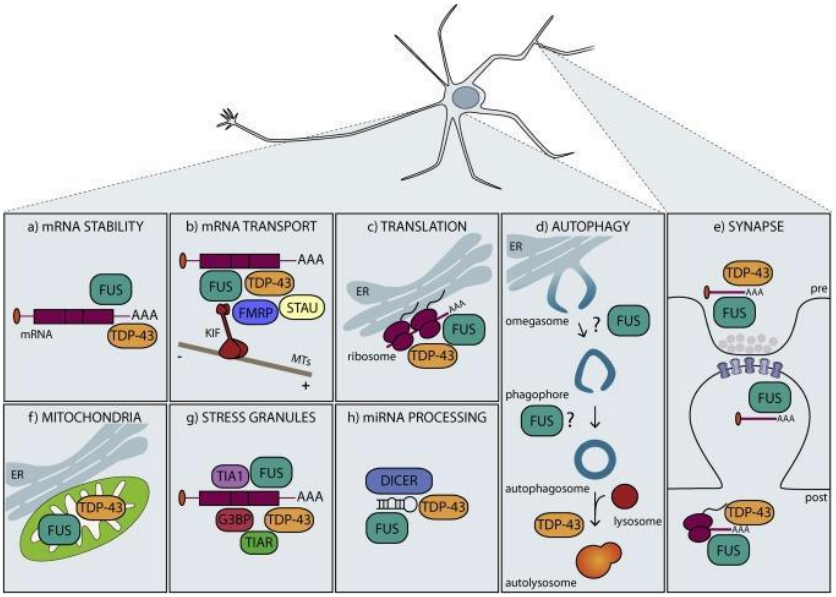

Figure 2. Functions of TDP-43 and FUS and their roles in ALS [54]. *Abbreviations: FUS (Fused in Sarcoma), TDP-43 (TAR DNA-binding Protein 43, product of the TARDBP gene), FMRP (Fragile X Mental Retardation Protein), STAU (Staufen), KIF (Kinesin Family), MTs (Microtubules), ER (Endoplasmic Reticulum), TIA1 (T-Cell Intracellular Antigen 1), TIAR (TIA1-Related Protein),*

G3BP (GTPase Activating Protein, SH3 Domain, Binding Protein), DICER (Dicer enzyme).

Under stress conditions, TDP-43 is translocated to form part of cytoplasmic aggregates known as "stress granules" (membraneless structures composed of mRNAs, upstream transcription factors, 40S ribosomes, and RNA-binding proteins), where it is sequestered along with different RNAs not involved in the stress response. Once the stress is overcome, the aggregates dissociate (by peptidases and chaperones), and TDP-43 returns to the nucleus, releasing RNAs that can be translated again. Prolonged stress and/or TDP-43 mutations induce the sequestration of mRNAs and proteins in stress granules, inhibiting their translation [55].

Silencing of the TARDBP and FUS genes has not been identified as a cause of ALS, ruling out loss of function as the origin of the disease [56]. Cytoplasmic TDP-43 inclusions are observed in approximately 97% of all ALS cases [27]. While TDP-43 typically resides in the nucleus, in ALS, it is often found mislocated in the cytoplasm, where it undergoes significant post-translational modifications or truncations [57]. This mislocalization disrupts the normal processing of RNA, affecting critical proteins like stathmin-2 (STMN2), which is essential for the stability of microtubules. The reduction in STMN2 levels compromises axonal growth and the functionality of MNs [58]. Notably, the

presence of TDP-43 inclusions does not coincide with aggregates of FUS or SOD1, despite TDP-43 and FUS sharing functions as DNA (deoxyribonucleic acid)/RNA (ribonucleic acid) binding proteins involved in the regulation of transcription, RNA splicing, localization, and degradation [59,60].

The remaining ALS-associated mutations (Table 1) are less frequent and/or occur in geographically isolated locations [61–64]. The inheritance pattern in the majority of FALS cases is autosomal dominant. However, although rare, recessive inheritance patterns can also be observed in FALS, exhibiting X-linked dominant inheritance where only males are affected [64,65].

Table 1. Genes associated with ALS identified between 1993 and 2016 (modified from [63]).

GENE	YEAR	LOCI	GENETIC EFFECT	DISEASE FEATURES
C21ORF2	2016	21q22.3	AD, RF	Cytoskeletal organization
CCNF	2016	16p13.3	AD	Proteostasis
NEK1	2016	4q33	AD, AR	Cytoskeletal organization, DNA damage, and cell cycle
TBK1	2015	12q14.2	AD, DN	Autophagy; neuroinflammation
CHCHD10	2014	22q11.23	AD	Mitochondrial function, cellular bioenergetics
MATR3	2014	5q31.2	AD	Ribostasis

TUBA4A	2014	2q35	AD	Cytoskeletal organization, axonal transport
HNRNPA1	2013	12q13	AD, DN, RF	Ribostasis
HNRNPA2B1	2013	7p15	AD, RF	Ribostasis
PFN1	2012	17p13	AD	Cytoskeletal organization, axonal growth and transport
C9ORF72	2011	9p21	AD	Intracellular trafficking, autophagy, proteostasis, global RNA alterations, nucleocytoplasmic transport
SQSTM1	2011	5q35	AD	Autophagy, neuroinflammation
UBQLN2	2011	Xp11	AD, XL	Proteostasis
ATXN2	2010	12q24	AD, RF	Ribostasis, nucleocytoplasmic transport
OPTN	2010	10p13	AD, AR	Autophagy; neuroinflammation
SPG11	2010	15q14	AR	DNA damage
VCP	2010	9p13	AD, DN	Proteostasis
ANG	2006	14q11	RF	Angiogenesis
ELP3	2009	8p21	UD	Ribostasis, cytoskeletal integrity
FUS	2009	16p11	AD, AR, DN	Ribostasis, nucleocytoplasmic transport
TARDBP	2008	1p36	AD, AR, DN	Ribostasis, nucleocytoplasmic transport
CHMP2B	2006	3p11	AD	Vesicular trafficking, proteostasis
VAPB	2004	20q13	AD	Proteostasis

DCTN1	2003	2p13	AD, RF	Axonal transport
ALS2	2001	2q33	AR	Vesicular trafficking
SETX	1998	9q34	AD	Ribostasis
NEFH	1994	22q12	AD, RF	Axonal transport
SOD1	1993	21q22	AD, AR, DN	Proteostasis, oxidative stress

Abbreviations: NA (not available), AD (autosomal dominant), AR (autosomal recessive), DN (de novo), RF (risk factor), UD (undefined), XL (X-linked), ANG (Angiogenin), C21ORF2 (Chromosome 21 Open Reading Frame 2), CCNF (Cyclin F), NEK1 (NIMA-Related Kinase 1), TBK1 (TANK Binding Kinase 1), CHCHD10 (Coiled-Coil-Helix-Coiled-Coil-Helix Domain Containing 10), MATR3 (Matrin 3), TUBA4A (Tubulin Alpha-4A), HNRNPA1 (Heterogeneous Nuclear Ribonucleoprotein A1), HNRNPA2B1 (Heterogeneous Nuclear Ribonucleoprotein A2/B1), PFN1 (Profilin 1), C9ORF72 (Chromosome 9 Open Reading Frame 72), SQSTM1 (Sequestosome 1), UBQLN2 (Ubiquilin 2), ATXN2 (Ataxin 2), OPTN (Optineurin), SPG11 (Spastic Paraplegia 11), VCP (Valosin-Containing Protein), ELP3 (Elongator Acetyltransferase Complex Subunit 3), FUS (Fused in Sarcoma), TARDBP (TAR DNA-Binding Protein), CHMP2B (Charged Multivesicular Body Protein 2B), VAPB (VAMP-Associated Protein B), DCTN1 (Dynactin Subunit 1), ALS2 (Alsin Rho Guanine Nucleotide Exchange Factor ALS2), SETX (Senataxin), NEFH (Neurofilament Heavy Chain), SOD1 (Superoxide Dismutase 1).

The identified ALS risk genes (Table 1) converge on several key biological pathways, including oxidative stress, dysregulation of mitochondrial function, protein homeostasis, RNA processing, axonal transport, nucleocytoplasmic transport, neuroinflammation, excitotoxicity, and DNA damage [63].

Susceptibility to ALS and the pathogenic nature of its associated genes can differ significantly. Genes directly related to the onset of ALS, such as TARDBP, SOD1, and FUS, usually cause the disease. In contrast, other genes such as angiogenin (ANG),

ataxin 2 (ATXN2), and dynactin subunit 1 (DCTN1) do not directly cause ALS but increase the risk of developing the disease. However, it is important to note that even genes directly associated with the onset of ALS do not necessarily guarantee that the disease will manifest, as these genes are not fully penetrant. Moreover, environmental factors can further modify the risk. To complicate matters, a single mutation can lead to different clinical presentations, suggesting that varying mechanisms influence outcomes. Additionally, similar ALS phenotypes can result from different mutations, implying that ALS is a syndrome originating from different potential causes that share common pathophysiological pathways [66].

Considering the late presentation of symptoms and the possible recessive pattern of inheritance, it is feasible that some cases of FALS may be erroneously considered sporadic [65]. In any case, the clinical manifestations of FALS and SALS forms are identical, except for the fact that in FALS, the age of onset is usually earlier by approximately 10 years [25].

1.3.2. ALS Risk Factors

The only well-established risk factors for ALS are age and family history. However, genetic mutations are not sufficient to explain the onset and the progression rates of ALS. Even within families, not all carriers of the genetic mutation develop ALS, and the age of onset and severity of the disease can vary widely among

individuals with the same mutation [67]. This makes evident that environmental and metabolic modifiers must be considered to explain the complexity of ALS etiopathogenesis

Exposure to heavy metals (especially lead and selenium), pesticides, electromagnetic fields, solvents, β-methylamino-L-alanine, and methylphenyltetrahydropyridine has been epidemiologically linked to ALS risk [14,25,68]. It is important to mention that most of these risk factors promote oxidative stress, one of the most important mechanisms involved in ALS pathophysiology, which will be discussed later.

Physical activity, especially when linked to head injuries and physical trauma, is a documented ALS risk factor [69,70]. Football players, who are likely to suffer from head injuries, have been found to have a high incidence of ALS among American and European athletes [71]. More recently, an animal model demonstrated that repeated/chronic traumatic brain injuries induced long-lasting deficits in motor function, decreased cortical thickness, shrinkage of the corpus callosum, and early onset of ALS symptoms [72]. The high prevalence of ALS in military veterans has also been correlated to high physical demands, head injuries, exposure to environmental risk factors, or chronic and high stress [73,74].

ALS patients lose weight throughout the course of the disease, and this weight loss is a strong predictor of shortened survival.

Additionally, some studies seem to suggest that increased body mass in earlier life is associated with a lower incidence of ALS [25,75,76].

Like other neurodegenerative diseases, ALS tends to be considered the final result of interactions between genes, ageing and environmental factors/conditions. In this regard, each subject has a determined genetic load, some degree of cell damage according to aging, and a variety of environmental risk exposures. The development of ALS would then occur when the sum of these factors reaches a certain threshold [77]. In FALS cases, the genetic load and the MN damage related to ageing would be sufficient to develop the disease without the environmental influences [78]. This would be particularly relevant in aged subjects harboring ALS genetic risk variants, in which risk environmental factors could be determinants in developing ALS or not [65].

Al Chalabi et al. studied 49 ALS twin pairs [79]. Among them, 5 were concordant-affected, and 44 monozygotic were discordant-affected. After applying several statistical tests, the authors estimated the heritability of SALS around 0.6, with an unshared environmental component of 0.4 [79]. This reinforces the importance of the interaction between hereditary and environmental factors, although their respective roles or mechanisms involved in ALS etiology are largely unknown [25].

1.4. Symptomatology

As previously mentioned, ALS affects UMN and/or LMN (Figure 3) [1,2,80]. In the vast majority of cases, the sensory system, cognitive functions, control of eye movements, and anal and bladder sphincters remain unaffected [81].

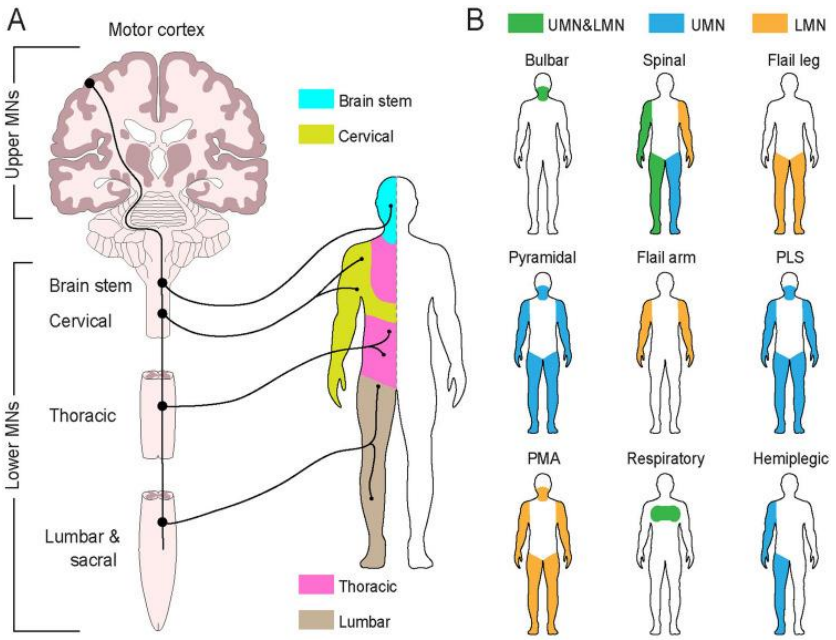

Figure 3. Anatomical Overview of ALS Phenotypic Variants and Their Impact on Motor Function Patterns [80]. *(A) Diagram of the human central nervous system showing locations and innervation distribution of various MNs, including UMN and LMN. (B) Patterns of motor involvement in ALS phenotypes, ranging from cranial nerve paralysis to limb-specific or generalized muscle degeneration, including respiratory forms [80].*

The highest incidence of SALS is typically observed between the ages of 50-75, and 40-60 for FALS [14]. However, there are cases occurring in individuals under the age of 25, which is classified as

juvenile ALS (JALS) [4]. The most common genetic basis associated with JALS includes variants in FUS, alsin Rho guanine nucleotide exchange factor (ALS2), senataxin (SETX), and spastic paraplegia 11 (SPG11) genes. In addition, several other genes have been linked to JALS based on single case reports or case series [82].

Clinical manifestations differ depending on whether UMN or LMN are initially affected. Spinal involvement of LMN is the most frequent form (about 70%) and manifests with asymmetric loss of strength (gradually developing in the extremities), early onset of fasciculations and cramps that may progress to hypotonia, progressive muscle weakness, areflexia, atrophy, and paralysis that eventually affects both parts of the body. On the other hand, bulbar involvement (25-30% of cases) is usually less frequent but is characterized by a worse prognosis due to its rapid evolution. Symptoms usually include tongue twitching, difficulties in controlling facial expression, slurred or slow speech that can be difficult to understand (dysarthria), chewing, swallowing (dysphagia), etc. [18,83].

Primary ALS is considered when the UMN are initially affected without involvement of the LMN. In this case, the initial symptoms are loss of dexterity, stiffness, spasticity, clumsiness, and the inability to make difficult movements. Typically, the mouth, throat (or both) are affected first, and it eventually

spreads to the extremities. Deep muscle reflexes (regulated at the medullary level by the myotatic reflex arch) are released due to lack of cortical control, resulting in hyperreflexia [84].

The symptoms that arise from damage to the LMN of the brainstem and spinal cord are referred to as LMN syndrome. Damage to LMN cell bodies or their peripheral axons results in paralysis (loss of movement) or paresis (weakness) of the affected muscles. In addition to paralysis and/or paresis, LMN syndrome includes a loss of reflexes (areflexia) due to interruption of the efferent (motor) limb of the sensory motor reflex arcs. Damage to LMN also entails a loss of muscle tone, since tone is in part dependent on the monosynaptic reflex arc that links the muscle spindles to the LMN. A somewhat later effect is atrophy of the affected muscles due to denervation and disuse. The muscles involved may also exhibit fibrillations and fasciculations, which are spontaneous twitches characteristic of single denervated muscle fibers or motor units, respectively. These phenomena arise from changes in the excitability of denervated muscle fibers in the case of fibrillation and from abnormal activity of injured α MNs in the case of fasciculations. These spontaneous contractions can be readily recognized in an electromyogram, providing an especially helpful clinical tool in diagnosing lower MN disorders [85].

If the corticobulbar pathway is bilaterally affected (pseudo-bulbar syndrome or disorder of inappropriate emotional expression), affected patients suffer from a lack of control to express proportional emotions, resulting, for example, in a tendency to cry or laugh uncontrollably [86].

Frontotemporal dementia (FTD) is the second most prevalent type of dementia in individuals under 65, marked by the gradual deterioration of the frontal and/or temporal lobes. The relationship between FTD and ALS is evident based on clinical, pathological, and genetic features [87,88]. Both conditions are linked to mutations in a shared set of genes, with the most significant being the GGGGCC hexanucleotide repeat expansion in the first intron of the C9orf72 gene [89]. However, this genetic common background is not absolute. Variants in genes such as SOD1, FUS, and TDP-43, while predominantly linked to ALS, are infrequently associated with FTD [90]. Additionally, while mutations in genes like CHMP2B and TREM2 are rare and found in both FTD and ALS, a wider range of genes including TARDBP, DCTN1, FUS, valosin containing protein (VCP), UBQLN2, sequestosome 1 (SQSTM1), CHCHD10, TANK binding kinase 1 (TBK1), and CCNF contribute to a diverse spectrum of disorders bridging FTD and ALS (Figure 4) [91].

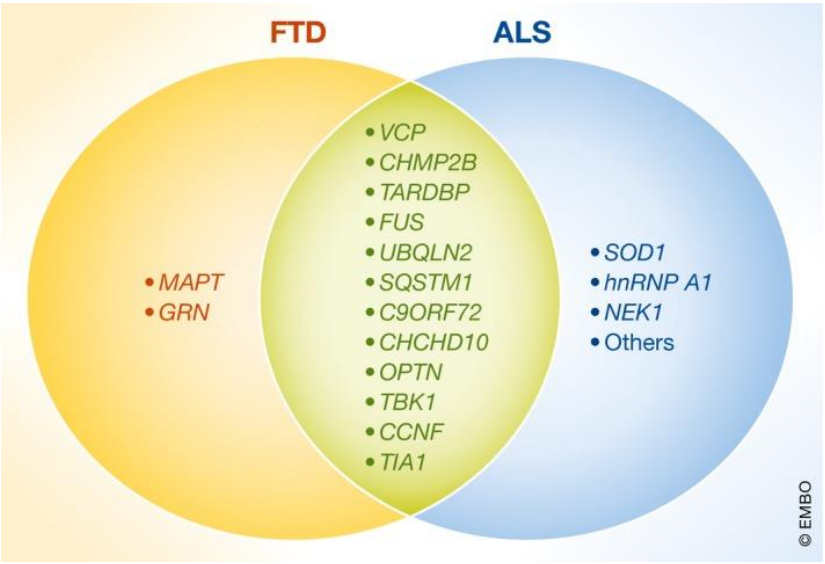

Figure 4. Genes involved in FTD, ALS or both [89]. *Abreviations: MAPT (Microtubule-Associated Protein Tau), GRN (Granulin), VCP (Valosin-Containing Protein), CHMP2B (Charged Multivesicular Body Protein 2B), TARDBP (TAR DNA-Binding Protein), FUS (Fused in Sarcoma), UBQLN2 (Ubiquilin 2), SQSTM1 (Sequestosome 1), C9ORF72 (Chromosome 9 Open Reading Frame 72), CHCHD10 (Coiled-Coil-Helix-Coiled-Coil-Helix Domain Containing 10), OPTN (Optineurin), TBK1 (TANK-Binding Kinase 1), CCNF (Cyclin F), TIA1 (T-Cell Intracellular Antigen 1), SOD1 (Superoxide Dismutase 1), hnRNP A1 (Heterogeneous Nuclear Ribonucleoprotein A1), NEK1 (NIMA-Related Kinase 1).*

Typically, affected individuals first exhibit symptoms characteristic of the behavioral variant FTD, such as changes in behavior, deficits in executive functions, and difficulties in language processing [92]. These symptoms precede the development of ALS indicators as the disease advances, and it is estimated that 3-20% of ALS patients will be diagnosed with or develop FTD. The link between ALS and dementia may not be restricted to FTD, as epidemiological investigations reveal an

elevated dementia risk among ALS patient families overall, particularly those with the C9orf72 hexanucleotide repeat expansion [93–96]. Moreover, approximately one quarter of ALS patients display subtle cognitive deficits, underscoring the complex interplay between ALS and cognitive disorders.

1.5. ALS Diagnosis

The clinical picture in advanced ALS is rather typical, but the diagnosis may not be clear at the onset of the disease. The early stages of ALS are distinguished by their wide clinical diversity rather than by presenting specific and consistent symptoms. This variability, combined with the absence of biological markers, makes early and accurate diagnosis of the disease extremely difficult [97]. Furthermore, initial symptoms of ALS mimic spinal cord diseases and mononeuropathies. The average time from symptom onset to diagnosis is approximately 1 year [98,99].

Therefore, diagnostic criteria have been developed that focus on the identification of certain clinical signs to facilitate a more rapid and accurate differential diagnosis of ALS. In 1990, a workshop on ALS was held in El Escorial (Spain) sponsored by the Federation of Neurology Subcommittee on Motor Neuron Diseases to develop ALS clinical diagnostic criteria, known as the "El Escorial criteria", which were published in 1994 [100].

According to the El Escorial criteria, clinical evidence of UMN and LMN impairment in four anatomically segmented body regions (bulbar, cervical, thoracic and lumbar) is surveyed for the diagnosis. Additionally, the progressive spreading of symptoms and the absence of electrophysiological and neuroimaging evidence of other causing diseases must be fulfilled. Patients are stratified into four categories of diagnostic certainty based on the number of affected regions and the extent of MN involvement: suspected, possible, probable, and definite ALS [100]. Although these criteria were proposed to standardize diagnosis for clinical trials, their value in allowing early clinical trial entry has been questioned, as they proved to have low diagnostic sensitivity [1].

The criteria were revised (termed as "revised El Escorial criteria") in 2000 to improve diagnostic sensitivity (Table 2). Diagnostic categories were refined with the following terms: definite, probable, clinically probable with laboratory support, and possible ALS, while the category of suspected ALS was excluded. The electrophysiological examination was implemented to support clinical findings and identify LMN involvement, with signs of active and chronic denervation by electromyography (EMG) and the exclusion of motor neuropathy by nerve conduction studies. The category of "probable with laboratory support" enhanced sensitivity, including cases with confirmatory

electrodiagnostic testing but without full clinical manifestation [101].

Table 2. Revised El Escorial classification of ALS [102].

DIAGNOSTIC CATEGORY	INCLUSION CRITERIA
DEFINITE ALS	Presence of UMN and LMN signs in three anatomical regions.
PROBABLE ALS	Presence of UMN and LMN signs in at least two regions with UMN sign rostral to LMN signs.
PROBABLE ALS, LABORATORY RESULTS SUPPORTED	Presence of UMN and LMN signs in one region with evidence by EMG of LMN involvement in another region.
POSSIBLE ALS	Presence of UMN and LMN signs in one region or UMN signs in two or three regions, such as monomelic ALS, progressive bulbar palsy, and primary lateral sclerosis.

The Awaji criteria, introduced in 2008, represented a significant advance by including electrophysiological tests, such as fibrillation and positive sharp waves, to identify LMN dysfunction, thus increasing diagnostic sensitivity [103]. The evolution of the criteria has enabled more precise and earlier diagnosis, which is crucial for the appropriate inclusion of patients in clinical studies [104]. However, the El Escorial and Awaji criteria, despite being designed to enhance the diagnostic precision of ALS, have proven complex and susceptible to misinterpretations, as reflected by the low reliability scores

[105]. Furthermore, these criteria do not predict disease progression [106].

The Gold Coast criteria were introduced to streamline the diagnostic process by clearly categorizing conditions into ALS and non-ALS [107]. To date, studies evaluating the feasibility of the Gold Coast criteria have shown an increase in diagnostic sensitivity with largely preserved high specificity [2,108]. The Gold Coast criteria have been proposed for incorporation into routine practice and clinical trial settings; however, they are not widely used at this time [109].

Although the diagnosis of ALS is primarily clinical and based on the identification of signs of dysfunction of both UMN and LMN, several tests and complementary assessments are used to support this diagnosis and exclude other conditions with similar symptoms, such as electrodiagnostic studies [110,111], magnetic resonance imaging [112], cerebrospinal fluid (CSF) analysis [113,114], and/or genetic studies [115].

Accurate and rapid diagnosis of ALS is relevant for many reasons. A definite diagnosis will relieve anxiety for the patient and their family. Diagnosis also allows initiation of earlier clinical management including possible entry into a clinical trial and permits earlier life planning and adaptations, as well requesting the necessary healthcare system support [116]. Developing diagnostic tools or blood-selective biomarkers can help

encourage general practitioners to consider ALS and make an urgent referral to ALS specialists, providing patients a more rapid diagnosis [2].

1.6. Pathophysiology

In line with the etiology, the pathophysiological mechanisms promoting the development of the disease, as well as why only MNs are affected, remain unknown. Many of the proposed mechanisms have been inferred from the functions of genes mutated in FALS (Table 1) [30,63,117–119]. These mechanisms (Figure 5), in an effort to simplify, can be grouped into the following categories: glutamate excitotoxicity [120,121], alterations in DNA repair [122,123] and RNA transport [53], abnormal protein metabolism, epigenetic mechanisms [124], formation of stress aggregates and/or granules [125,126], defective clearance of abnormal proteins [127], reactive phenotypes in astrocytes and microglia [128], neuroinflammation, oxidative stress with potentiation of the inflammatory response [129,130], mitochondrial injury [131–133], alterations in autophagy/mitophagy [134], microtubule dysfunction [135], and other problems that, in one way or another, affect axonal transport [136], neurotransmitter release [137], or induce neuronal death [138].

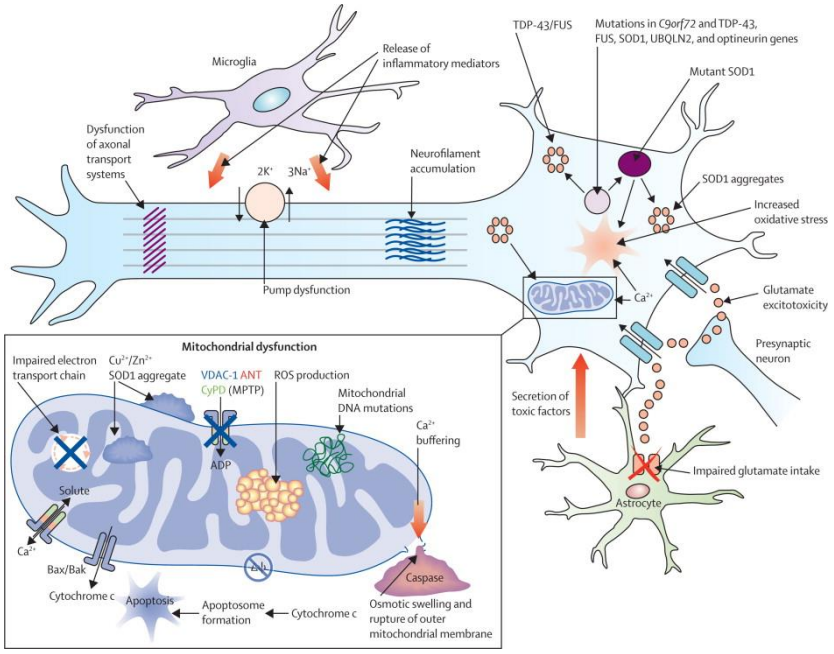

Figure 5. Mechanisms involved in ALS-associated neurodegeneration (modified from [139]). *Abbreviations: TDP-43 (TAR DNA-binding Protein 43), FUS (Fused in Sarcoma), SOD1 (Superoxide Dismutase 1), UBQLN2 (Ubiquilin 2), C9orf72 (Chromosome 9 Open Reading Frame 72), ROS (Reactive Oxygen Species), VDAC-1 (Voltage-Dependent Anion Channel 1), ANT (Adenine Nucleotide Translocator), CyPD (Cyclophilin D), MPTP (Mitochondrial Permeability Transition Pore), ADP (Adenosine Diphosphate), Ca^{2+} (Calcium ion), Bax/Bak (Bcl-2-associated X protein/Bcl-2 homologous antagonist killer), Cu/Zn (Copper/Zinc).*

1.6.1. Glutamate-Mediated Excitotoxicity

Glutamate is the most important excitatory neurotransmitter in the central nervous system (CNS) of mammals. It is synthesized from glutamine in both presynaptic neurons and glial cells. Scofield et al. demonstrated that glutamate elevation in primary cultures of cholinergic MNs favors the translocation of TDP-43 to

the cytoplasm, causing post-translational modifications that promote ALS [140].

Glutamate is removed from synapses by excitatory amino acid transporters (EAATs), with astrocyte EAAT2 being the most important in preventing synaptic accumulation [141]. The down-regulation of EAAT2 in ALS patients has been reproduced in transgenic mice expressing human SOD1 with the G93A mutation ($SOD1^{G93A}$), which is responsible for some cases of FALS [142]. MNs from $SOD1^{G93A}$ mice are sensitive to glutamate due to decreased EAAT2 expression and activity, which is exacerbated by exposure to environmental mycotoxins. Studies with knock-out models for the EAAT2 transporter resulted in neuronal death, and abnormalities in EAAT2 expression were detected in brain and spinal tissues in 80% of ALS patient autopsies [141]. Consistent with these findings, it was observed that EAAT2 overexpression in these transgenic models delayed the onset of motor deficits by increasing glutamate clearance [33].

Glutamate accumulation, EAAT2 deficit, and/or over-activation of ionotropic receptors [AMPA or N-Methyl-D-Aspartate (NMDA) and/or kainate receptors], are associated with excitatory states in pre-symptomatic stages of ALS [141,143]. This accumulation induces the activation of Ca^{2+}-dependent enzymatic cascades (MNs are particularly vulnerable due to their

poor capacity to buffer cytosolic Ca^{2+} variations), oxidative stress, and reduced glutathione (GSH) depletion, which especially affects mitochondrial function, favoring the release of proapoptotic factors [141,144]. All this compromises axonal transport [highly adenosine 5'-triphosphate (ATP)-dependent], favors the release of pro-inflammatory mediators, and leads to neuronal death [68,139].

1.6.2. Axonal Transport Damage

The extensive length of axons in MNs makes essential the transport of different cell components such as mRNA, proteins, and organelles, in both anterograde and retrograde directions. Axonal retraction and denervation occur before the loss of neuronal bodies, highlighting the relevance of axonal dynamics in disease development [50]. Increased markers of axonal damage, such as TAU and progranulin, have been observed in the CSF of ALS patients, and neuropathological analyses of post-mortem tissues have shown abnormal accumulations in MNs of phosphorylated neurofilaments (a pathological hallmark of ALS), damaged mitochondria, lysosomes, and axonal spheroids containing vesicles [136].

The most frequent associated mutations in FALS (FUS, TDP-43, and C9orf72) negatively affect axonal transport [145]. In both SOD1 models and patients, axonal transport is compromised due

to ATP depletion caused by mitochondrial dysfunction, kinesin dysfunction, and the presence of abnormal protein aggregates [146–148]. Reduced microtubule light chain expression has been observed in MNs of ALS patients [149]. Profilin-1 is crucial for actin filament polymerization, and its mutations impede axonal growth, thus favoring retraction and denervation [150].

Mutations in SOD1 and dynactin result in failures of retrograde axonal transport [151]. In addition, mutations in genes encoding neurofilament heavy chain, peripherin, dynactin, and alsin, among others, have been associated with FALS [145]. In contrast, factors that promote axonal growth and regeneration, such as endothelial growth factor, have demonstrated neuroprotective potential. Therefore, all of the above factors can influence the flow of molecules and organelles through axons, compromising MN function [43].

1.6.3. Neurotrophic Factor Deficiency

Neurotrophic factors are crucial for neurogenesis, development, and maintenance of neuronal plasticity. A decrease in these factors [CTNF, brain-derived neurotrophic factor (BDNF), GDNF, and insulin-like growth factor 1 (IGF-1)] has been reported in both post-mortem samples from patients and ALS preclinical models [152,153]. BDNF production is decreased due to glutamate-induced excitotoxicity. Similarly, mice lacking the

hypoxia response element in the VEGF promoter show an ALS-like phenotype [154]. Furthermore, BDNF, ciliary neurotrophic factor (CNTF), GDNF, GDNF, IGF-1, VEGF, hepatocyte growth factor (HGF), granulocyte-colony stimulating factor (G-CSF), and erythropoietin have been shown to offer protection against cell death, promote the maintenance of neuromuscular function, and improve survival in mouse models [155]. However, their application in clinical trials to date has not yielded the expected results [156–158].

1.6.4. Protein Aggregation

A main pathological feature of ALS is the abnormal accumulation of misfolded or aggregated proteins in affected neurons and glia [159,160]. The most common mutations in FALS (SOD1, C9orf72, FUS or TDP-43) affect RNA synthesis and transport into the cytoplasm, or promote the formation of aggregates in neuronal axons, triggering cytotoxic effects [43,161]. In TDP-43 FALS cases, the aggregates contain the mutated protein, and ubiquitinated and hyperphosphorylated cytoplasmic inclusions of aggregated TDP-43 are present in nerve cells in almost all SALS cases (>95%) [162]. The presence of these aggregates is directly related to disease progression [159], but their relationship with ALS etiopathology and progression remains unclear. In physiological conditions, when misfolded proteins

accumulate in the cytoplasm, a stress response is induced in order to facilitate their removal [56]. However, if the stress response is prolonged due to factors like ongoing accumulation, nutrient deficiency, ischemia, or toxicity, chromatolysis can occur. This process involves the fragmentation and dissolution of the endoplasmic reticulum (ER)'s cisternae, further worsening the damage and leading to the activation of programmed cell death mechanisms [25,77,159].

Lead (Pb) and zinc (Zn) have both been shown to induce TDP-43 aggregation and to be significantly elevated in ALS CSF samples. Oxidative stress has been considered a possible cause of TDP-43 aggregation because inducers of oxidative stress have been found to dislocate TDP-43 into the cytoplasm, where it forms aggregates [163]. Furthermore, the formation of TDP-43 inclusions has been linked to mitochondrial damage, which is influenced by the activation of caspases and calpains [164]. Consequently, TDP-43 inclusions can lead to neuronal toxicity either by a toxic gain of function or via disruption of physiological functions of TDP-43 in the nucleus, where its presence becomes diminished [165].

TDP-43 is not redistributed in mouse models of SOD1 mutation, suggesting a distinct pattern of TDP-43 pathology in individuals with these mutations [166,167]. This view is somewhat contested by reports indicating possible shared pathways

between FALS linked to SOD1 mutations and SALS, as some cases of SOD1-related FALS show cytoplasmic inclusions of TDP-43 [88,168]. Recent research by Robertson et al. highlighted the misplacement of TDP-43 into the cytoplasm and its link to ubiquitinated inclusions in two cases of FALS with SOD1 mutations [166]. Further studies revealed that changes in TDP-43 could play a role in the death of MNs in the spinal cord of $SOD1^{G93A}$ mice [169]. Overexpression of TDP-43 in both neurons and oligodendrocytes has been associated with MN degeneration in $SOD1^{G93A}$ mice models [170]. Additionally, SALS patient inclusions have been found to contain misfolded versions of both TDP-43 and SOD1 [88,171–173]. The connection between the alteration of TDP-43 and the onset of SOD1-related FALS remains to be understood, with comprehensive mechanisms of how SOD1 and TDP-43 interact still undiscovered.

1.6.5. Endoplasmic Reticulum Dysfunction

Extensive research highlights the critical role of ER stress in the progression of ALS [160,174,175]. The ER is pivotal for several cellular processes, including the folding of secreted proteins, calcium signaling through its role as a major calcium store, and the modification of proteins after their translation. Ca^{2+} ions are essential for transmitting neuronal depolarization and synaptic

activity. Maintaining calcium balance is crucial for synaptic plasticity and neuron survival. Disruptions in calcium balance can lead to neurotoxic effects, contributing to neurodegenerative disease progression. Furthermore, the buildup of misfolded proteins can exacerbate ER stress. If the stress response is prolonged, it can lead to ER dysfunction and impair the ubiquitin-proteasome system, which in turn causes oxidative and nitrosative stress [160]. Activation of the unfolded protein response, a mechanism to mitigate such stress, can diminish the capacity of glial cells to support synapses and is linked to neuronal death [160].

Additionally, abnormalities in the ER's mitochondrial-associated membranes can disrupt neuronal calcium balance, affect mitochondrial function and dynamics, ER operations, and autophagy processes, all of which can lead to axonal degeneration [176]. This complex interplay underscores the importance of ER stress in ALS pathology, influencing both cellular survival mechanisms and the progression of neurodegenerative conditions.

1.6.6. Alterations in Autophagy

Autophagy is a critical process that prevents the accumulation of protein aggregates and restores cellular homeostasis. Numerous ALS-related mutations, including SOD1, C9orf72, TDP-43, FUS,

P62, OPTN, VCP, Ubiquilin-2, and TBK1, have been observed to negatively affect autophagy, autophagosome transport, and/or the fusion process between autophagosomes and lysosomes, resulting in the accumulation of protein aggregates [177,178]. This disruption contributes to the development and/or acceleration of symptomatology [178]. Additionally, genetic mutations that indirectly affect autophagy can also destabilize this mechanism. For example, dynactin, which together with dynein forms an essential motor complex for retrograde vesicle transport, can compromise autophagic flux and cause FALS when mutated [179].

Recent research suggests that TDP-43 stabilizes mRNAs involved in the expression of crucial components of the autophagic machinery. Consequently, the loss of function of TDP-43 inhibits autophagic flux [178]. Although the presence of protein aggregates can initiate the autophagic process, their accumulation eventually obstructs the movement of lysosomes and the fusion process, leading to the accumulation of autophagic structures in the cytoplasm of MNs, which promotes neuronal death [177]. Several autophagy regulators, such as fluphenazine and methotrimeprazine, have been tested in TDP-43 and SOD1 mutant models, achieving increased survival and reduced delocalization of TDP-43 to the cytoplasm [180].

1.6.7. Prion Behavior of Proteins Involved in ALS

Prions are proteins that can change from their normal form (PrPC) to an infectious variant, called a "prion" (or PrPres), which has the ability to replicate, spread from cell to cell, and transmit disease without the need for DNA or RNA [181], causing neuronal damage [182]. Neurodegenerative diseases such as ALS share several features with prion diseases, including the accumulation of toxic proteins in the cytoplasm that become resistant to proteases [181], and their spread along neuroanatomical pathways, which can ultimately lead to neuronal damage [182,183]. *In vitro* studies indicate that mutant SOD1, mutant TDP-43, mutant FUS, and mutant C9orf72 proteins can behave similarly to prions [126,183], whereas only mutant SOD1 and TDP-43 have this ability *in vivo* [182,184].

1.6.8. Neuroinflammation

ALS is characterized by the presence of reactive astrocytes and microglia, moderate infiltration of peripheral immune cells, and elevated levels of inflammatory mediators in motor areas of the CNS [185–187]. Microglial cells are the first line of immune defense in the CNS, and when they are unable to eliminate a toxic insult, they remain reactive and continue to recruit astrocytes and oligodendrocytes, setting up an inflammatory process that becomes chronic [188]. In samples from patients

and murine models of ALS, abnormal proliferation of astrocytes (astrogliosis) surrounding degenerating MNs, as well as overexpression of inflammatory markers, including cyclooxygenase-2 (COX-2), inducible nitric oxide (NO) synthase (iNOS), nuclear NO synthase (nNOS), and molecules that impede the repair of damaged axons, are observed [189]. Spinal cord-derived astrocytes from SALS or FALS patients have been shown to exert a cytotoxic effect on cultured MNs [190]. Furthermore, in murine models of ALS, mast cells and neutrophils accumulate around the motor axons of the extensor digitorum longus muscle, sciatic nerve, and ventral roots, indicating that immune cell infiltration has far-reaching consequences along the entire peripheral motor pathway [191].

In activated microglia cells, there is evidence of increased ER-associated stress, a marked increase in autophagic vesicles and secretion of pro-inflammatory cytokines [e.g., TNF-α, interleukin-1 beta (IL-1β), interleukin-12 (IL-12), interferon gamma (IFN-γ)] with neurotoxic effects on MNs [185]. Cytokines such as interleukin-1 receptor-associated kinase 1 (IL-1α), TNF-α, and C1q (Complement Component 1q) further induce the A1 subtype of reactive astrocytes, which have been shown to be key in neuronal death in ALS and other neurodegenerative diseases [190]. Pro-inflammatory cytokines such as GM-CSF, interleukin-2 (IL-2), interleukin-6 (IL-6), interleukin-15 (IL-15), interleukin-17

(IL-17), monocyte chemoattractant protein-1 (MCP-1), macrophage inflammatory protein 1 alpha (MIP-1α), TNF-α, and VEGF appear normally elevated in the CSF of patients [192] and murine models of ALS [130,193,194]. IL-6 levels in astrocyte-derived exosomes are increased in ALS patients [195], and a significant negative correlation between the ALS Functional Rating Scale-Revised (ALSFRS-R) global score and serum IL-6 levels has also been described in ALS patients [196], suggesting the possibility of using it as indicative biomarker of progression.

Despite increasing evidence linking neuroinflammatory processes and neuronal death in ALS, during the early stages of the disease, the immune response seems to have a protective effect [197]. Glial and T cells, antibody-mediated immune response inducers (Th-2), regulatory T lymphocytes (Treg), and especially M2 macrophages/microglia, control the inflammatory response, favoring the viability of MNs [198,199]. However, as the disease progresses and MN injury accelerates, a second phase of rapid progression is activated, characterized by an increase in the activity of M1 macrophages/microglia and helper T lymphocytes with pro-inflammatory effects (Th1 and Th17) [200]. In contrast, M2/Treg/Th2-mediated neuroprotective pathways are down-regulated, resulting in self-propagation of the inflammatory response and disease progression [201]. This evidence indicates the importance of neuroinflammation in the

pathophysiology of FALS and SALS (with or without associated FTD) [202].

1.6.9. Oxidative Stress

ROS are highly reactive molecules [e.g., $O_2^{\bullet -}$, H_2O_2, hydroxyl radicals ($^{\bullet}OH$), and others] generated as natural byproducts of cellular metabolism. Oxidative stress refers to an imbalance between the production of ROS and the ability of a biological system to detoxify these reactive intermediates. Thus, oxidative stress can be induced by ROS overproduction or impaired mechanisms for ROS elimination [203]. If repair mechanisms are overwhelmed, the disruption of homeostasis leads to the accumulation of molecular/cellular damage, resulting in dysfunction and, eventually, cell death [204,205]. In fact, oxidative stress is implicated in a wide range of pathology-related conditions, including aging, neurodegenerative and cardiovascular diseases, diabetes, cancer, and inflammatory disorders [129,205]. The combination of high metabolic activity, elevated oxygen consumption, limited antioxidant defenses, long axons, and limited regenerative capacity makes MNs particularly sensitive to oxidative stress [206,207].

There is abundant evidence indicating a key role for oxidative damage in the pathophysiology of ALS. Several studies have reported elevated levels of oxidative stress and inflammation

markers in the serum, spinal cord, muscle, urine, and brain samples of patients with ALS, as well as in transgenic mouse models [208,209]. Increased 3-nitrotyrosine levels, a marker of oxidative damage mediated by peroxynitrite ($^{-}$OONO), were detected in FALS and SALS patients, who also carry SOD1 mutations [210]. Biomarkers of lipid peroxidation (e.g., 4-hydroxynonenal, malondialdehyde), oxidative damage to DNA (8-hydroxy-2'-deoxyguanosine), and protein carbonyl levels are increased in the serum and CSF of patients with ALS [209,211]. Mechanisms that protect against oxidative stress are weakened in MNs obtained from ALS samples. GSH depletion promotes neurological deficits, mitochondrial dysfunction, and MN degeneration in mutant SOD1 ALS mice [212]. Levels of GSH are lower in the motor cortex of ALS patients compared to healthy volunteers [213].

In addition, the nuclear factor erythroid 2-related factor 2 (Nrf2) seems to be impaired in ALS patients as well as in cell cultures and animal models of the disease [214,215]. Nrf2 protein levels were also shown to be reduced in primary MN cultures from SOD1^{G93A} transgenic mice compared to wild-type (WT) animals [130], although the experimentally induced overexpression of Nrf2 in SOD1^{G93A} cells was able to significantly decrease oxidative stress and increase cell survival [130,215].

Biochemical and cellular studies have shown that mutations in genes such as SOD1, TARDBP, and/or the accumulation of native proteins in cytoplasmic aggregates induce oxidative stress in MNs [163]. Oxidative stress promotes the formation of acetylated TDP-43 aggregates [216]. Additionally, oxidative stress causes misplacement of both TDP-43 and FUS proteins in cellular models of ALS, indicating a disruption in RNA processing [217]. Prolonged oxidative stress also facilitates growth arrest and DNA damage-inducible protein 34 (GADD34)-mediated phosphorylation of TDP-43, a key feature of TDP-43 proteinopathy [218]. The aggregation of TDP-43 in the cytoplasm traps specific microRNAs (miRNAs) and proteins, including those encoded by the nuclear genome for mitochondrial functions, disrupting mitochondrial activity and further increasing oxidative stress. This creates a cycle of escalating oxidative stress, protein aggregation, and mitochondrial dysfunction [219].

In addition, oxidative stress exacerbates other pathophysiological processes, such as glutamate excitotoxicity and mitochondrial damage, which compromises neurotransmitter release and is aggravated by the formation of protein aggregates, ER stress [220], and activation of the inflammatory response, along with loss of neurotrophic factors, all leading to neurodegeneration [221].

Although evidence of oxidative damage in ALS pathogenesis has been largely described in the literature, excepting edavarone, most antioxidants tested in patients (vitamin E, coenzyme Q10, dexpramipexole, melatonin, AEOL 10150) have so far failed. These facts question whether antioxidant therapies may be effective for ALS treatment [129].

1.6.10. Mitochondrial Dysfunction

MNs are particularly vulnerable to mitochondrial damage (Figure 6) due to their high ATP requirements (to maintain electrical activity, axonal transport, etc.), their sensitivity to alterations in Ca^{2+} homeostasis (linked to neurotransmitter release), and because the accumulation of oxidative stress damage is favored by their long biological lifetime [144,163,222]. In fact, mitochondrial dysfunction is considered a key neuropathological signal in ALS, to the extent that some works suggest that ALS may be a mitochondrial neuropathy [223–225,133]. Several evidences support this hypothesis [226]: a) the mitochondrial morphological alterations observed in spinal cord samples from ALS patients [227]; b) the activity of complexes I-IV of the electron transport chain is reduced in circulating lymphocytes from ALS patients [228]; c) several genetic mutations causing FALS are associated with mitochondrial dysfunction [229,230]; and d) other mitochondrial alterations, such as—voltage-

dependent anion channel inhibition, inactivation of mitochondrial sirtuins (SIRTs), or defects in autophagy/mitophagy mechanisms have been detected in ALS murine models or patients [133,231].

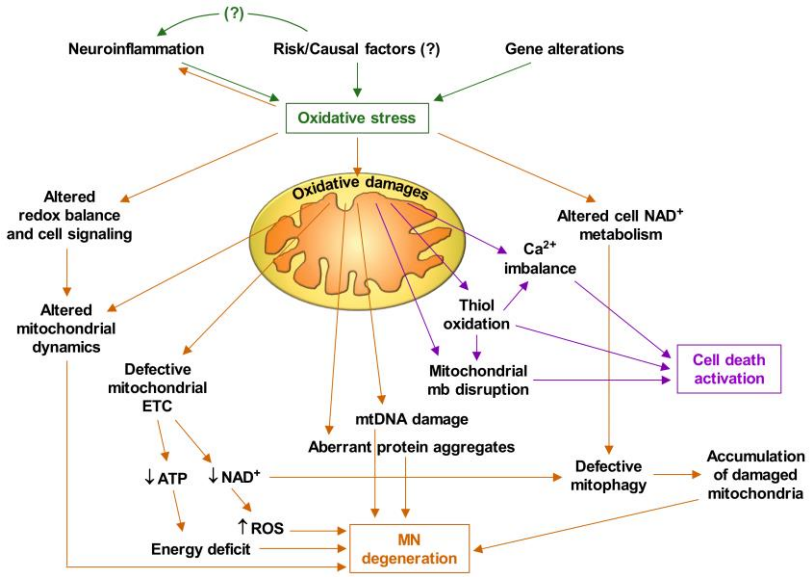

Figure 6. Oxidative stress and inflammation lead to mitochondrial dysfunction [232]. *Abbreviations: ETC (electron transport chain), mtDNA (mitochondrial DNA), mb (membrane). It is suspected that this cascade of events gradually damages MNs until (a still undefined) a-point-of-no-return threshold is reached and cell deterioration and death are irreversible.*

SIRTs are a class of proteins that possess either mono-ADP-ribosyltransferase or deacylase activity, including deacetylase, desuccinylase, demalonylase, demyristoylase, and depalmitoylase activity. From *in vitro* studies, SIRTs are implicated in influencing cellular processes like transcription,

apoptosis, inflammation and stress resistance, as well as energy efficiency and alertness during low-calorie situations [233,234]. In particular, Sirtuin 3 (SIRT3) regulates the expression of several mitochondrial enzymes (such as acetyl-CoA synthase-2 and glutamate dehydrogenase) and prevents oxidative damage to mitochondria. Its deficit causes hyperacetylation (and consequent loss of function) of superoxide dismutase 2 (SOD2) and other important mitochondrial proteins [e.g., cyclophilin D, which promotes opening of the transient permeability pore (TPP)] involved in the adaptive responses of neurons to stress and resistance to degeneration [235]. On the other hand, increased sirtuin 1 (SIRT1) expression (predominantly localized in the nucleus in normal cells) contributes to preventing oxidative stress [130,236] and maintaining mitochondrial homeostasis and mitophagy, and has been hypothetically linked to increased longevity [237]. Both SIRTs are negatively regulated as ALS progresses [238], which favors the release of proapoptotic signals and the consequent neuronal death. Reduced intracellular nicotinamide adenine dinucleotide (NAD^+) content reduces the activity of SIRTs, with deleterious effects on mitochondrial biogenesis and function [239], worsening ALS progression [130,240]. In contrast, elevated NAD^+ levels attenuate the neurotoxic phenotype of astrocytes in $SOD1^{G93A}$

mice [241] and likely contribute to delay disease progression [130,193,194,240].

Mitochondrial abnormalities in skeletal muscle have also been described in ALS patients, including increased mitochondrial volume, presence of paracrystalline inclusions, ruptured cristae, etc. [242]. Mitochondrial SOD2 is the enzyme responsible for superoxide radical scavenging, and its expression is reduced by 40% in skeletal muscle samples from ALS patients [243]. Consistent with this, oxidative stress damages have been evidenced in skeletal muscle from ALS patients and $SOD1^{G93A}$ mice [244]. These mice also showed increased expression of cyclophilin D, thus favoring mitochondrial membrane depolarization, additional ROS generation and release of proapoptotic signals [245]. The importance of mitochondrial dysfunction in the origin and progression of ALS is supported by the conclusions of a recent meta-analysis that compiles the results of 73 publications showing that therapies aimed at treating mitochondrial dysfunction in animal models of ALS significantly improve the survival of treated groups, provided that treatment is initiated before the development of the disease or in its early stages [246].

The complex nature of ALS pathophysiology overlaps different mechanisms and makes necessary to validate early

diagnosis/prognosis biomarkers to ensure that each patient receives the best treatment options (Figure 7).

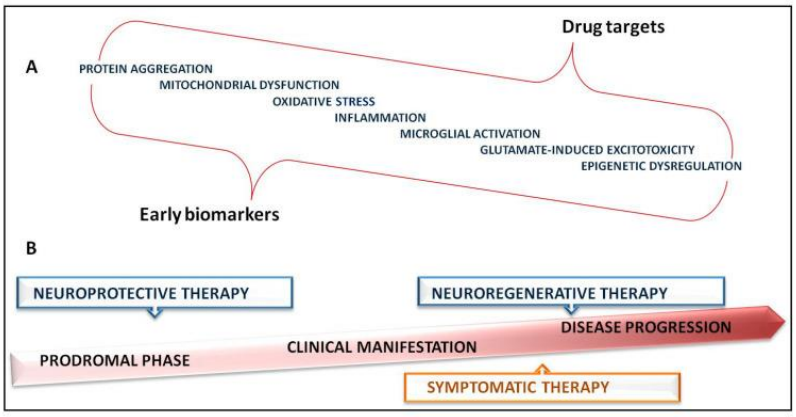

Figure 7. Main mechanism involved in ALS pathophysiology condition and therapeutic strategies for ALS patients [226]. *(A) Pathogenic mechanisms crucial for the identification of biomarkers and drug targets; (B) timeline of therapeutic possibilities.*

1.7. ALS Treatment

Currently, there is no cure for this fatal disease. In most countries, the only approved medications for treating ALS are Rilutek (riluzole), Radicava (edaravone), Qalsody (tofersen), and Relyvrio (sodium phenylbutyrate/taurursodiol) [247]. These drugs have shown the ability to significantly slow the progression of the disease in some patients, as measured by the ALSFRS-R. Nevertheless, at best, these medications can provide a few months of extension in autonomy and increase life expectancy

[248–251]. In any case, early diagnosis is crucial to improving treatment effectiveness [175].

Due to the absence of effective treatments, patients are offered supportive treatment to alleviate symptoms and improve their quality of life. This supportive healthcare is most effectively delivered by integrated, multidisciplinary teams consisting of different professionals i.e., physicians, pharmacists, physical therapists, occupational therapists, speech therapists, respiratory therapists, nutritionists, social workers, clinical psychologists, as well as home care and hospice nurses.

1.7.1. Specific Pharmacological Treatment

As stated above, approved drugs for ALS are quite limited.

1.7.1.1. Riluzole

Riluzole (1,6-(trifluoromethoxy)-2-benzothiazolamine, PK 26124, RP 54274, RILUTEK) was originally investigated for its anesthetic and anticonvulsant properties, both linked to its capacity to interfere with glutamate neurotransmission in biochemical, electrophysiological, and behavioral experiments [252]. Riluzole has neuroprotective effects *in vitro*, protecting primary cultures of rat cortical neurons against anoxic stress and against an exctotoxic factor present in CSF of ALS patients. Furthermore, riluzole protected the wobbler mouse, one of the most useful models of MNs degeneration, from glutamate

excitotoxic effects and increase motor behavior, thus diminishing MNs loss [253]. Despite the absence of a clear consensus on the exact mechanism of action of riluzole in ALS *in vivo* [157], the drug received in 1993 a marketing authorization by the *Food and Drug Administration* (FDA) based on the results of three phase III clinical trials [254–256]. These studies, involving more than 1,000 patients, showed a modest increase in survival of 2-4 months in those treated with riluzole. Although it has been noted that the drug may delay the need for tracheostomy, there is no evidence that it improves motor or pulmonary function, fasciculations, or muscle strength [257]. The adoption of riluzole in ALS treatment was reflected a desperate need for therapeutic options [258].

As schematized in Figure 8, this drug inactivates voltage-dependent sodium channels in the pre-synapse (1), a vital process in the modulation of neuronal activity [259]. At higher doses, riluzole also impacts Ca^{2+} channels (2), effectively reducing the release of glutamate, an essential but potentially harmful neurotransmitter if released in excess. At concentrations higher than those commonly used *in vivo*, riluzole inhibits NMDA (4) and kainate (6) receptors at the postsynapse, hence contributing to the regulation of neuronal excitability [257,260]. In addition, riluzole increases the amount of EAAT2 (7) transporters in glial cells [261]. This action favors

the clearance of glutamate from the synaptic space, maintaining a proper balance and preventing excitotoxicity.

In inflammation, riluzole inhibits phospholipase A2, reducing arachidonic acid production, protein kinase C activity, and the consequent release of pro-inflammatory substances [262].

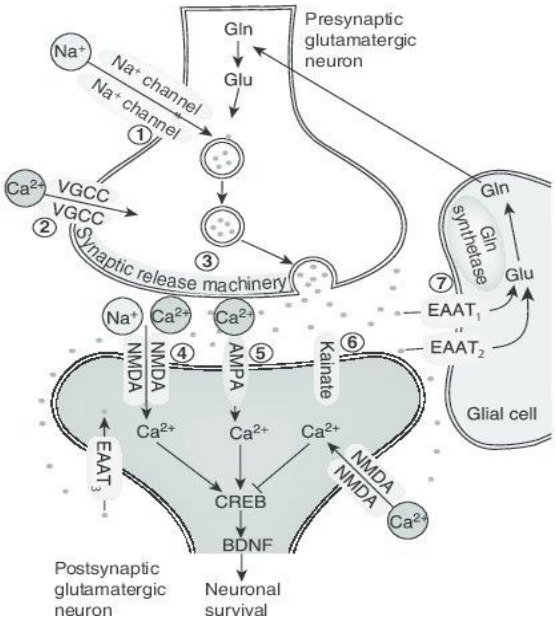

Figure 8. Proposed mechanisms of action of riluzole [259]. *Abbreviations: BDNF (brain-derived neurotrophic factor), Ca^{2+} (calcium ion), CREB (cyclic adenosine monophosphate response element binding protein), Gln (glutamine), Glu (glutamate), Na^{+} (sodium ion). See text for details.*

At even higher doses, the drug enhances axonal transport by inhibition of neurofilament phosphorylation, a crucial aspect for the maintenance of neuronal function [175]. This mechanism is important to ensure efficient transport of nutrients and signaling in neurons. In addition, it stimulates the production of

neurotrophic factors such as NGF, GDNF and BDNF in astrocytes and/or neurons [257,263]. These factors are vital for nerve cell survival and regeneration, underscoring riluzole's ability to promote neuronal health and support. Some authors recommend its use in combination with antioxidant vitamins (E and C) and creatinine, although there are no controlled studies demonstrating the benefits of these combinations [264].

1.7.1.2. Edavarone

Edaravone (3-methyl-1-phenyl-2-pyrazolin-5-one) is a drug used in both Japan and the US to treat stroke, and was approved by the FDA for the treatment of ALS in May 2017. Its therapeutic efficacy is based on its antioxidant effects and its ability to neutralize free radicals, slowing, according to clinical trials, disease progression [265,266]. In ALS mouse models , it has been shown to slow the functional deterioration of MNs [267]. In addition, it proved to be effective in the wobbler mouse model, where high doses (10 mg/kg) significantly reduced muscle mass loss and forelimb atrophy, as well as the number of astrocytes [265]. These reductions are associated with decreased neuroinflammation, consistent with its inhibitory effects on lipoxygenase activity [265].

This treatment seems to increase survival by a few months, being effective mainly in early stages of the disease, specifically

when the patient is still able to work and perform domestic activity [268]. However, in more advanced stages, where the patient lives independently but cannot work and needs assistance for activities, its effectiveness is very limited or null [269]. It is commonly used in combination with riluzole in stage 1 patients with preserved vital capacity [267].

The drug is administered intravenously (i.v.) in daily cycles for two weeks, followed by two weeks without treatment [267]. The half-life of the drug is approximately 4.5-6.0 hours, suggesting that more frequent administration may be beneficial. It is contraindicated in children, old adults, during pregnancy and lactation, and in cases of renal and liver disease [270].

1.7.1.3. Relyvrio

Relyvrio is an innovative treatment for ALS, approved by the FDA in 2022. This drug is a combination of two compounds: sodium phenylbutyrate and taurursodiol, each with a mechanism of action targeting different aspects of ALS pathogenesis. Sodium phenylbutyrate acts by reducing ER stress in nerve cells, while taurursodiol protects and helps to maintain mitochondria function [271].

According to the results of the CENTAUR trial (NCT03127514), published in the *New England Journal of Medicine*, patients treated with Relyvrio showed a slower decline in function

compared to those who did not receive the treatment [271]. Participants from the CENTAUR trial were eligible for enrollment into the Open-Label Extension (OLE) trial (NCT03488524) evaluating the long-term effects of Relyvrio in patients with ALS for a duration of up to 132 weeks. The survival analysis of participants in CENTAUR indicated that the risk of death was 44% lower among those originally randomized to the trial medication compared with those randomized to placebo (hazard ratio [HR], 0.56; 95% CI, 0.34-0.92; P = 0.023). The median survival duration was 25 months for the treatment arm versus 18.5 months for the placebo arm [272]. These findings suggested that Relyvrio may have a positive impact on the survival of ALS patients, although further studies are required to confirm these long-term benefits. Nevertheless, recently, Amylyx Pharmaceuticals announced that Relyvrio did not show significant benefit in the PHOENIX phase III trial (NCT05021536) and may be withdrawn from the market.

1.7.2. Therapy for Symptomatology Relief

To treat the symptoms derived from the pathogenic processes of this disease, the following drugs are commonly used (adELA, 2014) [273]:

- Spasticity: due to degeneration of UMN. Treatments of choice: Baclofen, Diazepam, or botulinum toxin injections.

- Sialorrhea: to minimize the difficulty in swallowing saliva, amitriptyline, anticholinergics, antihistamines (e.g. diphenhydramine), glycopyrrolate, scopolamine patches, and atropine sulfate can be administered. If salivary secretion is very dense, propanolol can be added. Another option is the infiltration of botulinum toxin.
- Pain: Pain can be treated with non-steroidal anti-inflammatory drugs, tricyclic antidepressants, antiepileptics (for neuropathic pain) and opioids.
- Pseudobulbar symptoms: manifested as swallowing and phonation disorders, loss of tongue mobility and spasmodic laughter. The drug of choice is amitriptyline. Others: SSRIs, lithium carbonate, and L-dopa.
- Fasciculations: due to contractions of motor units secondary to impulses arising in the distal part of the motor axons. It is recommended to reduce caffeine and nicotine intake. They are treated with benzodiazepines (lorazepam), magnesium, or antiepileptics (phenytoin, carbamazepine, or gabapentin).
- Cramps due to hyperexcitability: quinine sulfate or antiepileptics (phenytoin, carbamazepine, or gabapentin) is the therapy of choice.
- Edemas: produced by prolonged immobility and lack of muscular pumping. The treatment of choice is diuretics.

- Constipation: dietary modifications and hydration, as well as laxatives such as lactulose.

1.7.3. Support Therapies

Supportive therapies involve various disciplines and strategies that focus on physical, emotional, and nutritional aspects to improve patients' quality of life and control symptoms as the disease progresses. Respiratory care is paramount, given its direct association with patient mortality, requiring devices such as insufflators to clear the airway and, when necessary, invasive ventilation [274,275]. Nutritional support is vital due to the impact of ALS on patients' nutritional status, so dieticians ensure adequate nutrition [276] and may recommend gastrostomy in severe cases to prevent malnutrition, which can accelerate disease progression [277].

Physiotherapy aims to optimize mobility and control spasticity [278], while occupational therapy enables patients to adapt daily activities to maintain their independence through assistive devices and energy conservation technique [279]. Early intervention by speech therapists addresses communication and swallowing difficulties, offering strategies and devices for safer feeding and communication [280]. Psychological support helps patients and their families overcome the emotional challenges

of ALS by providing counselling, support groups, and therapies for mental health problems [281].

This holistic approach underscores the multidisciplinary strategy needed to treat ALS, focusing on physical, emotional, and nutritional well-being to improve patients' quality of life.

1.8. Fundamentals of Our Therapeutic Proposal

As previously discussed, the progression of ALS involves complex mechanisms where oxidative stress, mitochondrial dysfunction, and neuroinflammation play a crucial role. Han et al. reported that resveratrol treatment delayed disease onset and increased survival in $SOD1^{G93A}$ mice [282]. The therapeutic benefits of resveratrol were attributed to enhanced SIRT1 activation, as evidenced by the deacetylation of p53, a key target of SIRT1. Similar results were reported by Mancuso et al., who observed delayed disease onset, prolonged survival, and improved spinal MN function in $SOD1^{G93A}$ mice, with increases in SIRT1 activation in the spinal cord [283]. However, the low bioavailability of resveratrol has restricted its clinical application [284].

Pterostilbene (PT, 3,5-dimethoxy-4’-hydroxystilbene) is a naturally derived stilbenoid primarily found in blueberries and the heartwood of the *Pterocarpus marsupium*. PT substitutes two hydroxyl groups in the resveratrol molecule with methoxy groups, a structural modification that increases PT’s lipophilicity

and half-life, allowing PT to cross the blood-brain barrier (BBB) and elevate SIRT1 and Nrf2 levels, potentially enhancing antioxidant defenses (Figure 8) in the CNS [285]. In addition to modulating the activity of antioxidant enzymes involved in the phase II response, PT has an intrinsic antioxidant capacity and has been shown to increase plasma antioxidant capacity and decrease lipid peroxidation [286]. PT mitigates inflammation (Figure 9) by decreasing inflammatory mediators, notably tumor necrosis factor α (TNF-α), interleukin (IL)-1beta (IL-1β), and interleukin-6 (IL-6); and by blocking nuclear factor kappa-light-chain-enhancer of activated B cells (NF-κB) activation, a primary promoter of inflammation [287,288]. Evidence from animal studies suggests that PT can attenuate inflammatory cell infiltration, thus helping to limit tissue damage and the propagation of the inflammatory response [289]. Interestingly, PT has also been shown to attenuate early brain injury following subarachnoid hemorrhage by inhibiting the nucleotide-binding oligomerization domain-like receptor family pyrin domain-containing 3 (NLRP3) inflammasome and NOX2-related oxidative stress, mechanisms relevant to ALS pathology given that microglial NLRP3 inflammasomes are activated by ALS-associated proteins [290,291]. The antioxidant and anti-inflammatory properties of PT suggest a valuable therapeutic role in ALS management [292].

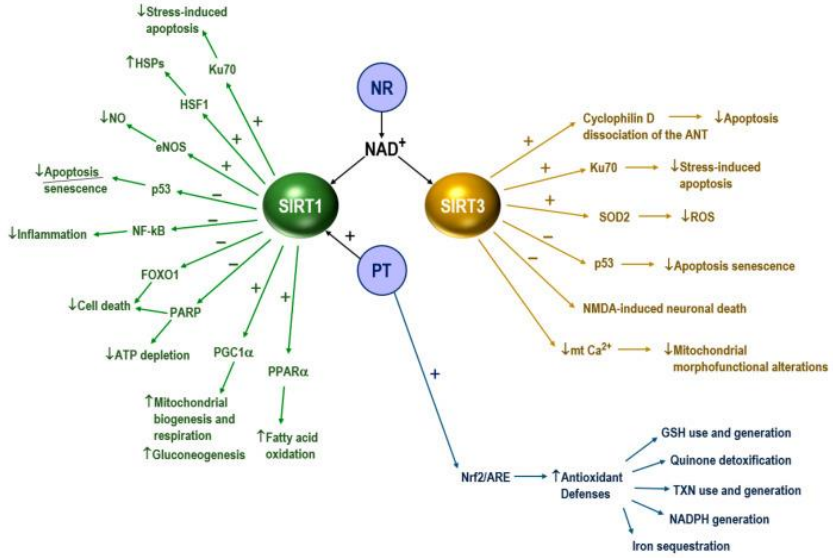

Figure 9. Molecular interactions underlying the beneficial effects of NR and PT in ALS [144]. *Abbreviations: NR (nicotinamide riboside), PT (pterostilbene) SIRT1 (sirtuin 1), SIRT3 (sirtuin 3), HSPs (heat-shock proteins), HSF1 (heat-shock factor 1), NF-kB (nuclear factor kappa-light-chain-enhancer of activated B cells), FOXO1 (forkhead box protein O1), PARP (poly (ADP-ribose) polymerase), PGC1α (peroxisome proliferator-activated receptor gamma coactivator 1-alpha), LXRs (liver X receptors), eNOS (endothelial nitric oxide synthase), PPARα (peroxisome proliferator-activated receptor alpha), Nrf2/ARE (transcription factor Nrf2, NF-E2-related factor 2, antioxidant responsive element), ANT (adenine nucleotide translocator), SOD2 (superoxide dismutase 2), NMDA (N-methyl-D-aspartate), GSH (glutathione), TXN (thioredoxin). NR increases the availability of NAD+, which supports the activity of SIRT1 and SIRT3 and their downstream targets. PT activates SIRT1 and Nrf2. Activation of Nrf2 in motor neurons (MNs) leads to the induction of many cytoprotective proteins, including but not limited to the following: (1) GSH utilization and generation (γ-glutamyl-cysteine synthase, GSH reductase, xCT (a component of the cysteine/glutamate transporter), GSH peroxidase 2, various GSH transferase isoenzymes); (2) quinone detoxification (NAD(P)H dehydrogenase (quinone 1)); (3) thioredoxin utilization and generation (thioredoxin 1, peroxiredoxin 1, thioredoxin reductase 1); (4) iron sequestration (heme oxygenase 2); (5) NADPH generation (glucose-6-phosphate dehydrogenase, phosphogluconate dehydrogenase, malic enzyme 1, isocitrate dehydrogenase 1).*

Cellular processes including redox chemistry, glycolysis, metabolism, mitochondrial respiration, and bioenergetics are dependent on electron transfer from NADH and nicotinamide adenine dinucleotide phosphate (NADPH). NAD^+ is a coenzyme that plays a fundamental role in the process of ROS detoxification and, also, in energy metabolism and mitochondrial function (Figure 9) [293]. Studies have found that NAD^+ decreases with age in certain tissues, and age-related NAD^+ depletion affects physiological functions and contributes to various aging-related diseases, including neurodegenerative diseases [294], and axon degeneration [295]. The altered expression of enzymes involved in NAD^+ synthesis (nicotinamide phosphoribosyltransferase and nicotinamide nucleotide adenyltransferase 2), and the decreased sirtuin 6 (SIRT6) expression found in the spinal cord of ALS patients suggest that ALS pathophysiology can be associated with NAD^+ deficits [296]. In fact, supplementation of NAD^+ precursors significantly elevates NAD^+ levels in murine tissues, effectively mitigates metabolic syndrome, enhances cardiovascular health, protects against neurodegeneration, and boosts muscular strength [297]. Since NAD^+ depletion is associated with neuronal death [298], it has been proposed that increasing NAD^+ availability may be neuroprotective [299]. Indeed, NAD^+ and related metabolites

are involved in the adaptation of neurons to a wide range of physiological stressors and in counteracting processes in different neurodegenerative diseases, including ALS [300]. Gerdts et al. demonstrated, using a model of sterile alpha and TIR motif-constraining 1-induced axonal death, that NAD^+ levels are rapidly depleted following axonal injury. Their findings revealed that treatment with a NAD^+ precursor effectively prevented both axonal degeneration and cell death in this context [301]. SIRTs link NAD^+ levels to mitochondrial function, dynamics and biogenesis, and to cellular antioxidant defenses [232,294]. Interestingly, under the conditions of reduced cellular energy (as occurs in the MNs during the progression of ALS), SIRTs may not consume sufficient NAD^+ to preclude any cell survival-promoting effects of its deacetylase action on protein substrates. It is also important to mention that high NAD^+ levels in ALS astrocytes increase their oxidative stress resistance and reverts their toxicity towards MNs. Enhancing of the NAD^+ salvage pathway reverses the toxicity of primary astrocytes expressing ALS-linked mutant SOD1 [241]. Consumption of NAD^+ without an adequate method of replenishment can result in decreased activity of SIRT-dependent processes, and a consequential deleterious effect on mitochondrial biogenesis, function and mitophagy [239]. Therefore, it is plausible to deduce that SIRTs deactivation may contribute to the

mitochondrial dysfunction associated with ALS. All these facts (Figure 9) suggest that ensuring the maintenance of NAD^+ levels can contribute to delaying ALS progression. We selected nicotinamide riboside (NR) as an NAD^+ precursor because of its superior pharmacokinetic profile compared to other forms of vitamin B3 such as nicotinic acid and nicotinamide [302]. Moreover, although nicotinamide mononucleotide (NMN) is a direct precursor of NAD^+, orally consumed NMN is technically a precursor NR and must be converted to NR before it can pass through cell membranes. Inside the cell, the NR converts back to NMN, and then to NAD^+ [303,304]. Given that NR can enter cells, this distinction is important to make when it comes to efficiency.

Until now, most ALS treatments have been tested using individual molecules. However, ALS is a complex pathology with multiple cellular and signaling interactions, and thus, we consider that a combined treatment should be a better therapeutic strategy. In my master's thesis, I demonstrated that a combined therapy with NR and PT is able to protect MNs against oxidative stress, increasing the expression of SIRT1, SIRT3, and antioxidant enzymes, thus slowing the loss of function and neurodegeneration associated with ALS [130,240]. In addition, treatment with NR+PT mitigated oxidative stress and mitochondrial dysfunction, and significantly prolonged survival of $SOD1^{G93A}$ mice [130]. This

combined treatment is now being evaluated in the NO-ALS Study: A Phase II Trial of Nicotinamide/Pterostilbene Supplement in ALS (NCT04562831, Norway).

Considering that neuromotor deterioration is accelerated by the inflammatory response (mainly mediated by glial cells) and loss of neurotrophic factors, our starting hypothesis is that it is possible to increase the efficacy of the NR+PT treatment by adding an anti-inflammatory drug. In order to select the best option, I conducted an exhaustive literature review, verifying the low efficacy of most of the anti-inflammatory/immunosuppressant therapies clinically assessed for ALS treatment [305–307]. For instance, treatment with anakinra (an IL-1 receptor antagonist) showed no significant difference in disease progression compared to controls, as measured by the ALSFRS-R (NCT01277315) [308]. Similarly, a recent trial (NCT02059759) testing low-dose human recombinant IL-2 (proleukin) in ALS patients found a dose-dependent increase in Treg markers, which suggests an alteration and inhibition of inflammatory pathways. However, no correlation with ALS progression was noted in the study [306]. Comparable outcomes were observed in a clinical trial using tocilizumab (an antibody blocking the IL-6 receptor) (NCT02469896) [307].

Additionally, NP001, which modulates monocytes and macrophages to transition from an inflammatory to a non-inflammatory phenotype, was tested in a phase II trial in ALS patients (NCT01281631). Although it was found to be safe and well-tolerated, NP001 did not achieve its primary endpoints [309].

Other trials at immune suppression in ALS patients include treatment with minocycline (NCT00047723) to reduce microglial activation, which resulted in worsened patient outcomes [310]. Total body irradiation and stem cell therapy showed no benefit in ALS [311,312]. Furthermore, several trials and case reports have also explored corticosteroid treatments, which generally lacked efficacy [313]. One of the most recent ones (NCT01884571) enrolled 31 ALS patients to assess the effect of immune modulation on disease progression biomarkers. Despite the use of a combination of multiple immunosuppressants (basiliximab, tacrolimus, mycophenolate mofetil, and prednisone) the regimen did not impact the rate of ALSFRS-R decline compared to the rate of decline before treatment [314].

The limited effectiveness of treatments like celecoxib (a COX-2 inhibitor) and corticosteroids can be attributed to the difficulty in reaching effective doses in the CNS, a fact that result from their limited capacity to cross the BBB; and, in addition, to the proteolytic effects of corticosteroids, which are entirely

counterproductive in a ALS patients [313,315]. Conversely, masitinib, a tyrosine kinase inhibitor, has shown potential in reducing the neuro-inflammatory activity of ALS by targeting macrophages, mast cells, and microglia in different ALS models [316,317]. It downregulates pro-inflammatory cytokines, reduces inflammation, and induces neuroprotection [317]. In a phase 2/3 clinical trial combined with riluzole (NCT02588677), masitinib demonstrated improved ALS functional rating scale results, slowed disease progression, and enhanced the quality of life of patients [318]. However, the *European Medicines Agency* (EMA) did not approve masitinib for ALS treatment due to concerns about the analysis of the trial groups. A multicenter phase III trial evaluating masitinib in ALS is currently underway (NCT03127267).

Emerging evidence demonstrates that cyclic nucleotide phosphodiesterases (PDEs), enzymes that degrade cyclic nucleotides like cyclic mdenosine monophosphate (cAMP) and cyclic guanosine monophosphate (cGMP), are implicated in the pathophysiological mechanisms of neurodegenerative diseases. PDEs regulate a wide variety of cellular functions, including inflammatory responses, cell survival, apoptosis, neuronal plasticity, neurotransmitters regulation, neurotrophic factors, synaptic function, intracellular calcium levels, astrocytic

function, oxidative stress, autophagy, and mitochondrial homeostasis [319].

Rolipram, a selective PDE4 inhibitor, has demonstrated neuroprotective effects in various models of neurodegenerative diseases by positively regulating cAMP levels in nerve cells and by modulating immune and inflammatory responses [320]. Although it has shown promise in preclinical studies due to its ability to cross the BBB, clinical trial outcomes have not been consistently effective, partly limited by significant side effects such as nausea and sleep disturbances [320,321].

Roflumilast, a PDE-4 inhibitor approved by the FDA to treat chronic obstructive pulmonary disease, has shown broad anti-inflammatory effects across various cell types and tissues [322]. Clinical trials have demonstrated its effectiveness. However, roflumilast is also associated with significant side effects, including diarrhea, weight loss, nausea, headache, and psychiatric disturbances, which can impact patient compliance [320,323].

Apremilast is marketed to treat psoriatic arthritis and moderate to severe plaque psoriasis unresponsive to topical glucocorticoid therapy [320,324–326]. Preclinical studies have demonstrated that oral administration of apremilast effectively reduces epidermal thickness and curbs irregular cell proliferation and the expression of intercellular adhesion molecule 1 (ICAM-1),

Human Leukocyte Antigen-DR isotype (HLA-DR), and TNF-α in affected skin [324]. However, clinical trials have reported several adverse effects associated with apremilast, including headache, abdominal pain, depression, weight loss, nausea, diarrhea, vomiting, nasopharyngitis, and upper respiratory tract infections [327].

Ibudilast (IBU), also known as MN-166 (3-isobutyryl-2-isopropylpyrazol-[1,5-a]pyridine) [328], is a relatively nonselective phosphodiesterase (PDE) inhibitor, available as an oral formulation, and initially used to treat asthma and stroke [319,329]. IBU effectively inhibits several PDEs, including PDE2, PDE4, PDE5, PDE10, and PDE11 [312], with a noted preferential inhibition for PDE4 [330]. As it is shown in Figure 10, IBU reduces neuroinflammation and microglial activation by downregulating pro-inflammatory cytokines such as TNF-α, IL-1β, and IL-6, and by upregulating the anti-inflammatory cytokine (interleukin-10) IL-10 [331,332]. It promotes the expression of various neurotrophic factors, including GDNF, NT-3, NT-4, and NGF, and prevents mitochondrial dysfunction by restoring mitochondrial membrane potential [332,333]. Additionally, IBU impacts the autophagy-lysosomal pathway by regulating the (mechanistic target of rapamycin complex 1 (mTORC1)-transcription factor EB (TFEB) pathway and promoting the clearance of TDP-43 and SOD1 aggregates, which helps suppress abnormal protein

aggregation [334]. Furthermore, it modulates the ubiquitin-proteasome system by regulating TLR-related ubiquitin ligase, and protects against glutamate-induced neurotoxicity by reducing Ca^{2+} influx (Figure 10). IBU also protects neurons from apoptosis by downregulating caspase-3 and upregulating B-cell lymphoma 2 (Bcl-2), and it may reduce oxidative stress by decreasing the production of ROS [319,335]. Beyond PDE inhibition, IBU also inhibits the macrophage migration inhibitory factor (MIF) and the Toll-like receptor 4 (TLR-4), which may lead to a reduction in the production of pro-inflammatory cytokines via the NF-κB pathway [319,336,337].

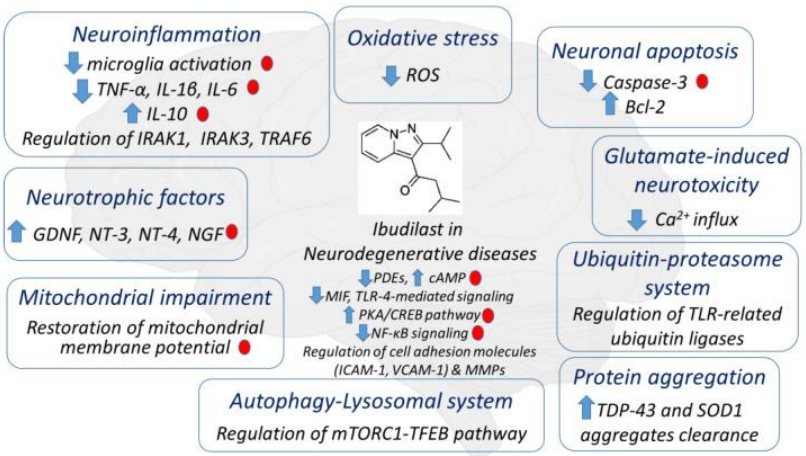

Figure 10. Potential effects of IBU on neurodegenerative diseases [319]. *Abbreviation: TNF-α (Tumor Necrosis Factor Alpha), IL-18 (Interleukin 18), IL-6 (Interleukin 6), IL-10 (Interleukin 10), IRAK1 (Interleukin-1 Receptor-Associated Kinase 1), IRAK3 (Interleukin-1 Receptor-Associated Kinase 3), TRAF6 (TNF Receptor-Associated Factor 6), ROS (Reactive Oxygen Species), Caspase-3, Bcl-2 (B-cell lymphoma 2), Ca2+ (Calcium) influx, GDNF (Glial cell line-Derived Neurotrophic Factor), NT-3 (Neurotrophin-3), NT-4 (Neurotrophin-4), NGF (Nerve Growth Factor), TLR (Toll-Like Receptor),*

TDP-43 (TAR DNA-binding Protein 43), SOD1 (Superoxide Dismutase 1), mTORC1 (Mechanistic Target of Rapamycin Complex 1), TFEB (Transcription Factor EB), PDEs (Phosphodiesterases), cAMP (Cyclic Adenosine Monophosphate), MIF (Macrophage Migration Inhibitory Factor), TLR-4 (Toll-Like Receptor 4), PKA (Protein Kinase A)/CREB (cAMP Response Element-Binding Protein) pathway, NF-κB (Nuclear Factor kappa-light-chain-enhancer of activated B cells), ICAM-1 (Intercellular Adhesion Molecule 1), VCAM-1 (Vascular Cell Adhesion Molecule 1), MMPs (Matrix Metalloproteinases).

Although the exact mechanisms by which IBU mediates these diverse cellular and molecular effects are not fully understood, the small red circles in Figure 10 highlight the specific mechanisms that seems the consequence of the IBU-induced PDE activity inhibition.

Based on the above evidence, IBU has gained increasing attention against neurodegeneration, and it is being investigated in several clinical trials for neurodegenerative diseases, including multiple sclerosis (SPRINT-MS study (SPRINT-MS, NCT01982942, study) and ALS (COMBAT-ALS, phase IIb/III NCT04057898) [326].

2. HYPOTHESIS AND OBJECTIVES

2.1. Hypothesis

ALS is a multifaceted neurodegenerative disorder characterized by intricate cellular and signaling network interactions. Our group has demonstrated that PT and NR, as a combined therapy, protect MNs against oxidative stress, slow neurodegeneration, and significantly prolong the survival of $SOD1^{G93A}$ mice [130]. Neuroinflammation (involving reactive astrocytes and microglia, and increased levels of inflammatory mediators) enhances oxidative/nitrosative stress and is involved in ALS progression. Thus, adding an anti-inflammatory agent could help improve the efficacy of PT and NR [338,339].

Previous research indicate that PDE inhibitors can reduce glial cell activation, suggesting a potential strategy to mitigate neuroinflammation [333]. In fact, these inhibitors are being considered as a possible anti-inflammatory strategy for ALS and other neurodegenerative diseases [340], and can be a good option to increase the efficacy of the NR+PT treatment.

Here we propose to test if IBU synergizes with NR and PT treatment for the following reasons:

a) PDE4 is essential for the activation of native immunity and the inflammatory response in the CNS [333].

b) IBU inhibits the release of pro-inflammatory cytokines, NO and $O_2^{\bullet-}$ production, and has the ability to cross the BBB exerting neuroprotective effects [333,334].

c) IBU facilitates the clearance of TDP-43 and SOD1 aggregates in ALS models [334].

d) As presented in the results (section 4.1), the efficacy of other PDE inhibitors (rolipram, roflumilast, and apremilast) was limited by their side effects in the ALS animal models used in this thesis.

2.2. General Objective

The aim of this contribution was to investigate whether IBU could enhance the protective effects of the NR and PT in two murine models of ALS ($SOD1^{G93A}$ and FUS^{R521C}), as well as to explore the molecular mechanisms underlying the potential therapeutic efficacy.

2.3. Specific Objectives

1. Evaluate the toxicity of PDE4 inhibitors to select the safest therapeutic option
2. To investigate the effect of NR+PT+IBU on the survival and neuromotor functions in murine models of ALS.

3. To conduct histopathological studies of the spinal cord to obtain direct morphological evidence of the effects of therapy.
4. To evaluate cell death, autophagy/mitophagy, SIRT activities, enzymes and Nrf2-dependent redox metabolites in MNs isolated from control and treated (NR+PT+IBU) mice to investigate how the treatment affects oxidative/nitrosative stress markers and mitochondrial dysfunction associated with ALS progression.

3. MATERIAL AND METHODS

3.1. ALS Murine Models and Controls

I used two transgenic mouse models ($SOD1^{G93A}$ and FUS^{R521C}) from Jackson Laboratory (Mount Desert Island, ME) chosen for their significance in neurodegenerative disease research. These models were selected due to their ability to replicate key features of ALS, making them essential tools for studying disease mechanisms and evaluating potential therapies.

$SOD1^{G93A}$: B6.Cg-Tg(SOD1*G93A)1Gur/J is hemizygous for the SOD1*G93A transgene, expressing a mutant form of human SOD1 with the G93A mutation. This genetic modification makes it a relevant model for ALS study due to the pathological aggregation of the mutant SOD1 protein. The G93A mutation in the SOD1 gene is well-documented for inducing ALS-like pathology in humans, including MN degeneration and progressive muscle paralysis [341,342].

FUS^{R521C}: B6.SJL-Tg(Prnp-FUS*R521C)3313Ejh/J expresses the mutant FUS protein R521C under the control of the Prnp promoter, leading to the accumulation of FUS^{R521C} in the cytoplasm. The R521C mutation causes cytoplasmic accumulation of FUS linked to ALS pathogenesis and has been shown to cause contributing to neurodegeneration [343,344].

Wild-type (WT): B6SJLF1/J mice [produced by crossing a C57BL/6J (B6) female with an SJL/J (SJL) male] (www.jax.org) were used as WT controls.

The experiments started when the mice were 4 weeks old and weighed between 14 and 16 grams. They were randomly distributed into different experimental groups to ensure the validity and reproducibility of the results obtained. Their health status was assessed following NIH standards (www.nih.gov), and the cages were placed in a specific pathogen-free (SPF) area to prevent contaminations that could affect the study results. They had *ad libitum* access to tap water and standard pellet feed (Altromin®, Germany), except for the mice treated with PT (see PT administration), ensuring their well-being and reducing stress, which could influence experimental outcomes.

All procedures adhered to international laws and policies (EEC Directive 86/609, OJ L 358.1, December 12, 1987; and NIH Guide for the Care and Use of Laboratory Animals, NIH Pub. No. 85-23, 1985). The mice were kept under controlled conditions, with 12-hour light-dark cycles and an ambient temperature maintained at 22°C. The experiments adhered to the 3R principles (replacement, reduction, and refinement) promoted by our institution's Animal Experimentation Ethics Committee, aiming to minimize the impact on the animals used and maximize the relevance and applicability of the study results.

3.2. NR, PT, and IBU administration

Transgenic mouse models and WT mice were treated as follows [345]:

- PT was incorporated into the feed at a dose of 30 mg/kg/day, thus facilitating continuous intake without direct intervention in the daily feeding of the mice [130]. The quantity of PT that was added to the commercial pellets was calculated from the normal diet consumed ad libitum by a mouse for 1 week. Diets were prepared by the pulverization of a commercial pelleted rodent diet (Harlan Teklad, Indianapolis, IN) into a Bapitaurus food chopper (Taurus, Berlin, Germany), followed by the addition of the required amount of PT and 150 mL of 5% gum arabic solution (Sigma-Aldrich, St. Louis, MO). The mixture was carefully homogenized, and pellets were reconstituted using a stainless-steel welded wire mesh and allowed to dry for 24 h. The concentration of PT in the reconstituted pellet was determined by high-performance liquid chromatography (HPLC) analyses. Control and IBU groups were fed with commercial pelleted rodent diet containing the same percentage of gum arabic as above. The food was stored at 4 °C and protected from light until used.
- NR (3-aminocarbonyl-1-β-D-ribofuranosyl-pyridinium, Elysium Health, Inc., New York, NY) was dissolved in vaccination-grade water, and the pH of the solution

neutralized (pH 7.0) before oral administration (185 mg/kg × day). The administration was done daily using a micropipette tip, with a volume of 25 µL per mouse.

- IBU (from Merck, Taufkirchen, Germany) was dissolved in physiological saline (PS) and administered orally at 12 mg/kg/day using a suitable tip to ensure complete ingestion [345].

The administration of NR and IBU was carried out without the need for sedation or anesthesia, between 10:00 and 10:30 am, ensuring minimal variation in experimental conditions [345].

The WT mice were treated with NR+PT, IBU and NR+PT+IBU (same doses and timing used for the ALS models), and we found no changes in cytokine levels in the CSF, in the number of MNs in the grey matter of the ventral horns, or in the neuromotor functionality, as compared to untreated WT mice (results not shown). Thus, indicating that treatment with NR, PT and IBU does not cause toxicity per se [345].

3.3. L-NAME administration

L-NAME (L-NG-nitro arginine methyl ester) was sourced from Abmole Bioscience Inc., Houston, TX, and administered via intraperitoneal (i.p.) injection. The dosage was set at 20 mg/kg daily, starting in the 18th week of the experiment and continuing

until the demise of the last mouse in the study. This method allowed us to assess the prolonged effects of NO synthase inhibition on mice ALS mice models, a crucial element in our biochemical research.

3.4. Assessment of Neuromotor Functionality

3.4.1. Neurological Score

To monitor the progression of the disease and the effectiveness of treatments in ALS mouse models, the assessment scale proposed by Weydt et al. was used. This scale objectively quantifies the severity and evolution of ALS-specific symptoms in mice, using a scoring system that ranges from "0" to "5" [346]:

- *Score 0*: Indicates a completely healthy mouse with no clinical signs associated with ALS.
- *Score 1*: Presence of tremors in the hind legs, an early symptom of the disease.
- *Score 2*: Difficulty in separating the hind legs when the mouse is suspended by the tail, suggesting initial muscle weakness.
- *Score 3*: Locomotion difficulties, evidenced by stumbling or wobbly walking, indicating progression of muscle weakness.
- *Score 4*: Inability to walk properly, with dragging of the hind legs, indicating advanced neuromotor dysfunction.
- *Score 5*: Inability of the mouse to right itself after being placed in an inverted position for 30 seconds, at which point it is

considered that the animal's quality of life has significantly deteriorated.

The progression of symptoms and the effectiveness of experimental treatments were monitored weekly in all mouse groups. The "onset" of the disease was defined as the earliest time when mice exhibited symptoms with a score less than "4", thus allowing for detailed and ongoing assessment of ALS progression. When animals reach a score of "4", food pellets are placed on the cage floor to ensure all transgenic mice have easy access to food and water. This measure guarantees their nutritional status despite the deterioration of their neuromotor functions. If a mouse reaches a score of "5", euthanasia is performed for ethical reasons to prevent unnecessary suffering.

3.4.2. Rotarod Test

For this test, a Rotarod apparatus (Rota Rod, Harvard Apparatus, Holliston, MA) was used. The objective was to measure the maximum time (in seconds) that mice could remain on a rotating rod (3.5 cm in diameter) at a constant speed of 15 revolutions per minute (rpm) without falling.

Each mouse was given up to three attempts to reach the set time limit of 1,200 seconds. The longest time that each mouse could stay on the rotating rod during any of the attempts was recorded. Variations in the performance of the different mouse groups were monitored weekly, allowing for the assessment of

the impact of treatments and the progression of diseases on neuromotor skills.

3.5. Pathology

At 17-18 weeks of age for $SOD1^{G93A}$ mice and 17-19 weeks for FUS^{R521C} mice, 4-5 mice per group were perfused with 4% chilled paraformaldehyde in phosphate buffered saline (PBS, pH 7.4) through the left ventricle. The lumbar and thoracic segments of the spinal cord were surgically isolated and fixed for 24 hours. They were subsequently embedded in paraffin for preservation and analysis.

Serial sections [2 µm thick, 20 sections at different levels (L2-L5, T5-T10)] were cut using a Leica RM2255 microtome (Leica Biosystems, Wetzlar, Germany). The sections were stained with hematoxylin and eosin (HE) to visualize the general cellular structure.

MNs were immunohistochemically stained with anti-choline acetyltransferase antibody (rabbit anti-ChAT polyclonal antibody AB143, Millipore, Burlington, MA). Microglia were stained using anti-ionized calcium-binding adapter molecule 1 (Iba1) monoclonal antibodies (mAbs) (ab5076, Abcam, Cambridge, UK). Astroglia were stained using anti-glial fibrillary acidic protein (GFAP) mAbs (ab8975, Abcam).

To quantify MNs in the spinal cord, a stereological method previously described [347] was employed to precisely delimit the counting area in the gray matter of the ventral horns. All neurons with visible nuclei were outlined using a Nikon drawing tube. The drawings were then scanned into a computer using an HP flat-bed scanner. Several parameters, including the number and size of MNs and their nuclear size, were measured from these drawings using *MetaMorph* software. Sections (28–30 per segment and animal) stained with anti-ChAT antibodies were used for quantification. Only MNs with diameters >25 µm and <25 µm and a polygonal shape were counted using a Leica DMD 108 microscope and Leica's LAS X image analysis software.

To quantify microglial and astroglial immunoreactivity, after setting the threshold for background correction, the integrated density of Iba1 or GFAP labeling was measured (14–15 sections per segment and animal) using *ImageJ* software. The integrated density represents the area above the threshold for the mean density minus the background. The *Image J Sliding Paraboloid* processing was applied to each image to minimize potential over-signaling.

3.6. Quantification of Cytokines

The procedure for collecting CSF from a mouse began by administering buprenorphine (0.1 mg/kg) to anesthetize the

mouse, confirmed by the absence of a withdrawal response to a toe pinch test. After achieving full anesthesia, the hair from the back of the head to the neck was removed. The mouse's head was then secured at a 45° angle using a mouse adapter and ear bars. The depth of anesthesia was monitored by checking the respiratory rates and toe pinch response. The dissection exposed the base of the skull with minimal muscle covering the cisterna magna. The dura mater was then carefully cleaned and dried to facilitate safe and efficient CSF collection.

For the CSF collection, a glass capillary was positioned at a 30-45° angle behind the base of the mouse's head. The system was purged using a syringe to ensure no contaminants and to maintain negative pressure. The capillary was delicately moved closer to the membrane using a micromanipulator until resistance was felt but without premature puncturing. After proper alignment, the membrane was gently punctured under microscopic observation. The CSF began to collect, and adjustments were made to the syringe to optimize the collection. After collecting the desired amount (a total amount of ~ 10–15 µL of CSF in 10–30 minutes), the system's pressure was stabilized, and the capillary was gently withdrawn. The CSF was then transferred to a microtube containing a protease inhibitor, briefly centrifuged, and stored at -80°C for analysis.

This method minimized tissue damage and contamination, ensuring precise collection.

Quantification of various cytokines in the CSF (TNF-α, IFN-γ, IL-1β, IL-2, IL-6, and GM-CSF) was performed using xMAP technology on a MAGPIX Luminex 200 platform (Thermo Fisher Scientific, Waltham, MA, USA) [130]. The procedure involved an hour-long incubation of 50 µL of CSF samples with a specific monoclonal antibody-conjugated bead population, followed by further incubation with detection antibodies (30 minutes) and a streptavidin-phycoerythrin-conjugated solution (10 minutes). The beads were then washed, resuspended in the assay buffer, shaken for 1 minute, and read by the *MAGPIX* instrument. Data were analyzed using *xPONENT 4.2®* software (Luminex, Austin, TX, USA).

3.7. Isolation and Culture of MNs, Astrocytes, and Microglia

The isolation of pure MNs, astrocytes, and microglia from adult mouse spinal cords was based on the methodology described by Beaudet et al. [348]. The spinal cords were isolated from mice anesthetized with isoflurane and then decapitated. After the removal of the pia mater, the spine was rapidly microdissected under a surgical microscope, extracting the gray matter columns from the ventral horns without significant contamination from

the dorsal horns or surrounding white matter. The gray matter from six mice was incubated with papain [2 mg/mL in Hank's Balanced Salt Solution (HBSS) supplemented with glucose and sucrose] from Sigma-Aldrich, chopped into small pieces, and digested for 30 minutes in a tissue culture incubator (5% CO_2 and 95% O_2 at 37°C). Subsequently, cold medium was added, and the remaining tissue was gently homogenized at low speed using a cold pestle tissue grinder (Thomas Scientific, Swedesboro, NJ). This step was repeated three times, and cells were centrifuged at 280 x g for 10min at 4 °C for MN extraction or at 300 x g for glia. Adult glial cells were ready to plate after this step. After this spin, the MN-enriched pellet was resuspended in 100 µL of PBS, pH 7.4, and fixed with 1 mL of 4% paraformaldehyde for cell characterization, or in 5 mL of cold L-15 medium (Thermo Fisher Scientific) and layered over a 1.06-g/mL Nycoprep density solution (Progen, Heidelberg, Germany) and spun at 900 x g for 20 minutes at 4 °C. MNs were collected at the interface of the Nycoprep solution and transferred to a collection tube. The MN collection tubes were centrifuged at 425 x g for 10 minutes in a swinging bucket centrifuge at 4 °C, and glia collecting tubes were centrifuged at 300 x g for 10 minutes.

MN pellets were gently resuspended at 100,000 cells/cm^2 (in plastic flasks coated with 10 µg/mL poly-D-lysine) in a 1:1 (v/v) ratio of the following two culture media: Neurobasal™-A

medium supplemented with 2% B-27 serum-free supplement and 0.5 mM glutamine (Invitrogen, Carlsbad, CA); DMEM/F12 medium (3:1, v/v ratio) containing 0.4 µg/mL hydrocortisone, 5 µg/mL bovine insulin (Sigma-Aldrich), and 10% fetal bovine serum (Thermo Fisher Scientific). This mixture of both media was further supplemented with 10 ng/mL human neurotrophin-3, 10 ng/mL human BDNF, 10 ng/mL rat glial-derived neurotrophic factor (GDNF), 25 ng/mL rat CNTF, and antibiotics (100 U/mL penicillin G and 25 µg/mL gentamycin) (all from Sigma-Aldrich). Adult glial cells were resuspended in this fibroblast-conditioned medium. They were placed in T75 flasks coated with poly-D-lysine (10 µg/mL) at a density of 500,000 cells per flask and incubated in a humidified incubator at 37°C for 4 days, without moving the flasks, to allow the cells to adhere. After 4 days, the cells were washed twice with complete DH medium, and fresh fibroblast-conditioned medium was added three times a week until confluence was reached.

Once confluence was reached, the cells were separated. The medium was saved for microglia culture, and the cells were treated with trypsin (0.05%) and EDTA (0.1%) at room temperature to allow the astrocytes to detach, but not the microglia. The adult astrocytes were transferred to a tube with complete medium, counted, and centrifuged at 300 x g for 10 minutes. The pellet was resuspended in fibroblast-conditioned

medium supplemented with B-27 (2%) and placed in T75 flasks coated with poly-D-lysine at a density of 500,000 cells per flask.

The purified medium for microglia was obtained by filtering the astrocyte-conditioned medium using a 0.22 μm filter, mixed in a 1:1 ratio with complete DH medium, and supplemented with 1× B-27, 40 ng/mL basic fibroblast growth factor (FGF) (Cell Sciences), 20 ng/mL epidermal growth factor (Austral Biologicals), and 5 ng/mL GM-CSF (Invitrogen). Adult microglia could take up to a month to start proliferating, and the medium was changed three times a week. When the microglia reached confluence, they were purified using a three-step Percoll gradient (Sigma-Aldrich).

For this, the cells were treated with trypsin (0.25%) and EDTA (0.1%), transferred to a tube with complete DH medium, and centrifuged at 300 x g for 10 minutes. The pellet was resuspended in 10 mL of 70% isotonic Percoll, overlaid with 20 ml of 50% isotonic Percoll, and finally with 10 mL of 1x HBSS. The gradient was centrifuged at 1,200 x g for 45 minutes in a swing-bucket centrifuge without braking. The microglia were collected from the 50-70% interface, transferred to a new tube, and filled with complete medium. The cells were counted and centrifuged again at 300 x g for 10 minutes. The pellet was resuspended in purified microglia medium and placed in T75 flasks coated with poly-D-lysine at a density of 1,000,000 cells per flask.

The purity of MNs was determined by calculating the ratio of ChAT-positive cells for each extraction over the number of unstained but 4',6-diamidino-2-phenylindole (DAPI)-positive cells after 2 days of culture. For each MN extraction, four random fields were selected for purity evaluation. Our procedure generated a cell suspension containing at least 99% MNs. To eliminate residual glial cells in the MN culture, MNs were treated 24 hours after plating with 10 µM cytosine β-D-arabinofuranoside hydrochloride (Sigma-Aldrich) for 48 hours. MNs obtained from WT and transgenic mice were stained positive for ChAT and TUJ1 (a neuron-specific marker) (mouse anti-TUJ1 monoclonal antibody, MyBiosource, San Diego, CA). The number of MNs extracted varied from 30,000 to 70,000 MNs per mouse.

3.8. MNs Compartmentation

Cytosolic and mitochondrial compartments were rapidly separated, as previously reported in detail for cancer cells [349], using digitonin and centrifugation through a layer of silicon oil. The methodology used to ensure the correct separation of the cytosolic and mitochondrial compartments was the determination of enzymatic activities present only in one of the two compartments. To this end, the activities determined as internal controls in every experiment were phosphate-

dependent glutaminase and SOD2 for the mitochondrial fraction, and LDH for the cytosolic fraction. The fractionation technique ensures that, at least, 97% of total phosphate-dependent glutaminase and SOD2 activities are in the mitochondrial fraction, and an equivalent % of the total LDH activity is in the cytosolic fraction.

To assay phosphate-dependent glutaminase activity, we followed the method described by Matsuda et al. [29], with the following modifications. Instead of using non-radioactive glutamine (Gln), we used ^{14}C-Gln with a specific activity of 250 mCi/mmol (PerkinElmer, Waltham, MA). For each assay tube, a reaction mixture containing 0.5 mCi of ^{14}C-Gln was prepared, with the total volume adjusted to 1 mL.

First, the reaction mixture was prepared by adding ^{14}C-Gln at the specified concentration. The reaction mixture included the substrate and glutaminase enzyme in the presence of phosphate, allowing the enzyme to catalyze the conversion of ^{14}C-Gln into glutamate and ammonia. The reaction was carried out at a controlled temperature of 37°C for 30 minutes.

Upon completion of the incubation, the reaction was terminated by adding 2 mL of 10% trichloroacetic acid. The mixture was then centrifuged to separate the supernatant, which contained the reaction products. The supernatant was introduced into a *Selligson-Shibata* diffusion apparatus to determine the amount

of ammonia released. After a 20-minute diffusion period at room temperature, the ammonia was quantified using the Nesslerization method.

The Nesslerization method involves the addition of Nessler's reagent (a solution of potassium iodide, mercury iodide, and potassium hydroxide) to the sample. In the presence of ammonia, the reagent forms a colored complex, the intensity of which can be measured spectrophotometrically. The color intensity is directly proportional to the ammonia concentration, allowing for precise quantification.

3.9. Lactate Dehydrogenase Activity

Lactate Dehydrogenase (LDH) activity was determined using a standard kit from Merck (MAK066, Darmstadt, Germany).

- LDH Activity Assay Kit

To prepare the reagents, allow the LDH Assay Buffer to reach room temperature before use. Reconstitute the LDH Substrate Mix in 1 mL of water, mix well by pipetting, and keep cold during use. Prepare the NADH Standard by reconstituting it in 400 µL of water, mixing well by pipetting, and keeping it cold during use. Both solutions are stable for one week at 4 °C and one month at –20 °C. Reconstitute the LDH Positive Control in 200 µL of LDH

Assay Buffer (50 mL solution of buffer components) before use. Use 2–5 µL as the positive control and keep on ice during use.

For the procedure, first prepare the NADH Standards for colorimetric detection by adding 0, 2, 4, 6, 8, and 10 µL of the NADH Standard (1.25 mM reconstituted in 400 µL water) into a 96-well plate in duplicate. This will generate standards of 0 (blank), 2.5, 5, 7.5, 10, and 12.5 nmol/well. Add LDH Assay Buffer to each well to a final volume of 50 µL. For sample preparation, homogenize 100 mg of tissue, $1x10^6$ cells, or 200 µL of erythrocytes on ice in 500 µL of cold LDH Assay Buffer. Centrifuge the homogenate at 10,000 x g for 15 minutes at 4 °C to remove insoluble material. Use the supernatant for the assay. Serum samples can be assayed directly by adding 2–50 µL into the wells of a 96-well plate. Adjust the final volume of each sample to 50 µL with LDH Assay Buffer.

Next, set up the assay reaction by preparing the Master Reaction Mix, combining 48 µL of LDH Assay Buffer (buffer components) and 2 µL of LDH Substrate Mix (1 mL reconstituted in water) for each reaction. Add 50 µL of this Master Reaction Mix to each well containing standards or samples. Mix well using a horizontal shaker or by pipetting, and protect the plate from light during incubation. After 2-3 minutes, take the initial absorbance measurement at 450 nm ($T_{initial}$). Incubate the plate at 37 °C, taking absorbance measurements every 5 minutes. Continue

taking measurements until the value of the most active sample exceeds the highest standard (12.5 nmol/well). The final absorbance measurement (T_{final}) should be taken before the sample values exceed the linear range.

To calculate the results, correct the final measurements by subtracting the absorbance of the blank standard from the absorbance of the samples. The difference between the final and initial absorbance is calculated using the following formula:

$$\Delta A450 = (A450)_{final} - (A450)_{initial}$$

A standard curve was used to relate the ΔA450 to the amount of NADH generated (B) for each sample.

Calculate the LDH activity using the formula:

$$LDH\ Activity\ = \frac{B\ \times Sample\ Dilution\ Factor}{Reaction\ Time\ \times V}$$

Where:

- B = Amount (nmol) of NADH generated between $T_{initial}$ and T_{final}.

- Reaction Time = $T_{final} - T_{initial}$ (minutes).

- V = Sample volume (mL) added to well.

- LDH activity is reported as nmol/min/mL

3.10. Isolation and culture of endothelial cells

Tissue digestion was carried out at 37 °C by sequential perfusion (through the left ventricle) with type-E pronase (0.04 % in HBSS) plus collagenase A (0.08 % in HBSS) (Boehringer, Mannheim, Germany) (15 mL, 1 mL x minute), and then with 0.1 % type-E pronase (10 mL, 1 mL x minute) [350]. Then the medulla was surgically isolated, minced and stirred (10 minutes) in another solution containing pronase (0.04 %), collagenase (0.08 %) and DNAase (type I deoxyribonuclease; Merck) (0.0005 %).

After enzymatic digestion, the solution was diluted in HBSS medium, and the entire volume was filtered through sterile nylon gauze. The filtrate was centrifuged (10 minutes, 450 g) at 4 °C and the same washing was repeated. The cell pellet was resuspended in 2.5 mL of HBSS and mixed with metrizamide previously dissolved in HBSS without Na+. Endothelial cells were separated in a 17.5 % (w/v) metrizamide gradient. After centrifugation at 950 g x 15 minutes (4 °C), the cells located in the upper gradient were separated, resuspended in DMEM, and seeded. Purity (>98 %) was checked by immunochemistry using an anti-RECA-1 monoclonal antibody (ab197727, abcam). Cultures of endothelial cells were established and maintained in pyrogen-free Dulbecco's modified Eagle's medium (DMEM; Gibco Labs., Grand Island, NY), pH 7.4, supplemented with 10 % fetal calf serum (Gibco), 10 mM 4-(2-hydroxyethyl)-1-

piperazineethanesulfonic acid (HEPES), 40 mM NaHCO3, 100 U/mL penicillin and 100 µg/mL streptomycin. Differential adhesion of endothelial cells to the collagen matrix and washing allows a complete elimination of other cell types (macrophages, lymphocytes, glia and neurons) from the culture flasks. No significant morphological differences were found comparing cells isolated from WT and SOD^{1G93A} or FUS^{R521C} mice (for more information check [345], Additional File 1: Fig. S1). Isolated endothelial cells were cultured for 24 h before any addition or measurement.

3.11. Cell Death Analysis

To differentiate between apoptotic and necrotic cell death, we employed fluorescence microscopy. Specifically, we incubated MNs with 10 mM Hoechst (Invitrogen, 33342), which stains all cell nuclei, and 10 mM propidium iodide, which targets the nuclei of cells with damaged plasma membranes. This incubation lasted for 3 minutes. Observations were made using a Nikon Diaphot 300 fluorescence microscope set to an excitation wavelength of 360 nm.

Nuclei of viable cells appeared as blue and round, nuclei of necrotic cells showed up as pink and round, and nuclei of apoptotic cells were either blue or pink and fragmented. We

counted approximately 1,000 cells for each analysis to ensure accuracy.

Additionally, to assess DNA strand breaks in apoptotic cells, we used the "In Situ Cell Death Detection Kit" (TUNEL) (Roche, 11684795910). For sample preparation, adherent cells were fixed with a 4% paraformaldehyde solution in PBS (phosphate-buffered saline, pH 7.4) for 1 hour at room temperature, followed by a rinse with PBS. The cells were then permeabilized with a 0.1% Triton X-100 solution in 0.1 % sodium citrate (freshly prepared) for 2 minutes on ice and rinsed again with PBS. Regarding reaction controls, a negative control was included by incubating fixed and permeabilized cells with 50 µL of labeling solution (without terminal transferase) instead of the TUNEL reaction mixture. A positive control was established by incubating fixed and permeabilized cells with recombinant DNase I to induce DNA strand breaks prior to labeling procedures. For the labeling protocol, the TUNEL reaction mixture was prepared by mixing 450 µl of labeling solution with 50 µL of enzyme solution, resulting in 500 µl of TUNEL reaction mixture, which was kept on ice until use. Then, 50 µL of the TUNEL reaction mixture was applied to the adherent cells, covered with parafilm or a coverslip to ensure even distribution and prevent evaporation, and incubated for 60 minutes at 37 °C in a humidified, dark environment. Following incubation, the

cells were rinsed three times with PBS. For fluorescence microscopy analysis, the samples were observed under a fluorescence microscope using appropriate filters for fluorescein (excitation: 450-500 nm, emission: 515-565 nm), where the nuclei of apoptotic cells displayed green fluorescence due to the incorporation of fluorescein-dUTP at DNA strand breaks.

3.12. ROS and NO Generation

The assays for the generation of H_2O_2 and superoxide anion ($O_2^{\bullet -}$) were conducted following methodologies previously described [351,352]. Cells were plated immediately after the isolation procedure, and measurements of H_2O_2 and NOx were performed 24 hours later. The H_2O_2 production assay was based on the H_2O_2-dependent oxidation of homovanillic acid (3-methoxy-4-hydroxyphenylacetic acid) to a fluorescent dimer (2,2'-dihydroxydiphenyl-5,5'-diacetic acid), mediated by horseradish peroxidase (HRP). A reaction mixture containing homovanillic acid (1 mM) and HRP (0.2 U/mL) in an appropriate buffer was added to T25. Plates were incubated at 37°C for 30 minutes to allow the oxidation reaction. The fluorescence of the resulting dimer was measured using a microplate reader with an excitation wavelength of 312 nm and an emission wavelength of 420 nm.

The generation of $O_2^{\bullet-}$ was determined by flow cytometry using dihydroethidium (DHE) as a probe [352]. For the preparation of the cell suspension, cells were collected and diluted to a concentration of 200,000 cells/mL in a physiological buffer. DHE was added to the cell suspensions at a final concentration of 2 µg/mL. The mixture was incubated at 37°C for 30 minutes in the dark. A *FACS Aria Fusion* flow cytometer (BD, Franklin Lakes, NJ) was used to acquire data from 10,000 individual cells per sample. The fluorescent signal of the oxidized probe was detected in the appropriate fluorescence channel.

To ensure the accuracy and validity of the results, several controls were implemented:

- Negative Controls: Unstained samples and samples stained with DHE but without oxidative treatment were included as negative controls to establish baseline fluorescence.
- Positive Controls: Treatments known to induce the generation of H_2O_2 and $O_2^{\bullet-}$ were used as positive controls to validate the assay's sensitivity.
- Repeatability and Reproducibility: All experiments were performed in triplicate and on different days to evaluate the assays' repeatability and reproducibility.

Data obtained from fluorescence and flow cytometry assays were analyzed using specialized statistical software. ANOVA test

was employed as appropriate to determine the statistical significance of the results obtained.

The determination of nitrite (NO_2^-) and nitrate (NO_3^-) was based on the methodology described by Braman and Hendrix [353]. Total NOx (NO_2^- plus NO_3^-) was assessed by monitoring NO evolution from a sample placed into a boiling VCl_3/HCl solution, which reduces both NO_2^- and NO_3^- to NO. Quantitation was accomplished using a standard curve made up of known amounts of NO_2^- and NO_3^- [354].

3.13. GSH and GSSG Quantification

To determine the amount of glutathione in MNs we used the reduced (GSH) and oxidized glutathione (GSSG) quantification kit (Sigma-Aldrich, 38185).

3.13.1. Sample Preparation

MNs were collected by centrifugation at 200 x g for 10 minutes at 4°C, and the supernatant was discarded. The cells were washed with 300 µLof PBS, and centrifuged again at 200 x g, for 10 minutes at 4°C, discarding the supernatant. Subsequently, 80µLof 10 mmol/L HCl were added, and the cells were lysed by freezing and thawing twice. To further process the lysate, 20 mL of 5% sulfosalicylic acid (SSA) were added, followed by centrifugation at 8,000 x g for 10 minutes. The supernatant was

transferred to a new tube and ddH2O was added to reduce the SSA concentration to 0.5% for the assay.

Two sets of sample solutions (200 µL each x 2) were prepared for both GSH and GSSG determinations. For GSSG measurement, 200 µL of the sample were added to a microtube, followed by 4 µL of Masking solution, and mixed using a vortex mixer (Sample A). For total glutathione measurement, a 200 µL sample was prepared (Sample B).

3.13.2. Preparation of Standard Solutions

To prepare the GSSG standard solution, 100 µL of 100 µmol/L GSSG standard solution were mixed with 300 µL of 0.5% SSA solution to create a 25 µmol/L GSSG standard solution. Serial dilutions were then performed using 0.5% SSA solution to obtain the following concentrations: 25.0, 12.5, 6.25, 3.13, 1.57, 0.78, and 0 µmol/L. To all prepared GSSG standard solutions, 4 µL of Masking solution were added and mixed using a vortex mixer.

For the GSH standard solution, 100 µL of 200 µmol/L GSH standard solution were mixed with 300 µL of 0.5% SSA solution to create a 50 µmol/L GSH standard solution. Serial dilutions were performed using 0.5% SSA solution to obtain the following concentrations: 50.0, 25.0, 12.5, 6.25, 3.13, 1.57, and 0 µmol/L.

3.13.3. Measurement

For the measurement, 40 µL of GSSG standard solution, GSH standard solution, Sample A, or Sample B were added to each well, with triplicate measurements per sample recommended for accuracy. Next, 120 µL of Buffer solution were added to each well. The plate was incubated at 37°C for 1 hour, using a well cap to prevent evaporation. After incubation, 20 µL of substrate working solution were added to each well, followed by 20 µL of coenzyme working solution and then 20 µL of enzyme working solution, using a multichannel pipette to avoid reaction time lag. The plate was incubated at 37°C for 10 minutes. Absorbance was read at 405 or 415 nm using a microplate reader.

The concentration of GSSG in Sample A was determined using a GSSG calibration curve, and the concentration of total glutathione (GSH + GSSG) in Sample B was determined using a GSH calibration curve.

3.13.4. Calculation of Glutathione Concentrations

The concentration of GSH is calculated using the following equation from the concentrations of total glutathione (GSH + GSSG) and GSSG:

$$GSH = \text{Total glutathione (GSH + GSSG)} - GSSG \times 2$$

3.14. Preparation of NO and $^{-}$OONO solutions

Solution of NO was produced by first bubbling nitric acid gas through Dulbecco's PBS, thereby saturating the solution with NO. This process involved several steps: Two small tubes were equipped with airtight septa and glass tubes for the intake and release of gases. The initial tube contained 5 M potassium hydroxide, while the second tube, connected to the first via tygon tubing, was filled with Dulbecco's PBS (GIBCO). Argon gas (prepurified, Matheson) was introduced into these tubes at a flow rate of 10 mL/minute. After 15 minutes, the argon was replaced by NO (Matheson) at the same flow rate. 15 minutes later, the NO solution was extracted and stored under argon at a temperature of 4°C. Thionitrobenzoic acid was used to characterize the stability of NO solution. NO levels were quantified in the gas phase using a Sievers NOA 270B Chemiluminescence Analyzer (Sievers NOA, Boulder, Colorado). This device employs the chemical reaction between NO and ozone to generate activated nitrogen dioxide (NO_2*), which emits light in the red to far-red spectrum. To initiate the measurement, 100 µl samples of cell culture medium were injected into a nitrogen-purged vessel containing a 1% sodium iodide solution in glacial acetic acid. This process released gaseous NO from the dissolved NO and NO_2^- in the sample. The gas was then exposed to ozone within the vessel to produce

NO_2*, detected by a red-sensitive photomultiplier tube. The resulting signal was captured using an integrating pen recorder. The area under the curve for each sample was translated into picomoles of NO by using a calibration curve, which was developed following the analysis of various sodium nitrite standards.

A method described by Uppu and Pryor [355] was used to synthesize $^{-}$OONO, which involves a biphasic displacement reaction where the hydroperoxide anion in the aqueous phase displaces the isoamyl group from isoamyl nitrite in the organic phase, producing $^{-}$OONO in the aqueous phase and isoamyl alcohol in the organic phase. The reaction is effectively carried out at a pH greater than 12.5 to enhance the nucleophilicity of the hydroperoxide anion and minimize the alkaline hydrolysis of isoamyl nitrite, which would otherwise produce NO_2^-. Isoamyl nitrite, a water-insoluble alkyl nitrite, is used as the nitrosating species and the reaction presumably takes place at the liquid-liquid interface, requiring vigorous stirring of the reactants in both phases. After the reaction, phase separation is facilitated by brief centrifugation, allowing the aqueous phase containing $^{-}$OONO to be easily separated from the alcoholic product and excess alkyl nitrite using a separatory funnel. $^{-}$OONO solutions may contain H_2O_2 as an impurity, which can be reduced to less than 1 mM by passing the solution through a manganese dioxide

column. The $^{-}$OONO solutions are then stored under controlled conditions, often at 4°C under an argon atmosphere, to maintain stability and prevent decomposition. The concentration of $^{-}$OONO was measured spectrophotometrically (extinction coefficient of 1,670 M^{-1} x cm^{-1} at 302 nm).

3.15. Measurement of ATP Levels

To determine ATP levels, the ATP Determination Kit (Invitrogen, A22066) was employed, which utilizes a bioluminescence assay involving recombinant firefly luciferase and its substrate, D-luciferin. This assay is highly sensitive and can detect as little as 0.1 picomole of ATP, making it suitable for various applications, including detecting ATP production in enzymatic reactions and assessing bacterial contamination. The kit includes the following components:

- D-Luciferin (Component A): 5 vials, each containing 3 mg of lyophilized powder
- Firefly Luciferase (Component B): 40 µL of a 5 mg/mL solution in 25 mM Tris-acetate, pH 7.8, with 0.2 M ammonium sulfate, 15% (v/v) glycerol, and 30% (v/v) ethylene glycol
- Dithiothreitol (DTT) (Component C): 25 mg
- ATP (Component D): 400 µL of a 5 mM solution in TE buffer

- 20X Reaction Buffer (Component E): 10 mL of 500 mM Tricine buffer, pH 7.8, with 100 mM $MgSO_4$, 2 mM EDTA, and 2 mM sodium azide.

The kit is sufficient for 200 ATP assays using 500 µL sample volumes or 1,000 ATP assays using 100 µL sample volumes.

For reagent preparation, a 1X Reaction Buffer was made by adding 50 µL of 20X Reaction Buffer (Component E) to 950 µL of deionized water (dH_2O). A 10 mM D-Luciferin stock solution was prepared by adding 1 mL of 1X Reaction Buffer to one vial of D-luciferin (Component A) and protecting it from light until use. This solution was stored at ≤ –20°C. A 100 mM DTT stock solution was made by adding 1.62 mL of dH_2O to the bottle containing 25 mg of DTT (Component C), aliquoting it into ten 160 µL volumes, and storing it at ≤–20°C. Low-concentration ATP standard solutions were prepared by diluting the 5 mM ATP solution (Component D) in dH_2O to achieve ATP concentrations ranging from 1 nM to 1 µM, and stored at ≤ –20°C.

To prepare the standard reaction solution, 8.9 mL dH_2O, 0.5 mL 20X Reaction Buffer, 0.1 mL 0.1 M DTT, 0.5 mL of 10 mM D-Luciferin, and 2.5 µL of firefly luciferase (5 mg/mL stock solution) were combined. The mixture was gently inverted to mix and protected from light until use. This solution may be stored at 2–

6°C for several days, though assay sensitivity diminishes over time.

For the standard curve, an appropriate volume of the standard reaction solution was placed in the luminometer and the background luminescence was measured. The reaction was initiated by adding the desired amount of dilute ATP standard solution, ensuring the ATP standard solution volume was no more than 10% of the total assay volume. Background luminescence was subtracted, and a standard curve for a series of ATP concentrations was generated, ensuring consistent sample volume.

For sample analysis, the directions given in the standard curve were followed, substituting ATP-containing samples for the ATP standard solutions. The total volume of the experimental sample assays was equal to that of the ATP standard assays, with the sample amounting to no more than 10% of the total assay volume. The ATP amount in the experimental samples was calculated from the standard curve.

3.16. Determination of Caspase 3 Activity

This activity was measured using a highly sensitive colorimetric substrate, N-acetyl-Asp-Glu-Val-Asp p-nitroanilide (Ac-DEVD-pNA) following the manufacturer's instructions (CalBiochem, La Jolla, CA). Cells (5 x 10^5) were lysed in lysis buffer [50 mM HEPES

(pH 7.4), 100 mM NaCl, 0.1 % (v/v) CHAPS, 1 mM dithiothreitol and 0.1 mM EDTA] on ice for 10 minutes, then centrifuged at 10,000 x g for 10 minutes (4 °C). Equal volumes of the supernatants were added to equal volumes of assay buffer [50 mM HEPES (pH 7.4), 100 mM NaCl, 0.1 % (v/v) CHAPS, 10 mM dithiothreitol, 0.1 mM EDTA, and 10 % glycerol] and incubated at 37 °C for 10 minutes. Then, freshly prepared Ac-DEVD-pNA (200 mM) was added to the mixture and A405 was monitored every 20 minutes for 3 hours at room temperature. Cultures without cell lysates were used as controls. Enzyme activity was calculated as pmol/min using manufacturer's formulae.

Z-DEVD-FMK (Z-Asp-Glu-Val-Asp-fluoromethylketone; CalBiochem), dissolved in dimethyl sulfoxide (DMSO), was used as an irreversible caspase-3 inhibitor.

3.17. Mitochondrial membrane potential

Quantitative determination of the mitochondrial membrane potential (MMP) was performed by the uptake of the radiolabeled lipophilic cation methyl triphenylphosphonium (TPMP), which enables small changes in potential to be determined [356]. Cells (2 X 10^6) were incubated at 37 °C for 60 minutes in 1 mL DMEM, supplemented as mentioned above but including 1 mM TPMP, 250 nCi 3HTPMP (Amersham, Bucks, UK), and 1 mM sodium tetraphenylboron. After incubation, the cells

were pelleted by centrifugation (1,000 g for 5 min), 100 mL of the supernatant were removed, the pellet resuspended in 100 mL 10 % Triton X-100, and the radioactivity (disintegrations/min) was measured using a *Tri-Carb Liquid Scintillation Counter* from PerkinElmer (Waltham, MA).

3.18. Oxygen Consumption

O_2 concentration and rate of O_2 consumption in isolated MN was continuously recorded using a high-resolution oxygraph (Oroboros Instruments Corp., Innsbruck, Austria). Isolated MNs were resuspended in respiration medium (DMEM 4,500 mg/L glucose to which 5 mM pyruvate was added) that had been pre-warmed to 37 °C. A volume of 2.0 mL of cell suspension was added to the O_2 electrode chamber, where it was magnetically stirred and kept at 37 °C. The chamber was sealed, and the cells were incubated until a stable respiratory rate was reached.

3.19. Analysis of Mitophagy

To analyze late-stage mitophagy, we examined the percentage of lysosomes that colocalize with mitochondria [357]. For this purpose, we used *MitoTracker™ Green FM* (Thermo Fisher Scientific, M7514) to stain the mitochondria and *LysoTracker™ Red DND-99* (Life Technologies, Carlsbad, CA, USA) to stain the

lysosomes in MNs. The protocols followed were those provided by the respective manufacturers:

3.19.1. MitoTracker Protocol

Isolated MNs were cultured in 6-well plates at a density of approximately 5,000-10,000 cells per cm^2. Twenty-four hours after seeding, *MitoTracker™ Green FM* was added to achieve a final concentration of 100 nM and incubated for 30 minutes at 37°C. This was followed by three washes with PBS and a replacement with fresh DMEM. Images were captured using a *Leica TCS SP8* confocal microscope with a 63x objective and a 2.5x zoom.

3.19.2. LysoTracker Protocol

Similarly, isolated MNs were cultured in 6-well plates at the same cell density. After 24 hours*, LysoTracker™ Red DND-99* was added to reach a concentration of 75 nM and incubated for 30 minutes at 37°C. Following the incubation, the cells were washed three times with PBS and the medium was replaced with fresh DMEM. For imaging, we used the same *Leica TCS SP8* confocal microscope, equipped with a 63x objective and a 2.5x zoom.

3.20. Enzymes Expression and Activities

The assays for enzyme activities were conducted using specific protocols to ensure precise and reproducible results. Cells were

washed twice at 4 °C in Krebs-Henseleit bicarbonate medium (pH 7.4) without added Ca^{2+} or Mg^{2+}, and containing 0.5 mM ethylene glycol tetraacetic acid (EGTA). Subsequently, the cells were resuspended and homogenized in ice-cold lysis buffer, composed of 0.1 M PBS (pH 7.2), 1 mM phenylmethylsulfonyl fluoride (PMSF), 10 µg/mL aprotinin, 10 µg/mL leupeptin, and 5 µg/mL pepstatin A (Sigma), at a density of approximately 15 × 10^6 cells/mL.

SOD activity was measured following the methodology detailed by Flohé and Ötting [358], which employs the xanthine-xanthine oxidase-cytochrome c system. This assay differentiates between the SOD2 and the SOD1 using cyanide. The protocol involves adding 2 mM cyanide to the assay medium to inhibit SOD1, allowing for the specific measurement of SOD2 activity. The SOD1 activity is determined by measuring the remaining activity in the presence of 50 µM cyanide, which partially inhibits SOD1 by 13%. The SOD2 activity is then calculated by subtracting the contribution of SOD1 activity at 2 mM cyanide from the total activity measured. The supernatant from the homogenized sample, after centrifugation at 20,000 x g for 10 minutes at 4°C, is used in the xanthine-xanthine oxidase-cytochrome c assay, where the inhibition of cytochrome c reduction by SOD is measured spectrophotometrically at 550 nm.

Catalase (CAT) activity was measured using the protocol by Aebi [359], which involves the decomposition of H_2O_2 and monitoring the decrease in absorbance at 240 nm. The homogenate is appropriately diluted, and 2.0 mL of the enzyme solution is added to 1.0 mL of 30 mM H_2O_2 in 50 mM phosphate buffer (pH 7.0). The reaction is initiated by adding H_2O_2, and the decrease in absorbance at 240 nm is recorded for 30 seconds. The rate constant (k) is calculated using the formula:

$$k = \frac{2.3}{\Delta t} log\left(\frac{A_1}{A_2}\right)$$

Where $A1$ and $A2$ are the absorbance readings at times t_1 and t_2 , respectively, and $\Delta t = t_2 - t_1$ is the measured time interval in seconds. This rate constant is used as a direct measure of the CAT concentration. The velocity constant k obtained is used as a direct measure of the CAT concentration in the sample.

Glutathione peroxidase (GPX) activity, specifically selenium-dependent GPX, was measured using the method outlined by Flohé and Günzler [360], with H_2O_2 as a substrate. A mixture of 0.1 M potassium phosphate buffer (pH 7.0), 1 mM EDTA, the enzyme sample, and 4 mM GSH is preincubated at 37 °C. The reaction is initiated by adding 500 µL of 5 mM H_2O_2 pre-warmed to 37 °C. After 60 seconds, the reaction is stopped by adding 2.0 mL of 1.18 M $HClO_4$. The GSH content is then measured

polarographically, and the activity is calculated by determining the logarithmic decrease in GSH concentration over time.

For the NOS activity assay, 100 µL of supernatant was added to a reaction mixture containing HEPES (20.0 mmol/L, pH 7.4), 0.2 mM L-arginine (Sigma), and 2 mM NADPH (Sigma) in a total volume of 0.5 mL. The mixture was then incubated with constant air bubbling (1 mL/min) at 37 °C for 120 minutes. The blank sample contained all reaction components except NADPH. NOS activity was determined by calculating the difference between the sample readings and the blank readings.

RT-PCR analysis was performed as previously described [130]. RNA was extracted from the MNs using Qiagen RNAeasy mini kits. Quantitative and qualitative analyses of RNA samples were performed using a 2100 Bioanalyzer (Agilent Technologies) to ensure they were of sufficient quality to generate reliable data (RIN10). 1 x 10^5 cells were mixed with lysis solution (Thermo Fisher Scientific) and incubated for 5 min at room temperature to lyse the cells and remove gDNA. Then, the stop solution (Thermo Fisher Scientific) was added and incubated for 2 minutes at room temperature. Samples were stored at −80 °C. Real time quantitation of each mRNA relative to glyceraldehyde-3-phosphate dehydrogenase (GAPDH) mRNA was performed with a SYBR Green I assay and an iCycler detection system (Bio-Rad). Target cDNAs were amplified in separate tubes using as

follows: 10 minutes at 95 °C to ensure complete denaturation of the cDNA and then 40 cycles of amplification (denaturation at 95 °C for 30 s and annealing and extension at 60 °C for 1 min per cycle).

PCR Master Mix and AmpliTaq Gold DNA polymerase (Applied Biosystems) containing specific primers (Sigma Genosys) were then added:

- SOD1 (forward, *5'-TGGGTTCCACGTCCATCAG-3'*; reverse, *5'-ACACCGTCCTTTCCAGCAG-3'*),
- SOD2 (forward, *5'-ATGCAGCTGCACCACAGCAA-3'*; reverse, *5'-ACTTCAGTGCAGGCTGAAGAG-3'*),
- CAT (forward, *5'-ATGGTCTGGGACTTCTGGAGTCTTC-3'*; reverse, *5'-GTTTCCTCTCCTCCTCATTCAACAC-3'*),
- GPX (forward, *5'-GGGACTACACCGAGATGAACGA-3'*; reverse, *5'-ACCATTCACTTCGCACTTCTCA-3'*),
- iNOS, 5'-*CGGATATCTCTTGCAAGTCCAAA* (forward) and 5'-*AAGTATGTGTCTGCAGATATG* (reverse);
- eNOS, 5'-*CACCAGGAAGAAGACCTTTAAGGA* (forward) and 5'-*CACACGCTTCGCCATCAC* (reverse).

The increase in fluorescence was measured in real time during the extension step. The threshold cycle (CT) was determined, and then the relative gene expression was expressed as follows:

fold change = $2^{-\Delta(\Delta CT)}$, where ΔC_T = C_T target - C_T GAPDH, and Δ (ΔC_T) = ΔC_T treated - ΔC_T control.

3.21. Western Blott

3.21.1. Sample Preparation

To extract proteins from cells using the radioimmunoprecipitation assay (RIPA) protocol, the following steps were taken: In a cell culture hood, the culture medium was first removed from adherent cells. The cells were then washed with PBS and treated with trypsin to detach them, using approximately 1.5 mL of trypsin for T25 flasks. The trypsin was neutralized by adding a volume of culture medium equal to twice the volume of trypsin used, and the cell suspension was transferred to 15 mL conical tubes. The cells were then centrifuged at 500 X g for 5 minutes to pellet them, and the supernatant was carefully removed without disturbing the cell pellet. The pellet was resuspended in 1 mL of PBS and transferred to an Eppendorf tube.

Outside of the hood, the cell suspension in PBS was centrifuged at 4°C for 10 minutes at 500 x g. The supernatant was carefully removed and discarded. A RIPA buffer solution with protease inhibitor was prepared at the following ratio: for 5,000,000 viable cells, 1 mL of RIPA and 10 µl of protease inhibitor (1:100 ratio) were added. The volumes of RIPA and protease inhibitor

were adjusted based on the cell viability of the sample; for more than 5,000,000 cells, an additional 1 mL of RIPA was added. The cell pellet was resuspended in the RIPA solution with protease inhibitor (1X) and incubated on ice for 15 minutes to promote cell lysis. The suspension was then centrifuged at maximum speed (16,100 rpm) for 20 minutes. The supernatant containing the soluble proteins was carefully collected and transferred to a clean, properly labeled Eppendorf tube, and the pellet was discarded. Finally, if necessary, the protein sample was stored in a freezer at -20°C for preservation.

3.21.2. Protein Quantification

For protein quantification using the bicinchoninic acid (BCA) method (Thermo Fisher Scientific, 23225), a standard curve using BSA was prepared. Forty milligrams of BSA were dissolved in 1 mL of double-distilled water to make a 40 mg/mL stock solution. The standard curve was prepared by performing serial 1:2 dilutions, resulting in concentrations ranging from 20 mg/mL to 0.3125 mg/mL. The volume of reagent needed was calculated, considering the number of wells required. A 50:1 dilution of Reagents A and B was prepared, respectively. For example, if 20 wells were needed (16 for the standard curve and 4 for samples), 260 µL per well were multiplied, resulting in 5,200 µl. Seven milliliters of reagent were prepared to ensure a slight excess: 7,000 µl total volume, divided by 50 for Reagent B, gave 140 µl

of Reagent B. This was subtracted from the total volume to get 6,860 µl of Reagent A. The reagents were mixed well and covered with aluminum foil to protect them from light.

A 96-well plate was taken, and 3 µl of each concentration from the standard curve were loaded into separate wells, followed by 3 µl of each sample into different wells. Each condition was duplicated. A template indicating the location of each sample on the plate was created. Then, 260 µl of the prepared reagent were added to each well. The plate was incubated at 37°C in the dark, and the absorbance was read at 562 nm using spectrophotometry.

3.21.3. Gel Electrophoresis and Immunodetection

The next step was to perform gel electrophoresis to separate the proteins by size. First, the samples were denatured with 4x Laemmli buffer at 95°C for 5 minutes and briefly centrifuged to collect any remaining solution. Then, 20-40 µg of protein from each sample were loaded onto a 12.5 % acrylamide gel (the composition described in Table 3). The internal standard (5 µM/well) was from Thermo Scientific (ref. 26623). After electrophoresis, the proteins were transferred to a polyvinylidene fluoride membrane (Amersham Hybond™-P, GE).

Table 3. Composition of acrylamide gels

12.5% ACRYLAMIDE GELS	Volume (mL)		
	1 Gel	2 Gels	4 Gels
H2O	2673,3	5346,7	10692,0
TRIS 1,5M PH8,8	1333,3	2666,7	5333,3
Acrylamide 40%	1214,7	2430,7	4860,0
SDS 10%	53,3	106,7	213,3
APS 10%	53,3	106,7	213,3
TEMED	5,3	10,7	21,3

Abbreviations: SDS (Sodium Dodecyl Sulfate), APS (Ammonium Persulfate), TEMED (Tetramethylethylenediamine), TRIS (Tris(hydroxymethyl)aminomethane).

To perform the immunodetection of the proteins, the membrane was first blocked to prevent non-specific binding using a solution of 5% BSA in 1x TBST (Tris-Buffered Saline with Tween 20) for 1 hour at room temperature with gentle agitation. After blocking, the membrane was incubated with primary antibodies specific to each protein overnight at 4 °C with gentle agitation. The membrane was then incubated with an HRP-conjugated secondary antibody for 1 hour at room temperature with gentle agitation. The primary and secondary antibodies used are detailed in Table 4.

Table 4. Primary and secondary antibodies used in western blotting.

ANTIBODIES	REFERENCES	SUPPLIER	DILUTIONS
ANTI-SOD1	ab51254	Abcam	1:50,000
ANTI-SOD2	ab68155	Abcam	1:1,000
ANTI-CAT	ab209211	Abcam	1:2,000
ANTI-GPX1	ab108427	Abcam	1:200
ANTI-iNOS	ab178945	Abcam	1:1,000
ANTI-eNOS	ab300071	Abcam	1:1,000
ANTI-CYTOCHROME C	ab133504	Abcam	1:500
ANTI-TLS/FUS [BLR023E]	ab243880	Abcam	1:2,000
ANTI-SOD1 (ALS MUTANT), CLONE MS785	MABN834	Merck Millipore	1:1,000
GAPDH	ab8245	Abcam	1:2000
GOAT ANTI-RABBIT IGG	ab205718	Abcam	1:2,000

Finally, immunodetection was performed by adding the Immobilon Crescendo Western HRP Substrate (Millipore) to the membrane (2-5 minutes) and visualizing the results using the ImageQuantTM LAS 4000 imaging system. The results were normalized to housekeeping proteins, specifically GAPDH. The analysis was performed by densitometry of the obtained bands using AlphaEase FC software (Bonsai Technologies Group, S.A., Madrid, Spain).

3.22. Measurement of $^{\bullet}OH$ and $^{-}OONO$ levels

3.22.1. Measurement of $^{\bullet}OH$ levels

The measurement of $^{\bullet}OH$ was conducted following the methodology described by Deng et al. [361]. The detection starts with the NO_2^- release from nitroimidazoles upon its specific reaction with $^{\bullet}OH$ radicals, followed by NO_2^- quantification by Griess reagent, which forms a red substance. The color development is proportional to the amount of $^{\bullet}OH$.

The Griess reagent, is composed of two solutions: 1% p-amino benzene sulfonamide in an aqueous solution (R1) and 0.1% N-1-naphthylethylenediamine in aqueous solution (R2). R2, obtained from Cayman, was used as supplied. R1 was prepared by dissolving 500 mg of p-amino benzene sulfonamide in 50 mL of a 5% phosphoric acid solution, following standard protocols. These components were mixed immediately prior to each assay to ensure freshness. In the assay procedure, 100 µL of the freshly mixed Griess reagent (combining R1 and R2) was dispensed into each well of a 96-well plate. This was followed by the addition of 50 µL of NO_2^--containing samples into each well. Under acidic conditions, the NO_2^- ions react with R1 to form a reactive diazonium salt. This intermediate then reacts with R2 to produce a red azo dye, which exhibits maximum absorbance at 540 nm. The plates were then incubated in the dark at room temperature

for 10 minutes before the absorbance was measured using a plate reader.

For the establishment of the standard curve, various concentrations of sodium nitrite solutions were freshly prepared. Fifty microliters of each solution were added to the Griess reagent in separate wells for colorimetric analysis. Each sample was tested in triplicate. DMSO, known for its ability to neutralize •OH radicals, was used in the control assay. DMSO was added to the reaction mixture to a final concentration of 4% to assess the specificity of the reaction. The absorbance readings at 540 nm, after subtracting the background values from the reagent control, were plotted against the concentrations of NO_2^-. All assays were conducted at room temperature (25 °C), unless specified otherwise.

3.22.2. Measurement of $^-$OONO levels

The Peroxynitrite Assay Kit was used to quantify $^-$OONO levels. This assay employs a specialized fluorescent probe that reacts with $^-$OONO to yield a vivid green fluorescence.

3.22.2.1. Reagent Preparation

Peroxynitrite Sensor Green stock solution (500X): Add 20 µL of DMSO into the vial of Peroxynitrite Sensor Green and mix well to make 500X stock solution.

Peroxynitrite Sensor Green working solution (10X): Add 10 µL of 500X DMSO reconstituted Peroxynitrite Sensor Green (from step 5.1) into 500 µL of Assay Buffer and mix well.

3.22.2.2. Sample Preparation

Cells were seeded at a density of 75,000 cells per 100 µL in each well of a 96-well plate and incubated overnight in growth medium.

3.22.2.3. Run the $^{-}$OONO assay

1. Add 10 µL/well of Peroxynitrite Sensor Green working solution (10X) in 90 µL cell culture per well in the cell plate (96-well plate).

2. Co-incubate cells with Peroxynitrite Sensor Green (10X) at 37 °C for 1 hour, protected from light.

3. Measure the fluorescence using a microplate reader at Ex/Em=490/530 nm.

3.23. Nitrosative stress biomarkers

The acid-soluble fractions (200 µL) obtained for GSH determination were added to 25 µL of 2.0 % ammonium sulfamate. To the mixtures were added 200 µL of 0.5 N HCl containing 0.25 % $HgCl_2$ and 5 % sulfanilamide. Then, 250 µL of a 0.5 N HCl solution containing 0.25 % N-(1-naphthyl)ethylenediamide dihydrochloride were added to the mixtures. After incubation for 30 minutes at 25 °C, the amount

of S-nitrosothiols (RSNO) was determined spectrophotometrically at 550 nm using S-nitrosoglutathione (GSNO) as a standard [362]. Fresh GSNO solution was obtained, before each experiment, by incubating equimolar GSH and sodium nitrite in acidified water at 0 °C as previously described [363]. GSNO concentration was determined spectrophotometrically at 335 nm (ε = 992 $dm^3 \times mol^{-1} \times cm^{-1}$) and at 545 nm ($\varepsilon$ = 15.9 $dm^3 \times mol^{-1} \times cm^{-1}$). No significant decomposition of GSNO occurred during the assay procedures. Formation of 3-nitrotyrosine was measured using the enzyme-linked Immunosorbent assay (ELISA) kit from Cell Biolabs (San Diego, CA).

3.24. Stadistical analysis

In this study, G*Power 3.1.9.2 software was used to determine the sample size, set up for a four-group analysis of variance (ANOVA), with an effect size of 0.21, a significance level (α) of 0.05, and a statistical power (β) of 0.80, to ensure sufficient statistical power to detect significant differences between groups. Survival data were analyzed using Kaplan-Meier curves and the LogRank (Mantel–Cox) test, techniques used to evaluate survival function and compare the efficacy of treatments across different groups. Analyses were conducted using either one- or two-way ANOVA or unpaired t-tests as applicable (SPSS Statistics

29 for Windows; SPSS Inc., Chicago, IL). The Levene test was applied to assess the homogeneity of variances among the groups, a crucial step to validate the assumptions of ANOVA. The null hypothesis was accepted for all test values where the F value was not significant at $P \geq 0.05$. Data for which the F value was significant were examined using Tukey's test at $P < 0.05$ to identify specific differences between pairs of groups, providing a detailed and comprehensive analysis of the treatment effects

4. RESULTS

4.1. PDE inhibitors tolerance and selection

Previous research indicates that PDE inhibitors can reduce glial cell activation, suggesting a potential strategy to mitigate inflammation [333]. Thus, we considered the possibility of assaying one of them to increase the efficacy of the NR+PT treatment. To select the most suitable option, we evaluated the tolerance of different and currently used PDE4 inhibitors (Table 5). We tested rolipram (which promotes the clearance of abnormal proteins through the proteasome), roflumilast (with demonstrated anti-inflammatory effects), apremilast (which inhibits TNF-α generation by different cells), and IBU (with anti-inflammatory and neuroprotective properties).

Table 5. Side effects observed in SOD1^{G93A} and FUS^{R521C} mice treated with different PDE4 inhibitors. *Murine doses were calculated using human doses and the conversion factor recommended by the FDA (www.fda.gov). All PDE4 inhibitors were from Monmouth Junction, NJ. Rolipram was administered subcutaneously daily (in saline with 10% ethanol). Roflumilast (suspended in 4% methylcellulose, 1.5% polyethylene glycol 400) was given once a day by oral gavage. Apremilast (suspended in PS containing 10% Tween-80) was administered orally once a day. The administration of PDE4 inhibitors started 4 weeks after birth (see under Methods). The number of mice per treatment group was n=15. Control mice were treated with vehicles and for the same time period and showed no side effects (results not shown).*

PDE4 INHIBITOR	MURINE DOSE	DIARRHEA	MUSCLE SPASMS	PAIN (HUNCHED POSTURE)
	(mg/kg x day)	(days after the start of treatment)		
ROLIPRAM	12	10-12	--	--
ROFLUMILAST	1	11-12	12-13	--
APREMILAST	50	8-10	--	13-14
IBU	12	--	--	--

To calculate the dose to be administered, the FDA conversion factor to transform pharmacological doses in humans into equivalent doses in mice was used [323]. As shown in Table 5, within two weeks of treatment, mice treated with rolipram, roflumilast, or apremilast developed gastrointestinal disturbances (diarrhea), muscle spasms (in mice treated with roflumilast), and signs of pain (in mice treated with apremilast, which exhibited a characteristic hunched posture as treatment progressed). The experiment was stopped when muscular spams or pain were evident and/or when the diarrhea caused a loss of body weight >20%.

Considering the significant side effects observed with the administration of the PDE4 inhibitors rolipram, roflumilast, and apremilast in ALS mouse models, as described in previous studies [323], we consider IBU to be the safest and most viable therapeutic option. The absence of relevant adverse effects with IBU reinforces its potential as a key component in the therapeutic combination with NR and PT for treating ALS.

4.2. NR, PT, and IBU Delay ALS-Related Loss of Neuromotor Functions

Neuromotor functions were assessed in $SOD1^{G93A}$ and FUS^{R521C} mice using a standard neurological scoring system focused on hind limb abilities (Figure 11A) and the rotarod test, which assesses balance, coordination, and general fitness (Figure 11B). The onset of

symptomatology appeared around postnatal week 12 in $SOD1^{G93A}$ mice and week 7 in FUS^{R521C} mice. Both IBU alone and the NR+PT treatment delayed the onset of the neurological symptomatology in both ALS models compared to the control groups (Figure 11A and B).

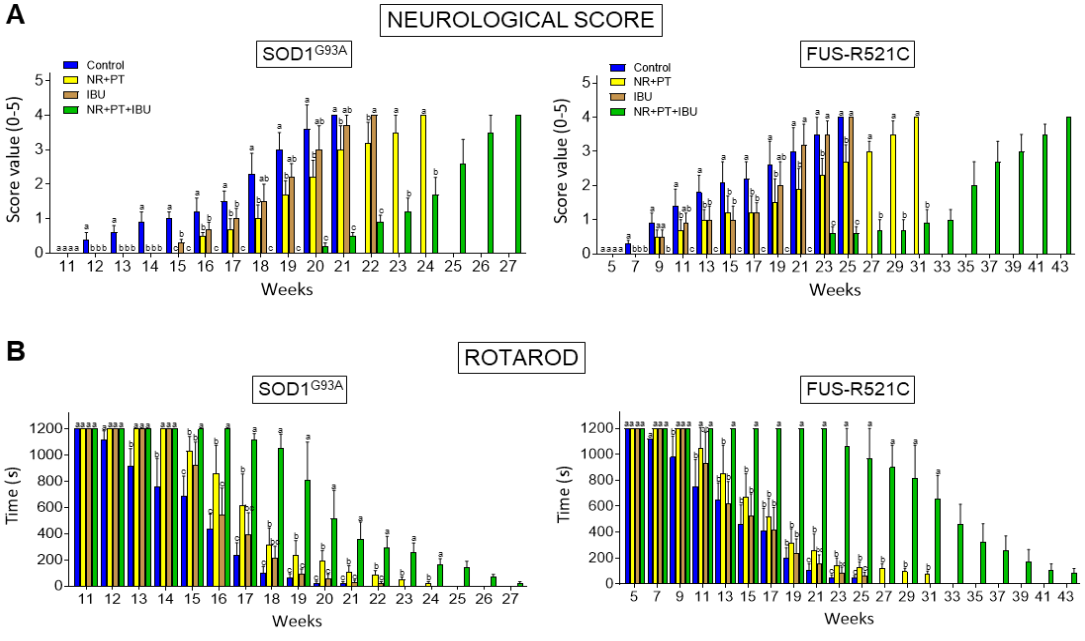

Figure 11. NR+PT+IBU delays the loss of functional performance in SOD1^{G93A} and FUS^{R521C} mice. *(A) Neurological score. (B) Rotarod test. Treatment arms were as follows: PS-treated transgenic mice (SOD1^{G93A} or FUS^{R521C} controls), SOD1^{G93A} or FUS^{R521C} mice treated with NR and PT, SOD1^{G93A} or FUS^{R521C} mice treated with IBU, and SOD1^{G93A} or FUS^{R521C} mice treated with NR, PT, and IBU. Both neuromotor tests (A and B) were performed twice a week. On the days of the week in which the animals were not scored, they were trained on the rotarod. Control experiments performed in WT mice (n = 10) rendered a neurological score of 0 and a performance time of 1,200 s in the rotarod test in all cases. A one-way analysis of variance (ANOVA) was used to make comparisons among the different treatments at each time point. Different letters indicate statistical differences, P < 0.05 (A, B). (A and B, n=20)*

However, this delay was most notable in mice treated with the triple combination (NR+PT+IBU) compared to the other treatments (Figure 11A and B). These results highlight the synergistic potential of the combined therapy.

4.3. NR, PT, and IBU Extend Survival in Murine ALS Models

Survival of $SOD1^{G93A}$ and FUS^{R521C} transgenic mice was studied using the same treatments as in the neuromotor function studies (Figure 11). NR+PT or the use of IBU alone increased survival rates compared to controls. However, the use of the triple therapy (NR+PT+IBU) significantly enhanced survival rates compared to controls or to those treated with NR+PT or IBU alone (Figure 12).

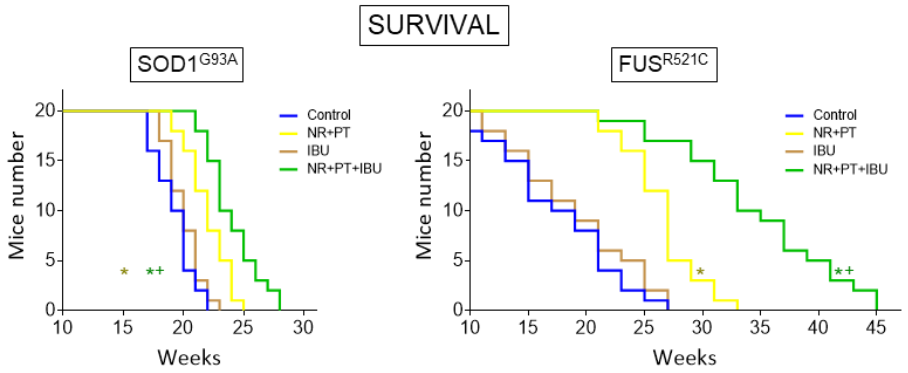

Figure 12. Combined treatment with NR+PT+IBU significantly extends survival in $SOD1^{G93A}$ and FUS^{R521C} mice. *Treatment arms were as Figure 11. Survival data were analyzed with Kaplan-Meier curves and LogRank (Mantel-Cox) test (*P < 0.01 comparing all groups versus controls; *P < 0.01 comparing mice treated with NR+PT+IBU versus mice treated with NR+PT) (n=20).*

These findings suggest that the therapeutic combination could offer substantial benefits in terms of extending life and reducing disease progression in ALS patients, with effects superior to those of the individual molecules alone. This further underscores the synergistic potential of the treatment (NR+PT+IBU).

4.4. NR, PT and IBU Decrease Microgliosis, Astrogliosis and MN Degeneration

ALS progression is associated with microgliosis and astrogliosis affecting the anterior horns of the medulla. Therefore, immunohistopathological analysis was performed at postnatal week 18 (advanced state of progression) to quantify these changes in both murine models ($SOD1^{G93A}$ and FUS^{R521C}), using Iba1 immunohistochemical staining for microgliosis and GFAP staining for astrogliosis. Treatments with NR+PT or the combination of NR+PT+IBU showed a reduction in both types of neuroinflammation-related gliosis (Figure 13A and B). However, in the case of microgliosis, only the triple combination was significantly more effective than the NR+PT treatment (Figure 13A). As an example, microscopic images comparing thoracic spinal cord sections obtained from mice treated with PS and mice treated with the triple combination are shown (Figure 13A and B).

The number of MN cell bodies in the anterior horns of the thoracic spinal cord was better preserved in both mouse models treated with

PT+NR or with PT+NR+IBU (Figure 13C). In fact, the state of MNs in treated groups (NR+PT+IBU) was similar to the count found in WT mice (data not shown). The histological assessment of spinal cord samples, using HE staining, showed a significant reduction of MNs in control $SOD1^{G93A}$ and FUS^{R521C} mice treated with PS. In contrast, MNs appeared to be better preserved in mice treated with NR+PT+IBU (Figure 13C). However, the mere count or morphology of these MNs does not indicate whether they are fully functional or have suffered any damage.

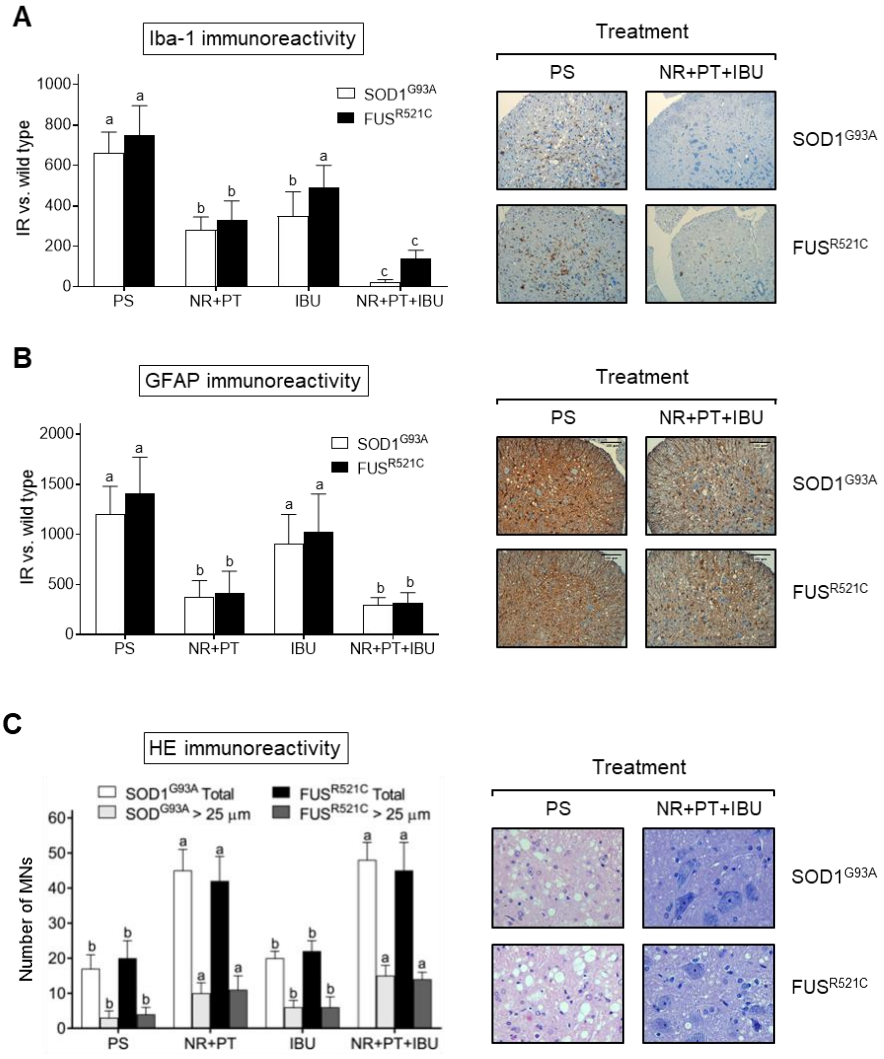

Figure 13. NR+PT+IBU reduces MN degeneration and neuroinflammation in the anterior horn of the medulla. *(A) Iba-1 staining and immunoreactivity. (B) GFAP staining and immunoreactivity. (C) Number of MNs per section and HE staining. Tissue samples were obtained at postnatal week 18 (advanced state of progression) from SOD1^{G93A} and FUS^{R521C} mice. Representative images of microglia (Iba-1) staining (A), astroglia (GFAP) staining (B), and HE staining (C) of the anterior horns of the thoracic spinal cord are shown, comparing mice treated with PS, or NR+PT, or, IBU, or NR+PT+IBU. (A, B) Glia quantification (IR, immunoreactivity). Reactive glia is quantified based on the immunostaining signal (arbitrary units), where the data*

obtained with the different treatments in ALS mice are subtracted from the data obtained in WT mice treated with PS. A one-way ANOVA was used to make comparisons among the different treatments. Different letters indicate statistical differences, P < 0.05 (A and B, n = 7; C, n = 14).

The significant reduction of reactive microglia and astrogliosis in the spinal cord of mice treated with NR, PT, and IBU demonstrates the positive impact of the therapeutic combination in mitigating neuroinflammation and preserving MNs. These results support the hypothesis that the combined therapy can effectively intervene in the inflammatory pathways that exacerbate neuronal degeneration in ALS.

4.5. NR, PT, and IBU Reduce Pro-inflammatory Cytokine Levels

The next step was to study a possible correlation between neuroinflammation and molecular signaling. To this end, we measured several important pro-inflammatory cytokines in CSF samples obtained from WT, $SOD1^{G93A}$, and FUS^{R521C} mice at week 18. As shown in Figure 14, the levels of all measured cytokines increased in the CSF of control $SOD1^{G93A}$ and FUS^{R521C} mice treated with PS as compared to WT mice. NR+PT treatment significantly reduced IFN-γ and IL-6 levels, whereas treatment with IBU alone was remarkably effective in decreasing TNF-α levels. Comparing the groups treated with NR+PT and those treated with NR+PT+IBU, only a significant difference in

TNF-α levels was observed. These data indicate that, in both ALS models, IBU specifically targets and reduces TNF-α levels (Figure 14).

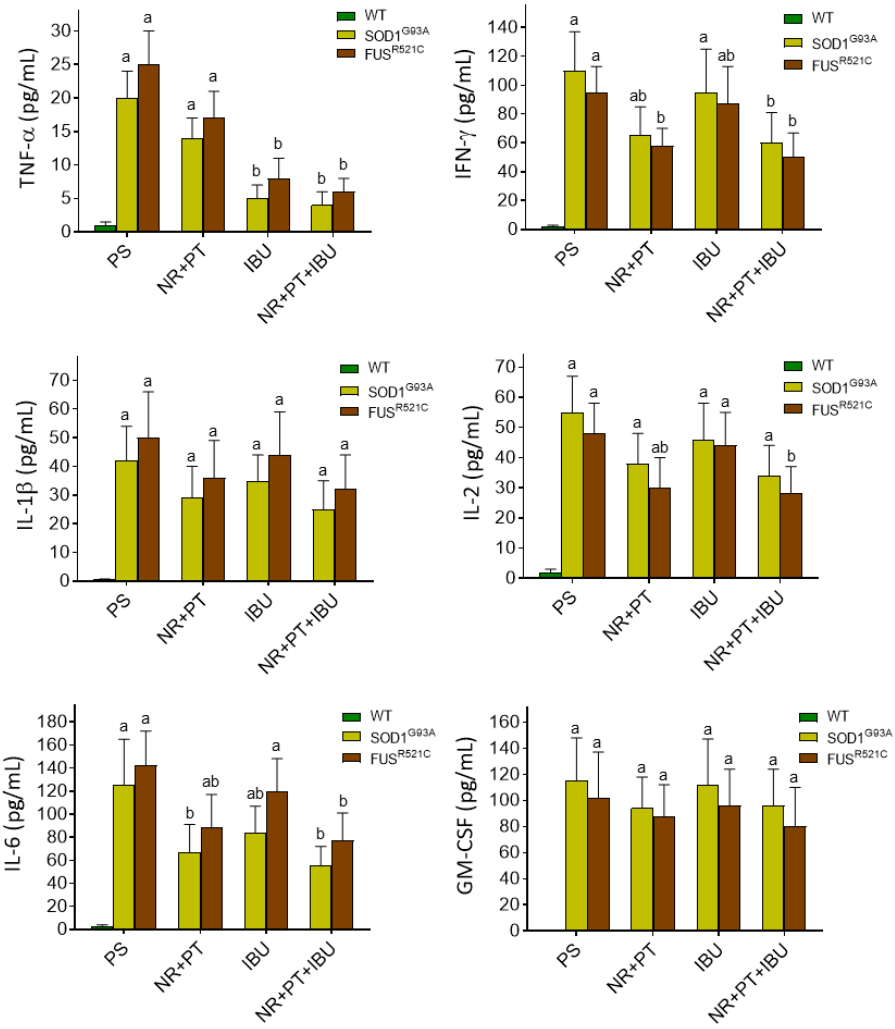

Figure 14. Levels of pro-inflammatory cytokines in the CSF of WT, SOD1^{G93A}, and FUS^{R521C} mice. *CSF samples were obtained at week 18. A one-way ANOVA was used to make comparisons among the different treatments. Different letters indicate statistical differences, P < 0.05 (n = 7 in all cases).*

The significant decrease in TNF-α, IFN-γ, and IL-6 levels in the CSF of mice treated with NR, PT, and IBU underscores the efficacy of the therapeutic combination in reducing systemic and local inflammation in ALS. These anti-inflammatory effects may be crucial for disrupting the cycle of inflammation/oxidative stress/neuronal damage, suggesting a promising approach for the treatment of ALS.

4.6. Cytokine Induction of Oxidative/Nitrosative Stress

Oxidative stress and neuroinflammation are integral to the pathophysiology of ALS [232]. Studies on the interactions of metastatic and endothelial cells have shown that cytokines such as TNF-α, IFN-γ, and IL-1β can induce the production of ROS and reactive nitrogen species (RNS) [364]. Furthermore, NO and H_2O_2 produced by vascular endothelium were found to be cytotoxic to the metastatic cells [364].

Therefore, we explored potential connections between oxidative/nitrosative stress and different cells in the MN microenvironment. As shown in Figure 15, TNF-α, IFN-γ, and IL-1β significantly increased NO (expressed as NOx: NO_2^- plus NO_3^-) and H_2O_2 generation by MNs, astrocytes, microglia, and endothelial cells isolated from $SOD1^{G93A}$ and FUS^{R521C} mice, in contrast to similar cells isolated from WT mice. This effect was particularly pronounced, except in astrocytes, when all three cytokines were incubated together (Figure 15), reflecting *in vivo* conditions more accurately (Figure 14). The other cytokines measured in CSF, such as IL-2, IL-6, and

granulocyte-macrophage colony-stimulating factor (GM-CSF) (Figure 14), did not affect H_2O_2 or NO production in the cells analyzed (data not shown).

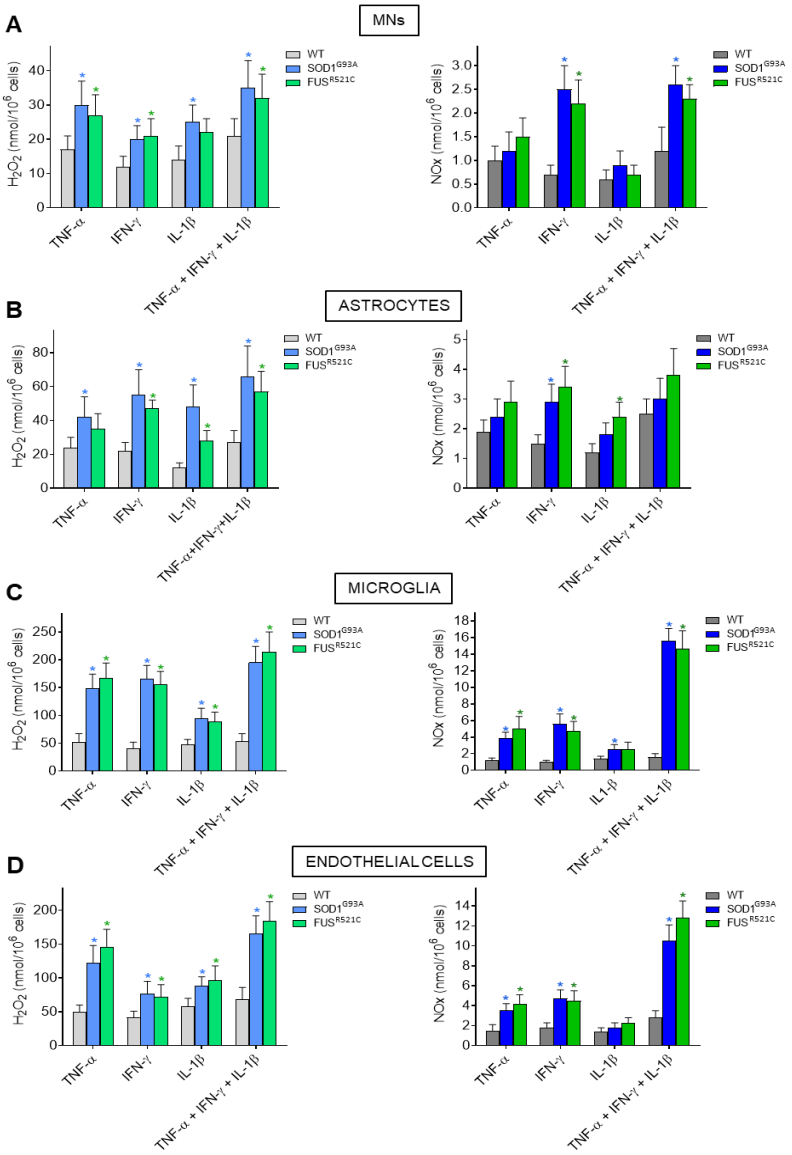

Figure *15*. *In vitro* production of H_2O_2 and NO by cytokine-activated MNs (A), astrocytes (B), microglia (C), and endothelial cells (D). *Cells were isolated from mice*

*at week 18 of progression, plated immediately afterwards, and incubated x 24 hours before the addition of the cytokines. The concentrations of each cytokine were selected based on the results obtained in Figure 14. rmTNF-α concentrations in the culture medium were 1 pg/mL (cells isolated from WT mice) or 25 pg/mL (cells isolated from $SOD1^{G93A}$ or FUS^{R521C} mice). rmIFN-γ concentrations in the culture medium were 2 pg/mL (cells isolated from WT mice) or 100 pg/mL (cells isolated from $SOD1^{G93A}$ or FUS^{R521C} mice). rmIL-1β concentrations in the culture medium were 0.5 pg/mL (cells isolated from WT mice) or 50 pg/mL (cells isolated from $SOD1^{G93A}$ or FUS^{R521C} mice). H_2O_2 and NOx were measured 6 hours after adding the cytokines to the culture flasks. Values are means ± standard deviation (SD) of 5-6 different experiments. *P < 0.05 (t-test) comparing cells isolated from $SOD1^{G93A}$ or FUS^{R521C} mice versus cells isolated from WT mice.*

These results provide evidence that pro-inflammatory cytokines induce the production of ROS and RNS, exacerbating oxidative/nitrosative stress in MNs and other cells in the microenvironment. The combination of NR, PT, and IBU effectively reduced these stress markers, highlighting its potential to protect MNs from the harmful effects of oxidative and nitrosative stress in ALS.

4.7. NR, PT, and/or IBU Protect MNs Against Oxidative/ Nitrosative Stress

H_2O_2 and NO generation was also investigated in different cell types (MNs, astrocytes, microglia, and endothelial cells) isolated from $SOD1^{G93A}$ and FUS^{R521C} mice, which were either used as controls or treated *in vivo* with NR+PT, IBU, or NR+PT+IBU. As shown in Table 6, treatment with NR and PT significantly reduced cytokine (TNF-α, IFN-γ, and IL-1β)-induced H_2O_2 and NO production in all cell types, except for H_2O_2 in FUS^{R521C} astrocytes and NO in $SOD1^{G93A}$ astrocytes.

Treatment with IBU alone decreased H_2O_2 production in microglia and endothelial cells. Moreover, NR+PT+IBU treatment further reduced H_2O_2 and NO production in microglia and endothelial cells compared with NR+PT treatment. Notably, H_2O_2 and NO generation was more substantial in microglia and endothelial cells than in MNs and astrocytes.

Table *6.* Cytokines (rmTNF-α, rmIFN-γ, and rmIL-1β)-induce H_2O_2 and NO production by MNs, astrocytes, microglia, and endothelial cells. *Cells were isolated from mice treated with PS, NR, PT, and/or IBU as in Figure 11 at week 18 of progression. Cytokines were incubated at the concentrations and for the time period indicated in Figure 15. Values are means ± SD of 4-5 different experiments. A one-way ANOVA was used to make comparisons among the different treatments. Different letters indicate statistical differences, P<0.05.*

	Control (nmol/10^6 cells)		**NR+PT** (nmol/10^6 cells)		**IBU** (nmol/10^6 cells)		**NR+PT+IBU** (nmol/10^6 cells)	
	SOD1^{G93A}	**FUS-R521C**	**SOD1^{G93A}**	**FUS-R521C**	**SOD1^{G93A}**	**FUS-R521C**	**SOD1^{G93A}**	**FUS-R521C**
MNs								
H_2O_2	35 ± 8^{a}	32 ± 7^{a}	18 ± 4^{b}	16 ± 4^{b}	25 ± 5^{ab}	24 ± 6^{ab}	12 ± 3^{b}	10 ± 2^{b}
NOx	2.6 ± 0.4^{a}	2.3 ± 0.3^{a}	1.5 ± 0.4^{b}	1.2 ± 0.3^{b}	2.5 ± 0.7^{a}	2.4 ± 0.8^{a}	1.4 ± 0.4^{b}	1.3 ± 0.4^{b}
Astrocytes								
H_2O_2	66 ± 18^{a}	57 ± 12^{a}	39 ± 8^{b}	42 ± 11^{a}	50 ± 17^{ab}	51 ± 18^{a}	30 ± 7^{b}	28 ± 6^{b}
NOx	3.0 ± 0.7^{a}	3.8 ± 0.9^{a}	2.0 ± 0.5^{b}	2.4 ± 0.5^{b}	2.8 ± 0.8^{a}	3.6 ± 1.0^{ab}	1.8 ± 0.3^{b}	2.0 ± 0.5^{b}
Microglia								
H_2O_2	195 ± 29^{a}	214 ± 36^{a}	110 ± 18^{b}	126 ± 23^{b}	137 ± 21^{b}	156 ± 27^{ab}	65 ± 20^{c}	74 ± 16^{c}
NOx	15.6 ± 1.5^{a}	14.6 ± 2.2^{a}	8.5 ± 1.2^{b}	7.4 ± 0.9^{b}	14.2 ± 1.3^{a}	12.7 ± 2.0^{a}	5.7 ± 1.2^{b}	5.0 ± 1.1^{b}
Endothelial cells								
H_2O_2	166 ± 26^{a}	184 ± 29^{a}	84 ± 17^{b}	96 ± 17^{bc}	114 ± 19^{b}	129 ± 19^{b}	43 ± 15^{c}	55 ± 18^{c}
NOx	10.5 ± 1.6^{a}	12.8 ± 1.7^{a}	8.6 ± 1.3^{a}	9.2 ± 1.5^{a}	9.6 ± 1.6^{a}	11.5 ± 1.7^{a}	5.4 ± 1.2^{b}	5.7 ± 1.5^{b}

In accordance with these results, our subsequent experiments focused on microglia and endothelial cells, where we evaluated a number of enzymatic activities directly related to H_2O_2 and NO metabolism. As shown in Table 7, SOD1, SOD2, CAT, and NOS activities were increased in microglia and endothelial cells isolated from $SOD1^{G93A}$ and FUS^{R521C} mice compared to data obtained in the same cells isolated from WT mice. Treatment with NR+PT+IBU significantly decreased SOD1 and NOS activities in both cell types, and SOD2 in microglia (Table 7).

Table 7. Effect of NR, PT, and IBU on oxidative/nitrosative stress-related enzyme activities in microglia and endothelial cells. *Cells were isolated from mice at week 18 of progression. Mice were treated as in Figure 11. Enzyme activities were measured as described under Methods. *P < 0.05, **P < 0.01 comparing activities in the murine models of ALS versus those measured in cells isolated from WT mice; +P < 0.05, ++P < 0.01 comparing in each cell type treatment with NR+PT+IBU versus controls (untreated) (n = 5-6).*

	WT		**SOD1^{G93A}**				**FUS^{R521C}**			
	Microglia	**Endot. cells**	**Microglia**		**Endot. cells**		**Microglia**		**Endot. cells**	
In vivo pretreatment with NR+PT+IBU	**–**	**–**	**–**	**+**	**–**	**+**	**–**	**+**	**–**	**+**
SOD1 (U/10^6 cells)	1.4 ± 0.3	1.0 ± 0.3	3.2 ± 0.5**	1.5 ± 0.4^{++}	2.5 ± 0.4**	1.2 ± 0.3^{++}	3.6 ± 0.5**	1.5 ± 0.4^{++}	3.0 ± 0.4**	1.4 ± 0.3^{++}
SOD2 (U/10^6 cells)	0.3 ± 0.1	0.2 ± 0.1	0.7 ± 0.2*	0.3 ± 0.1^{+}	0.5 ± 0.2*	0.2 ± 0.1	0.9 ± 0.3**	0.4 ± 0.1^{+}	0.6 ± 0.2*	0.3 ± 0.1
CAT (mU/10^6 cells)	2.5 ± 0.6	2.1 ± 0.7	3.7 ± 0.5*	3.0 ± 0.4	3.2 ± 0.6	2.5 ± 0.4	4.2 ± 1.1*	3.1 ± 0.6	3.5 ± 0.5*	2.3 ± 0.4^{++}
GPX (mU/10^6 cells)	6.2 ± 1.3	5.8 ± 1.2	7.7 ± 1.2	6.2 ± 1.3	7.0 ± 0.9	6.0 ± 1.2	7.9 ± 1.5	6.5 ± 1.0	7.3 ± 1.5	6.0 ± 1.0
NOS (pmol NO/mg protein x min)	1.5 ± 0.4	2.6 ± 0.7	6.5 ± 1.4**	2.7 ± 0.8^{*++}	8.4 ± 1.7**	3.2 ± 0.7^{++}	6.0 ± 0.9**	2.1 ± 0.5^{++}	10.2 ± 2.1**	3.8 ± 0.9^{++}

These changes in enzyme activity reflect changes in H_2O_2 and NO production, as described in Table 6, and correlate with measurements of enzyme expression (Figure 16) and enzyme levels (Figure 17).

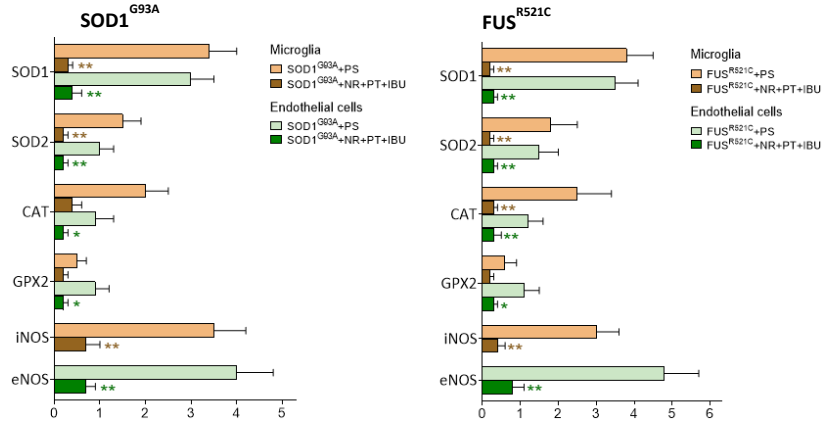

Figure 16. Effect of NR, PT, and IBU on the expression (RT-PCR) of oxidative- and nitrosative stress-related enzyme activities in microglia and endothelial cells. *Cells were isolated from mice at week 18 of progression. Mice were treated as in Figure 11. Data, expressed as fold change versus WT mice (quantitative RT-PCR; see Methods), show mean values ± SD for 5 different cell isolation procedures in each case. *P < 0.05, **P < 0.01 comparing ALS mice treated with NR+PT+IBU versus controls treated with PS.*

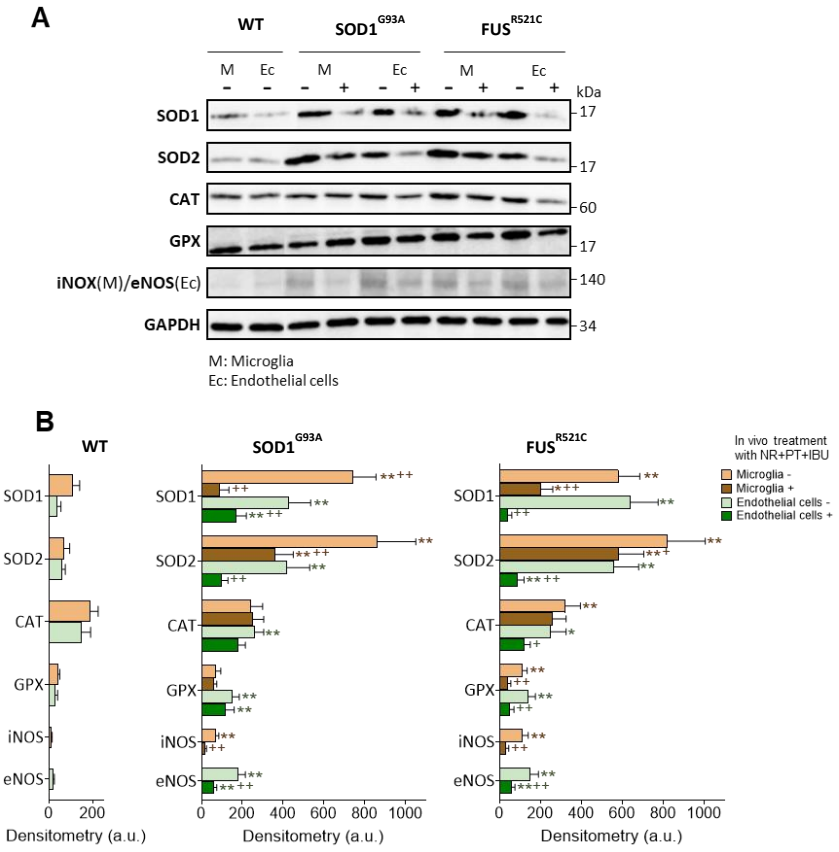

Figure 17. Effect of NR, PT, and IBU on levels of oxidative and nitrosative stress-related enzyme activities in microglia and endothelial cells. *Cells were isolated from WT mice or from ALS mice at week 18 of progression. Mice were treated as in Figure 11. (A) Western blots. (B) Densitometric analysis of the blots represents the mean values ± SD for 4–5 different cell isolation procedures per molecule and experimental condition. *P < 0.05, **P < 0.01 comparing each cell type (microglia and endothelial cells) in untreated or treated ALS mice versus the equivalent data in WT mice treated with PS. $^{+}P < 0.05$, $^{++}P < 0.01$ comparing each cell type in ALS mice treated with NR+PT+IBU versus control ALS mice treated with PS.*

All these results demonstrate that specific pro-inflammatory cytokines can induce oxidative and nitrosative stress in the MN

microenvironment. Additionally, the combined treatment of NR, PT, and IBU showed a significant ability to reduce the production of H_2O_2 and NO in cells isolated from ALS mouse models, and modulate the activity of key enzymes such as SOD1, SOD2, CAT, and NOS [345]. This highlights the efficacy of the therapeutic combination in protecting MNs against oxidative/nitrosative damage.

4.8. Metal presence enhances RNS/ROS-induced MN cytotoxicity

The mechanism by which H_2O_2 and NO can induce MN cytotoxicity was further investigated in isolated MNs exposed to pathophysiological concentrations of stress promoters. The concentrations chosen for H_2O_2 and NO were based on the amounts collectively generated by the different cells (Table 6, controls, cells isolated at day 18 of *in vivo* progression). As presented in Table 8, H_2O_2 or NO alone caused minimal cytotoxicity (<10%) in both models compared to MNs treated with basal medium. However, when H_2O_2 and NO were combined, a significant increase in MN cytotoxicity (approximately 40% above control levels) was observed (Table 8). Furthermore, $^{-}$OONO exhibited even greater cytotoxicity than H_2O_2 or NO alone (Table 8), suggesting that the combination of H_2O_2 and NO is likely responsible for the increased cytotoxicity in MNs. Incubation of MNs with NO and SOD, which removes $O_2^{\bullet-}$ released into the extracellular medium and

increases H_2O_2 levels, caused more cytotoxicity than NO alone (Table 8).

Table 8. Metal presence enhances RNS/ROS-induced MN cytotoxicity. *MNs were cultured for 24 hours before any addition. NO (10 µM), H_2O_2 (100 µM), SOD (100 units/mL, Merck), $^{-}$OONO (10 µM), EGTA (0.5 mM), or ebselen (10 µM, Merck) were added at 24 hours of culture. $FeCl_3$ (1 mM) was added 5 minutes after EGTA addition. Cytotoxicity is expressed as the percentage of MNs that lost viability within a 3-hour period of incubation. Data are means ± SD of seven different experiments. A one-way ANOVA was used to make comparisons among the different treatments. Different letters indicate statistical differences, P < 0.05.*

ADDITIONS	MN CYTOTOXICITY (%)	
	$SOD1^{G93A}$	FUS-R521C
BASAL MEDIUM	2 ± 1^{d}	1 ± 0.5^{d}
NO	10 ± 4^{c}	8 ± 3^{c}
H_2O_2	7 ± 3^{cd}	10 ± 4^{c}
NO + H_2O_2	42 ± 7^{a}	38 ± 8^{a}
$^{-}$OONO	28 ± 5^{b}	30 ± 7^{a}
NO + SOD	25 ± 6^{b}	28 ± 6^{ab}
NO + H_2O_2 + EGTA	14 ± 4^{c}	10 ± 3^{c}
NO + H_2O_2 + EGTA + $FECL_3$	50 ± 7^{a}	45 ± 10^{a}
NO + H_2O_2 + EBSELEN	15 ± 3^{c}	17 ± 4^{bc}

The Fenton reaction is central to the generation of hydroxyl radicals, which play a pivotal role in enhancing nitrosative stress. This reaction involves the transition metal ion (typically iron, Fe^{2+}) catalyzing the decomposition of H_2O_2 to generate $^{\bullet}OH$, one of the most reactive and damaging ROS [365]. The basic reaction can be summarized as follows:

$$Fe^{2+} + H_2O_2 \rightarrow Fe^{3+} + OH^{-} + {}^{\cdot}OH$$

The hydroxyl radicals produced in this reaction are extremely reactive and can cause significant damage to cellular components, including lipids, proteins, and DNA. EGTA was added to the culture media to

chelate metal ions. Under these conditions, H_2O_2- and NO-induced cytotoxicity decreased to levels similar to those observed in the presence of NO alone, whereas the addition of $FeCl_3$ again enhanced the MN cytotoxicity (Table 8). Ebselen, a synthetic organoselenium drug that mimics GPX activity and thus reduces H_2O_2 levels [366], also decreased the cytotoxicity in MNs induced by H_2O_2 and NO (Table 8). Taken together, these results suggest that a trace metal-catalyzed process exists within a mechanism where different reactions can take place, i.e., (but not limited to):

$$NO + H_2O_2 \rightarrow NO_2 + {}^{\bullet}OH + H^+$$

$$Fe^{3+} + NO + H_2O_2 \rightarrow Fe^{2+} + {}^{-}OONO + 2H^+$$

$${}^{\bullet}OH + H_2O_2 \rightarrow {}^{-}OOH + H_2O$$

$${}^{\bullet}OOH + NO \rightarrow {}^{-}OONO + H^+$$

4.9. NR, PT, and IBU Attenuates Oxidative/Nitrosative Stress

Mechanisms that produce potent oxidants, such as ${}^{\bullet}OH$ and ${}^{-}OONO$, could be primarily responsible for the NO- and H_2O_2-induced MN death. To prove this hypothesis, we also quantified the generation of these highly reactive species by microglia and endothelial cells, the cell types that produce higher levels of H_2O_2 and NO (Table 6). As illustrated in Figure 18, microglia and endothelial cells isolated from ALS mice generated higher levels of NO_2^- (which indirectly reflects the

generation of $^{\bullet}OH$ through the following reaction: $^{\bullet}OH + NO \rightarrow NO_2^-$) and ^-OONO compared to their counterparts from WT mice.

The treatment with NR+PT and NR+PT+IBU decreases NO_2^- and ^-OONO levels in both types of murine ALS, with the NR+PT+IBU combination being more effective (Figure 18). This aligns with the findings reported for H_2O_2 and NO in Table 6.

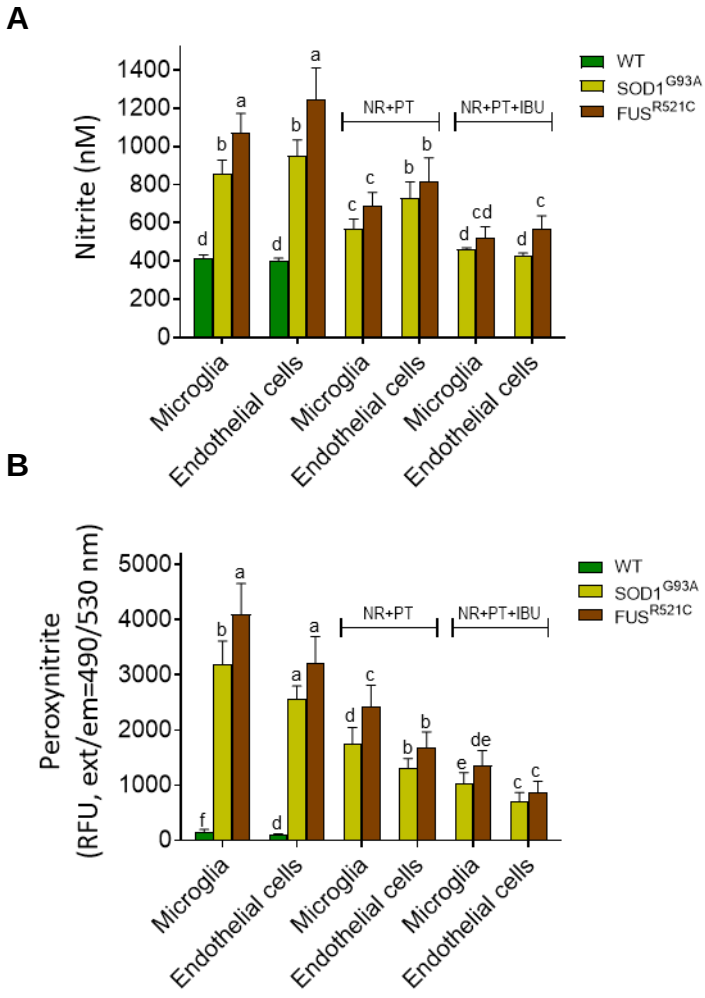

Figure 18. Generation of $^{\bullet}OH$ (A) and $^{-}OONO$ (B) by microglia and endothelial cells isolated from WT, control, NR+PT or NR+PT+IBU-treated ALS mice. *Based on the methodology (see under Material and Methods), data are expressed as NO_2^- levels or relative fluorescence units (RFU) ($^{-}OONO$). n= 4-5 different mice per experimental condition. A one-way ANOVA was used to make comparisons among the different treatments. Different letters in each cell type indicate statistical differences, P<0.05 (mean values ± SD).*

These results highlight the ability of NR, PT, and IBU to prevent the generation of highly damaging reactive species such as $^{\bullet}OH$ and $^{-}OONO$ in microglia and endothelial cells. This underscores the potential of this combination to break the vicious cycle of oxidative and nitrosative damage in ALS.

4.10. Oxidative and Nitrosative Stress Trigger MN Death

As a proof of concept, we explored the effect of pathophysiological concentrations of H_2O_2 and NO on the viability of MNs isolated from FUS^{R521C} mice. As shown in Figure 19A, oxidative/nitrosative stress-induced MN death is mainly apoptotic. According to the data presented in Table 8, the number of dead MNs was higher when H_2O_2 and NO were combined (Figure 19A). This finding correlates with molecular alterations related to the activation of the mitochondria-dependent apoptotic cell death, including reduced mitochondrial membrane potential, depletion of GSH and ATP, increased mitochondrial O_2 consumption, and elevated levels of cytosolic caspase 3 and cytochrome C activity (Figure 19B).

In addition, several studies have demonstrated that a decrease in autophagy/mitophagy can lead to an increase in ROS generation, which, in turn, can activate immune signaling pathways and trigger the release of inflammatory cytokines [367]. We found that mitophagy (based on the percentage of lysosomes colocalizing with mitochondria) was also increased in MNs isolated from mice treated

with NR+PT or NR+PT+IBU compared to controls (Figure 19C). This effect was more pronounced in mice treated with the triple combination compared with those receiving NR+PT (Figure 19c). These observations suggest that protective treatments enhance the clearance of damaged mitochondria through lysosomes.

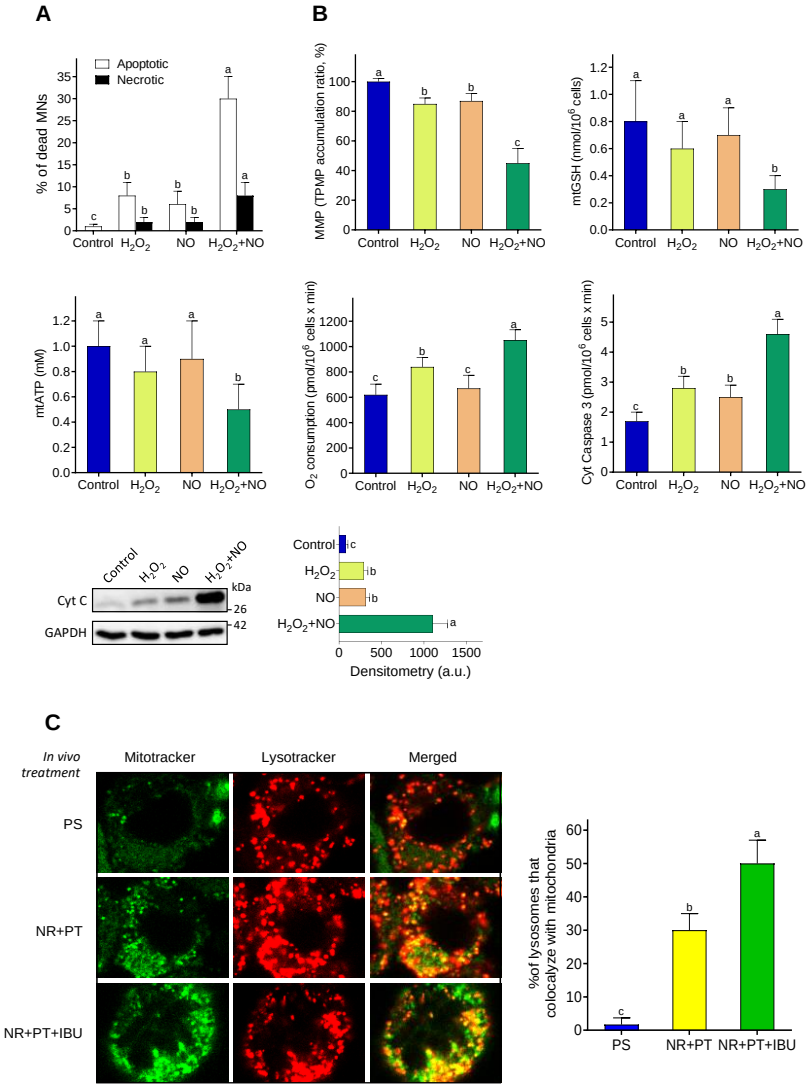

Figure 19. H_2O_2- and NO-induced activation of MN death. *MNs were isolated from FUS^{R521C} mice (week 18). For the analysis of cell death (A) and the tests related to the molecular activation of apoptosis (B), cells were treated as indicated in Table 8. Data are means ± SD of 4-5 different experiments. (C) Mitophagy analyses using lysosomal- and mitochondrial specific fluorescent dyes in live MNs. The graph corresponds to the average percentage of lysotracker puncta that colocalize with mitochondria (mean values ± SD for 4–5 different mice per experimental condition). A one-way ANOVA was used to make comparisons among the different treatments. Different letters indicate statistical differences, P < 0.05.*

4.11. NOS Inhibition Increases Survival in ALS Mice

To further investigate the role of NO in ALS progression and its contribution to MN damage, we studied the effects of *in vivo* administration of L-NAME, a specific inhibitor of NOS activity, in $SOD1^{G93A}$ and FUS^{R521C} mice. The treatment with L-NAME, initiated at week 18 (advanced stage of disease progression), resulted in reduced levels of nitrosative stress biomarkers, including nitrosothiols and nitrotyrosine (Figure 20A). In addition, L-NAME administration decreased NOx production (NO_2^- plus NO_3^-) by MNs, astrocytes, microglia, and endothelial cells (Figure 20B).

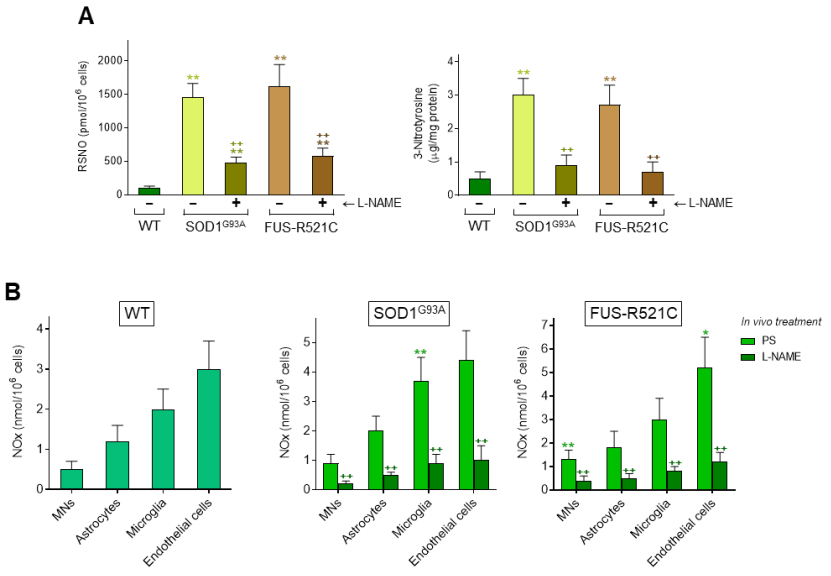

Figure 20. Treatment with L-NAME prevents nitrosative stress. *(A) Nitrosative stress biomarkers were measured in MNs isolated from WT mice and from ALS mice treated with PS or with L-NAME (i.p.), respectively. *P < 0.05, **P < 0.01 comparing ALS versus WT mice: ++P < 0.01 comparing ALS mice treated with L-NAME versus control ALS mice treated with PS (n = 4–5). (B) NOx (NO_2^- plus NO_3^-) generated by MNs, astrocytes, microglia, and endothelial cells (isolated from WT and ALS mice) during 3*

*hours of in vitro incubation. *P < 0.05, **P < 0.01 comparing cells isolated from ALS mice versus cells isolated from WT mice; **P < 0.01 comparing cells isolated from L-NAME-treated ALS mice versus cells isolated from control ALS mice treated with PS (n = 4–5, t-test).*

L-NAME treatment significantly increased the survival of $SOD1^{G93A}$ and $FUSR^{521C}$ mice compared with control mice, providing evidence of the importance of nitrosative stress in ALS progression (Figure 21). L-NAME administration began at week 18 to ensure the treatment duration was not extended, thereby avoiding potential systemic toxicities associated with L-NAME, such as hypertension [368], liver and intestinal toxicity [369], or nephrotoxicity [370]. Taken together, these results (see also Table 8) confirm our hypothesis that NO, and consequently nitrogen and oxygen-derived mixed reactive species, cytokines, and neuroinflammation, play a key role in the mechanism leading to the damage of MNs.

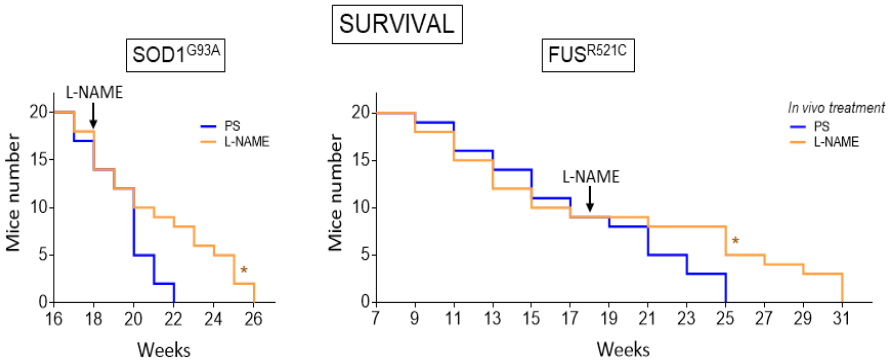

Figure 21. Treatment with L-NAME increases survival in ALS mice. The dosage was set at 20 mg/kg daily (i.p.), starting in the 18th week of the experiment and continuing until the demise of the last mouse in the study. Data were analyzed with Kaplan-Meier curves and LogRank (Mantel-Cox) test (*P < 0.01 comparing L-NAME-treated mice versus controls treated with PS, n = 20).

4.12. NR+PT+IBU Reduces the Cytoplasmic Accumulation of Mutant FUS Protein in MN

We also investigated whether mutant SOD1 and FUS protein levels could be affected by the treatments shown above. To this purpose, we analyzed these protein levels by western blots in control mice (treated with PS) and in mice treated with IBU, NR+PT, NR+PT+IBU, or L-NAME, following their respective treatment protocols as described above (Figure 22). The analysis was performed on MNs obtained from mice at an advanced stage of disease progression, ensuring that the results were directly comparable with previous experiments.

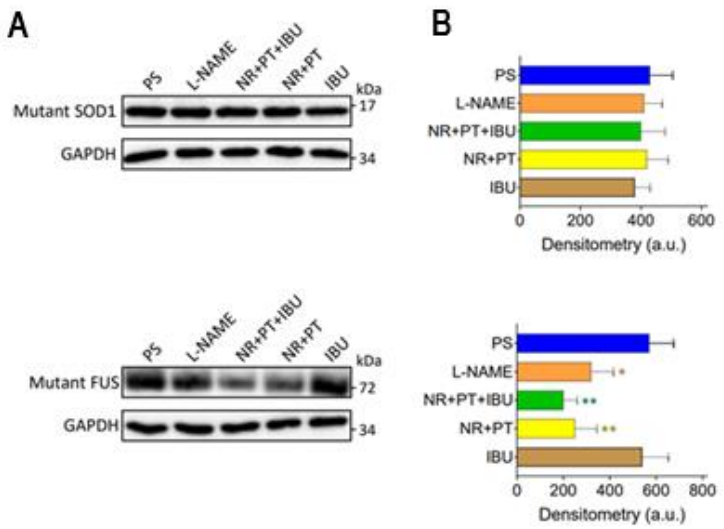

Figure 22. Effect of *in vivo* treatment with NR+PT, IBU, NR+PT+IBU or L-NAME on the levels of mutant SOD1 and FUS proteins in MNs isolated from SOD1^{G93A} or FUS^{R521C} mice. *Cells were isolated from WT mice or from ALS mice at week 18 of progression. Mice were treated as described in Material and Methods. (A) Western blots. (B) Densitometry analysis of the blots represents the mean values ± SD for 4 different cell isolation procedure per molecule and experimental condition. *P < 0.05, **P < 0.01 comparing all treatments versus control ALS mice treated with PS.*

As indicated in Figure 22, none of the experimental treatments altered the intracellular levels of the SOD1 mutant. This suggests that the effectiveness of the treatments in SOD1^{G93A} mice affected the pathophysiological consequences of the mutation and not its genetic background. However, the situation was different in the case of FUS mice. Treatment with NR+PT+IBU or with L-NAME decreased the accumulation of FUS mutant protein within MNs (Figure 22). This fact can be interpreted in different ways. Treatments may influence the pathophysiological consequences of the mutation, as observed in SOD1^{G93A} mice. Alternatively, alterations in cytokine, ROS, RNS, or NO levels could also affect transcriptional mechanisms via the C/EBP (CCAAT/Enhancer-Binding Protein) homologous protein (CHOP) transcription factor, leading to mutant protein synthesis [371]. Additionally, it is possible that the mutant FUS protein is being removed more efficiently, potentially through mechanisms such as the ubiquitin-proteasome system [372]. In any of the cases, the decreased accumulation of FUS mutant protein within MNs must contribute to maintaining MN function and, consequently, ALS mice survival [345,373].

5. DISCUSSION

Increasing evidence indicates that neuroinflammation and oxidative stress pave the way for neurodegeneration in ALS [144]. As the disease progresses, microglia and astrocytes in the anterior horn of the medulla undergo a phenotypic transition, proliferate, and secrete pro-inflammatory cytokines [144,185–187,374]. Neuroinflammation is associated with the release of cytokines that represent potential apoptosis (i.e., TNF-α, IFN-γ, IL-1β), whereas TNF-α also interferes with the normal electron flow in the mitochondria and increases the generation of ROS [375]. Pro-inflammatory cytokines such as GM-CSF, IL-2, IL-6, IL-15, IL-17, MCP-1, MIP-1α, TNF-α, and VEGF are typically elevated in the CSF of patients [192] and murine models of ALS [130,193,194]. Reactive astrocytes in ALS express inflammatory markers, including COX-2, inducible NOS, and neuronal NOS, and inhibitory molecules that block regrowth of a damaged axon [144]. Glial and infiltrated immune cells are major producers of ROS and RNS in pathological conditions of the CNS, thus chronic inflammation enhances oxidative stress linked to MN damage [376].

NAD^+ is a vital coenzyme involved in various cellular processes. It functions in redox reactions, serves as donor of ADP-ribose for ADP-ribosylation reactions, acts as a precursor of cyclic ADP-ribose, and functions as a substrate for SIRTs, which use this cofactor to deacetylate proteins [294]. SIRTs, particularly SIRT1 and SIRT3, regulate mitochondrial biogenesis and function. SIRTs also help mitigate oxidative stress by deacetylating and activating antioxidant

enzymes [294,377]. PT can cross the BBB, possesses intrinsic antioxidant capacity, and has been shown to increase nuclear Nrf2, thus promoting the antioxidant defenses in the CNS [285,286]. PT mitigates inflammation (Figure 9) by decreasing inflammatory mediators, i.e., TNF-α, IL1-β and IL-6 [292,293], which may further support its therapeutic potential in ALS treatment [70].

The efficacy of NR+PT as a potential treatment for ALS is evidenced by several studies promoted by our group [130,240]. NR and PT treatment helps maintain neuromotor functions according to a placebo-controlled double-blind human pilot study in ALS patients (NCT03489200) [240]. In this study, NR+PT treatment significantly slowed the progression of ALS as measured by ALSFRS-R score, forced vital capacity and Medical Research Council grading scale when compared to the placebo group [240].

My master's thesis results evidence that NR and PT enhance Nrf2-dependent antioxidant defenses and increase SIRT1 and SIRT3 activity in MNs from $SOD1^{G93A}$ mice (Figure 23). PT promoted SIRT1 overexpression and the nuclear translocation of Nrf2, while NR provides NAD^+ for poly [ADP-Ribose] polymerase 1 (PARP-1) and SIRT-catalyzed reactions [130]. The NR+PT treatment reduced oxidative stress, potentially decreasing the release of proapoptotic signals from mitochondria through a complex mechanism involving factors such as Ca^{2+} accumulation, mitochondrial DNA damage, changes in mitochondrial membrane potential, and alterations in the

proapoptotic/antiapoptotic protein balance [130,232,292]. The combined treatment slowed the loss of neuromotor functions and significantly prolonged survival of $SOD1^{G93A}$ mice [130]. PT+NR treatment is now being evaluated in the NO-ALS Study: A Phase II Trial of Nicotinamide/Pterostilbene Supplement in ALS (NCT04562831, Norway).

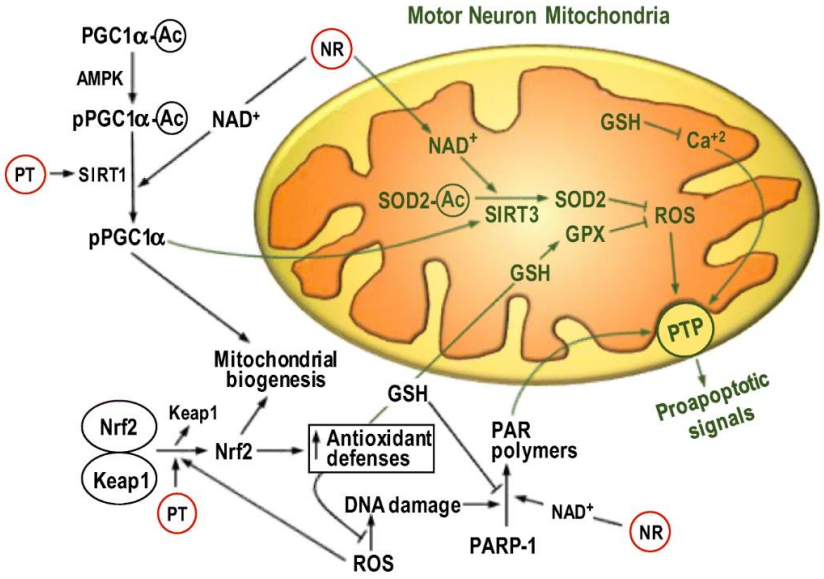

Figure 23. NR and PT decrease the release of mitochondrial proapoptotic molecular signals [130]. *Abbreviations: PGC-1α (peroxisome proliferator-activated receptor gamma coactivator 1-alpha), AMPK (AMP-activated protein kinase), Ac (acetylated), P (phosphorylated), Nrf2 (nuclear factor erythroid 2-related factor 2), Keap1 (Kelch-like ECH-associated protein 1), PARP-1 (poly [ADP-ribose] polymerase 1), GPX (glutathione peroxidase), SIRT (sirtuin), SOD2 (superoxide dismutase 2).*

ALS is a multifaceted neurodegenerative disorder, and single agent therapies have failed to increase survival. Therefore, we consider that a combined strategy is a better therapeutic option, and in our case,

the addition of an anti-inflammatory agent can further increase the efficacy of NR and PT. As many anti-inflammatory agents like celecoxib or corticosteroids have failed to demonstrate any survival advantage, we looked at PDE inhibitors for their capacity of cross the BBB and reduce glial cell activation, [333]. We tested rolipram, roflumilast, apremilast, and IBU, with doses converted to murine equivalents using FDA guidelines [323]. Rolipram, roflumilast, and apremilast had significant side effects, including diarrhea, muscle spasms, and pain, which necessitated early termination of treatment. In contrast, IBU did not cause significant side effects, making it the safest and most viable therapeutic option.

Here we show that treatment with NR+PT+IBU, compared to NR+PT alone, can further delay the progression of neuromotor damage (Figure 11) and increase survival in two ALS murine models [345]. Notably, the inclusion of IBU in the combined NR and PT treatment increases survival by 2 more weeks in $SOD1^{G93A}$ mice and by 11 weeks in FUS^{R521C} mice, compared to the NR+PT treatment alone (Figure 12). These effects were associated with reduced neuroinflammation (Figure 13A and B) and decreased levels of various pro-inflammatory cytokines in CSF (Figure 14).

High O_2 consumption is needed to produce ATP to maintain the neuronal membrane potential through Na^+ and K^+ gradients. The mitochondrial respiratory chain, responsible for most oxygen consumption, can leak electrons to reduce molecular O_2 and form $O_2^{\bullet -}$

[378]. Although mechanisms exist to eliminate $O_2^{\bullet-}$ from the cell via enzymatic catalysis by SOD enzymes, the kinetically favorable reaction of $O_2^{\bullet-}$ with NO, facilitated by metals like iron, will ultimately lead to $^{-}$OONO formation before $O_2^{\bullet-}$ can be eliminated [379]. NO is produced by NOS, which are expressed in different isoforms. For example, endothelial cells produce NO through eNOS, neurons through nNOS, and immune cells such as macrophages and microglia through iNOS. Additionally, other cell types, such as astrocytes, can also produce NO using these isoforms [379]. Free radicals are important at physiological concentrations as they can act as cellular signaling molecules, but during oxidative stress, they are produced at high levels and can damage lipids, proteins, and nucleic acids [378,379]. As MNs are rich in functional lipids, they are especially susceptible to oxidative stress damage. Zhao et al. demonstrated that microglia, activated by lipopolysaccharide (LPS) or IgG immune complexes, induced injury in primary cultures of MNs [380]. This injury was prevented by a microglia-iNOS inhibitor, as well as by CAT or GSH. On the other hand, Pehar et al. observed that cultured embryonic MNs expressing p75(NTR) were not vulnerable to nerve growth factor unless exposed to an exogenous influx of NO [381]. We found that different cytokines (TNF-α, IFN-γ, and IL-1β) increased H_2O_2 and NO generation by MNs, astrocytes, microglia, and endothelial cells isolated from ALS mice (Figure 15). PT alone has been shown to reduce NO production in microglia stimulated by LPS, without directly scavenging NO radicals

[382]. Further studies revealed that PT might inhibit LPS-induced NO and TNF-α production in microglia by blocking IKβα phosphorylation and degradation [383], presumably preventing NF-κB activation associated with IKβα phosphorylation. The binding of LPS to toll-like receptor 4 (TLR4) of microglia can trigger the activation of downstream signaling pathways such as NF-κB and mitogen-activated protein kinases (MAPKs), subsequently inducing the expression of inflammation-related genes such as COX-2 and various pro-inflammatory cytokines [384]. All this suggests that NO plays an important role in the pathophysiological cascade of ALS.

Here we present evidence showing that the combined treatments, either NR+PT or NR+PT+IBU, cause a significant decrease in NO production in all tested cells (Table 6). IBU significantly reduced TNF-α levels in the CSF (Figure 14) and H_2O_2 generation by microglia and endothelial cells (Table 6). Unexpectedly, exposing MNs to pathophysiological concentrations of H_2O_2 or NO individually resulted in minimal cytotoxicity (Table 8). However, the cytotoxicity to MNs was notably increased when H_2O_2 and NO were combined. This can be attributed to the formation of potent oxidants, i.e., $^{\bullet}OH$ and $^{-}OONO$ radicals (Figure 18), through a trace metal-dependent process (Table 8).

These results suggest that oxidative and nitrosative stress, triggered by pro-inflammatory cytokines, significantly harms MNs, and that different cells in the anterior horn microenvironment play a role in this

process, i.e., microglia, astrocytes, endothelial cells, and likely infiltrating immune cells [187,345]. Importantly, microglia exhibits different phenotypes throughout ALS progression, transitioning from a vigilant state in the early phases to activated M1 and M2 states in advanced stages, characterized by harmful and protective gene expression, respectively [385]. Although our methodology to isolate microglial cells does not differentiate between the different phenotypes, we have evidence that microglia isolated at week 18 of progression release pro-inflammatory cytokines (Figure 15C).

The concentrations of H_2O_2 and NO used in the experiments displayed in Table 8 are derived from the amounts generated by different cells present in the anterior horns (Table 6, cells isolated on day 18 of *in vivo* progression). Therefore, these concentrations may approach the pathophysiological maximum levels. However, complex tissue architecture, the flow of blood, lymph, and CSF, along with various regulatory molecules, serve as significant limiting factors that are not present in the *in vitro* experimental setting. Therefore, it is plausible to expect that, *in vivo*, MNs are exposed to lower levels of H_2O_2 and NO. Moreover, given that ALS often progresses in sporadic flares, the exposure of MNs to toxic levels of ROS and RNS may not be constant [386]. These observations suggest a scenario more consistent with the gradual deterioration experienced by patients. Additionally, the cellular and neuroanatomical specificity of the ALS-related degeneration is often accompanied by aberrant misfolding,

aggregation, and deposition of specific proteins, such as SOD1 [38], TDP-43 [88], or FUS [343]. This is important (and coherent with our findings) because both ROS and RNS can favor abnormal protein aggregation [219,387,388].

Several works evidence the importance of metals in the damage induced by oxidative stress. Free iron can react with H_2O_2 via the Fenton reaction, a primary cause of lipid peroxidation and a mechanism that has been implicated in several CNS injuries/disorders, such as, stroke, epilepsy, Friedreich's ataxia [389], and (as we show in our study) is also active in ALS [345]. The SOD mutation is involved in oxidative injury through increased generation of hydroxyl radicals, increased peroxidase activity, or increased nitration of tyrosine by $^{-}OONO$ [390]. The ALS mutant SODs have reduced affinity for zinc. Furthermore, neurofilament subunits bind zinc with sufficient affinity to remove zinc from SOD. The increased loss of zinc from SOD will diminish the scavenging of superoxide and increase the catalysis of tyrosine nitration by $^{-}OONO$ [390]. Singh et al. were first to suggest that the loss of zinc from SOD may enhance $^{-}OONO$ formation and MN death in ALS [389] and also evidenced the importance of the Fenton reactions in the promotion of MN toxicity [390].

Previous studies have reliably identified iron deposition in the motor cortex as potential pathogenesis of ALS [391,392]. On the cellular and molecular level, excessive iron deposition may lead to oxidative stress-associated neural apoptosis [393]. Moreover, a recent meta-analysis

reported unusual changes in iron status linked to ALS [394]. According to this study, serum ferritin levels were higher and transferrin levels were lower in ALS patients, compared to healthy controls. The ability of transferrin to decrease free iron levels in circulation suggests that this protein may have a protective effect on neurons in ALS progression. The conclusions of the study suggest possible iron metabolism abnormalities in ALS patients, thus supporting the importance of iron in the oxidative stress toxicity on MNs shown in this work (Table 8). Therefore, controlling metal serum levels, as well as their dietary or accidental intake, could be important for ALS patients.

IBU, an anti-inflammatory drug initially developed to treat asthma, is a cyclic nucleotide PDE inhibitor that acts primarily by increasing cAMP and cGMP levels, while decreasing pro-inflammatory factors such as TNF-α, MIF, and TLR-4 [395,396]. Pharmacologically, IBU significantly prolongs the time to first relapse and attenuates brain volume reduction in patients with relapsing-remitting and/or secondary progressive multiple sclerosis [319]. Experimentally, IBU's neuroprotective effects are thought to stem from reduced neuroinflammation, apoptosis inhibition, or actions on the ubiquitin-proteasome pathway [319,397,398]. The observed reduction of TNF-α levels in the CSF depicted in Figure 14 also indicates a potential decrease in the production of mitochondria-derived ROS (Table 6, see also [130]). Hennet et al. [399] and Goossens et al. [400] first reported that TNF-α promotes ROS formation by mitochondria. Consequently,

the reduction in TNF-α levels induced by IBU suggests a probable decrease in mitochondria-derived ROS, positioning IBU as a good candidate to complement the therapeutic benefits obtained by NR and PT. However, although treatment with NR and PT did not show any significant toxicity in the $SOD1^{G93A}$ model [130] or in ALS patients [240], the use of IBU might encounter challenges due to potential side effects, including gastrointestinal and/or skin disorders [401]. In this study, mouse models were treated with a daily single dose of 12 mg/kg, equivalent to approximately 0.97 mg/kg per day in humans, based on the FDA-accepted conversion factor. Therefore, a patient of approximately 70 kg body weight should take a daily oral dose of 67.9 mg, and IBU shows an excellent safety profile at 60 mg/day [401].

Our results show that the combination of NR, PT, and IBU enhances the protection of MNs in murine models of ALS. This combined treatment significantly attenuates the oxidative and nitrosative stress caused by pro-inflammatory cytokines, which is highly deleterious to MNs (Figure 24). Thus, the use of NR+PT+IBU or NOS inhibitors currently under investigation in clinical trials (NCT04562831, NCT05095571, and NCT04057898) [402], emerges as a promising strategy against ALS.

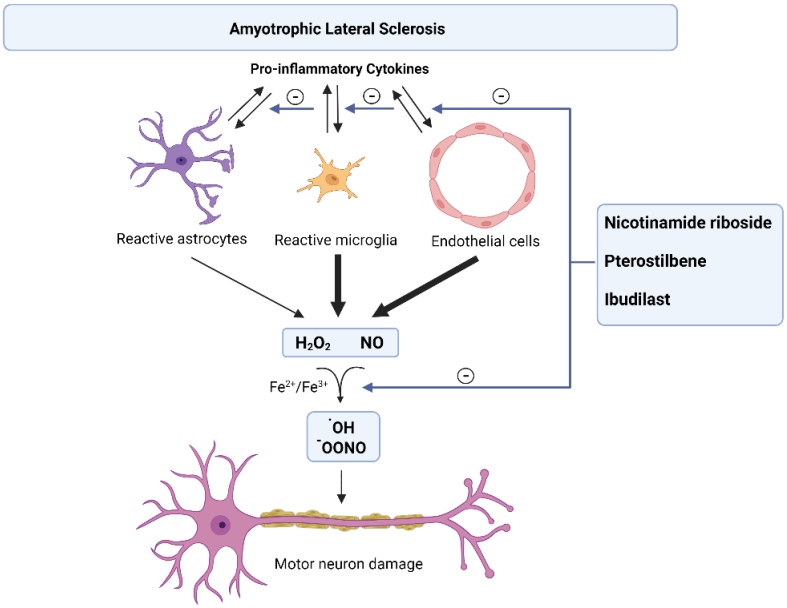

Figure 24. Diagram of the neuroprotective effects of the experimental treatment (NR+PT+IBU). *Figure created with BioRender.*

Additionally, this study provides strong evidence that potent oxidants, such as $^{\bullet}OH$ and $^{-}OONO$, which are primarily responsible for lipid, protein, and DNA oxidation, play a crucial role in the cascade of events leading to neuronal damage, involving catalysis by trace metals. This cascade of molecular events likely feed into itself, generating a vicious cycle of accumulated damage.

In conclusion, our results clearly suggest that a judicious combination of several drugs may be more beneficial than the use of individual drugs [247,345]. The treatment with NR+PT+IBU has significantly improved motor functions and survival in FUS and SOD mice. We believe this treatment could offer substantial benefits to ALS patients.

In fact, we are already working to promote the development of a clinical trial involving patients.

Furthermore, the complex pathophysiology of the disease, as well as the negative results of many clinical trials, also suggests that targeting patients early in their disease may be crucial. In this, it is important to consider that symptoms become evident (measurable) only after the death of a sufficient number of MNs, where progressive damage accumulates. Murine models of ALS are transgenic, and we know from the beginning that the mutation will cause the development of MN damage and approximately when it will occur. This is not the case in ALS patients, where treatments generally start (at best) after pre-diagnosis, when initial symptoms are already evident. When we planned experiments in a previous paper [130], we observed that if treatment (NR+PT) was started approximately 3 weeks before the onset of the symptoms, survival increased over time (by an average time of approximately 1 week longer in the case of $SOD1^{G93A}$ mice) compared to starting treatment just at the time of the symptom onset. Weaning in our mouse models occurs 3 weeks after birth. Therefore, we decided to start treatment 1 week after weaning (following the same strategy in the present work) [345]. These facts exemplify the need for early biomarkers that could indicate, in humans, the presence of a neuromotor disorder potentially associated with ALS. This would allow treatment to be applied before the clinical symptoms become evident. In practice, even before the onset of symptoms, early

treatment should be considered in individuals with known mutations associated with the etiology of FALS. Naturally, without reliable biomarkers, clinical decisions are much more complicated in cases of SALS [403].

6. CONCLUSIONS

Based on the results presented in this doctoral thesis, we can draw the following conclusions:

1. IBU emerged as the most tolerable PDE4 inhibitor, demonstrating a lack of significant side effects in both $SOD1^{G93A}$ and FUS^{R521C} mouse models.
2. The NR+PT+IBU treatment significantly reduce pro-inflammatory cytokine levels (INF-γ, IL-1β, IL-2, IL-6, and GM-CSF) in CSF, with IBU being particularly effective in inhibiting the production of TNF-α. This supports the synergistic anti-inflammatory effect exerted by the combined treatment.
3. Treatment with NR+PT+IBU effectively prevents the production of H_2O_2 and NO in MNs, astrocytes, microglia, and endothelial cells, thereby enhancing the survival of MNs isolated from ALS transgenic mice.
4. The significant increase in survival with L-NAME treatment confirms the critical role of NO-mediated nitrosative stress in ALS progression.
5. Attenuating inflammation reduces oxidative/nitrosative stress, which is a key driver of neurodegeneration in ALS. This not only curbs further inflammation but also improves neuromotor function, effectively breaking the destructive cycle. These findings provide valuable insights into the mechanisms underlying MNs survival in ALS.

6. IBU enhances neuroprotection exerted by NR and PT in the context of ALS. This combined treatment significantly delays the loss of neuromotor functions and increases survival in both $SOD1^{G93A}$ and FUS^{R521C} mouse models.

7. REFERENCES

1. de Carvalho M, Swash M. Diagnosis and differential diagnosis of MND/ALS: IFCN handbook chapter. Clin Neurophysiol Pract. 19 de diciembre de 2023;9:27-38.

2. Vidovic M, Müschen LH, Brakemeier S, Machetanz G, Naumann M, Castro-Gomez S. Current State and Future Directions in the Diagnosis of Amyotrophic Lateral Sclerosis. Cells. 24 de febrero de 2023;12(5):736.

3. Testa D, Lovati R, Ferrarini M, Salmoiraghi F, Filippini G. Survival of 793 patients with amyotrophic lateral sclerosis diagnosed over a 28-year period. Amyotroph Lateral Scler Mot Neuron Disord Off Publ World Fed Neurol Res Group Mot Neuron Dis. diciembre de 2004;5(4):208-12.

4. Traxinger K, Kelly C, Johnson BA, Lyles RH, Glass JD. Prognosis and epidemiology of amyotrophic lateral sclerosis: Analysis of a clinic population, 1997-2011. Neurol Clin Pract. agosto de 2013;3(4):313-20.

5. Requardt MV, Görlich D, Grehl T, Boentert M. Clinical Determinants of Disease Progression in Amyotrophic Lateral Sclerosis—A Retrospective Cohort Study. J Clin Med. enero de 2021;10(8):1623.

6. An exceptional man. BMJ. 22 de junio de 2002;324(7352):1478.

7. Ma YL, Li ZP. [Jean-Martin Charcot, discovery and nomenclature of amyotrophic lateral sclerosis]. Zhonghua Yi Shi Za Zhi Beijing China 1980. 28 de enero de 2019;49(1):14-8.

8. Al-Chalabi A, Kwak S, Mehler M, Rouleau G, Siddique T, Strong M, et al. Genetic and epigenetic studies of amyotrophic lateral sclerosis. Amyotroph Lateral Scler Front Degener. 16 de mayo de 2013;14.

9. A manual of diseases of the nervous system - Digital Collections - National Library of Medicine [Internet]. [citado 16 de abril de 2024]. Disponible en: https://collections.nlm.nih.gov/catalog/nlm:nlmuid-101509155-bk

10. Text-book of nervous diseases for physicians and students / by H. Oppenheim. [Internet]. Wellcome Collection. [citado 16 de abril de 2024]. Disponible en: https://wellcomecollection.org/works/f2rzbv4g

11. Henson RA. Russell Brain, DM, FRCP, FRS 1895-1966. Arch Neurol. 1 de mayo de 1967;16(5):559-60.

12. Freemon FR. Brain's Diseases of the Nervous System. JAMA. 10 de agosto de 1970;213(6):1041.

13. Wijesekera LC, Leigh PN. Amyotrophic lateral sclerosis. Orphanet J Rare Dis. 2009;4:3.

14. Ingre C, Roos PM, Piehl F, Kamel F, Fang F. Risk factors for amyotrophic lateral sclerosis. Clin Epidemiol. 2015;7:181-93.

15. Arthur K, Calvo A, Price T, Geiger J, Chió A, Traynor B. Projected increase in amyotrophic lateral sclerosis from 2015 to 2040. Nat Commun. 11 de agosto de 2016;7:12408.

16. Fontana A, Marin B, Luna J, Beghi E, Logroscino G, Boumédiene F, et al. Time-trend evolution and determinants of sex ratio in Amyotrophic Lateral Sclerosis: a dose-response meta-analysis. J Neurol. agosto de 2021;268(8):2973-84.

17. Ilieva H, Vullaganti M, Kwan J. Advances in molecular pathology, diagnosis, and treatment of amyotrophic lateral sclerosis. The BMJ. 27 de octubre de 2023;383:e075037.

18. Couratier P, Corcia P, Lautrette G, Nicol M, Preux PM, Marin B. Epidemiology of amyotrophic lateral sclerosis: A review of literature. Rev Neurol (Paris). enero de 2016;172(1):37-45.

19. Nona RJ, Xu Z, Robinson GA, Henderson RD, McCombe PA. Age of Onset and Length of Survival of Queensland Patients with Amyotrophic Lateral Sclerosis: Details of Subjects with Early Onset and Subjects with Long Survival. Neurodegener Dis. octubre de 2023;22(3-4):104-21.

20. Carrera-Juliá S, Estrela JM, Zacarés M, Navarro MÁ, Vega-Bello MJ, de la Rubia Ortí JE, et al. Nutritional, Clinical and Sociodemographic Profiles of Spanish Patients with Amyotrophic Lateral Sclerosis. Nutrients. 25 de enero de 2024;16(3):350.

21. Camacho A, Esteban J, Paradas C. Informe de la Fundación Del Cerebro sobre el impacto social de la esclerosis lateral amiotrófica y las enfermedades neuromusculares. Neurología. enero de 2018;33(1):35-46.

22. Xu L, Liu T, Liu L, Yao X, Chen L, Fan D, et al. Global variation in prevalence and incidence of amyotrophic lateral sclerosis: a systematic review and meta-analysis. J Neurol. 1 de abril de 2020;267(4):944-53.

23. Logroscino G, Piccininni M. Amyotrophic Lateral Sclerosis Descriptive Epidemiology: The Origin of Geographic Difference. Neuroepidemiology. 2019;52(1-2):93-103.

24. Logroscino G, Urso D, Tortelli R. The challenge of amyotrophic lateral sclerosis descriptive epidemiology: to estimate low incidence rates across complex phenotypes in different geographic areas. Curr Opin Neurol. octubre de 2022;35(5):678-85.

25. Duan QQ, Jiang Z, Su WM, Gu XJ, Wang H, Cheng YF, et al. Risk factors of amyotrophic lateral sclerosis: a global meta-summary. Front Neurosci. 24 de abril de 2023;17:1177431.

26. Byrne S, Bede P, Elamin M, Kenna K, Lynch C, McLaughlin R, et al. Proposed criteria for familial amyotrophic lateral sclerosis. Amyotroph Lateral Scler Off Publ World Fed Neurol Res Group Mot Neuron Dis. mayo de 2011;12(3):157-9.

27. Hardiman O, Al-Chalabi A, Chio A, Corr EM, Logroscino G, Robberecht W, et al. Amyotrophic lateral sclerosis. Nat Rev Dis Primer. 5 de octubre de 2017;3:17071.

28. Renton AE, Chiò A, Traynor BJ. State of play in amyotrophic lateral sclerosis genetics. Nat Neurosci. enero de 2014;17(1):17-23.

29. Turner MR, Al-Chalabi A, Chio A, Hardiman O, Kiernan MC, Rohrer JD, et al. Genetic screening in sporadic ALS and FTD. J Neurol Neurosurg Psychiatry. 1 de diciembre de 2017;88(12):1042-4.

30. Goutman SA, Hardiman O, Al-Chalabi A, Chió A, Savelieff MG, Kiernan MC, et al. Emerging insights into the complex genetics and pathophysiology of ALS. Lancet Neurol. mayo de 2022;21(5):465-79.

31. Majounie E, Renton AE, Mok K, Dopper EGP, Waite A, Rollinson S, et al. Frequency of the C9orf72 hexanucleotide repeat expansion in patients with amyotrophic lateral sclerosis and frontotemporal dementia: a cross-sectional study. Lancet Neurol. abril de 2012;11(4):323-30.

32. DeJesus-Hernandez M, Mackenzie IR, Boeve BF, Boxer AL, Baker M, Rutherford NJ, et al. Expanded GGGGCC hexanucleotide repeat in noncoding region of C9ORF72 causes chromosome 9p-linked FTD and ALS. Neuron. 20 de octubre de 2011;72(2):245-56.

33. Turner MR, Hardiman O, Benatar M, Brooks BR, Chio A, de Carvalho M, et al. Controversies and priorities in amyotrophic lateral sclerosis. Lancet Neurol. marzo de 2013;12(3):310-22.

34. Babić Leko M, Župunski V, Kirincich J, Smilović D, Hortobágyi T, Hof PR, et al. Molecular Mechanisms of Neurodegeneration Related to C9orf72 Hexanucleotide Repeat Expansion. Behav Neurol. 15 de enero de 2019;2019:2909168.

35. Flynn JM, Melov S. SOD2 in mitochondrial dysfunction and neurodegeneration. Free Radic Biol Med. septiembre de 2013;62:4-12.

36. Zelko IN, Mariani TJ, Folz RJ. Superoxide dismutase multigene family: a comparison of the CuZn-SOD (SOD1), Mn-SOD (SOD2), and EC-SOD (SOD3) gene structures, evolution, and expression. Free Radic Biol Med. 1 de agosto de 2002;33(3):337-49.

37. Fukai T, Ushio-Fukai M. Superoxide dismutases: role in redox signaling, vascular function, and diseases. Antioxid Redox Signal. 15 de septiembre de 2011;15(6):1583-606.

38. Rosen DR, Siddique T, Patterson D, Figlewicz DA, Sapp P, Hentati A, et al. Mutations in Cu/Zn superoxide dismutase gene are associated with familial amyotrophic lateral sclerosis. Nature. 4 de marzo de 1993;362(6415):59-62.

39. Reaume AG, Elliott JL, Hoffman EK, Kowall NW, Ferrante RJ, Siwek DF, et al. Motor neurons in Cu/Zn superoxide dismutase-deficient mice develop normally but exhibit enhanced cell death after axonal injury. Nat Genet. mayo de 1996;13(1):43-7.

40. Brown RH. Amyotrophic lateral sclerosis: recent insights from genetics and transgenic mice. Cell. 10 de marzo de 1995;80(5):687-92.

41. Tak YJ, Park JH, Rhim H, Kang S. ALS-Related Mutant SOD1 Aggregates Interfere with Mitophagy by Sequestering the Autophagy Receptor Optineurin. Int J Mol Sci. 13 de octubre de 2020;21(20):7525.

42. Trist BG, Fifita JA, Hogan A, Grima N, Smith B, Troakes C, et al. Co-deposition of SOD1, TDP-43 and p62 proteinopathies in ALS: evidence for multifaceted pathways underlying neurodegeneration. Acta Neuropathol Commun. 25 de agosto de 2022;10(1):122.

43. Taylor JP, Brown RH, Cleveland DW. Decoding ALS: from genes to mechanism. Nature. 10 de noviembre de 2016;539(7628):197-206.

44. Bruijn LI, Houseweart MK, Kato S, Anderson KL, Anderson SD, Ohama E, et al. Aggregation and motor neuron toxicity of an ALS-linked SOD1 mutant

independent from wild-type SOD1. Science. 18 de septiembre de 1998;281(5384):1851-4.

45. Brasil A de A, de Carvalho MDC, Gerhardt E, Queiroz DD, Pereira MD, Outeiro TF, et al. Characterization of the activity, aggregation, and toxicity of heterodimers of WT and ALS-associated mutant Sod1. Proc Natl Acad Sci [Internet]. 17 de diciembre de 2019 [citado 6 de abril de 2024];116(51):25991-6000. Disponible en: https://www.pnas.org/doi/full/10.1073/pnas.1902483116

46. Bunton-Stasyshyn RKA, Saccon RA, Fratta P, Fisher EMC. SOD1 Function and Its Implications for Amyotrophic Lateral Sclerosis Pathology: New and Renascent Themes. Neurosci Rev J Bringing Neurobiol Neurol Psychiatry. octubre de 2015;21(5):519-29.

47. Benkler C, O'Neil AL, Slepian S, Qian F, Weinreb PH, Rubin LL. Aggregated SOD1 causes selective death of cultured human motor neurons. Sci Rep [Internet]. 6 de noviembre de 2018 [citado 6 de abril de 2024];8(1):16393. Disponible en: https://www.nature.com/articles/s41598-018-34759-z

48. Thomas EV, Fenton WA, McGrath J, Horwich AL. Transfer of pathogenic and nonpathogenic cytosolic proteins between spinal cord motor neurons in vivo in chimeric mice. Proc Natl Acad Sci [Internet]. 11 de abril de 2017 [citado 6 de abril de 2024];114(15):E3139-48. Disponible en: https://www.pnas.org/doi/abs/10.1073/pnas.1701465114

49. Hayashi Y, Homma K, Ichijo H. SOD1 in neurotoxicity and its controversial roles in SOD1 mutation-negative ALS. Adv Biol Regul. enero de 2016;60:95-104.

50. Robberecht W, Philips T. The changing scene of amyotrophic lateral sclerosis. Nat Rev Neurosci. abril de 2013;14(4):248-64.

51. Ranganathan R, Haque S, Coley K, Shepheard S, Cooper-Knock J, Kirby J. Multifaceted Genes in Amyotrophic Lateral Sclerosis-Frontotemporal Dementia. Front Neurosci [Internet]. 7 de julio de 2020 [citado 6 de abril de 2024];14:684. Disponible en: https://www.ncbi.nlm.nih.gov/pmc/articles/PMC7358438/

52. Kim G, Gautier O, Tassoni-Tsuchida E, Ma XR, Gitler AD. ALS Genetics: Gains, Losses, and Implications for Future Therapies. Neuron [Internet]. 9 de diciembre de 2020 [citado 6 de abril de 2024];108(5):822-42. Disponible en: https://www.ncbi.nlm.nih.gov/pmc/articles/PMC7736125/

53. Butti Z, Patten SA. RNA Dysregulation in Amyotrophic Lateral Sclerosis. Front Genet. 2018;9:712.

54. Birsa N, Bentham MP, Fratta P. Cytoplasmic functions of TDP-43 and FUS and their role in ALS. Semin Cell Dev Biol. marzo de 2020;99:193-201.

55. Aulas A, Vande Velde C. Alterations in stress granule dynamics driven by TDP-43 and FUS: a link to pathological inclusions in ALS? Front Cell Neurosci. 2015;9:423.

56. Guerrero EN, Wang H, Mitra J, Hegde PM, Stowell SE, Liachko NF, et al. TDP-43/FUS in motor neuron disease: Complexity and challenges. Prog Neurobiol. 2016;145-146:78-97.

57. Wood A, Gurfinkel Y, Polain N, Lamont W, Lyn Rea S. Molecular Mechanisms Underlying TDP-43 Pathology in Cellular and Animal Models of ALS and FTLD. Int J Mol Sci. 29 de abril de 2021;22(9):4705.

58. Klim JR, Williams LA, Limone F, Guerra San Juan I, Davis-Dusenbery BN, Mordes DA, et al. ALS-implicated protein TDP-43 sustains levels of STMN2, a mediator of motor neuron growth and repair. Nat Neurosci. febrero de 2019;22(2):167-79.

59. Mackenzie IR, Rademakers R, Neumann M. TDP-43 and FUS in amyotrophic lateral sclerosis and frontotemporal dementia. Lancet Neurol. octubre de 2010;9(10):995-1007.

60. Ling SC, Polymenidou M, Cleveland DW. Converging mechanisms in ALS and FTD: disrupted RNA and protein homeostasis. Neuron. 7 de agosto de 2013;79(3):416-38.

61. Al-Chalabi A, van den Berg LH, Veldink J. Gene discovery in amyotrophic lateral sclerosis: implications for clinical management. Nat Rev Neurol. febrero de 2017;13(2):96-104.

62. Mejzini R, Flynn LL, Pitout IL, Fletcher S, Wilton SD, Akkari PA. ALS Genetics, Mechanisms, and Therapeutics: Where Are We Now? Front Neurosci [Internet]. 6 de diciembre de 2019 [citado 13 de diciembre de 2020];13. Disponible en: https://www.ncbi.nlm.nih.gov/pmc/articles/PMC6909825/

63. Chia R, Chiò A, Traynor BJ. Novel genes associated with amyotrophic lateral sclerosis: diagnostic and clinical implications. Lancet Neurol. enero de 2018;17(1):94-102.

64. Goutman SA, Hardiman O, Al-Chalabi A, Chió A, Savelieff MG, Kiernan MC, et al. Emerging insights into the complex genetics and pathophysiology of amyotrophic lateral sclerosis. Lancet Neurol. 1 de mayo de 2022;21(5):465-79.

65. Feldman EL, Goutman SA, Petri S, Mazzini L, Savelieff MG, Shaw PJ, et al. Amyotrophic lateral sclerosis. The Lancet. 15 de octubre de 2022;400(10360):1363-80.

66. Gordon PH. Amyotrophic Lateral Sclerosis: An update for 2013 Clinical Features, Pathophysiology, Management and Therapeutic Trials. Aging Dis. 1 de octubre de 2013;4(5):295-310.

67. Liscic RM, Alberici A, Cairns NJ, Romano M, Buratti E. From basic research to the clinic: innovative therapies for ALS and FTD in the pipeline. Mol Neurodegener. 1 de junio de 2020;15(1):31.

68. Riancho J, Gonzalo I, Ruiz-Soto M, Berciano J. Why do motor neurons degenerate? Actualisation in the pathogenesis of amyotrophic lateral sclerosis. Neurol Engl Ed. 1 de enero de 2019;34(1):27-37.

69. Chen H, Richard M, Sandler DP, Umbach DM, Kamel F. Head Injury and Amyotrophic Lateral Sclerosis. Am J Epidemiol. 1 de octubre de 2007;166(7):810-6.

70. Liu G, Ou S, Cui H, Li X, Yin Z, Gu D, et al. Head Injury and Amyotrophic Lateral Sclerosis: A Meta-Analysis. Neuroepidemiology. 23 de febrero de 2021;1-9.

71. Chapman L, Cooper-Knock J, Shaw PJ. Physical activity as an exogenous risk factor for amyotrophic lateral sclerosis: a review of the evidence. Brain. 2 de mayo de 2023;146(5):1745-57.

72. Thomsen GM, Ma AM, Ko A, Harada MY, Wyss L, Haro PS, et al. A model of recurrent concussion that leads to long-term motor deficits, CTE-like tauopathy and exacerbation of an ALS phenotype. J Trauma Acute Care Surg. diciembre de 2016;81(6):1070.

73. McKay KA, Smith KA, Smertinaite L, Fang F, Ingre C, Taube F. Military service and related risk factors for amyotrophic lateral sclerosis. Acta Neurol Scand. enero de 2021;143(1):39-50.

74. Weisskopf MG, O'Reilly EJ, McCullough ML, Calle EE, Thun MJ, Cudkowicz M, et al. Prospective study of military service and mortality from ALS. Neurology. 11 de enero de 2005;64(1):32-7.

75. O'Reilly ÉJ, Wang M, Adami HO, Alonso A, Bernstein L, van den Brandt P, et al. Prediagnostic body size and risk of amyotrophic lateral sclerosis death in 10 studies. Amyotroph Lateral Scler Front Degener. agosto de 2018;19(5-6):396-406.

76. Nakken O, Meyer HE, Stigum H, Holmøy T. High BMI is associated with low ALS risk: A population-based study. Neurology. 30 de julio de 2019;93(5):e424-32.

77. Riancho J, Bosque-Varela P, Perez-Pereda S, Povedano M, de Munaín AL, Santurtun A. The increasing importance of environmental conditions in amyotrophic lateral sclerosis. Int J Biometeorol. 1 de agosto de 2018;62(8):1361-74.

78. Al-Chalabi A, Hardiman O. The epidemiology of ALS: a conspiracy of genes, environment and time. Nat Rev Neurol. noviembre de 2013;9(11):617-28.

79. Al-Chalabi A, Fang F, Hanby MF, Leigh PN, Shaw CE, Ye W, et al. An estimate of amyotrophic lateral sclerosis heritability using twin data. J Neurol Neurosurg Psychiatry. diciembre de 2010;81(12):1324-6.

80. Ovsepian SV, O'Leary VB, Martinez S. Selective vulnerability of motor neuron types and functional groups to degeneration in amyotrophic lateral sclerosis: review of the neurobiological mechanisms and functional correlates. Brain Struct Funct. enero de 2024;229(1):1-14.

81. van Es MA, Hardiman O, Chio A, Al-Chalabi A, Pasterkamp RJ, Veldink JH, et al. Amyotrophic lateral sclerosis. Lancet Lond Engl. 4 de noviembre de 2017;390(10107):2084-98.

82. de Souza PVS, Serrano P de L, Farias IB, Machado RIL, Badia B de ML, de Oliveira HB, et al. Clinical and Genetic Aspects of Juvenile Amyotrophic Lateral Sclerosis: A Promising Era Emerges. Genes. 28 de febrero de 2024;15(3):311.

83. Swinnen B, Robberecht W. The phenotypic variability of amyotrophic lateral sclerosis. Nat Rev Neurol. noviembre de 2014;10(11):661-70.

84. Bali T, Miller TM. Management of Amyotrophic Lateral Sclerosis. Mo Med [Internet]. 2013 [citado 1 de enero de 2024];110(5):417-21. Disponible en: https://www.ncbi.nlm.nih.gov/pmc/articles/PMC6179867/

85. Garg N, Park SB, Vucic S, Yiannikas C, Spies J, Howells J, et al. Differentiating lower motor neuron syndromes. J Neurol Neurosurg Psychiatry. junio de 2017;88(6):474-83.

86. Goldin DS. Pseudobulbar Affect: An Overview. J Psychosoc Nurs Ment Health Serv. 1 de septiembre de 2020;58(9):19-24.

87. Renton AE, Majounie E, Waite A, Simón-Sánchez J, Rollinson S, Gibbs JR, et al. A hexanucleotide repeat expansion in C9ORF72 is the cause of chromosome 9p21-linked ALS-FTD. Neuron. 20 de octubre de 2011;72(2):257-68.

88. Neumann M, Sampathu DM, Kwong LK, Truax AC, Micsenyi MC, Chou TT, et al. Ubiquitinated TDP-43 in frontotemporal lobar degeneration and amyotrophic lateral sclerosis. Science. 6 de octubre de 2006;314(5796):130-3.

89. Gao F, Almeida S, Lopez-Gonzalez R. Dysregulated molecular pathways in amyotrophic lateral sclerosis–frontotemporal dementia spectrum disorder. EMBO J. 16 de octubre de 2017;36(20):2931-50.

90. Abramzon YA, Fratta P, Traynor BJ, Chia R. The Overlapping Genetics of Amyotrophic Lateral Sclerosis and Frontotemporal Dementia. Front Neurosci [Internet]. 5 de febrero de 2020 [citado 19 de marzo de 2024];14. Disponible en: https://www.frontiersin.org/journals/neuroscience/articles/10.3389/fnins.2020.00042/full

91. Häkkinen S, Chu SA, Lee SE. Neuroimaging in genetic frontotemporal dementia and amyotrophic lateral sclerosis. Neurobiol Dis. 1 de noviembre de 2020;145:105063.

92. Neary D, Snowden JS, Gustafson L, Passant U, Stuss D, Black S, et al. Frontotemporal lobar degeneration: a consensus on clinical diagnostic criteria. Neurology. diciembre de 1998;51(6):1546-54.

93. Majoor-Krakauer D, Ottman R, Johnson WG, Rowland LP. Familial aggregation of amyotrophic lateral sclerosis, dementia, and Parkinson's disease: evidence of shared genetic susceptibility. Neurology. octubre de 1994;44(10):1872-7.

94. Huisman MHB, de Jong SW, Verwijs MC, Schelhaas HJ, van der Kooi AJ, de Visser M, et al. Family history of neurodegenerative and vascular diseases in ALS: a population-based study. Neurology. 4 de octubre de 2011;77(14):1363-9.

95. Byrne S, Heverin M, Elamin M, Bede P, Lynch C, Kenna K, et al. Aggregation of neurologic and neuropsychiatric disease in amyotrophic lateral sclerosis kindreds: a population-based case-control cohort study of familial and sporadic amyotrophic lateral sclerosis. Ann Neurol. noviembre de 2013;74(5):699-708.

96. Fallis BA, Hardiman O. Aggregation of neurodegenerative disease in ALS kindreds. Amyotroph Lateral Scler Off Publ World Fed Neurol Res Group Mot Neuron Dis. abril de 2009;10(2):95-8.

97. Caballero-Hernandez D, Toscano MG, Cejudo-Guillen M, Garcia-Martin ML, Lopez S, Franco JM, et al. The «Omics» of Amyotrophic Lateral Sclerosis. Trends Mol Med. enero de 2016;22(1):53-67.

98. Paganoni S, Macklin EA, Lee A, Murphy A, Chang J, Zipf A, et al. Diagnostic timelines and delays in diagnosing amyotrophic lateral sclerosis (ALS). Amyotroph Lateral Scler Front Degener. septiembre de 2014;15(5-6):453-6.

99. Kraemer M, Buerger M, Berlit P. Diagnostic problems and delay of diagnosis in amyotrophic lateral sclerosis. Clin Neurol Neurosurg. febrero de 2010;112(2):103-5.

100. Brooks BR. El Escorial World Federation of Neurology criteria for the diagnosis of amyotrophic lateral sclerosis. Subcommittee on Motor Neuron Diseases/Amyotrophic Lateral Sclerosis of the World Federation of Neurology Research Group on Neuromuscular Diseases and the El Escorial «Clinical limits of amyotrophic lateral sclerosis» workshop contributors. J Neurol Sci. julio de 1994;124 Suppl:96-107.

101. Brooks BR, Miller RG, Swash M, Munsat TL, World Federation of Neurology Research Group on Motor Neuron Diseases. El Escorial revisited: revised criteria for the diagnosis of amyotrophic lateral sclerosis. Amyotroph Lateral Scler Mot Neuron Disord. diciembre de 2000;1(5):293-9.

102. Verma A. Clinical Manifestation and Management of Amyotrophic Lateral Sclerosis. En: Araki T, editor. Amyotrophic Lateral Sclerosis [Internet]. Brisbane (AU): Exon Publications; 2021 [citado 26 de febrero de 2024]. Disponible en: http://www.ncbi.nlm.nih.gov/books/NBK573427/

103. de Carvalho M, Dengler R, Eisen A, England JD, Kaji R, Kimura J, et al. Electrodiagnostic criteria for diagnosis of ALS. Clin Neurophysiol Off J Int Fed Clin Neurophysiol. marzo de 2008;119(3):497-503.

104. Tao QQ, Wu ZY. Amyotrophic Lateral Sclerosis: Precise Diagnosis and Individualized Treatment. Chin Med J (Engl) [Internet]. 5 de octubre de 2017 [citado 19 de abril de 2024];130(19):2269-72. Disponible en: https://www.ncbi.nlm.nih.gov/pmc/articles/PMC5634073/

105. Johnsen B, Pugdahl K, Fuglsang-Frederiksen A, Kollewe K, Paracka L, Dengler R, et al. Diagnostic criteria for amyotrophic lateral sclerosis: A multicentre study of inter-rater variation and sensitivity. Clin Neurophysiol Off J Int Fed Clin Neurophysiol. febrero de 2019;130(2):307-14.

106. Traynor BJ, Codd MB, Corr B, Forde C, Frost E, Hardiman OM. Clinical features of amyotrophic lateral sclerosis according to the El Escorial and Airlie House diagnostic criteria: A population-based study. Arch Neurol. agosto de 2000;57(8):1171-6.

107. Shefner JM, Al-Chalabi A, Baker MR, Cui LY, de Carvalho M, Eisen A, et al. A proposal for new diagnostic criteria for ALS. Clin Neurophysiol Off J Int Fed Clin Neurophysiol. agosto de 2020;131(8):1975-8.

108. Turner MR, UK MND Clinical Studies Group. Diagnosing ALS: the Gold Coast criteria and the role of EMG. Pract Neurol. junio de 2022;22(3):176-8.

109. Hannaford A, Pavey N, van den Bos M, Geevasinga N, Menon P, Shefner JM, et al. Diagnostic Utility of Gold Coast Criteria in Amyotrophic Lateral Sclerosis. Ann Neurol. mayo de 2021;89(5):979-86.

110. Krarup C. Lower motor neuron involvement examined by quantitative electromyography in amyotrophic lateral sclerosis. Clin Neurophysiol Off J Int Fed Clin Neurophysiol. febrero de 2011;122(2):414-22.

111. Joyce NC, Carter GT. Electrodiagnosis in Amyotrophic Lateral Sclerosis. PM R [Internet]. mayo de 2013 [citado 1 de enero de 2024];5(5 0):S89-95. Disponible en: https://www.ncbi.nlm.nih.gov/pmc/articles/PMC4590769/

112. Kollewe K, Körner S, Dengler R, Petri S, Mohammadi B. Magnetic Resonance Imaging in Amyotrophic Lateral Sclerosis. Neurol Res Int [Internet]. 2012 [citado 1 de enero de 2024];2012:608501. Disponible en: https://www.ncbi.nlm.nih.gov/pmc/articles/PMC3400399/

113. Dreger M, Steinbach R, Otto M, Turner MR, Grosskreutz J. Cerebrospinal fluid biomarkers of disease activity and progression in amyotrophic lateral sclerosis. J Neurol Neurosurg Psychiatry [Internet]. abril de 2022 [citado 1 de enero de 2024];93(4):422-35. Disponible en: https://www.ncbi.nlm.nih.gov/pmc/articles/PMC8921583/

114. Leonardi A, Abbruzzese G, Arata L, Cocito L, Vische M. Cerebrospinal fluid (CSF) findings in amyotrophic lateral sclerosis. J Neurol. 1984;231(2):75-8.

115. Andersen PM, Al-Chalabi A. Clinical genetics of amyotrophic lateral sclerosis: what do we really know? Nat Rev Neurol. 11 de octubre de 2011;7(11):603-15.

116. Gwathmey KG, Corcia P, McDermott CJ, Genge A, Sennfält S, de Carvalho M, et al. Diagnostic delay in amyotrophic lateral sclerosis. Eur J Neurol. septiembre de 2023;30(9):2595-601.

117. Mejzini R, Flynn LL, Pitout IL, Fletcher S, Wilton SD, Akkari PA. ALS Genetics, Mechanisms, and Therapeutics: Where Are We Now? Front Neurosci. 2019;13:1310.

118. Mead RJ, Shan N, Reiser HJ, Marshall F, Shaw PJ. Amyotrophic lateral sclerosis: a neurodegenerative disorder poised for successful therapeutic translation. Nat Rev Drug Discov. marzo de 2023;22(3):185-212.

119. Zhou W, Xu R. Current insights in the molecular genetic pathogenesis of amyotrophic lateral sclerosis. Front Neurosci. 2023;17:1189470.

120. Foran E, Bogush A, Goffredo M, Roncaglia P, Gustincich S, Pasinelli P, et al. Motor neuron impairment mediated by a sumoylated fragment of the glial glutamate transporter EAAT2. Glia. noviembre de 2011;59(11):1719-31.

121. Provenzano F, Torazza C, Bonifacino T, Bonanno G, Milanese M. The Key Role of Astrocytes in Amyotrophic Lateral Sclerosis and Their Commitment to Glutamate Excitotoxicity. Int J Mol Sci. 21 de octubre de 2023;24(20):15430.

122. Tandan R, Robison SH, Munzer JS, Bradley WG. Deficient DNA repair in amyotrophic lateral sclerosis cells. J Neurol Sci. junio de 1987;79(1-2):189-203.

123. Konopka A, Atkin JD. DNA Damage, Defective DNA Repair, and Neurodegeneration in Amyotrophic Lateral Sclerosis. Front Aging Neurosci. 2022;14:786420.

124. Bennett SA, Tanaz R, Cobos SN, Torrente MP. Epigenetics in amyotrophic lateral sclerosis: a role for histone post-translational modifications in neurodegenerative disease. Transl Res J Lab Clin Med. febrero de 2019;204:19-30.

125. Dudman J, Qi X. Stress Granule Dysregulation in Amyotrophic Lateral Sclerosis. Front Cell Neurosci. 2020;14:598517.

126. Arnold FJ, Nguyen AD, Bedlack RS, Bennett CL, La Spada AR. Intercellular transmission of pathogenic proteins in ALS: Exploring the pathogenic wave. Neurobiol Dis. agosto de 2023;184:106218.

127. Chen W, Guo L, Li M, Wei C, Li S, Xu R. The pathogenesis of amyotrophic lateral sclerosis: Mitochondrial dysfunction, protein misfolding and epigenetics. Brain Res. 1 de julio de 2022;1786:147904.

128. Calafatti M, Cocozza G, Limatola C, Garofalo S. Microglial crosstalk with astrocytes and immune cells in amyotrophic lateral sclerosis. Front Immunol. 2023;14:1223096.

129. Cunha-Oliveira T, Montezinho L, Mendes C, Firuzi O, Saso L, Oliveira PJ, et al. Oxidative Stress in Amyotrophic Lateral Sclerosis: Pathophysiology and Opportunities for Pharmacological Intervention. Oxid Med Cell Longev. 2020;2020:5021694.

130. Obrador E, Salvador R, Marchio P, López-Blanch R, Jihad-Jebbar A, Rivera P, et al. Nicotinamide Riboside and Pterostilbene Cooperatively Delay Motor Neuron Failure in ALS SOD1G93A Mice. Mol Neurobiol. abril de 2021;58(4):1345-71.

131. Wiedemann FR, Manfredi G, Mawrin C, Beal MF, Schon EA. Mitochondrial DNA and respiratory chain function in spinal cords of ALS patients. J Neurochem. febrero de 2002;80(4):616-25.

132. Gunnarsson LG, Bodin L. Amyotrophic Lateral Sclerosis and Occupational Exposures: A Systematic Literature Review and Meta-Analyses. Int J Environ Res Public Health. 26 de octubre de 2018;15(11):2371.

133. Zhao J, Wang X, Huo Z, Chen Y, Liu J, Zhao Z, et al. The Impact of Mitochondrial Dysfunction in Amyotrophic Lateral Sclerosis. Cells. 28 de junio de 2022;11(13):2049.

134. Evans CS, Holzbaur ELF. Autophagy and mitophagy in ALS. Neurobiol Dis. febrero de 2019;122:35-40.

135. Alami NH, Smith RB, Carrasco MA, Williams LA, Winborn CS, Han SSW, et al. Axonal transport of TDP-43 mRNA granules is impaired by ALS-causing mutations. Neuron. 5 de febrero de 2014;81(3):536-43.

136. De Vos KJ, Hafezparast M. Neurobiology of axonal transport defects in motor neuron diseases: Opportunities for translational research? Neurobiol Dis. septiembre de 2017;105:283-99.

137. Teleanu RI, Niculescu AG, Roza E, Vladâcenco O, Grumezescu AM, Teleanu DM. Neurotransmitters—Key Factors in Neurological and Neurodegenerative Disorders of the Central Nervous System. Int J Mol Sci. 25 de mayo de 2022;23(11):5954.

138. Le Gall L, Anakor E, Connolly O, Vijayakumar UG, Duddy WJ, Duguez S. Molecular and Cellular Mechanisms Affected in ALS. J Pers Med. 25 de agosto de 2020;10(3):101.

139. Kiernan MC, Vucic S, Cheah BC, Turner MR, Eisen A, Hardiman O, et al. Amyotrophic lateral sclerosis. The Lancet. 12 de marzo de 2011;377(9769):942-55.

140. Scofield MD, Korutla L, Jackson TG, Kalivas PW, Mackler SA. Nucleus Accumbens 1, a Pox virus and Zinc finger/Bric-a-brac Tramtrack Broad protein binds to TAR DNA-binding protein 43 and has a potential role in Amyotrophic Lateral Sclerosis. Neuroscience. 27 de diciembre de 2012;227:44-54.

141. Rosenblum LT, Trotti D. EAAT2 and the Molecular Signature of Amyotrophic Lateral Sclerosis. Adv Neurobiol. 2017;16:117-36.

142. Bendotti C, Tortarolo M, Suchak SK, Calvaresi N, Carvelli L, Bastone A, et al. Transgenic SOD1 G93A mice develop reduced GLT-1 in spinal cord without alterations in cerebrospinal fluid glutamate levels. J Neurochem. 2001;79(4):737-46.

143. Do-Ha D, Buskila Y, Ooi L. Impairments in Motor Neurons, Interneurons and Astrocytes Contribute to Hyperexcitability in ALS: Underlying Mechanisms and Paths to Therapy. Mol Neurobiol. 2018;55(2):1410-8.

144. Obrador E, Salvador R, López-Blanch R, Jihad-Jebbar A, Vallés SL, Estrela JM. Oxidative Stress, Neuroinflammation and Mitochondria in the Pathophysiology of Amyotrophic Lateral Sclerosis. Antioxid Basel Switz. 22 de septiembre de 2020;9(9).

145. Burk K, Pasterkamp RJ. Disrupted neuronal trafficking in amyotrophic lateral sclerosis. Acta Neuropathol (Berl). junio de 2019;137(6):859-77.

146. Clark JA, Southam KA, Blizzard CA, King AE, Dickson TC. Axonal degeneration, distal collateral branching and neuromuscular junction architecture alterations occur prior to symptom onset in the SOD1(G93A) mouse model of amyotrophic lateral sclerosis. J Chem Neuroanat. octubre de 2016;76(Pt A):35-47.

147. Nicolas A, Kenna KP, Renton AE, Ticozzi N, Faghri F, Chia R, et al. Genome-wide Analyses Identify KIF5A as a Novel ALS Gene. Neuron. 21 de marzo de 2018;97(6):1268-1283.e6.

148. Bilsland LG, Sahai E, Kelly G, Golding M, Greensmith L, Schiavo G. Deficits in axonal transport precede ALS symptoms in vivo. Proc Natl Acad Sci U S A. 23 de noviembre de 2010;107(47):20523-8.

149. Volkening K, Leystra-Lantz C, Yang W, Jaffee H, Strong MJ. Tar DNA binding protein of 43 kDa (TDP-43), 14-3-3 proteins and copper/zinc superoxide dismutase (SOD1) interact to modulate NFL mRNA stability. Implications for altered RNA processing in amyotrophic lateral sclerosis (ALS). Brain Res. 11 de diciembre de 2009;1305:168-82.

150. Giampetruzzi A, Danielson EW, Gumina V, Jeon M, Boopathy S, Brown RH, et al. Modulation of actin polymerization affects nucleocytoplasmic transport in multiple forms of amyotrophic lateral sclerosis. Nat Commun. 23 de agosto de 2019;10(1):3827.

151. Kieran D, Hafezparast M, Bohnert S, Dick JRT, Martin J, Schiavo G, et al. A mutation in dynein rescues axonal transport defects and extends the life span of ALS mice. J Cell Biol. 23 de mayo de 2005;169(4):561-7.

152. Dubowsky M, Shepheard SR, Rogers ML. Neurotrophic Therapy for ALS/MND. En: Kostrzewa RM, editor. Handbook of Neurotoxicity [Internet]. Cham: Springer International Publishing; 2022 [citado 7 de marzo de 2024]. p. 1893-929. Disponible en: https://doi.org/10.1007/978-3-031-15080-7_34

153. Anand P, Parrett A, Martin J, Zeman S, Foley P, Swash M, et al. Regional changes of ciliary neurotrophic factor and nerve growth factor levels in post mortem spinal cord and cerebral cortex from patients with motor disease. Nat Med. febrero de 1995;1(2):168-72.

154. Oosthuyse B, Moons L, Storkebaum E, Beck H, Nuyens D, Brusselmans K, et al. Deletion of the hypoxia-response element in the vascular endothelial growth factor promoter causes motor neuron degeneration. Nat Genet. junio de 2001;28(2):131-8.

155. Henriques A, Pitzer C, Schneider A. Neurotrophic Growth Factors for the Treatment of Amyotrophic Lateral Sclerosis: Where Do We Stand? Front Neurosci. 11 de junio de 2010;4:32.

156. Tovar-y-Romo LB, Ramírez-Jarquín UN, Lazo-Gómez R, Tapia R. Trophic factors as modulators of motor neuron physiology and survival: implications for ALS therapy. Front Cell Neurosci. 28 de febrero de 2014;8:61.

157. Petrov D, Mansfield C, Moussy A, Hermine O. ALS Clinical Trials Review: 20 Years of Failure. Are We Any Closer to Registering a New Treatment? Front Aging Neurosci. 2017;9:68.

158. Gouel F, Rolland AS, Devedjian JC, Burnouf T, Devos D. Past and Future of Neurotrophic Growth Factors Therapies in ALS: From Single Neurotrophic Growth Factor to Stem Cells and Human Platelet Lysates. Front Neurol. 2 de agosto de 2019;10:835.

159. Parakh S, Atkin JD. Protein folding alterations in amyotrophic lateral sclerosis. Brain Res. 1 de octubre de 2016;1648(Pt B):633-49.

160. Jeon YM, Kwon Y, Lee S, Kim HJ. Potential roles of the endoplasmic reticulum stress pathway in amyotrophic lateral sclerosis. Front Aging Neurosci. 15 de febrero de 2023;15:1047897.

161. Saxena S, Caroni P. Selective Neuronal Vulnerability in Neurodegenerative Diseases: from Stressor Thresholds to Degeneration. Neuron. 14 de julio de 2011;71(1):35-48.

162. Mackenzie IRA, Bigio EH, Ince PG, Geser F, Neumann M, Cairns NJ, et al. Pathological TDP-43 distinguishes sporadic amyotrophic lateral sclerosis from amyotrophic lateral sclerosis with SOD1 mutations. Ann Neurol. mayo de 2007;61(5):427-34.

163. Bozzo F, Mirra A, Carrì MT. Oxidative stress and mitochondrial damage in the pathogenesis of ALS: New perspectives. Neurosci Lett. 01 de 2017;636:3-8.

164. Nakagawa Y, Yamada S. A novel hypothesis on metal dyshomeostasis and mitochondrial dysfunction in amyotrophic lateral sclerosis: Potential pathogenetic mechanism and therapeutic implications. Eur J Pharmacol. 5 de febrero de 2021;892:173737.

165. Ash PEA, Dhawan U, Boudeau S, Lei S, Carlomagno Y, Knobel M, et al. Heavy Metal Neurotoxicants Induce ALS-Linked TDP-43 Pathology. Toxicol Sci Off J Soc Toxicol. 1 de enero de 2019;167(1):105-15.

166. Robertson J, Sanelli T, Xiao S, Yang W, Horne P, Hammond R, et al. Lack of TDP-43 abnormalities in mutant SOD1 transgenic mice shows disparity with ALS. Neurosci Lett. 13 de junio de 2007;420(2):128-32.

167. Turner BJ, Bäumer D, Parkinson NJ, Scaber J, Ansorge O, Talbot K. TDP-43 expression in mouse models of amyotrophic lateral sclerosis and spinal muscular atrophy. BMC Neurosci. 28 de octubre de 2008;9:104.

168. Tan CF, Eguchi H, Tagawa A, Onodera O, Iwasaki T, Tsujino A, et al. TDP-43 immunoreactivity in neuronal inclusions in familial amyotrophic lateral sclerosis with or without SOD1 gene mutation. Acta Neuropathol (Berl). mayo de 2007;113(5):535-42.

169. Cai M, Lee KW, Choi SM, Yang EJ. TDP-43 modification in the hSOD1(G93A) amyotrophic lateral sclerosis mouse model. Neurol Res. marzo de 2015;37(3):253-62.

170. Lu Y, Tang C, Zhu L, Li J, Liang H, Zhang J, et al. The Overexpression of TDP-43 Protein in the Neuron and Oligodendrocyte Cells Causes the Progressive Motor Neuron Degeneration in the SOD1 G93A Transgenic Mouse Model of Amyotrophic Lateral Sclerosis. Int J Biol Sci. 2016;12(9):1140-9.

171. Blokhuis AM, Groen EJN, Koppers M, van den Berg LH, Pasterkamp RJ. Protein aggregation in amyotrophic lateral sclerosis. Acta Neuropathol (Berl). junio de 2013;125(6):777-94.

172. Deng HX, Zhai H, Bigio EH, Yan J, Fecto F, Ajroud K, et al. FUS-immunoreactive inclusions are a common feature in sporadic and non-SOD1 familial amyotrophic lateral sclerosis. Ann Neurol. junio de 2010;67(6):739-48.

173. Forsberg K, Jonsson PA, Andersen PM, Bergemalm D, Graffmo KS, Hultdin M, et al. Novel antibodies reveal inclusions containing non-native SOD1 in sporadic ALS patients. PloS One. 14 de julio de 2010;5(7):e11552.

174. Sasaki S. Endoplasmic reticulum stress in motor neurons of the spinal cord in sporadic amyotrophic lateral sclerosis. J Neuropathol Exp Neurol. abril de 2010;69(4):346-55.

175. Sawada H. Considerations for pharmacotherapy use in patients with amyotrophic lateral sclerosis: the earlier it starts, the better the results. Expert Opin Pharmacother. octubre de 2019;20(14):1671-4.

176. Bernard-Marissal N, Chrast R, Schneider BL. Endoplasmic reticulum and mitochondria in diseases of motor and sensory neurons: a broken relationship? Cell Death Dis. 28 de febrero de 2018;9(3):333.

177. Ramesh N, Pandey UB. Autophagy Dysregulation in ALS: When Protein Aggregates Get Out of Hand. Front Mol Neurosci. 2017;10:263.

178. Nguyen DKH, Thombre R, Wang J. Autophagy as a common pathway in amyotrophic lateral sclerosis. Neurosci Lett. 1 de abril de 2019;697:34-48.

179. Budini M, Buratti E, Morselli E, Criollo A. Autophagy and Its Impact on Neurodegenerative Diseases: New Roles for TDP-43 and C9orf72. Front Mol Neurosci. 30 de mayo de 2017;10:170.

180. Barmada SJ, Serio A, Arjun A, Bilican B, Daub A, Ando DM, et al. Autophagy induction enhances TDP43 turnover and survival in neuronal ALS models. Nat Chem Biol. agosto de 2014;10(8):677-85.

181. Yuan F, Yang L, Zhang Z, Wu W, Zhou X, Yin X, et al. Cellular prion protein (PrPC) of the neuron cell transformed to a PK-resistant protein under oxidative stress, comprising main mitochondrial damage in prion diseases. J Mol Neurosci MN. septiembre de 2013;51(1):219-24.

182. Ayers JI, Cashman NR. Prion-like mechanisms in amyotrophic lateral sclerosis. Handb Clin Neurol. 2018;153:337-54.

183. Bräuer S, Zimyanin V, Hermann A. Prion-like properties of disease-relevant proteins in amyotrophic lateral sclerosis. J Neural Transm Vienna Austria 1996. abril de 2018;125(4):591-613.

184. Porta S, Xu Y, Restrepo CR, Kwong LK, Zhang B, Brown HJ, et al. Patient-derived frontotemporal lobar degeneration brain extracts induce formation and spreading of TDP-43 pathology in vivo. Nat Commun. 11 de octubre de 2018;9(1):4220.

185. Philips T, Rothstein JD. Glial cells in amyotrophic lateral sclerosis. Exp Neurol. 1 de diciembre de 2014;262:111-20.

186. Liu J, Wang F. Role of Neuroinflammation in Amyotrophic Lateral Sclerosis: Cellular Mechanisms and Therapeutic Implications. Front Immunol [Internet]. 2017 [citado 14 de octubre de 2019];8. Disponible en: https://www.frontiersin.org/articles/10.3389/fimmu.2017.01005/full

187. Calafatti M, Cocozza G, Limatola C, Garofalo S. Microglial crosstalk with astrocytes and immune cells in amyotrophic lateral sclerosis. Front Immunol. 26 de julio de 2023;14:1223096.

188. Ransohoff RM. How neuroinflammation contributes to neurodegeneration. Science. 19 de agosto de 2016;353(6301):777-83.

189. Radford RA, Morsch M, Rayner SL, Cole NJ, Pountney DL, Chung RS. The established and emerging roles of astrocytes and microglia in amyotrophic lateral sclerosis and frontotemporal dementia. Front Cell Neurosci. 2015;9:414.

190. Liddelow SA, Guttenplan KA, Clarke LE, Bennett FC, Bohlen CJ, Schirmer L, et al. Neurotoxic reactive astrocytes are induced by activated microglia. Nature. 26 de 2017;541(7638):481-7.

191. Trias E, King PH, Si Y, Kwon Y, Varela V, Ibarburu S, et al. Mast cells and neutrophils mediate peripheral motor pathway degeneration in ALS. JCI Insight. 04 de 2018;3(19).

192. Chen X, Hu Y, Cao Z, Liu Q, Cheng Y. Cerebrospinal Fluid Inflammatory Cytokine Aberrations in Alzheimer's Disease, Parkinson's Disease and Amyotrophic Lateral Sclerosis: A Systematic Review and Meta-Analysis. Front Immunol. 2018;9:2122.

193. López-Blanch R, Salvador-Palmer R, Estrela JM, Obrador E. An Intercellular Flow of Glutathione Regulated by Interleukin 6 Links Astrocytes and the Liver in the Pathophysiology of Amyotrophic Lateral Sclerosis. Antioxidants. 16 de diciembre de 2021;10(12):2007.

194. Obrador E, Jihad-Jebbar A, Salvador-Palmer R, López-Blanch R, Oriol-Caballo M, Moreno-Murciano MP, et al. Externally Applied Electromagnetic Fields and Hyperthermia Irreversibly Damage Cancer Cells. Cancers. 29 de junio de 2023;15(13):3413.

195. Chen Y, Xia K, Chen L, Fan D. Increased Interleukin-6 Levels in the Astrocyte-Derived Exosomes of Sporadic Amyotrophic Lateral Sclerosis Patients. Front Neurosci. 2019;13:574.

196. Wosiski-Kuhn M, Caress JB, Cartwright MS, Hawkins GA, Milligan C. Interleukin 6 (IL6) level is a biomarker for functional disease progression within IL6R358Ala variant groups in amyotrophic lateral sclerosis patients. Amyotroph Lateral Scler Front Degener. 3 de abril de 2021;22(3-4):248-59.

197. Murdock BJ, Bender DE, Segal BM, Feldman EL. The dual roles of immunity in ALS: injury overrides protection. Neurobiol Dis. mayo de 2015;77:1-12.

198. Chiu IM, Chen A, Zheng Y, Kosaras B, Tsiftsoglou SA, Vartanian TK, et al. T lymphocytes potentiate endogenous neuroprotective inflammation in a mouse model of ALS. Proc Natl Acad Sci U S A. 18 de noviembre de 2008;105(46):17913-8.

199. Beers DR, Zhao W, Wang J, Zhang X, Wen S, Neal D, et al. ALS patients' regulatory T lymphocytes are dysfunctional, and correlate with disease progression rate and severity. JCI Insight. 9 de marzo de 2017;2(5):e89530.

200. Hooten KG, Beers DR, Zhao W, Appel SH. Protective and Toxic Neuroinflammation in Amyotrophic Lateral Sclerosis. Neurother J Am Soc Exp Neurother. abril de 2015;12(2):364-75.

201. Henkel JS, Beers DR, Wen S, Rivera AL, Toennis KM, Appel JE, et al. Regulatory T-lymphocytes mediate amyotrophic lateral sclerosis progression and survival. EMBO Mol Med. 2013;5(1):64-79.

202. Oeckl P, Weydt P, Steinacker P, Anderl-Straub S, Nordin F, Volk AE, et al. Different neuroinflammatory profile in amyotrophic lateral sclerosis and frontotemporal dementia is linked to the clinical phase. J Neurol Neurosurg Psychiatry. 2019;90(1):4-10.

203. Matschke V, Theiss C, Matschke J. Oxidative stress: the lowest common denominator of multiple diseases. Neural Regen Res. febrero de 2019;14(2):238.

204. Sies H. Oxidative stress: a concept in redox biology and medicine. Redox Biol. 1 de abril de 2015;4:180-3.

205. Hajam YA, Rani R, Ganie SY, Sheikh TA, Javaid D, Qadri SS, et al. Oxidative Stress in Human Pathology and Aging: Molecular Mechanisms and Perspectives. Cells. 5 de febrero de 2022;11(3):552.

206. Barber SC, Shaw PJ. Oxidative stress in ALS: key role in motor neuron injury and therapeutic target. Free Radic Biol Med. 1 de marzo de 2010;48(5):629-41.

207. Turner MR, Bowser R, Bruijn L, Dupuis L, Ludolph A, McGrath M, et al. Mechanisms, models and biomarkers in amyotrophic lateral sclerosis. Amyotroph Lateral Scler Front Degener. mayo de 2013;14 Suppl 1(0 1):19-32.

208. Rogers ML, Schultz DW, Karnaros V, Shepheard SR. Urinary biomarkers for amyotrophic lateral sclerosis: candidates, opportunities and considerations. Brain Commun. 24 de octubre de 2023;5(6):fcad287.

209. Bogdanov M, Brown RH, Matson W, Smart R, Hayden D, O'Donnell H, et al. Increased oxidative damage to DNA in ALS patients. Free Radic Biol Med. 1 de octubre de 2000;29(7):652-8.

210. Beal MF, Ferrante RJ, Browne SE, Matthews RT, Kowall NW, Brown RH. Increased 3-nitrotyrosine in both sporadic and familial amyotrophic lateral sclerosis. Ann Neurol. octubre de 1997;42(4):644-54.

211. Arslanbaeva L, Bisaglia M. Activation of the Nrf2 Pathway as a Therapeutic Strategy for ALS Treatment. Molecules. 22 de febrero de 2022;27(5):1471.

212. Killoy KM, Harlan BA, Pehar M, Helke KL, Johnson JA, Vargas MR. Decreased glutathione levels cause overt motor neuron degeneration in hSOD1WT over-expressing mice. Exp Neurol. abril de 2018;302:129-35.

213. Weiduschat N, Mao X, Hupf J, Armstrong N, Kang G, Lange DJ, et al. Motor cortex glutathione deficit in ALS measured in vivo with the J-editing technique. Neurosci Lett. 6 de junio de 2014;570:102-7.

214. Sarlette A, Krampfl K, Grothe C, Neuhoff N von, Dengler R, Petri S. Nuclear erythroid 2-related factor 2-antioxidative response element signaling pathway in motor cortex and spinal cord in amyotrophic lateral sclerosis. J Neuropathol Exp Neurol. noviembre de 2008;67(11):1055-62.

215. Nanou A, Higginbottom A, Valori CF, Wyles M, Ning K, Shaw P, et al. Viral delivery of antioxidant genes as a therapeutic strategy in experimental models of amyotrophic lateral sclerosis. Mol Ther J Am Soc Gene Ther. agosto de 2013;21(8):1486-96.

216. Cohen TJ, Hwang AW, Restrepo CR, Yuan CX, Trojanowski JQ, Lee VMY. An acetylation switch controls TDP-43 function and aggregation propensity. Nat Commun. 5 de enero de 2015;6:5845.

217. Colombrita C, Zennaro E, Fallini C, Weber M, Sommacal A, Buratti E, et al. TDP-43 is recruited to stress granules in conditions of oxidative insult. J Neurochem. noviembre de 2009;111(4):1051-61.

218. Goh CW, Lee IC, Sundaram JR, George SE, Yusoff P, Brush MH, et al. Chronic oxidative stress promotes GADD34-mediated phosphorylation of the TAR

DNA-binding protein TDP-43, a modification linked to neurodegeneration. J Biol Chem. 5 de enero de 2018;293(1):163-76.

219. Zuo X, Zhou J, Li Y, Wu K, Chen Z, Luo Z, et al. TDP-43 aggregation induced by oxidative stress causes global mitochondrial imbalance in ALS. Nat Struct Mol Biol. febrero de 2021;28(2):132-42.

220. Kanekura K, Suzuki H, Aiso S, Matsuoka M. ER stress and unfolded protein response in amyotrophic lateral sclerosis. Mol Neurobiol. abril de 2009;39(2):81-9.

221. Pollari E, Goldsteins G, Bart G, Koistinaho J, Giniatullin R. The role of oxidative stress in degeneration of the neuromuscular junction in amyotrophic lateral sclerosis. Front Cell Neurosci. 13 de mayo de 2014;8:131.

222. Smith EF, Shaw PJ, De Vos KJ. The role of mitochondria in amyotrophic lateral sclerosis. Neurosci Lett. 25 de septiembre de 2019;710:132933.

223. Wiedemann FR, Manfredi G, Mawrin C, Beal MF, Schon EA. Mitochondrial DNA and respiratory chain function in spinal cords of ALS patients. J Neurochem. febrero de 2002;80(4):616-25.

224. Gunnarsson LG, Bodin L. Amyotrophic Lateral Sclerosis and Occupational Exposures: A Systematic Literature Review and Meta-Analyses. Int J Environ Res Public Health. 26 de 2018;15(11).

225. Calió ML, Henriques E, Siena A, Bertoncini CRA, Gil-Mohapel J, Rosenstock TR. Mitochondrial Dysfunction, Neurogenesis, and Epigenetics: Putative Implications for Amyotrophic Lateral Sclerosis Neurodegeneration and Treatment. Front Neurosci. 15 de julio de 2020;14:679.

226. Jankovic M, Novakovic I, Gamil Anwar Dawod P, Gamil Anwar Dawod A, Drinic A, Abdel Motaleb FI, et al. Current Concepts on Genetic Aspects of Mitochondrial Dysfunction in Amyotrophic Lateral Sclerosis. Int J Mol Sci. 11 de septiembre de 2021;22(18):9832.

227. Sasaki S, Iwata M. Mitochondrial alterations in the spinal cord of patients with sporadic amyotrophic lateral sclerosis. J Neuropathol Exp Neurol. enero de 2007;66(1):10-6.

228. Ghiasi P, Hosseinkhani S, Noori A, Nafissi S, Khajeh K. Mitochondrial complex I deficiency and ATP/ADP ratio in lymphocytes of amyotrophic lateral sclerosis patients. Neurol Res. 1 de abril de 2012;34(3):297-303.

229. Ferri A, Cozzolino M, Crosio C, Nencini M, Casciati A, Gralla EB, et al. Familial ALS-superoxide dismutases associate with mitochondria and shift their redox potentials. Proc Natl Acad Sci U S A. 12 de septiembre de 2006;103(37):13860-5.

230. Faes L, Callewaert G. Mitochondrial dysfunction in familial amyotrophic lateral sclerosis. J Bioenerg Biomembr. diciembre de 2011;43(6):587-92.

231. Muyderman H, Chen T. Mitochondrial dysfunction in amyotrophic lateral sclerosis - a valid pharmacological target? Br J Pharmacol. abril de 2014;171(8):2191-205.

232. Obrador E, Salvador-Palmer R, López-Blanch R, Jihad-Jebbar A, Vallés SL, Estrela JM. The Link between Oxidative Stress, Redox Status, Bioenergetics and Mitochondria in the Pathophysiology of ALS. Int J Mol Sci. 14 de junio de 2021;22(12):6352.

233. Satoh A, Imai SI, Guarente L. The brain, sirtuins, and ageing. Nat Rev Neurosci. 18 de mayo de 2017;18(6):362-74.

234. Bhatt V, Tiwari AK. Sirtuins, a key regulator of ageing and age-related neurodegenerative diseases. Int J Neurosci. diciembre de 2023;133(10):1167-92.

235. Bause AS, Haigis MC. SIRT3 regulation of mitochondrial oxidative stress. Exp Gerontol. 1 de julio de 2013;48(7):634-9.

236. Herskovits AZ, Hunter TA, Maxwell N, Pereira K, Whittaker CA, Valdez G, et al. SIRT1 deacetylase in aging-induced neuromuscular degeneration and amyotrophic lateral sclerosis. Aging Cell. 2018;17(6):e12839.

237. DiNicolantonio JJ, McCarty MF, O'Keefe JH. Nutraceutical activation of Sirt1: a review. Open Heart. 15 de diciembre de 2022;9(2):e002171.

238. Hor JH, Santosa MM, Lim VJW, Ho BX, Taylor A, Khong ZJ, et al. ALS motor neurons exhibit hallmark metabolic defects that are rescued by SIRT3 activation. Cell Death Differ. abril de 2021;28(4):1379-97.

239. Imai S ichiro, Guarente L. NAD+ and sirtuins in aging and disease. Trends Cell Biol. agosto de 2014;24(8):464-71.

240. Rubia JE de la, Drehmer E, Platero JL, Benlloch M, Caplliure-Llopis J, Villaron-Casales C, et al. Efficacy and tolerability of EH301 for amyotrophic lateral

sclerosis: a randomized, double-blind, placebo-controlled human pilot study. Amyotroph Lateral Scler Front Degener. 2 de enero de 2019;20(1-2):115-22.

241. Harlan BA, Pehar M, Sharma DR, Beeson G, Beeson CC, Vargas MR. Enhancing NAD+ Salvage Pathway Reverts the Toxicity of Primary Astrocytes Expressing Amyotrophic Lateral Sclerosis-linked Mutant Superoxide Dismutase 1 (SOD1). J Biol Chem. 13 de mayo de 2016;291(20):10836-46.

242. Napoli L. Ultrastructural Mitochondrial Abnormalities in Patients With Sporadic Amyotrophic Lateral Sclerosis. Arch Neurol. 1 de diciembre de 2011;68(12):1612.

243. Vielhaber S, Kunz D, Winkler K, Wiedemann FR, Kirches E, Feistner H, et al. Mitochondrial DNA abnormalities in skeletal muscle of patients with sporadic amyotrophic lateral sclerosis. Brain. 1 de julio de 2000;123(7):1339-48.

244. Park HR, Yang EJ. Oxidative Stress as a Therapeutic Target in Amyotrophic Lateral Sclerosis: Opportunities and Limitations. Diagn Basel Switz. 26 de agosto de 2021;11(9):1546.

245. Martin LJ, Gertz B, Pan Y, Price AC, Molkentin JD, Chang Q. The mitochondrial permeability transition pore in motor neurons: involvement in the pathobiology of ALS mice. Exp Neurol. agosto de 2009;218(2):333-46.

246. Mehta AR, Walters R, Waldron FM, Pal S, Selvaraj BT, Macleod MR, et al. Targeting mitochondrial dysfunction in amyotrophic lateral sclerosis: a systematic review and meta-analysis. Brain Commun. 6 de agosto de 2019;1(1):fcz009.

247. Tzeplaeff L, Wilfling S, Requardt MV, Herdick M. Current State and Future Directions in the Therapy of ALS. Cells [Internet]. 31 de mayo de 2023 [citado 4 de abril de 2024];12(11):1523. Disponible en: https://www.ncbi.nlm.nih.gov/pmc/articles/PMC10252394/

248. Cedarbaum JM, Stambler N, Malta E, Fuller C, Hilt D, Thurmond B, et al. The ALSFRS-R: a revised ALS functional rating scale that incorporates assessments of respiratory function. BDNF ALS Study Group (Phase III). J Neurol Sci. 31 de octubre de 1999;169(1-2):13-21.

249. Jaiswal MK. Riluzole and edaravone: A tale of two amyotrophic lateral sclerosis drugs. Med Res Rev. marzo de 2019;39(2):733-48.

250. Georgoulopoulou E, Fini N, Vinceti M, Monelli M, Vacondio P, Bianconi G, et al. The impact of clinical factors, riluzole and therapeutic interventions on

ALS survival: a population based study in Modena, Italy. Amyotroph Lateral Scler Front Degener. septiembre de 2013;14(5-6):338-45.

251. Hinchcliffe M, Smith A. Riluzole: real-world evidence supports significant extension of median survival times in patients with amyotrophic lateral sclerosis. Degener Neurol Neuromuscul Dis. 2017;7:61-70.

252. Grant P, Song JY, Swedo SE. Review of the Use of the Glutamate Antagonist Riluzole in Psychiatric Disorders and a Description of Recent Use in Childhood Obsessive-Compulsive Disorder. J Child Adolesc Psychopharmacol [Internet]. agosto de 2010 [citado 1 de enero de 2024];20(4):309-15. Disponible en: https://www.ncbi.nlm.nih.gov/pmc/articles/PMC2958461/

253. Fumagalli E, Bigini P, Barbera S, De Paola M, Mennini T. Riluzole, unlike the AMPA antagonist RPR119990, reduces motor impairment and partially prevents motoneuron death in the wobbler mouse, a model of neurodegenerative disease. Exp Neurol. marzo de 2006;198(1):114-28.

254. Bensimon G, Lacomblez L, Meininger V. A controlled trial of riluzole in amyotrophic lateral sclerosis. ALS/Riluzole Study Group. N Engl J Med. 3 de marzo de 1994;330(9):585-91.

255. Bensimon G, Lacomblez L, Delumeau JC, Bejuit R, Truffinet P, Meininger V, et al. A study of riluzole in the treatment of advanced stage or elderly patients with amyotrophic lateral sclerosis. J Neurol. mayo de 2002;249(5):609-15.

256. Lacomblez L, Bensimon G, Leigh PN, Guillet P, Meininger V. Dose-ranging study of riluzole in amyotrophic lateral sclerosis. Amyotrophic Lateral Sclerosis/Riluzole Study Group II. Lancet Lond Engl. 25 de mayo de 1996;347(9013):1425-31.

257. Bellingham MC. A Review of the Neural Mechanisms of Action and Clinical Efficiency of Riluzole in Treating Amyotrophic Lateral Sclerosis: What have we Learned in the Last Decade? CNS Neurosci Ther [Internet]. 17 de enero de 2011 [citado 1 de enero de 2024];17(1):4-31. Disponible en: https://www.ncbi.nlm.nih.gov/pmc/articles/PMC6493865/

258. Dharmadasa T, Kiernan MC. Riluzole, disease stage and survival in ALS. Lancet Neurol. 1 de mayo de 2018;17(5):385-6.

259. Pittenger C, Coric V, Banasr M, Bloch M, Krystal JH, Sanacora G. Riluzole in the treatment of mood and anxiety disorders. CNS Drugs. 2008;22(9):761-86.

260. Doble A. The pharmacology and mechanism of action of riluzole. Neurology. diciembre de 1996;47(6 Suppl 4):S233-241.

261. Azbill RD, Mu X, Springer JE. Riluzole increases high-affinity glutamate uptake in rat spinal cord synaptosomes. Brain Res. 21 de julio de 2000;871(2):175-80.

262. Noh KM, Hwang JY, Shin HC, Koh JY. A novel neuroprotective mechanism of riluzole: direct inhibition of protein kinase C. Neurobiol Dis. agosto de 2000;7(4):375-83.

263. Katoh-Semba R, Asano T, Ueda H, Morishita R, Takeuchi IK, Inaguma Y, et al. Riluzole enhances expression of brain-derived neurotrophic factor with consequent proliferation of granule precursor cells in the rat hippocampus. FASEB J Off Publ Fed Am Soc Exp Biol. agosto de 2002;16(10):1328-30.

264. Orient-López F, Terré-Boliart R, Guevara-Espinosa D, Bernabeu M. Tratamiento neurorehabilitador de la Esclerosis Lateral Amiotrófica.

265. Ikeda K, Iwasaki Y. Edaravone, a Free Radical Scavenger, Delayed Symptomatic and Pathological Progression of Motor Neuron Disease in the Wobbler Mouse. PloS One. 2015;10(10):e0140316.

266. Okada M, Yamashita S, Ueyama H, Ishizaki M, Maeda Y, Ando Y. Long-term effects of edaravone on survival of patients with amyotrophic lateral sclerosis. eNeurologicalSci. junio de 2018;11:11-4.

267. Sawada H. Clinical efficacy of edaravone for the treatment of amyotrophic lateral sclerosis. Expert Opin Pharmacother. mayo de 2017;18(7):735-8.

268. WRITING GROUP ON BEHALF OF THE EDARAVONE (MCI-186) ALS 17 STUDY GROUP. Exploratory double-blind, parallel-group, placebo-controlled extension study of edaravone (MCI-186) in amyotrophic lateral sclerosis. Amyotroph Lateral Scler Front Degener. octubre de 2017;18(sup1):20-31.

269. Pharmacoeconomic Review Report: Edaravone (Radicava): (Mitsubishi Tanabe Pharma Corporation): Indication: For the treatment of Amyotrophic Lateral Sclerosis (ALS) [Internet]. Ottawa (ON): Canadian Agency for Drugs and Technologies in Health; 2019 [citado 1 de enero de 2024]. (CADTH Common Drug Reviews). Disponible en: http://www.ncbi.nlm.nih.gov/books/NBK542526/

270. Luo L, Song Z, Li X, Huiwang null, Zeng Y, Qinwang null, et al. Efficacy and safety of edaravone in treatment of amyotrophic lateral sclerosis-a

systematic review and meta-analysis. Neurol Sci Off J Ital Neurol Soc Ital Soc Clin Neurophysiol. febrero de 2019;40(2):235-41.

271. Paganoni S, Macklin EA, Hendrix S, Berry JD, Elliott MA, Maiser S, et al. Trial of Sodium Phenylbutyrate-Taurursodiol for Amyotrophic Lateral Sclerosis. N Engl J Med. 3 de septiembre de 2020;383(10):919-30.

272. Alqallaf A, Cates DW, Render KP, Patel KA. Sodium Phenylbutyrate and Taurursodiol: A New Therapeutic Option for the Treatment of Amyotrophic Lateral Sclerosis. Ann Pharmacother. 1 de febrero de 2024;58(2):165-73.

273. Pota V, Sansone P, De Sarno S, Aurilio C, Coppolino F, Barbarisi M, et al. Amyotrophic Lateral Sclerosis and Pain: A Narrative Review from Pain Assessment to Therapy. Behav Neurol. 16 de marzo de 2024;2024:1228194.

274. Khairoalsindi OA, Abuzinadah AR. Maximizing the Survival of Amyotrophic Lateral Sclerosis Patients: Current Perspectives. Neurol Res Int. 2018;2018:6534150.

275. Dorst J, Ludolph AC. Non-invasive ventilation in amyotrophic lateral sclerosis. Ther Adv Neurol Disord [Internet]. 21 de junio de 2019 [citado 1 de enero de 2024];12:1756286419857040. Disponible en: https://www.ncbi.nlm.nih.gov/pmc/articles/PMC6589990/

276. Muscaritoli M, Kushta I, Molfino A, Inghilleri M, Sabatelli M, Rossi Fanelli F. Nutritional and metabolic support in patients with amyotrophic lateral sclerosis. Nutr Burbank Los Angel Cty Calif. octubre de 2012;28(10):959-66.

277. Dorst J, Dupuis L, Petri S, Kollewe K, Abdulla S, Wolf J, et al. Percutaneous endoscopic gastrostomy in amyotrophic lateral sclerosis: a prospective observational study. J Neurol. 2015;262(4):849-58.

278. Bello-Haas VD, Florence JM, Kloos AD, Scheirbecker J, Lopate G, Hayes SM, et al. A randomized controlled trial of resistance exercise in individuals with ALS. Neurology. 5 de junio de 2007;68(23):2003-7.

279. Majmudar S, Wu J, Paganoni S. Rehabilitation in amyotrophic lateral sclerosis: why it matters. Muscle Nerve. julio de 2014;50(1):4-13.

280. Beukelman D, Fager S, Nordness A. Communication Support for People with ALS. Neurol Res Int [Internet]. 2011 [citado 1 de enero de 2024];2011:714693. Disponible en: https://www.ncbi.nlm.nih.gov/pmc/articles/PMC3096454/

281. Pagnini F, Rossi G, Lunetta C, Banfi P, Corbo M. Clinical Psychology and Amyotrophic Lateral Sclerosis. Front Psychol [Internet]. 21 de julio de 2010 [citado 1 de enero de 2024];1:33. Disponible en: https://www.ncbi.nlm.nih.gov/pmc/articles/PMC3153752/

282. Han S, Choi JR, Soon Shin K, Kang SJ. Resveratrol upregulated heat shock proteins and extended the survival of G93A-SOD1 mice. Brain Res. 5 de noviembre de 2012;1483:112-7.

283. Mancuso R, del Valle J, Modol L, Martinez A, Granado-Serrano AB, Ramirez-Núñez O, et al. Resveratrol improves motoneuron function and extends survival in SOD1(G93A) ALS mice. Neurother J Am Soc Exp Neurother. abril de 2014;11(2):419-32.

284. Estrela JM, Ortega A, Mena S, Rodriguez ML, Asensi M. Pterostilbene: Biomedical applications. Crit Rev Clin Lab Sci. 2013;50(3):65-78.

285. Wang B, Liu H, Yue L, Li X, Zhao L, Yang X, et al. Neuroprotective effects of pterostilbene against oxidative stress injury: Involvement of nuclear factor erythroid 2-related factor 2 pathway. Brain Res. 15 de julio de 2016;1643:70-9.

286. Kosuru R, Rai U, Prakash S, Singh A, Singh S. Promising therapeutic potential of pterostilbene and its mechanistic insight based on preclinical evidence. Eur J Pharmacol [Internet]. 15 de octubre de 2016 [citado 1 de mayo de 2024];789:229-43. Disponible en: https://www.sciencedirect.com/science/article/pii/S0014299916304873

287. Liu P, Tang W, Xiang K, Li G. Pterostilbene in the treatment of inflammatory and oncological diseases. Front Pharmacol [Internet]. 8 de enero de 2024 [citado 1 de mayo de 2024];14:1323377. Disponible en: https://www.ncbi.nlm.nih.gov/pmc/articles/PMC10800393/

288. Liu H, Wu X, Luo J, Wang X, Guo H, Feng D, et al. Pterostilbene Attenuates Astrocytic Inflammation and Neuronal Oxidative Injury After Ischemia-Reperfusion by Inhibiting NF-κB Phosphorylation. Front Immunol. 2019;10:2408.

289. Liu J, Fan C, Yu L, Yang Y, Jiang S, Ma Z, et al. Pterostilbene exerts an anti-inflammatory effect via regulating endoplasmic reticulum stress in endothelial cells. Cytokine. enero de 2016;77:88-97.

290. Liu H, Zhao L, Yue L, Wang B, Li X, Guo H, et al. Pterostilbene Attenuates Early Brain Injury Following Subarachnoid Hemorrhage via Inhibition of the NLRP3

Inflammasome and Nox2-Related Oxidative Stress. Mol Neurobiol. octubre de 2017;54(8):5928-40.

291. Deora V, Lee JD, Albornoz EA, McAlary L, Jagaraj CJ, Robertson AAB, et al. The microglial NLRP3 inflammasome is activated by amyotrophic lateral sclerosis proteins. Glia. febrero de 2020;68(2):407-21.

292. Obrador E, Salvador-Palmer R, López-Blanch R, Dellinger RW, Estrela JM. NAD+ Precursors and Antioxidants for the Treatment of Amyotrophic Lateral Sclerosis. Biomedicines. 12 de agosto de 2021;9(8):1000.

293. Massudi H, Grant R, Guillemin GJ, Braidy N. NAD+ metabolism and oxidative stress: the golden nucleotide on a crown of thorns. Redox Rep Commun Free Radic Res. 2012;17(1):28-46.

294. Pehar M, Harlan BA, Killoy KM, Vargas MR. Nicotinamide Adenine Dinucleotide Metabolism and Neurodegeneration. Antioxid Redox Signal. 20 de 2018;28(18):1652-68.

295. Hopkins EL, Gu W, Kobe B, Coleman MP. A Novel NAD Signaling Mechanism in Axon Degeneration and its Relationship to Innate Immunity. Front Mol Biosci [Internet]. 8 de julio de 2021 [citado 1 de mayo de 2024];8:703532. Disponible en: https://www.ncbi.nlm.nih.gov/pmc/articles/PMC8295901/

296. Harlan BA, Killoy KM, Pehar M, Liu L, Auwerx J, Vargas MR. Evaluation of the NAD+ biosynthetic pathway in ALS patients and effect of modulating NAD+ levels in hSOD1-linked ALS mouse models. Exp Neurol. mayo de 2020;327:113219.

297. Poljšak B, Kovač V, Špalj S, Milisav I. The Central Role of the NAD+ Molecule in the Development of Aging and the Prevention of Chronic Age-Related Diseases: Strategies for NAD+ Modulation. Int J Mol Sci [Internet]. 3 de febrero de 2023 [citado 1 de mayo de 2024];24(3):2959. Disponible en: https://www.ncbi.nlm.nih.gov/pmc/articles/PMC9917998/

298. Zhou M, Ottenberg G, Sferrazza GF, Hubbs C, Fallahi M, Rumbaugh G, et al. Neuronal death induced by misfolded prion protein is due to NAD+ depletion and can be relieved in vitro and in vivo by NAD+ replenishment. Brain J Neurol. abril de 2015;138(Pt 4):992-1008.

299. Wang P, Xu TY, Guan YF, Tian WW, Viollet B, Rui YC, et al. Nicotinamide phosphoribosyltransferase protects against ischemic stroke through SIRT1-dependent adenosine monophosphate-activated kinase pathway. Ann Neurol. febrero de 2011;69(2):360-74.

300. Lautrup S, Sinclair DA, Mattson MP, Fang EF. NAD+ in Brain Aging and Neurodegenerative Disorders. Cell Metab. 1 de octubre de 2019;30(4):630-55.

301. Gerdts J, Brace EJ, Sasaki Y, DiAntonio A, Milbrandt J. SARM1 activation triggers axon degeneration locally via NAD^+ destruction. Science. 24 de abril de 2015;348(6233):453-7.

302. Trammell SAJ, Schmidt MS, Weidemann BJ, Redpath P, Jaksch F, Dellinger RW, et al. Nicotinamide riboside is uniquely and orally bioavailable in mice and humans. Nat Commun. 10 de octubre de 2016;7:12948.

303. Gilmour BC, Gudmundsrud R, Frank J, Hov A, Lautrup S, Aman Y, et al. Targeting NAD+ in translational research to relieve diseases and conditions of metabolic stress and ageing. Mech Ageing Dev. marzo de 2020;186:111208.

304. Alegre GFS, Pastore GM. NAD+ Precursors Nicotinamide Mononucleotide (NMN) and Nicotinamide Riboside (NR): Potential Dietary Contribution to Health. Curr Nutr Rep. septiembre de 2023;12(3):445-64.

305. Sever B, Ciftci H, DeMirci H, Sever H, Ocak F, Yulug B, et al. Comprehensive Research on Past and Future Therapeutic Strategies Devoted to Treatment of Amyotrophic Lateral Sclerosis. Int J Mol Sci. 22 de febrero de 2022;23(5):2400.

306. Giovannelli I, Bayatti N, Brown A, Wang D, Mickunas M, Camu W, et al. Amyotrophic lateral sclerosis transcriptomics reveals immunological effects of low-dose interleukin-2. Brain Commun [Internet]. 1 de julio de 2021 [citado 1 de mayo de 2024];3(3):fcab141. Disponible en: https://doi.org/10.1093/braincomms/fcab141

307. Milligan C, Atassi N, Babu S, Barohn RJ, Caress JB, Cudkowicz ME, et al. Tocilizumab is safe and tolerable and reduces C-reactive protein concentrations in the plasma and cerebrospinal fluid of ALS patients. Muscle Nerve [Internet]. septiembre de 2021 [citado 1 de mayo de 2024];64(3):309-20. Disponible en: https://www.ncbi.nlm.nih.gov/pmc/articles/PMC9132344/

308. Maier A, Deigendesch N, Müller K, Weishaupt JH, Krannich A, Röhle R, et al. Interleukin-1 Antagonist Anakinra in Amyotrophic Lateral Sclerosis--A Pilot Study. PloS One. 2015;10(10):e0139684.

309. Miller RG, Zhang R, Bracci PM, Azhir A, Barohn R, Bedlack R, et al. Phase 2B randomized controlled trial of NP001 in amyotrophic lateral sclerosis: Pre-specified and post hoc analyses. Muscle Nerve. julio de 2022;66(1):39-49.

310. Gordon PH, Moore DH, Miller RG, Florence JM, Verheijde JL, Doorish C, et al. Efficacy of minocycline in patients with amyotrophic lateral sclerosis: a phase III randomised trial. Lancet Neurol. diciembre de 2007;6(12):1045-53.

311. Appel SH, Engelhardt JI, Henkel JS, Siklos L, Beers DR, Yen AA, et al. Hematopoietic stem cell transplantation in patients with sporadic amyotrophic lateral sclerosis. Neurology. 21 de octubre de 2008;71(17):1326-34.

312. Lunetta C, Lizio A, Cabona C, Gerardi F, Sansone VA, Corbo M, et al. A phase I/IIa clinical trial of autologous hematopoietic stem cell transplantation in amyotrophic lateral sclerosis. J Neurol. octubre de 2022;269(10):5337-46.

313. Goslinga JA, Terrelonge Jr. M, Bedlack R, Barkhaus P, Barnes B, Bertorini T, et al. ALSUntangled #65: glucocorticoid corticosteroids. Amyotroph Lateral Scler Front Degener [Internet]. 3 de abril de 2023 [citado 1 de mayo de 2024];24(3-4):351-7. Disponible en: https://doi.org/10.1080/21678421.2022.2099746

314. Fournier CN, Schoenfeld D, Berry JD, Cudkowicz ME, Chan J, Quinn C, et al. An open label study of a novel immunosuppression intervention for the treatment of amyotrophic lateral sclerosis. Amyotroph Lateral Scler Front Degener [Internet]. 3 de abril de 2018 [citado 1 de mayo de 2024];19(3-4):242-9. Disponible en: https://doi.org/10.1080/21678421.2017.1421666

315. Cudkowicz ME, Shefner JM, Schoenfeld DA, Zhang H, Andreasson KI, Rothstein JD, et al. Trial of celecoxib in amyotrophic lateral sclerosis. Ann Neurol. julio de 2006;60(1):22-31.

316. Trias E, Ibarburu S, Barreto-Núñez R, Babdor J, Maciel TT, Guillo M, et al. Post-paralysis tyrosine kinase inhibition with masitinib abrogates neuroinflammation and slows disease progression in inherited amyotrophic lateral sclerosis. J Neuroinflammation. 11 de 2016;13(1):177.

317. Hamad AA, Amer BE, Hawas Y, Mabrouk MA, Meshref M. Masitinib as a neuroprotective agent: a scoping review of preclinical and clinical evidence. Neurol Sci Off J Ital Neurol Soc Ital Soc Clin Neurophysiol. mayo de 2024;45(5):1861-73.

318. Ketabforoush AHME, Chegini R, Barati S, Tahmasebi F, Moghisseh B, Joghataei MT, et al. Masitinib: The promising actor in the next season of the Amyotrophic Lateral Sclerosis treatment series. Biomed Pharmacother Biomedecine Pharmacother. abril de 2023;160:114378.

319. Angelopoulou E, Pyrgelis ES, Piperi C. Emerging Potential of the Phosphodiesterase (PDE) Inhibitor Ibudilast for Neurodegenerative Diseases: An Update on Preclinical and Clinical Evidence. Mol Basel Switz. 2 de diciembre de 2022;27(23):8448.

320. Crocetti L, Floresta G, Cilibrizzi A, Giovannoni MP. An Overview of PDE4 Inhibitors in Clinical Trials: 2010 to Early 2022. Molecules. enero de 2022;27(15):4964.

321. Schaal SM, Garg MS, Ghosh M, Lovera L, Lopez M, Patel M, et al. The Therapeutic Profile of Rolipram, PDE Target and Mechanism of Action as a Neuroprotectant following Spinal Cord Injury. PLOS ONE. 19 de septiembre de 2012;7(9):e43634.

322. Wu Q, Qi L, Li H, Mao L, Yang M, Xie R, et al. Roflumilast Reduces Cerebral Inflammation in a Rat Model of Experimental Subarachnoid Hemorrhage. Inflammation. agosto de 2017;40(4):1245-53.

323. Li H, Zuo J, Tang W. Phosphodiesterase-4 Inhibitors for the Treatment of Inflammatory Diseases. Front Pharmacol. 2018;9:1048.

324. Schafer PH, Parton A, Gandhi AK, Capone L, Adams M, Wu L, et al. Apremilast, a cAMP phosphodiesterase-4 inhibitor, demonstrates anti-inflammatory activity in vitro and in a model of psoriasis. Br J Pharmacol. febrero de 2010;159(4):842-55.

325. Edwards CJ, Blanco FJ, Crowley J, Birbara CA, Jaworski J, Aelion J, et al. Apremilast, an oral phosphodiesterase 4 inhibitor, in patients with psoriatic arthritis and current skin involvement: a phase III, randomised, controlled trial (PALACE 3). Ann Rheum Dis. 1 de junio de 2016;75(6):1065-73.

326. Huang Z, Liu S, Zhang L, Salem M, Greig GM, Chan CC, et al. Preferential inhibition of human phosphodiesterase 4 by ibudilast. Life Sci. 1 de mayo de 2006;78(23):2663-8.

327. Cada DJ, Ingram K, Baker DE. Apremilast. Hosp Pharm. septiembre de 2014;49(8):752-62.

328. Oliveros G, Wallace CH, Chaudry O, Liu Q, Qiu Y, Xie L, et al. Repurposing ibudilast to mitigate Alzheimer's disease by targeting inflammation. Brain J Neurol. 1 de marzo de 2023;146(3):898-911.

329. Rolan P, Hutchinson M, Johnson K. Ibudilast: a review of its pharmacology, efficacy and safety in respiratory and neurological disease. Expert Opin Pharmacother. diciembre de 2009;10(17):2897-904.

330. Souness JE, Villamil ME, Scott LC, Tomkinson A, Giembycz MA, Raeburn D. Possible role of cyclic AMP phosphodiesterases in the actions of ibudilast on eosinophil thromboxane generation and airways smooth muscle tone. Br J Pharmacol. abril de 1994;111(4):1081-8.

331. Grodin EN, Nieto SJ, Meredith LR, Burnette E, O'Neill J, Alger J, et al. Effects of Ibudilast on Central and Peripheral Markers of Inflammation in Alcohol Use Disorder: A Randomized Clinical Trial. Addict Biol. julio de 2022;27(4):e13182.

332. Schwenkgrub J, Zaremba M, Mirowska-Guzel D, Kurkowska-Jastrzębska I. Ibudilast: a non-selective phosphodiesterase inhibitor in brain disorders. Postepy Hig Med Doswiadczalnej Online. 2 de marzo de 2017;71(0):137-48.

333. Mizuno T, Kurotani T, Komatsu Y, Kawanokuchi J, Kato H, Mitsuma N, et al. Neuroprotective role of phosphodiesterase inhibitor ibudilast on neuronal cell death induced by activated microglia. Neuropharmacology. marzo de 2004;46(3):404-11.

334. Chen Y, Wang H, Ying Z, Gao Q. Ibudilast enhances the clearance of SOD1 and TDP-43 aggregates through TFEB-mediated autophagy and lysosomal biogenesis: The new molecular mechanism of ibudilast and its implication for neuroprotective therapy. Biochem Biophys Res Commun. 21 de mayo de 2020;526(1):231-8.

335. Yang D, Yang Y, Zhao Y. Ibudilast, a Phosphodiesterase-4 Inhibitor, Ameliorates Acute Respiratory Distress Syndrome in Neonatal Mice by Alleviating Inflammation and Apoptosis. Med Sci Monit Int Med J Exp Clin Res. 31 de marzo de 2020;26:e922281-1-e922281-8.

336. Wu NC, Wang JJ. Ibudilast, a Phosphodiesterase Inhibitor and Toll-Like Receptor-4 Antagonist, Improves Hemorrhagic Shock and Reperfusion-Induced Left Ventricular Dysfunction by Reducing Myocardial Tumor Necrosis Factor α. Transplant Proc. 2020;52(6):1869-74.

337. Sumaiya K, Selvambika P, Natarajaseenivasan K. Anti-macrophage migration inhibitory factor (MIF) activity of ibudilast: A repurposing drug attenuates the pathophysiology of leptospirosis. Microb Pathog. 1 de diciembre de 2022;173:105786.

338. Hensley K, Fedynyshyn J, Ferrell S, Floyd RA, Gordon B, Grammas P, et al. Message and protein-level elevation of tumor necrosis factor alpha (TNF alpha) and TNF alpha-modulating cytokines in spinal cords of the G93A-SOD1 mouse model for amyotrophic lateral sclerosis. Neurobiol Dis. octubre de 2003;14(1):74-80.

339. Brohawn DG, O'Brien LC, Bennett JP. RNAseq Analyses Identify Tumor Necrosis Factor-Mediated Inflammation as a Major Abnormality in ALS Spinal Cord. PloS One. 2016;11(8):e0160520.

340. Bhat A, Ray B, Mahalakshmi AM, Tuladhar S, Nandakumar DN, Srinivasan M, et al. Phosphodiesterase-4 enzyme as a therapeutic target in neurological disorders. Pharmacol Res. octubre de 2020;160:105078.

341. Gurney ME, Pu H, Chiu AY, Dal Canto MC, Polchow CY, Alexander DD, et al. Motor neuron degeneration in mice that express a human Cu,Zn superoxide dismutase mutation. Science. 17 de junio de 1994;264(5166):1772-5.

342. Turner BJ, Talbot K. Transgenics, toxicity and therapeutics in rodent models of mutant SOD1-mediated familial ALS. Prog Neurobiol. mayo de 2008;85(1):94-134.

343. Kwiatkowski TJ, Bosco DA, Leclerc AL, Tamrazian E, Vanderburg CR, Russ C, et al. Mutations in the FUS/TLS gene on chromosome 16 cause familial amyotrophic lateral sclerosis. Science. 27 de febrero de 2009;323(5918):1205-8.

344. Vance C, Rogelj B, Hortobágyi T, De Vos KJ, Nishimura AL, Sreedharan J, et al. Mutations in FUS, an RNA processing protein, cause familial amyotrophic lateral sclerosis type 6. Science. 27 de febrero de 2009;323(5918):1208-11.

345. López-Blanch R, Salvador-Palmer R, Oriol-Caballo M, Moreno-Murciano P, Dellinger RW, Estrela JM, et al. Nicotinamide riboside, pterostilbene and ibudilast protect motor neurons and extend survival in ALS mice. Neurother J Am Soc Exp Neurother. enero de 2024;21(1):e00301.

346. Weydt P, Hong SY, Kliot M, Möller T. Assessing disease onset and progression in the SOD1 mouse model of ALS. Neuroreport. 23 de mayo de 2003;14(7):1051-4.

347. Kong J, Xu Z. Massive mitochondrial degeneration in motor neurons triggers the onset of amyotrophic lateral sclerosis in mice expressing a mutant SOD1. J Neurosci Off J Soc Neurosci. 1 de mayo de 1998;18(9):3241-50.

348. Beaudet MJ, Yang Q, Cadau S, Blais M, Bellenfant S, Gros-Louis F, et al. High yield extraction of pure spinal motor neurons, astrocytes and microglia from single embryo and adult mouse spinal cord. Sci Rep. 18 de noviembre de 2015;5:16763.

349. Obrador E, Navarro J, Mompo J, Asensi M, Pellicer JA, Estrela JM. Glutathione and the rate of cellular proliferation determine tumour cell sensitivity to tumour necrosis factor in vivo. Biochem J. 1 de julio de 1997;325 (Pt 1):183-9.

350. Anasagasti MJ, Martin JJ, Mendoza L, Obrador E, Estrela JM, McCuskey RS, et al. Glutathione protects metastatic melanoma cells against oxidative stress in the murine hepatic microvasculature. Hepatol Baltim Md. mayo de 1998;27(5):1249-56.

351. Benlloch M, Obrador E, Valles SL, Rodriguez ML, Sirerol JA, Alcácer J, et al. Pterostilbene Decreases the Antioxidant Defenses of Aggressive Cancer Cells In Vivo: A Physiological Glucocorticoids- and Nrf2-Dependent Mechanism. Antioxid Redox Signal. 10 de junio de 2016;24(17):974-90.

352. Zhang Y, Dai M, Yuan Z. Methods for the detection of reactive oxygen species. Anal Methods. 4 de octubre de 2018;10(38):4625-38.

353. Braman RS, Hendrix SA. Nanogram nitrite and nitrate determination in environmental and biological materials by vanadium (III) reduction with chemiluminescence detection. Anal Chem. 15 de diciembre de 1989;61(24):2715-8.

354. Carretero J, Obrador E, Esteve JM, Ortega A, Pellicer JA, Sempere FV, et al. Tumoricidal activity of endothelial cells. Inhibition of endothelial nitric oxide production abrogates tumor cytotoxicity induced by hepatic sinusoidal endothelium in response to B16 melanoma adhesion in vitro. J Biol Chem. 13 de julio de 2001;276(28):25775-82.

355. Ahmed A, Dunk C, Kniss D, Wilkes M. Role of VEGF receptor-1 (Flt-1) in mediating calcium-dependent nitric oxide release and limiting DNA synthesis in human trophoblast cells. Lab Investig J Tech Methods Pathol. junio de 1997;76(6):779-91.

356. Scarlett JL, Sheard PW, Hughes G, Ledgerwood EC, Ku HH, Murphy MP. Changes in mitochondrial membrane potential during staurosporine-induced apoptosis in Jurkat cells. FEBS Lett. 23 de junio de 2000;475(3):267-72.

357. Dagda RK, Rice M. Protocols for assessing mitophagy in neuronal cell lines and primary neurons. Neuromethods. 2017;123:249-77.

358. Flohé L, Otting F. Superoxide dismutase assays. Methods Enzymol. 1984;105:93-104.

359. Aebi H. Catalase in vitro. Methods Enzymol. 1984;105:121-6.

360. Flohé L, Günzler WA. Assays of glutathione peroxidase. Methods Enzymol. 1984;105:114-21.

361. Deng T, Hu S, Huang XA, Song J, Xu Q, Wang Y, et al. A novel strategy for colorimetric detection of hydroxyl radicals based on a modified Griess test. Talanta. 1 de abril de 2019;195:152-7.

362. Nishikawa M, Sato EF, Kashiba M, Kuroki T, Utsumi K, Inoue M. Role of glutathione in nitric oxide-dependent regulation of energy metabolism in rat hepatoma cells. Hepatol Baltim Md. febrero de 1998;27(2):422-6.

363. Hart TW. Some observations concerning the S-nitroso and S-phenylsulphonyl derivatives of L-cysteine and glutathione. Tetrahedron Lett. enero de 1985;26(16):2013-6.

364. Carretero J, Obrador E, Esteve JM, Ortega A, Pellicer JA, Sempere FV, et al. Tumoricidal activity of endothelial cells. Inhibition of endothelial nitric oxide production abrogates tumor cytotoxicity induced by hepatic sinusoidal endothelium in response to B16 melanoma adhesion in vitro. J Biol Chem. 13 de julio de 2001;276(28):25775-82.

365. Miller CJ, Rose AL, Waite TD. Importance of Iron Complexation for Fenton-Mediated Hydroxyl Radical Production at Circumneutral pH. Front Mar Sci [Internet]. 4 de agosto de 2016 [citado 29 de mayo de 2024];3. Disponible en: https://www.frontiersin.org/articles/10.3389/fmars.2016.00134

366. Sies H, Arteel GE. Interaction of peroxynitrite with selenoproteins and glutathione peroxidase mimics. Free Radic Biol Med. 15 de mayo de 2000;28(10):1451-5.

367. Harris J, Deen N, Zamani S, Hasnat MA. Mitophagy and the release of inflammatory cytokines. Mitochondrion. julio de 2018;41:2-8.

368. Ignarro LJ, Napoli C, Loscalzo J. Nitric oxide donors and cardiovascular agents modulating the bioactivity of nitric oxide: an overview. Circ Res. 11 de enero de 2002;90(1):21-8.

369. Li B, He X, Lei SS, Zhou FC, Zhang NY, Chen YH, et al. Hypertensive Rats Treated Chronically With Nω-Nitro-L-Arginine Methyl Ester (L-NAME) Induced Disorder of Hepatic Fatty Acid Metabolism and Intestinal Pathophysiology. Front Pharmacol. 2019;10:1677.

370. Ragab TIM, Ali NA, El Gendy ANG, Mohamed SH, Shalby AB, Farrag ARH, et al. Renoprotective and therapeutic effects of newly water, ethanol, and butanol ginseng fractions in hypertensive and chronic kidney disease with L-NAME. Biomed Pharmacother Biomedecine Pharmacother. octubre de 2021;142:111978.

371. Yang L, Gal J, Chen J, Zhu H. Self-assembled FUS binds active chromatin and regulates gene transcription. Proc Natl Acad Sci U S A. 16 de diciembre de 2014;111(50):17809-14.

372. Perrotti D, Iervolino A, Cesi V, Cirinná M, Lombardini S, Grassilli E, et al. BCR-ABL prevents c-jun-mediated and proteasome-dependent FUS (TLS) proteolysis through a protein kinase CbetaII-dependent pathway. Mol Cell Biol. agosto de 2000;20(16):6159-69.

373. Grassano M, Brodini G, De Marco G, Casale F, Fuda G, Salamone P, et al. Phenotype Analysis of Fused in Sarcoma Mutations in Amyotrophic Lateral Sclerosis. Neurol Genet. octubre de 2022;8(5):e200011.

374. Lasiene J, Yamanaka K. Glial cells in amyotrophic lateral sclerosis. Neurol Res Int. 2011;2011:718987.

375. Hu S, Peterson PK, Chao CC. Cytokine-mediated neuronal apoptosis. Neurochem Int. 1997;30(4-5):427-31.

376. Liu J, Wang F. Role of Neuroinflammation in Amyotrophic Lateral Sclerosis: Cellular Mechanisms and Therapeutic Implications. Front Immunol. 2017;8:1005.

377. Morevati M, Fang EF, Mace ML, Kanbay M, Gravesen E, Nordholm A, et al. Roles of NAD+ in Acute and Chronic Kidney Diseases. Int J Mol Sci [Internet]. enero de 2023 [citado 3 de junio de 2024];24(1):137. Disponible en: https://www.mdpi.com/1422-0067/24/1/137

378. Kuntić M, Hahad O, Münzel T, Daiber A. Crosstalk between Oxidative Stress and Inflammation Caused by Noise and Air Pollution—Implications for Neurodegenerative Diseases. Antioxidants [Internet]. 22 de febrero de 2024 [citado 7 de junio de 2024];13(3):266. Disponible en: https://www.ncbi.nlm.nih.gov/pmc/articles/PMC10967531/

379. Daiber A, Kröller-Schön S, Oelze M, Hahad O, Li H, Schulz R, et al. Oxidative stress and inflammation contribute to traffic noise-induced vascular and cerebral dysfunction via uncoupling of nitric oxide synthases. Redox Biol. julio de 2020;34:101506.

380. Zhao W, Xie W, Le W, Beers DR, He Y, Henkel JS, et al. Activated microglia initiate motor neuron injury by a nitric oxide and glutamate-mediated mechanism. J Neuropathol Exp Neurol. septiembre de 2004;63(9):964-77.

381. Pehar M, Vargas MR, Robinson KM, Cassina P, Díaz-Amarilla PJ, Hagen TM, et al. Mitochondrial superoxide production and nuclear factor erythroid 2-related factor 2 activation in p75 neurotrophin receptor-induced motor neuron apoptosis. J Neurosci Off J Soc Neurosci. 18 de julio de 2007;27(29):7777-85.

382. Carey AN, Fisher DR, Rimando AM, Gomes SM, Bielinski DF, Shukitt-Hale B. Stilbenes and anthocyanins reduce stress signaling in BV-2 mouse microglia. J Agric Food Chem. 26 de junio de 2013;61(25):5979-86.

383. Meng XL, Yang JY, Chen GL, Wang LH, Zhang LJ, Wang S, et al. Effects of resveratrol and its derivatives on lipopolysaccharide-induced microglial activation and their structure-activity relationships. Chem Biol Interact. 10 de julio de 2008;174(1):51-9.

384. Fiebich BL, Batista CRA, Saliba SW, Yousif NM, de Oliveira ACP. Role of Microglia TLRs in Neurodegeneration. Front Cell Neurosci. 2 de octubre de 2018;12:329.

385. Geloso MC, Corvino V, Marchese E, Serrano A, Michetti F, D'Ambrosi N. The Dual Role of Microglia in ALS: Mechanisms and Therapeutic Approaches. Front Aging Neurosci. 2017;9:242.

386. Bono S, Feligioni M, Corbo M. Impaired antioxidant KEAP1-NRF2 system in amyotrophic lateral sclerosis: NRF2 activation as a potential therapeutic strategy. Mol Neurodegener. 18 de octubre de 2021;16(1):71.

387. Lévy E, El Banna N, Baïlle D, Heneman-Masurel A, Truchet S, Rezaei H, et al. Causative Links between Protein Aggregation and Oxidative Stress: A Review. Int J Mol Sci. 9 de agosto de 2019;20(16):3896.

388. Pirie E, Oh CK, Zhang X, Han X, Cieplak P, Scott HR, et al. S-nitrosylated TDP-43 triggers aggregation, cell-to-cell spread, and neurotoxicity in hiPSCs and in vivo models of ALS/FTD. Proc Natl Acad Sci U S A. 16 de marzo de 2021;118(11):e2021368118.

389. Adibhatla RM, Hatcher JF. Lipid oxidation and peroxidation in CNS health and disease: from molecular mechanisms to therapeutic opportunities. Antioxid Redox Signal. enero de 2010;12(1):125-69.

390. Singh RJ, Karoui H, Gunther MR, Beckman JS, Mason RP, Kalyanaraman B. Reexamination of the mechanism of hydroxyl radical adducts formed from the reaction between familial amyotrophic lateral sclerosis-associated Cu,Zn superoxide dismutase mutants and H2O2. Proc Natl Acad Sci U S A [Internet]. 9 de junio de 1998 [citado 7 de junio de 2024];95(12):6675-80. Disponible en: https://www.ncbi.nlm.nih.gov/pmc/articles/PMC22595/

391. Kwan JY, Jeong SY, Van Gelderen P, Deng HX, Quezado MM, Danielian LE, et al. Iron accumulation in deep cortical layers accounts for MRI signal abnormalities in ALS: correlating 7 tesla MRI and pathology. PloS One. 2012;7(4):e35241.

392. Langkammer C, Enzinger C, Quasthoff S, Grafenauer P, Soellinger M, Fazekas F, et al. Mapping of iron deposition in conjunction with assessment of nerve fiber tract integrity in amyotrophic lateral sclerosis. J Magn Reson Imaging JMRI. junio de 2010;31(6):1339-45.

393. Li Q, Zhu W, Wen X, Zang Z, Da Y, Lu J. Beyond the Motor Cortex: Thalamic Iron Deposition Accounts for Disease Severity in Amyotrophic Lateral Sclerosis. Front Neurol [Internet]. 24 de febrero de 2022 [citado 7 de junio de 2024];13:791300. Disponible en: https://www.ncbi.nlm.nih.gov/pmc/articles/PMC8907117/

394. Wang L, Li C, Chen X, Li S, Shang H. Abnormal Serum Iron-Status Indicator Changes in Amyotrophic Lateral Sclerosis (ALS) Patients: A Meta-Analysis. Front Neurol. 2020;11:380.

395. Yamazaki T, Anraku T, Matsuzawa S. Ibudilast, a mixed PDE3/4 inhibitor, causes a selective and nitric oxide/cGMP-independent relaxation of the intracranial vertebrobasilar artery. Eur J Pharmacol. 15 de enero de 2011;650(2-3):605-11.

396. Babu S, Hightower BG, Chan J, Zürcher NR, Kivisäkk P, Tseng CEJ, et al. Ibudilast (MN-166) in amyotrophic lateral sclerosis- an open label, safety and pharmacodynamic trial. NeuroImage Clin. 2021;30:102672.

397. Takuma K, Lee E, Enomoto R, Mori K, Baba A, Matsuda T. Ibudilast attenuates astrocyte apoptosis via cyclic GMP signalling pathway in an in vitro reperfusion model. Br J Pharmacol. julio de 2001;133(6):841-8.

398. Day JP, Lindsay B, Riddell T, Jiang Z, Allcock RW, Abraham A, et al. Elucidation of a structural basis for the inhibitor-driven, p62 (SQSTM1)-dependent intracellular redistribution of cAMP phosphodiesterase-4A4 (PDE4A4). J Med Chem. 12 de mayo de 2011;54(9):3331-47.

399. Hennet T, Richter C, Peterhans E. Tumour necrosis factor-alpha induces superoxide anion generation in mitochondria of L929 cells. Biochem J. 15 de enero de 1993;289 (Pt 2)(Pt 2):587-92.

400. Goossens V, Grooten J, Vos KD, Fiers W. Direct evidence for tumor necrosis factor-induced mitochondrial reactive oxygen intermediates and their involvement in cytotoxicity. Proc Natl Acad Sci [Internet]. 29 de agosto de 1995 [citado 14 de octubre de 2019];92(18):8115-9. Disponible en: https://www.pnas.org/content/92/18/8115

401. Rolan P, Gibbons JA, He L, Chang E, Jones D, Gross MI, et al. Ibudilast in healthy volunteers: safety, tolerability and pharmacokinetics with single and multiple doses. Br J Clin Pharmacol. diciembre de 2008;66(6):792-801.

402. Dao VTV, Elbatreek MH, Fuchß T, Grädler U, Schmidt HHHW, Shah AM, et al. Nitric Oxide Synthase Inhibitors into the Clinic at Last. Handb Exp Pharmacol. 2021;264:169-204.

403. Witzel S, Mayer K, Oeckl P. Biomarkers for amyotrophic lateral sclerosis. Curr Opin Neurol. 1 de octubre de 2022;35(5):699-704.